UNIVERSITÀ DEGLI STUDI DI NAPOLI "FEDERICO II"

Facoltà di Agraria

Dipartimento di Scienze del Suolo, della Pianta, dell'Ambiente e delle Produzioni Animali

Dottorato di Ricerca
in
AGROBIOLOGIA E AGROCHIMICA
XXI Ciclo

Ph.D. THESIS

PRESENTED BY

ALESSIO CIMMINO

Phytotoxins produced by pathogenic fungi for the integrated management of noxious weeds

Relator: Professor Antonio Evidente
2005-2008

CONTENTS

1. INTRODUCTION

1.1. Weed Management

The weed pest is one of the most serious problems for agriculture and environment. Infesting plants generate a great obstacle to the normal flow of superficial waters, destroy the natural habitat, seriously damage the archaeological and monumental areas, and cause heavy losses to crop production and to pasture industry. Many plants of agrarian interest may dieback when the weed grows in the same field absorbing water, food substances, and sunlight. Furthermore, they represent a serious impediment to the normal agrarian activity. The diffusion of weed reduces the pasture areas with consequent deterioration of animal food.

In agricultural fields, weeds seem to have coevolved with crop plants since prehistoric time as evidenced by pollen analysis techniques indicating that both share common evolutionary lines. Distribution of weeds is determined by various environmental and biological characteristics. Human activities are mainly responsible for their regional patterns and have certainly played an important role in their spread. Plant species are also affected when their habitat are disturbed (Harlan and deWelt, 1965). Weeds have evolved due to continuous selection pressure imposed by humans, technological advancement, and/or through agricultural practices. The role of humans in selecting crop plants vis-à-vis evolution of weeds is clear from the fact that over 40 percent of the world's total weed species belong to Asteracee (sunflower family) and Poacee (grass family), which happen to provide over half of world's food and food products (Kohli *et al*., 2006).

The effort to control weeds is as old as agriculture itself. Humans, however, were familiar with weeds even before the dawn of agriculture, as several aboriginal nomadic tribes suffered from allergies, hay fever, and other health problems caused by poisonous plants. The control of weed diffusion has been achieved with agrochemicals belonging to different class of organic compounds. They are usually used in very large amounts in

agriculture, thus causing serious problems to human and animal health and producing heavy environmental pollution. In fact, these substances have frequently low specificity and are weakly or not biodegradable, accumulate in food plants and in layer, and drinkable water. Furthermore, the chemical control has short-life and must usually be repeated on an annual or semi-annual basis. Nevertheless, it would not be wise to kill or eradicate weeds, as that would mean deliberate genetic erosion in the modern era of rapid biodiversity loss causing imbalance in the natural ecosystems. Thus an urgent need exists to get ride of adverse effects of weeds without affecting the natural balance. Management of weeds, should, therefore, be achieved through strategies that do not affect the sustainability of agroecosystems and the life support system. The biological agents offer the advantage of being compatible with the environment, often with high specificity and represent a long term solution also in the control of weed particularly resistant to chemical herbicides. Therefore, many efforts have been made to biologically control the weeds using their natural antagonists as microorganisms and/or insect. Among the microorganisms, fungi are the most common pathogens of plants and therefore for weeds as well. Some insects and fungi, which satisfy the criteria of efficacy, specificity and long-time persistence, have been already commercialised essentially outside from Europe (Bottiglieri *et al*., 2000). Recently, researches have been started to isolate phytotoxins produced by some fungi pathogenic for weeds and use them as natural herbicides. The goal of such a project is to use natural substances, their derivatives or synthetic analogues with increased efficacy and specificity to avoid the release of microorganisms, and the possibility that they became host of other organisms. There are many reasons why natural substances might be good sources of molecules or molecular templates for herbicides. These compounds are the result of coevolution of the producing organism and its biotic environment. Natural compounds often have a shorter environmental half life than synthetic compounds, thus reducing environmental impact. Since many phytotoxins isolated from fungi pathogenic

for agrarian plants are not specific, they may be considered as potential natural herbicides in native forms or as derivatives and analogues (Graniti *et al.*, 1989; Delfosse, 1990; Strobel, 1991; Strobel *et al.*, 1991).

The first approach is the isolation of microorganisms from tissues of infected infesting plants, followed by selection of the strains with higher specificity and virulence. The second step is to find appropriate conditions for the *in vitro* growth of the fungi to obtain culture filtrates with high phytotoxicity against the host plants. Next, the phytotoxins are isolated, characterised and in some cases derivatized before to be tested as potential herbicides. Finally, the knowledge of the chemical structure of these substances may allow the partial or total synthesis of the most appropriate natural herbicide. Furthermore, (if they are a virulent factor), the toxins could be used in indirect mode as biomarkers, to select the best fungal strain or to optimise for their large scale production (Evidente, 2006; Evidente and Abouzeid 2006) and in combination with low dose of herbicides and the phytopathogenic fungus, to develop integrated weed management strategy.

Phytotoxins are defined as microbial metabolites that are harmful to plants at very low concentrations. Most of the plant pathogenic fungi produce toxins in culture and in their hosts. Frequently, these compounds play an important role in the pathogenesis as reproduce some or even all of the symptoms of the disease. In many cases the toxins are low molecular weight compounds belonging to a variety of class of natural products. They are able to diffuse from the site of the infection to surrounding tissues or are translocable within the plant. The virulence of the plant pathogen may depend on its capability to synthesize one or more toxins. Only few phytotoxins are known as host-specific toxins, more frequently they are phytotoxic for a broad range of plant species. In some cases studies on their mode of action and their role as "vivo-toxin" have also been carried out

(Strobel, 1982, Graniti *et al.*, 1989; Ballio and Graniti., 1991; Evidente, 1997; Upadhyay and Mukerji, 1997; Evidente and Motta 2001).

The main aim of this research involving several worldwide institutions was either to isolate new promising strains of weed pathogenic fungi and/or to enhance its efficacy. Further experiments are still in progress to overcome the important problems that arise during the practical application of phytotoxins in integrated crop management. Unfortunately, these are seriously limited by the very low amounts of bioactive compounds frequently produced by weed pathogenic fungi. Therefore, the stereostructural determination of phytotoxins could assist in realizing their simple and convenient total synthesis, to furnish amount of metabolites sufficient to carry out experiments on their biological activities, mode of action, and toxicity. Furthermore, the synthetic phytotoxins could be used either to develop methods allowing the selection of fungal strains for mycoherbicide application or to prepare derivatives and analogues with modulated and/or increased biological activity and specificity, which could be used in greenhouse or field experiments in view of their practical application (Evidente and Abouzeid, 2006).

Some examples on the use of phytotoxic metabolites extracted and purified from different fungal species in the last years and applied for weed control researches are illustrated in the successive paragraph of this section.

1.2. Phytotoxins in the management of weeds infesting pasture and important agrarian crops

From infected leaves of *Erigeron annuus* L. a fungus identified as *Phoma putaminum* was isolated. *E. annuus*, commonly named annual fleabane, is an indigenous weed from North America widely found in field and pastures all over Europe, including Italy. The main phytotoxin present in the culture filtrates organic extract, named putaminoxin, was characterised by spectroscopic methods (essentially 1D and 2D ^{1}H- and

^{13}C-NMR and HRESI MS) as (5*S*)-5-hydroxy-9-propyl-6-nonen-9-olide (**1**, Fig. 1.1). The structure of this new 10-macrolide was confirmed by conversion of the toxin into the corresponding 5-*O*-acetyl- and 6,7-dihydro-derivatives by standard acetylation and catalytic hydrogenation, respectively. The absolute stereochemistry of the secondary alcohol at C-5 was determined by applying the GC Horeau's method (Evidente *et al.*, 1995). Further investigation was carried out to ascertain whether associated toxins could be responsible for the high phytotoxicity of the organic culture extract. Four structurally related metabolites, named putaminoxin B-E were identified (**2-5**, Fig. 1.1) (Evidente *et al*., 1997; 1998a). When assayed on annual fleabane by leaf-puncture assay, as well as on some weedy and cultivated plants, putaminoxin proved to be more toxic than the putaminoxin analogues and previous cited derivatives. The latter were all inactive due to a modification of the nonenolide ring and the alkyl side chain. On the basis of these results, the structural features that appeared to be of primary importance for the phytotoxic activity of the toxin were the presence of both the unchanged hydroxy group at C-5 and the alkyl side chain at C-9 (Evidente *et al*., 1998b).

Many of these structural features appear to be important for the activity of pinolidoxin (**6**, Fig 1.1), a phytotoxic metabolite isolated from *Ascochyta pinodes* solid culture, which is a pathogenic fungus responsible for pea anthracnose (Evidente *et al*., 1993b). In addition, three minor correlated toxins were isolated from the same fungus and characterized as 7-*epi*-, 5,6-dihydro-, and 5,6-epoxy-pinolidoxin (**7-9**, Fig. 1.1) (Evidente *et al*., 1993a). Pinolidoxin [2-(2,4-hexadienoloxy)-7,8-dihydroxy-9-propyl-5-nonen-9-olide] is another non specific phytotoxic nonenolide which, being structurally related to putaminoxin, may be proposed as a potential natural herbicide. Therefore, a structure-activity relationships study was carried out using pinolidoxin, three previously cited analogues and three synthetic derivatives (7,8-*O,O'*-diacetyl-, 7,8-*O,O'*-isopropylidene-, and 5,6,11,12,13,14-hexahydro-pinolidoxin). Pinolidoxin, compared to its analogues and

derivatives, showed the highest phytotoxicity on both cultivated plants and weeds. Therefore, also for the activity of pinolidoxin, primarily important features are the presence of an unmodified diol system between C-7 and C-8 with the correct stereochemistry and the functionalization and the conformational freedom of the nonenolide ring. The hexadienoyloxy residue at C-9 did not affect the activity (Evidente *et al.*, 1998b).

In view of a possible use as natural herbicides, the fungicide and zootoxic activity of both toxins putaminoxin and pinolidoxin (**1** and **6**) and some of their analogues and derivatives were assayed. On *Geothricum candidum*, none of the compounds tested proved to be toxic. Only the derivatives and analogues of pinolidoxin demostrated zootoxicity when assayed on larvae of brine shrimp (*Artemia salina* L.).

The conducted structure-activity relationship studies provided useful information on the variability of biological properties, with respect to the chemical structure, either the presence or absence of active groups and/or chain. The availability of these metabolites in large amounts or the use of large-scale production system could allow the testing of these toxins in greenhouse or field experiments to evaluate their potential practical application as new and original modified natural compounds (Evidente and Abouzeid, 2006).

Among the four species belonging to the genus *Xanthium* (namely, *X. occidentale*, *X. orientale* L., *X. italicum* Mor. and *X. cavanillesii* Schouw.), which constitute the Noogoora burr complex, *X. occidentale* was the first to be reported in Australia, and is becoming the most destructive and widespread species (Morin *et al.*, 1994). The biological control of this noxious weed, mainly with the use of plant pathogens, such as *Alternaria zinniae* has been proposed.

The structure of two metabolites (**10** and **11**, Fig. 1.2), was determined by extensive use of spectroscopic methods (1D and 2D ^{1}H- and ^{13}C-NMR and HRESI MS). The structure and the configuration of the two toxins were confirmed by X-ray analysis. From all the above data, **10** appeared to be identical to brefeldin A, the macrocyclic cytotoxic

and antimicrobial metabolite previously isolated from microscopic fungi (*Penicillium*, *Ascochyta*, *Alternaria*, and *Curvularia*) (Betina, 1992; Tietjen *et al.*, 1983; Coombe *et al.*, 1968), and **11** to the α,β-dehydrocurvularin, the octaketide lactone also produced by a number of fungal species (*Penicillium*, *Curvularia*, *Cercospora* and *Stemphylium* spp.) (Caputo and Viola, 1977; Robenson and Strobel, 1981; Arai *et al.*, 1989; Lai *et al.*, 1989). This was the first report on the production of these two phytotoxins by a strain of *A. zinniae*, a good candidate for the biological control of *X. occidentale* with the inundative approach (Vurro *et al.*, 1998). Even though some toxic properties of both compounds have already been reported (Suzuki *et al.*, 1970; Tietjen *et al.*, 1983; Robeson and Strobel, 1985; Betina, 1992), some aspects seemed to be interesting, even for a practical approach. Tietjen *et al.* (1983) demonstrated that brefeldin A was particularly active against species belonging to the *Asteraceae* family and only on two out of the twenty-two non *Asteraceae* species tested. In fact, the application of droplets containing around 0.3 μg of toxin caused the faster appearance of wide necrotic spots, both on host leaves and cotyledons. In contrast, the effect of this metabolite at the tested concentration on other non-host plants was lower or nil. Furthermore, the toxin caused severe necrosis also when it was applied on host leaves and cotyledons without puncture, which was not observable for non-host plants. This unusual observed effect suggested using the spray application.

Vurro and Ellis (1997) showed that some fungal toxins, applied at concentration which causes no macroscopic toxic effects, are able to suppress phenylalanine ammonia lyase induction, which can be one of the first steps of the mechanism of defence of plant from pathogen attack. Thus, a suitable application could be the possible use of brefeldin A at very low concentration, in a mycoherbicide suspension, together with *A. zinniae* conidia to block the defence reaction of *X. occidentale* and help the pathogen to cause a more severe disease, and hence to obtain a better control of the weed.

Striga hermontica (Del.) Benth, commonly called witchweed, is a parasitic weed which causes severe losses in many important cereal crops, mainly in sorghum, corn, millet, rice and sugarcane. The loss of grain-sorghum yield due to striga infestation may reach up 70% and in case of severe infestation there may no yield at all. *S. hermonthica* is still very difficult to control, even using herbicides and fertilisers, cultural methods and resistant crop varieties. Abbasher and Sauerborn (1992) suggested the use of pathogenic microorganisms, including *Fusarium nygamai* Burgess and Trimboli, which proved to be particularly promising. From the acidic organic extract of culture filtrates, the main phytotoxins were identified, using essentially spectroscopic method (^{1}H- and ^{13}C-NMR and FAB and EI MS), as fusaric and 9,10-dehydrofusaric acids (**12** and **14**, Fig. 1.2). Their corresponding methyl esters (**13** and **15**, Fig. 1.2) were also isolated for the first time as naturally occurring compounds at very low level (Capasso *et al.*, 1996). Fusaric acids (**12** and **14**) have been already described as toxic metabolites produced from other species of *Fusarium* (Turner, 1971; Turner and Aldridge, 1983; Luz *et al.*, 1990; Abraham and Hensenn, 1992). The phytotoxic properties of fusaric acids and their methyl esters, were further investigated using biological assay on striga plants, seedlings, leaves and seeds in order to test their possible use as natural herbicides. The application of very low amounts of toxins (10^{-6} M) caused a dramatic reduction of seed germination, while on punctured leaves caused the appearance of large necrotic spots. The use of these metabolites against *Striga*, possibly in combination with other cultural and biological methods, could assist in controlling this weed (Zonno *et al.*, 1996).

The perthotrophic fungal species *Ascochyta caulina* (P. Karst.) v.d. Aa and v. Kest. has been proposed as a mycoherbicide against *Chenopodium album* (Kempenaar, 1995), also known as common lambsquarter or fat hen, a common worldwide weed of many arable crops as sugar beet and maize (Holm *et al.*, 1977). The application of pycnidiospores of the fungus to *C. album* plants causes the appearance of large necrosis of

leaves and stems and, depending on the amount of necrosis developed, plants show retarded growth or death.

A. caulina belongs to a well-known toxin-producer genus (Strange, 1997), and the possible use of fungal toxins as an alternative or in addition to the use of pathogens in weed biocontrol (Strobel *et al.*, 1991), is under investigation. The culture filtrates of *A. caulina*, showing high phytotoxicity on leaves and cuttings both of host and non-host plants was examined to ascertain the chemical nature of the phytotoxic metabolites. Three toxins were isolated using gel-filtration combined to TLC methods and characterized using spectroscopic (essentially 1D and 2D ^{1}H and ^{13}C-NMR and ESI MS) and chemical methods. The main toxin, named ascaulitoxin (**16**, Fig. 1.3) was characterized as the N^2-β-D-glucopyranoside of the 2,4,7-triamino-5-hydroxyoctandioic acid (Evidente *et al.*, 1998c). The other two toxins, which as **16** are non-protein aminoacids, were characterized as the *trans*-4-amino-D-proline and the ascaulitoxin aglycone (**17** and **18**, Figure 1.3) (Evidente *et al*., 2000; 2001).

Tested on fat hen in the leaf-puncture assay, **16** caused the appearance of necrotic spots surrounded by chlorosis. Particularly relevant in size was necrosis on sugarbeet (*Beta vulgaris* L.). Clear necrosis also appeared both on some weeds and on cultivated plants. Still clear, but of reduced size, were necrosis on tomato (*Lycopersicon esculentum* Mill.) and redroot pigweed (*Amaranthus retroflexus* L.). Assayed on fungi (*G. candidum*) as well as on bacteria (*Pseudomonas syringae* and *Escherichia coli*), ascaulitoxin showed no antimicrobial activity (Evidente *et al.*, 1998c).

Considering its interesting phytotoxicity on *C. album*, and the lack of activity against fungi and bacteria, further studies are planned on the role of ascaulitoxin in the plant disease and on the mechanism of action. These aspects are important because the toxin could be used as natural herbicide, either in combination with toxic metabolites present in the culture filtrate of *A. caulina*, or with the pathogen itself, as well as with other

control methods in the integrated weed management approach (Evidente, 2006; Evidente and Abouzeid, 2006).

However, any pratical application of this toxin appears to be seriously limited by the very low amounts of this metabolite present in the fungal culture filtrates. Therefore, efforts were first directed to devise a convenient and simple method of total synthesis. Because the naturally occurring toxin, is only one of the possible sixteen stereoisomers, the determination of the relative configuration of the four chiral centres (C-2, C-4, C-5 and C-7) of ascaulitoxin appeared to be the most pressing and relevant problem to establish its absolute stereochemistry and to realize its stereoselective synthesis. The determination of the relative stereochemistry of the ascaulitoxin molecule was performed by NMR configuration analysis, based on the evaluation of the omo ($^3J_{HH}$)- and hetero ($^2J_{CH}$ and $^3J_{CH}$)- nuclear coupling constants, in combination with ROESY (Rotating Overhauser Effect Spectroscopy) responses (Matsumori *et al*., 1995, 1996, 1999, Wu *et al*., 2000; Bassarello *et al*., 2001).

Assayed on punctured leaves, **17** had a drastic effect on the host plant, causing the rapid appearance of large necrosis surrounding the puncture point. On other dicot leaves, the phytotoxicity varied from large necrotic areas (poppy, annual mercury, cucumber, wild cucumber), through medium ones (tree of heaven, tomato, common sowthistle), to small necrotic spots (black nightshade). An interesting aspect is the lack of toxicity when **17** was assayed on several monocots, both cultivated (wheat, oat, barley) as well as wild (canarygrass, slender foxtail, wild oat). When tested at up to 10^{-5} M on cut young fat hen seedlings, the toxin caused wide necrosis and dryeness of cotyledons, while no effect could be seen on stems (Evidente *et al*., 2000). The toxin lacks antifungal and antibiotic activities when assayed on *G. candidum* and on *P. syringae* ssp. *syringae* and *E. coli*, as already described for the ascaulitoxin, and has no zootoxicity when tested on brine shrimp larvae (*Artemia salina* L.).

To purify the three phytotoxins produced by *A. caulina*, an alternative method based on ion exchange chromatography was developed to overcome difficulties and high costs, and to obtain a mixture of all three toxins suitable for further experiments in view of their practical application. The mixture of toxic metabolites (350 mg/l) (Vurro *et al*., 2001), was used in greenhouse, field, and formulation experiments either alone or in combination with the pathogen, its culture filtrate, or with a low-dose herbicide, to biocontrol host plant. The efficacy of the toxins mixture was compared with that of the culture filtrate alone or in combination with the fungus. In glasshouse experiments it showed the same toxicity as culture filtrates when applied at the same concentration as the latter (2 mg/ml). The phytotoxins mixture influenced the growth of *C. album* even at the lowest concentration. Greenhouse experiments also showed that the use of solutions from the toxins mixture (1 mg/ml) in conjunction with spores of *A. caulina* (at 10^6/ml) improved the biocontrol efficacy of this fungus by more than 30 percent. Furthermore, the simultaneous application of toxins or fungal spores with low dose of herbicides at one-fifth of the labelled rate, such as metribuzin which act as an inhibitor of photosynthesis at the level of photosystem II, and rimsulfuron which is an aceto-lactate synthase inhibitor, gave better results than single-agent treatments. The efficacy improvement of rimsulfuron, which is nearly ineffective against *C. album* when used at the labelled concentration, could have an interesting practical application in terms of management of herbicide resistance. Furthermore, exploration of toxin activity could expand the action spectrum of herbicides or biocontrol agents (Vurro *et al*., 2001).

Formulations containing different combinations of *A. caulina* conidia, its phytotoxins, and low-dose herbicides have been tested. A significant improvement in the efficacy of the fungus was achieved in glasshouse trials with an aqueous formulation containing PVA (polyvinyl alcohol, 0.1 percent v/v), Psyllium (a plant derived polysaccharide, 0.4 percent w/v), Sylgard 309 (a surfactant, 0.1 percent v/v), nutrients, and

conidia (5 x 10^6/ml). Field trials have investigated the performance of *A. caulina* conidia applied at different development stages of *C. album* either as a single treatment or combined with sublethal doses of herbicides or with the fungal phytotoxin. With the available formulation, favourable weather conditions are needed to obtain the infection in the field. The efficacy of the strain of *A. caulina* used so far has proved to be inadequate to justify its development as a bioherbicide. This is probably due to its low virulence (Netland *et al*., 2001).

1.3. Biological control of grass weeds

In many countries, annual and perennial grasses are among the most problematic weeds for various crops (Holm *et al*., 1977). Of all the possible causes of loss in cereal yields, weeds, such as annual grasses are one of the most important; this is due to their similarity in morphology, physiology and ecology to the crop species.

Such weeds are difficult to control because of their prodigious seed production, which is responsible for their reproduction and diffusion, their tolerance to the chemical herbicides available, and their growth habits that can enable them to escape from chemical and mechanical control practices. Tactics that reduce the input of seed can improve long-term control of infesting grasses.

Considering the increasing number of weed species that are tolerant or resistant to the use of herbicides (Naylor, 2002), and the difficulties in finding new chemical active compounds, biocontrol microorganisms and new herbicides from natural sources are receiving a renewed interest. One such strategy could be the massive application of seed-borne pathogens as bioherbicides. Pathogens damaging the seed in the inflorescence or preventing flowering have also potential for biological control.

Some promising fungal pathogens have been identified, and their use as inundative agents has been proposed (Zhan and Watson, 1997; Chandramohan and Charudattan,

2001); furthermore, some fungal phytotoxins have been identified and considered as potential natural herbicides (Hallock *et al.*, 1988; Kastanias and Tokousbalides, 2000). Pathogenic fungi isolated from grass weeds were found in several fungal collections and many strains were collected (Fracchiolla, 2003). Such investigation was aimed at finding producers of toxic metabolites with herbicidal activities against grass weeds.

1.3.1. Biological control of *Bromus* spp.

Pathogens damaging the seed in the inflorescence or preventing flowering have also potential for biological control. Agents that attack the reproductive output of weeds are frequently used in biological control programmes against weeds in pastures, rangeland and natural habitats. *Pyrenophora semeniperda* (Brittlebank & Adam) Shoemaker, a seed-borne pathogen that causes several symptoms in infected plants, has been proposed as a bioherbicide (Campbell *et al*., 1996). *P. semeniperda* was first described in Europe in 1841, and later in Australia, New Zealand, North America and South Africa. The fungus infects seeds and leaves of over 35 genera of grasses including all the winter cereals and six dicotyledonous genera (Medd, 1992). In brome grass (*Bromus* spp.) and wheat (*Triticum aestivum* L.) it has been reported to cause death of seed primordia and subsequent abortion of seed (Neergard, 1979). The most striking symptom is the production of vegetative fungal stromata on infected seeds, which can lead to a reduction in the germination capacity or a decrease in seedling vigour. The ability of *P. semeniperda* to infect seeds, when applied as conidial suspension to the inflorescence of several grassy weed-species, has also been demonstrated. Since some annual grasses may occur in pastures or crops used as forage, any potential bioherbicidal agent should be devoid of toxic effects on livestock. Equally, there should be no risk of introducing toxins to grains that are harvested for human consumption.

It is well known that other species of *Pyrenophora* produce toxins, some of which are potentially dangerous (Bach *et al*., 1979; Friis *et al*., 1991). When grown on wheat kernels, *P. seminiperda* showed to produce cytochalasins, a large group of fungal metabolites having different biological activities (Natori and Yahara, 1991; Abate *et al*., 1997; Vurro *et al*., 1997; Evidente and Motta, 2001). Three new cytochalasans, named cytochalasins Z1, Z2 and Z3 (**19**, **20** and **21**, Fig. 1.4) were isolated and characterised by spectroscopic analysis carried out also in comparison with the spectral data of several cytochalasins already known (Cole and Cox, 1981; Vurro *et al*., 1997; Evidente and Motta 2001). Other cytochalasins isolated from the same organic extract were identified, using the same spectroscopic techniques, as the already known cytochalasins F, T, deoxaphomin and cytochalasin B (**28**-**30** and **26**, Fig. 1.5). Cytochalasins Z1 and Z2 proved to be structurally related to cytochalasin T, whereas cytochalasin Z3 was related to cytochalasin B, which was produced in very large amounts (Evidente *et al*., 2002).

In seedling assays on wheat and on tomato, the most active compounds were cytochalasin B, its 21,22-dihydroderivative (**31**, Fig. 1.5), prepared by $NaBH_4$ reduction of **26** (Bottalico *et al*., 1990), cytochalasins F, Z3 and deoxaphomin. They were all able to reduce the root length by about 50%. In the puncture assay, only deoxaphomin, at the used concentration, showed the ability to produce small necrotic lesions, whereas no effects were produced in the immersion assay by any of the tested cytochalasins. The existing structural correlation of cytochalasins Z1 and Z2 with cytochalasin T, and of cytochalasin Z3 with CB was also observed biologically. The first two were inactive, whereas the other two proved to be active in the root elongation assay (Evidente *et al*., 2002). These results were in accordance with those previously described in structure-activity relationship studies, which showed the important role of the hydroxy group at C-7 in conferring biological activity (Bottalico *et al*., 1990; Capasso *et al*., 1991; Vurro *et al*., 1997). These

results also showed that modification of the benzyl residue determine the lacking of activity.

Considering the potential applications and the availability of large amount of solid cultures of *Phoma exigua* var. *heteromopha* (Schulzer *et* Sacc.) Noordeloos *et* Boerema, which is a good producer of cytochalasins in solid and liquid culture (Vurro *et al*. 1997), an investigation, was carried out to look for new cytochalasins yielded by this fungus. *P. exigua* var. *heteromorpha* is the causal agent of a severe disease of Oleander (*Nerium oleander* L.) observed in 1985 in a nursery near Bari, Italy (Vurro *et al*., 1997).

Three new cytochalasans, named cytochalasins Z4, Z5, and Z6 (**22-24**, Fig. 1.4) were isolated from the wheat culture of *P. exigua* var. *heteromorpha* together with the known cytochalasin A, B, 7-*O*-acetylcytochalasin B, F, T, Z2, Z3, and deoxaphomin (**25-29**, Fig. 1.5, **20** and **21**, Fig. 1.4 and **30**, Fig. 1.5). All three new cytochalasins were characterised as 24-oxa[14]cytochalasans by extensive use of NMR and MS techniques. Cytochalasins Z4 and Z5 proved to be structurally related to cytochalasin B, whereas Z6 was related to cytochalasin F (Evidente *et al*., 2003).

Cytochalasins Z1 and Z5 represents the first two examples of a 24-oxa[14]cytochalasan bearing a *p*-hydroxybenzyl residue at C-3 of the perhydroisoindolyl-1-one moiety, and therefore, differed from the other [14] cytochalasans showing a phenyl, isopropyl or an indol-3-yl residue at C-10 and having a different functionalised macrocyclic ring (Cole and Cox, 1981; Natori and Yahara, 1991; Vurro *et al*., 1987). Furthermore, Z6 is the first 24-oxa[14]cytochalasan showing the epoxy group located between C-6 and C-7 of the perhydroisondolyl-1-one residue, the deoxygenation of C-20, and the hydroxylation of C-19, as already observed for Z3.

In tomato seedling assay, at 10^{-4} M, only Z6 proved to be slightly active causing 30% inhibition of root elongation, whereas Z4 and Z5 were inactive. When assayed at the same

concentration on brine shrimps (*A. salina* L.), only Z5 caused a quite low mortality of larvae (21%), whereas Z4 and Z6 were both inactive (Evidente *et al*., 2003).

Cytochalasins have been considered as potential mycotoxins. If high level of toxins were really produced *in vivo*, this could, in practice, make it hazardous to use these fungi as a biological control agent against grass weeds. Hence, studies are planned to quantify the presence of such toxins in naturally infected seeds, as well as to estimate their stability and impact in the environment.

1.3.2. Biological control of *Lolium perenne*

Some of the selected fungal strains were able to produce highly phytotoxic culture filtrates, particularly one strain of *Drechslera siccans*, isolated from *Lolium perenne* L., another annual and perennial grass which are one of the most important causes of loss in cereal yields. From the culture filtrates of *D. siccans*, a new phytotoxic trisubstituted naphthofuroazepinone, was isolated and named drazepinone (**32a**, Fig. 1.6). It was characterised as a 3,5,12a-trimethyl-2,5,5a,12a-tetrahydro-1*H*-naphtho[2',3':4,5]furo[2,3-*b*]azepin-2-one on the basis of its spectroscopic properties (essentially NMR and MS). The relative stereochemistry of drazepinone was based on NOESY correlations (**32b**, Fig. 1.6). Applied to wounded leaves, the toxin caused necrosis on almost all the species tested. Necrosis severity ranged from very wide, as in the case of *Urtica dioica*, to small ones as those observable applying the toxin to *Setaria viridis* and *L. perenne* leaves. The necrosis on *Euphorbia helioscopia* and *Mercurialis annua* leaves, both Euphorbiaceae, and *C. album* were also interesting. On the opposite, *Amaranthus retroflexus* and *Bromus* sp. were completely unaffected by the toxin. The symptoms caused by drazepinone and by the culture filtrates appeared to be almost the same, both in term of speed of appearance and size of necrosis, although the concentration of drazepinone in the culture filtrates is much

lower with respect to the pure solution. This could mean that, besides drazepinone, the main toxin in the culture extracts, the fungus could produce other bioactive compounds.

Drazepinone showed a weak fungistatic activity on *G. candidum* causing only a slight reduction of the fungal growth and it proved to be completely inactive when tested on *P. syringae* and *Lactobacillus plantarum* (a Gram- and a Gram+ bacterium, respectively). Assayed for zootoxic activity at 10^{-3} M, the metabolite caused the total mortality of shrimp larvae, which decreased to 81% and 12% when assayed at 10^{-4} and 10^{-5} M, respectively (Evidente *et al*., 2005).

Drechslera is a well-known genus producing phytotoxic metabolites. Most of those pathogens and their toxins have been deeply studied being agents of very severe diseases of cropped cereals (Tatum, 1971; Padmanabhan, 1973; Strobel *et al*., 1988). Some species were also isolated from grass weeds (Chandramohan and Charudattan, 2001), and their toxins proposed as potential natural herbicides (Kastanias and Tokousbalides, 2000; Kenfield *et al*., 1989a; 1989b). Toxins with structure completely different from drazepinone were previously isolated from other strains of the same fungus, such as de-*O*-methyldiaporthin (Hallock *et al*., 1998) and siccanol (Lim *et al*., 1996), an isocoumarin and a bicyclic sesterterpene, respectively. Siccanol completely inhibited the root of Italian ryegrass (*L. multiflorum* Lam.) seedlings at a level of 100 ppm (Lim *et al*., 1996). De-*O*-methyldiaporthin was almost inactive when assayed on host plants (*L. perenne* L. and *A. sativa* L.), whereas it was toxic when assayed on corn, crabgrass, and soybean, and on Barnyard grass and spiny amaranth (Hallock *et al*., 1998), with a toxicity resembling that caused by drazepinone.

The original chemical structure of drazepinone, the interesting phytotoxic activity, the low activity against fungi and bacteria, and the relatively low zootoxicity, suggest further studies for its use as an environmentally friendly and safe herbicide (Evidente and Motta, 2001).

1.3.3. Biological control of *Digitaria sanguinalis*

Drechslera gigantea Heald & Wolf is a cosmopolitan fungal pathogen found throughout North and South America, Japan, and other regions (Sivanesan, 1992). It causes a zonate eye-spot disease of grasses, banana, and coconut (Sivanesan, 1992; Farr *et al*., 1989). Under severe levels of disease, the leaf spots may coalesce, causing leaf lesions and leaf blight. Infected leaves may be killed. The extensive studies carried out over the past five years have shown that this fungus is effective for grass management under field conditions, alone and in combination with two other grass pathogens, *Exserohilum longirostratum* and *E. rostratum* (Chandramohan and Charudattan, 2001; Chandramohan *et al*. 2002). Typically, symptoms of *D. gigantea* leaf blight appear in about one week after the fungus is sprayed on the grass foliage and the disease progresses steadily over the following two to three weeks. The treated foliage is killed and the control lasts for 10 weeks or more. Rhizomes are not killed and the grasses will re-grow after a period of mycoherbicide-caused suppression.

Considering the potential of the genus in producing bioactive metabolites, and considering our interest in finding new toxins produced by weed pathogens to be tested as new natural herbicides, it seems of interest to investigate the production of novel metabolites by this proposed mycoherbicide isolated in Florida from diseased large crabgrass (*Digitaria sanguinalis*) (Photo 1), when growth in both liquid and solid cultures. This is one of the aims of the present thesis.

1.4. Biological control of *Cirsium arvense* and *Sonchus arvensis* (Asteracee)

Perennial weeds are common problem in different crops. They are especially harmful in agricultural systems with reduced herbicide usage because of their tolerance to traditional mechanical control methods. Such the typical plant species are *Cirsium arvense* (L.) Scop. (Photo 2) and *Sonchus arvensis* L. (Photo 3) (both from *Asteraceae*) commonly

called Canada thistle and perennial sowthistle, respectively (Donald, 1990; Lemna and Messersmith, 1990).

Canada thistle is a persistent perennial weed that grows vigorously, forming dense colonies and spreading by roots growing horizontally that give rise to aerial shoots. It spreads by seed, either by wind or as a contaminant in crop seed. Canada thistle is native to south Eastern Europe and the eastern Mediterranean area. It has spread to most temperate parts of the world and is considered an important weed all around the world as it infests many habitats such as cultivated fields, roadsides, pastures and rangeland, railway embankments, and lawns (Holm *et al*., 1977; 1997).

Classified as a noxious weed in many states and provinces, perennial sowthistle is a problem in several crops, where it causes economic losses due to reduced crop yields, increased cultivation and herbicide expenses, and land depreciation. At high densities (27 shoots/m^2), it has reduced spring wheat yields up to 45 percent in North Dakota. Perennial sowthistle is also a host of several economically important plant pests (Lemna and Messersmith 1990). A native of Eurasia, perennial sowthistle is distributed from Scandinavia south to Italy and east to the western portions of the former Soviet Union (Holm *et al*., 1977; 1997). Since its introduction to North America, it has spread widely throughout the northern United States and southern Canada. The plant has also established in South America, Australia, and New Zealand. Widely established in temperate regions, it is not found in the tropics (Lemna and Messersmith 1990).

Herbicides recommended for chemical control of the perennials in non-organic cropping systems are restricted to few active substances (clopyralid, dicamba, chlorsulfuron, bentazon, phenoxy-acids), and they are low selective (Lemna and Messersmith, 1990; Kloppenburg and Hall, 1990; Grekul *et al*., 2005). Obviously, new compounds should be actually developed as herbicides against the composite weeds.

The natural compounds acting as herbicides, phytotoxins or their synthetic analogues, could be used for the development of new agrochemicals against weeds (Evidente and Abouzeid, 2006; Rimando and Duke, 2006). Many plant pathogens, especially necrotrophic and hemibiotrophic fungi, produce phytotoxins responsible for disease development (Hoppe, 1998). Numerous surveys were carried out to find pathogens of *Cirsium arvense* (Berestetsky, 1997; Leth and Andreasen, 1999; Bailey *et al*., 2000). The mycobiota of *S. arvensis* was studied less extensively (Berestetski and Smolyaninova, 1998). Several pathogens, as *Stagonospora cirsii* Davis and *Ascochyta sonchi* (Sacc.) Grove (syn. *Phoma exigua* Desm. var. *exigua*) were found to be common for both host plants. *Phyllosticta cirsii* and *Phomopsis cirsii* were isolated from *Cirsium arvense* only.

The genus *Ascochyta* includes many phytopathogenic fungi that are responsible for severe diseases of many plant species (Mel'nik, 1971; 2000). They cause lesions on leaves, stems, blossoms and pods, and discoloration of the hypocotyl, cotyledons, and roots. Some of these pathogens are soil-borne and often persist in or on soil and plant debris. Some species have also been proposed as mycoherbicides for the biological control of noxious weeds, e.g.: *Ascochyta caulina* (P. Karst.) v.d. Aa and v. Kest. for the biological control of *Chenopodium album* L. (Netland *et al.*, 2001), or *Ascochyta cypericola* against *Cyperus rotundus* L. (Upadhyay *et al.*, 1991). These pathogens produce phytotoxins and their involvement in the appearance of symptoms has been proposed (Evidente *et al.*, 1993a; 1993b; 1998b; 2000; Strange, 1997).

Ascochyta sonchi (Sacc.) Grove was isolated from necrotic leaves of *Sonchus arvensis* L., and of *Cirsium arvense* L. (Scop.). Several strains of this fungus were isolated and their potential as mycoherbicides is under evaluation.

The main toxin, named ascosonchine (**33**, Fig. 1.7), was purified from the liquid culture of a strain of *A. sonchi* and chemically characterized and proposed as natural herbicide in addition or as an alternative to the use of the pathogen (Evidente *et al.*, 2004).

Ascosonchine is an enol tautomer of 4-pyridylpyruvic acid, characterised as (*Z*)-2-hydroxy-3-(4-pyridyl)-2-propenoic acid, showing interesting selective herbicidal properties, but is without antibacterial, antifungal, or zootoxic activities. The comparative assessment of virulence of many strains is difficult and time consuming. Thus attemptes were carried out to correlate the *in vitro* production of ascosonchine with its ability to cause the disease. If a positive correlation will be found, more virulent strains could be simply selected by quantifying the production of toxic metabolites *in vitro*. For this purpose, a HPLC method has been developed for the easy and rapid analysis of ascosonchine in the culture filtrates. This method has been applied to evaluate the production of ascosonchine by nine different *A. sonchi* strains isolated from different origins, as well as to optimize ascosonchine production conditions. The results obtained are reported in this thesis. In particular the method evidenced the presence of two atypical *Ascochyta* strains.

The pycnidial fungus *Stagonospora cirsii* J.J. Davis is a foliar pathogen of *C. arvense*, which biological potential for development of a mycoherbicide was demonstrated (Berestetskiy *et al*., 2005). In preliminary study it was found that fungus was capable of producing phytotoxins because its culture filtrate demonstrated phytotoxic activity to leaves and roots of the weed (Mitina *et al*., 2005). Recently, with the purpose of finding new natural potential herbicides, the main phytotoxic metabolite produced by *S. cirsii* in liquid culture, named stagonolide (**34**, Fig. 1.7), was isolated and characterized as a new phytotoxic nonenolide (Yuzikhin *et al*., 2007). **34** showed strong phytotoxicity on host and other non host and cultivated plants and a selective activity on seedling of *Cirsium arvense* and others Asteracee (Yuzikhin *et al*., 2007).

Considering the interesting results obtained on the basis of previous experiences made with phytopathogenic fungi, which in solid culture produced increased and/or different phytotoxins in respect to those isolated from liquid culture, the fungus has been

also grown on a solid medium, and the residue obtained by organic solvent extraction has been analysed with the aim of finding new phytotoxic metabolites.

Recently, the fungus *Phyllosticta cirsii* has been evaluated as a possible biocontrol agent of Canada thistle (Berestetskiy *et al*., 2005). Species belonging to the genus *Phyllosticta* are known to produce bioactive metabolites, including non-host phytotoxins, e.g.: phyllosinol, brefeldin and PM-toxin isolated by cultures of *Phyllosticta* sp., (Sakamura *et al*., 1965), *P. maydis* (Comstock *et al*., 1973) and *P. medicaginis*, (Entwistle *et al*., 1974) respectively.

Considering the interest for bioactive metabolites produced by weed pathogens as sources of novel natural herbicides, it seem of interest to investigate the production of toxins by the two atypical *Ascochyta sonchi* strains, *Stagonospora cirsii* and *Phyllosticta cirsii*. This is another main aim of the present thesis.

1.5. Biological control of parasitic weeds

Parasitic plants are among the worst weed problems, being responsible for major losses to many crops. *Orobanche* spp. (broomrapes) are holoparasitic plants which have lost their autotrophic way of life. This genus comprise together 170 species distributed predominantly in the Northern Hemisphere (Schneeweiss *et al*., 2004) and have adapted to obtain its organic and inorganic resources by parasitizing the roots of a range of plant species mainly in wild ecosystems. They are responsible for major losses to vegetable, legume, and sunflower crops by interfering with water and mineral intake and by affecting photosynthate partioning (Parker *et al*., 1993; Joel *et al*., 2007). *Orobanche* species vary in their host specificity. Most species have a rather narrow host range. For instance, species such as *O. densiflora* Salzm. ex Reut., *O. gracilis* Sm. and *O. hederae* Duby. are highly specialists parasitizing few wild species in nature. However, a few species of those genera have become weedy adapting to parasitize crops in agricultural environment. These are

usually more generalists. Species such as *O. aegyptiaca* (Pers.) (syn. *Phelipanche aegyptiaca*), *O. crenata* Forsk., *O. minor* Sm and *O. ramosa* (L.) Pomel (syn. *P. ramosa*) (Photos 4 and 5), parasitize a wide range of crops since antiquity (Sauerborn *et al*., 1991; Parker, 1994). However others are far more specific as *O. cumana* Wallr. parasitizing only sunflower (Parker *et al*., 1993; Joel *et al*., 2007) and *O. foetida* Poir that parasitizes many wild species of *Leguminosae* (Pujadas-Salvá, 2002), and only recently has been reported as weedy on faba bean (Kharrat *et al*., 1992) and vetch (Rubiales, 2005).

The *Orobanche* seeds germinate only if stimulated by the host root exudates. A radicle emerges through the seed coat which grows toward the host root and adheres to it by forming an appressorium. Subsequently the parasite penetrates the host root and connects the vascular tissue through an organ called haustorium which serves as an endophytic bridge through which the nutrient and water transfer is established from the host to the parasite. The parasite stores the resources stolen to the host in a storage organ called tubercle. Furthermore, the parasites have a long underground phase, and by the time they emerge much of the damage has already been produced.

Due to its unusual life cycle and the total dependence by the host, traditional control methods very often are impractical. The use of herbicides is not easy due to their economical or ecological unfeasibility, or lack of tolerance to the herbicides in some crops, which might overcome by the use of transgenic crops with target site herbicide resistance (Joel *et al*., 1995; Surov *et al*., 1997; Aviv *et al*., 2002).

Biological control is considered an attractive approach for broomrape control. Plant pathogens have also been proposed as source of natural herbicides (Strobel *et al*., 1991) because they produce many toxic metabolites (Evidente and Motta, 2001). A number of toxins such as fusaric and 9,10-dehydrofusaric acids have been isolated from *Fusarium* species isolated from *O. ramosa* plants. Organic extract from liquid culture caused total inhibition of seed germination (Abouzeid *et al*., 2004). Verrucarins, A, B, M and L acetate,

roridin A, isotrichoverrin B, and trichoverrol have been isolated from liquid cultures of the fungus *Myrothecium verrucaria*. Neosolaniol was isolated from *Fusarium compactum*. All these compounds belong to a different subgroup of trichothecenes and proved to be potent inhibitors of *O. ramosa* seed germination and possess strong zootoxic activity when assayed on *Artemia salina* brine shrimps (Andolfi *et al*., 2005). However at very low concentration (10^{-7}), roridin A showed very low zootoxic activity preserving a strong phytotoxic activity. These results suggest that roridin A could be proposed as a natural herbicide for the control of *O. ramosa*.

Considering that the seed germination of parasitic plants depends upon the presence of stimulating exudates produced by the roots of the host plant, an alternative approach for the management of parasitic host plants, the so called "suicidal germination", is under investigation. This latter consists in the induction of seeds germination by the application of a germination stimulant to the soil, in the absence of host. The parasite seeds germinate but, in the absence of the host will die in few days, resulting in a reduction of seed bank.

Therefore, much attention has been focused on the isolation and identification of germination stimulants (Humphrey *et al*., 2006). A number of compounds from the terpenoids group have been identified as germination stimulants, starting from strigol, which was isolated from the root exudates of cotton (Cook *et al*., 1972) and found also later in maize, millet, sorghum and clover (Siame *et al*., 1993; Sato *et al*., 2003; Yoneyama *et al*., 2004); sorgolactone, isolated from the root exudates of sorghum (Hauck *et al*., 1992); alectrol, isolated from cowpea and red clover (Müller *et al*., 1992); orobanchol, isolated from red clover (Yokota *et al*., 1998). Besides, 10 compounds have been detected as strigolactones in root exudates of pea, tomato, tobacco and other plant species (Yoneyama *et al*., 2006).

Recently some investigation were carried out on the fenugreek (*Trigonella foenum-graecum* L.) root exudates, which has been reported as having potential as trap crop of *O.*

ramosa as it induces *O. ramosa* seed germination but is little infected (Fernández-Aparicio *et al*., 2008), to ascertain its effects on the germination of *O. crenata*, *O. ramosa* and *O. foetida* seed and to determine the metabolites responsible on the interactions between different plants (Abebe *et al*., 2005). On the contrary, fenugreek roots have been suggested to inhibit *O. crenata* germination resulting in reduced infection in faba bean or pea intercropped with fenugreek (Bakheit *et al*., 2002; Evidente *et al*., 2007). The main inhibiting metabolite, named trigoxazonane, was isolated and chemically characterized as a new monosubstituted troxazonane (Evidente *et al*., 2007).

Among several fungal metabolites tested with the aim of finding new natural stimulants, Yoneama and co-authors (Yoneama *et al*., 1998) reported that cotylenins and fusicoccins induced high seed germination (>50%) of *S. hermonthica* (Del.) Benth and *O. minor* at concentrations as low as 10^{-5} M. They also reported that the answer of plants is species dependent.

Fusicoccin (FC, **35**, Fig. 1.8) is the major carbotricyclic phytotoxic diterpenoid produced by *Fusicoccum amygdali* Delacr., the causative fungal agent of peach and almond canker, isolated in 1962 (Ballio *et al*., 1964) and structurally described in 1968 (Ballio *et al*., 1968a; Barrow *et al*., 1968). Many studies were carried out on the chemical, biosynthetic and biological properties of this toxin and on structure-activity relationships (SAR) (Ballio and Graniti, 1991; Ballio *et al*., 1991; Evidente *et al*., 1984; Marrè, 1979). Ophiobolins, are sesterterpenoid phytotoxins close related to fusicoccins and cotylenins and are produced by the pathogenic fungi *Bipolaris* species, which usually infect rice, maize and sorghum. Many study were carried out on the organisms that produce the various ophiobolins, the structural variations of ophiobolins, the biological actions of ophiobolins in plants, animals and microrganisms, and the mode of actions and the possible use of ophiobolin A (**36**, Fig. 1.8) as a calmodulin antagonist (Au *et al*., 2000). The efficacy of FC in stimulating seed germination of parasitic plants was previously

reported (Ballio and Graniti, 1991; Marrè, 1979), and considering the availability of several derivatives and natural analogues of FC and its aglycone, as well as of cotylenol, due to previous works on the purification and identification of those compounds in Professor Evidente lab, a structure-activity study was carried out using the seeds of another parasitic plant species, *O. ramosa*, which proved to be useful in a preliminary screening. In both groups of glycosides and aglycones (including cotylenol), the most important structural feature to impart activity appeared to be the presence of the hydroxyl group at C-19 (Evidente *et al*., 2006). Furthermore, the dideacetyl FC, which is easy prepared by alkaline hydrolysis of FC, is a good candidate to promote a suicidal germination of *O. ramosa*.

Considering these results and that of the FC efficacy in stimulating seed germination of parasitic plant could be species dependent, we decided to carry out a study testing the effect of some FC derivatives and ophiobolin A on seed germination of different *Orobanche* species namely *O. aegyptiaca*, *O. ramosa*, *O. crenata*, *O. cumana*, *O. densiflora*, *O. foetida*, *O. gracilis*, *O. hederae*, and *O. minor*. This is the third aim of the present thesis.

2. OBJECTIVES

The first aim of the present thesis is to isolate and characterize by spectroscopic technique and chemical methods, the phytotoxic metabolites produced in liquid and solid cultures by *Dreschlera gigantea*, a potential mycoherbicide of grass weeds, isolated in Florida from naturally infected large crabgrass (*Digitaria sanguinalis*).

The second aim of the present thesis is to isolate and characterize by spectroscopic methods, the phytotoxins produced by fungi belonging to different genera as *Stagonospora cirsii* and *Phyllosticta cirsii*, proposed as mycoherbicides of *Cirsium arvense* and *Sonchus arvensis*, two noxious perennial weeds widely occurring in the temperate region of the world. Furthermore, the development of an analytical method to quantify the ascosonchine content in several *Ascochyta sonchi* strains, isolated from *C. arvense* and *S. arvensis* leaves, as well as the isolation and characterization by spectroscopic methods of phytotoxic metabolites produced in liquid and solid cultures by two atypical *A. sonchi* strains, is described.

The third aim of the present thesis is to use some natural compounds to stimulate the seed germination of the parasitic *Orobanche* spp. as an alternative and environmentally friendly approach, the so called “suicidal germination”. This work was carried out in collaboration with the agronomist groups.

Finally, the biological activity of the phytotoxins isolated as potential herbicides, carried out in collaboration with the plant pathologist groups involved, is described.

3. MATERIALS AND METHODS

3.1. Fungi

Dreschlera gigantea was isolated from Prof. R. Charudattan, during extensive field surveys in Florida, from naturally infected large crabgrass (*Digitaria sanguinalis*) (Chandramohan and Charudattan, 2001). It was stored in PDA slants both in the Biological Control of Weeds Collection at the Plant Pathology Department, University of Florida/IFAS, Gainesville, FL, USA (N. LCLF-1) and in the Collection of the Institute of Food Production Sciences, CNR, Bari, Italy (strain N. 7004).

Ascochyta sonchi strains were isolated by Dr. A. Berestetskiy, from necrotic lesions of diseased leaves of both *Cirsium arvense* and *Sonchus arvensis* collected from fields of different locations, as shown in Table 5.5.1, and identified as *A. sonchi* (Sacc.) Grove according to Mel'nik (2000). Fungal strains were maintained on agar slants (PDA) at 5 °C and deposited in the Collection of the All-Russian Institute of Plant Protection, St. Petersburg, Russia.

Two atypical *A. sonchi* strains were isolated as described above, identified as *A. sonchi* (Sacc.) Grove according to Mel'nik (2000), and then renamed to *Phoma exigua* Desm. var. *exigua* (Boerema *et al*., 2004). Fungal strains were maintained on agar slants (PDA) at 5 °C and deposited in the Collection of the All-Russian Institute of Plant Protection, St. Petersburg, Russia. For conidial production, the strains were grown on malt extract agar (Difco, Detroit, USA) or oatmeal agar (*25*) at 24 ± 2 °C, first for 4 days in the dark and then for 10 days under alternate near-UV light (14 h light/day). Under these conditions fungal colonies sporulated abundantly. The conidia were rinsed from the agar slants by adding sterile water (containing 0.01% Tween-20). Spore suspensions were then filtered through cheesecloth and the conidial concentrations were adjusted to $1x10^7$ conidia/ml. Measurements, description of fungal colonies, NaOH spot test were made using the *Phoma* manual (Boerema *et al*., 2004).

Stagonospora cirsii and *Phyllosticta cirsii*, isolated from diseased leaves of *Cirsium arvense* (L.) Scop., were supplied by Dr. A. Berestetskiy, All-Russian Institute of Plant Protection, St. Petersburg, Russia, and maintained in the Collection of the same institute. The strains were stored in sterile tubes containing potato-sucrose-agar (PDA) at 5°C and subcultured when needed.

3.2. Plant material

The weedy species assayed were collected by Dr. D. Olmedo Rubiales, Istitute for Sustainable Agriculture, CSIC, Cordoba, Spain. *O. aegyptiaca* was collected from plants parasitizing chickpea in Israel, *O. crenata* collected on faba bean in Spain, *O. cumana* collected on sunflower in Spain, *O. foetida* collected on faba bean in Tunisia, *O. minor* collected on red clover in Chile, and *O. ramosa* collected on tobacco in Spain. Additionally, some non-weedy species were included for comparisons: *O. densiflora* collected on *Lotus creticus* in Spain, *O. gracilis* collected on *Retama monogyna* in Spain and *O. hederae* collected on ivy in France.

Capsules were air dried and opened, allowing seeds extrusion. The material was then sifted through thin sieves to separate seeds from other vegetable residues, and finally clean seeds were collected and stored in plastic vials at 5 °C until their use.

3.3. General Procedures

Melting point was measured on an Axioskp Zeiss miscroscope coupled with a Metteler FP90 electric hot plate. Optical rotation was measured in $CHCl_3$ solution on a Jasco P-1010 digital polarimeter and the CD spectrum was recorded on a JASCO J-710 spectropolarimeter in MeOH solution.

IR spectra were recorded as neat on a Perkin-Elmer Spectrum One FT-IR Spectrometer and UV spectra were taken in MeCN solution on a Perkin-Elmer Lambda 25 UV/Vis spectrophotometer.

^{1}H- and ^{13}C-NMR spectra were recorded at 600, and at 150 and 75 MHz, respectively, in $CDCl_3$ on Bruker spectrometers. The same solvent was used as internal standard. Carbon multiplicities were determined by DEPT (Distortionless Enhancement by Polarization Transfer) spectra (Berger and Braun, 2004). DEPT, COSY-45 (Correlated Spectroscopy), HSQC (Heteronuclear Single Quantum Correlation), HMBC (Heteronuclear Multiple Quantum Correlation) and NOESY (Nuclear Overhauser Effect Spectroscopy) experiments (Berger and Braun, 2004), were performed using Bruker microprograms. Chemical shifts are in δ (ppm).

Coupling constants (*J*) are in Hertz. The following symbols were used: *s*=singlet; *br s*: broad singlet; *d*: doublet; *dd*: double doublet; *ddd*: doublet of double doublet; *t*: triplet; *q*: quartet; *m*: multiplet.

ESI (ElectroSpray Ionization) and HRESI MS (High Resolution ElectroSpray Ionization Mass Spectroscopy) spectra were recorded on Waters Micromass Q-TOF Micro Agilent 1100 coupled to JOEL AccuTOF (JMS-T100LC) spectrometers. EI MS spectra were taken at 70 eVon a QP 5050 Shimadzu spectrometer.

Analytical and preparative TLC were performed on silica gel (Merck, Kieselgel 60 F254, 0.25 and 0.50 mm, respectively) or reverse phase (Whatman, KC18 F254, 0.20 mm) plates; the spots were visualized by exposure to UV light and I_2 vapours or by spraying first with 10% H_2SO_4 in methanol and then with 5% phosphomolybdic acid in methanol, followed by heating at 110 °C for 10 min. Column chromatography was performed on silica gel (Merck, Kieselgel 60, 0.063-0.200 mm).

Analytical and HPLC grade solvents for chromatographic use were purchased from Carlo Erba (Milan, Italy). All other analytical grade chemicals were purchased from Merck

(Darmstadt, Germany). Water was HPLC quality, purified in a Milli-Q system (Millipore, Bedford, MA, USA). Disposable syringe filters, Anotop 10-0,2 μm, were purchased from Whatman (Springfield Mill, Maidstone, Kent, UK).

The HPLC system (Shimadzu, Tokyo, Japan) consisted of a Series LC-10AdVP pump, FCV-10AlVP valves, SPD-10AVVP spectrophotometric detector and DGU-14A degasser. The HPLC separations were performed using a Macherey-Nagel (Duren, Germany) high-density reversed-phase Nucleosil 100-5 C_{18} HD column (250x4.6 mm i.d.; 5 μm) provided with an in-line guard column from Alltech (Sedriano, Italy).

The sample of *p*-hydroxybenzaldehyde was purchased from Merck (Dramstadt, Germany).

4. EXPERIMENTAL

4.1. Production, extraction and purification of ophiobolins from *Dreschlera gigantea* culture filtrate

The fungus was grown and maintained on Petri dishes containing PDA (potato-dextrose-agar, Oxoid, England) by Dr. M. Vurro, Institute of Food Production Sciences, CNR, Bari, Italy. For the production of toxic metabolites, flasks (1 l) containing a mineral defined medium (350 ml), (Pinkerton and Strobel, 1976), were seeded with mycelium fragments obtained from colonies actively growing on PDA. The cultures were incubated under shaken conditions (100 rpm) at 25 °C in the dark for 8 days, then filtered, assayed for phytotoxic activity and lyophilized for the successive purification steps.

The lyophilized material obtained from the culture filtrates (2.7 l) was dissolved in distilled water (300 ml, final pH 4.2) and extracted with ethyl acetate (3x300 ml). The organic extracts were combined, dehydrated with Na_2SO_4, filtered and evaporated under reduced pressure. The brown oil residue (393.5 mg) proved to be highly toxic when assayed as described below on detached leaves of *Phalaris canariensis.* It was fractionated by column chromatography eluted with $CHCl_3$-*iso*-PrOH (96:4, v/v) yielding 10 groups of homogeneous fractions (1.3, 3.4, 149.0, 24.4, 2.6, 5.7, 26.0, 5.5, 9.3, 69.2 mg). The last fraction was eluted with methanol. The residue of the third fraction (149.0 mg) was crystallized three times with ethyl acetate-*n*-hexane (1:5) and gave the main metabolite (43 mg) as white crystals. The pure metabolite was identified as ophiobolin A (**36**). The residues obtained from the mother liquors of ophiobolin A crystallization (55 mg) were purified by preparative TLC [eluent EtOAC-*n*-hexane (5.5:4.5, v/v)] affording three bands. The first of them (R_f 0.55, 45 mg) was further purified by preparative TLC [$CHCl_3$-*iso*-PrOH (96:4, v/v)] yielding a further amount of ophiobolin A (24.5 mg) as a white crystalline solid, for a total of 67.5 mg (25.0 mg/l) and 6-*epi*-ophiobolin A (**37**, R_f 0.32, 4.1 mg, 1.5 mg/l). The second band of the first TLC (R_f 0.66) appeared to be a homogeneous

amorphous solid (R_f 0.62, eluent $CHCl_3$-*iso*-PrOH (96:4, v/v), 3.0 mg, 1.1 mg/l) and was identified as 3-anhydro-6-*epi*-ophiobolin A (**38**). The residue of the third band of the first TLC (R_f 0.80) gave a homogenous oil, named ophiobolin E (**40**, 1.3 mg, 0.48 mg/l). The residue of the seventh fraction (26.0 mg) of the first column, containing ophiobolin A and another metabolite, was further purified by two successive preparative TLC steps [EtOAC-*n*-hexane (5.5:4.5, v/v) and $CHCl_3$-*iso*-PrOH (94:6, v/v)], yielding a further amount of the main metabolite (**36**) (2.43 mg, for a total of 69.9 mg, 25.9 mg/l) and another amorphous solid identified as ophiobolin I (**39**) [R_f 0.20, eluent $CHCl_3$-*iso*-PrOH (94:6, v/v)0.8 mg, 0.3 mg/l].

4.1.1. Ophiobolin A (36)

Ophiobolin A, obtained as a white crystals, had: mp 182-185 °, $[\alpha]^{25}_D$ +270° (*c* 0.4), IR ν_{max} 3468 (O-H), 1740 (C=O), 1664 (C=C) cm^{-1}, UV λ_{max} nm (logε) 238 (4.1) [(Nozoe *et al*., 1965): mp 182°, $[\alpha]_D$ +270°, IR ν_{max}($CHCl_3$) 3500, 1743, 1633 cm^{-1}; UV λ_{max}(EtOH) nm (ε) 238 (13800)], [(Li *et al*., 1995): mp 170-172°, $[\alpha]_D$= +265.5° (c=1.0, $CHCl_3$), IR ν_{max} 3500, 1730, 1690, 1660, 1625 cm^{-1}], ^{1}H NMR spectrum differed from those reported (Li *et al*., 1995; Canales *et al*., 1988) for the following signals, δ: 2.04 and 1.37 (1H each, m, H_2C-13), 1.41 (1H, dd, *J*=12.0 and 3.8 Hz, H-12A); ^{13}C NMR spectrum was very similar to those already reported (Li *et al*., 1995): EI MS *m/z* (rel. int.): 401 $[M+H]^+$(11), 383 $[M+H-H_2O]^+$ (15), 319 $[M+H-C_6H_{10}]^+$ (28), 300 $[M-C_6H_{10}-H_2O]^+$ (33), 273 $[M-C_8H_{13}-H_2O]^+$ (32), 164 (100); ESI MS (+) *m/z*: 401 $[M+H]^+$, 423 $[M+Na]^+$, 439 $[M+K]^+$.

4.1.2. 6-*epi*-ophiobolin A (37)

6-*epi*-ophiobolin A, obtained as amorphous solid had: $[\alpha]^{25}_D$ +44° (*c* 0.1) [(Sugawara *et al*., 1987): $[\alpha]_D$ +46° (*c* 5.3, $CHCl_3$)]; IR ν_{max} 3445 (O-H), 1742 (C=O), 1683 (unsatureated C=O) cm^{-1}, [(Kim *et* al., 1984): IR ν_{max}^{film}: 3450, 1740, 1684, 1640

cm^{-1}]; UV λ_{max} nm (log ε) 235 (4.0); ^{1}H NMR spectrum differed from those reported (Canales *et al*., 1988; Sugawara *et al*., 1987) only for the following signals, δ: 2.18 (1H, br q, H-15), 1.80 and 1.40 (1H, each, m, H_2C-13); ^{13}C NMR spectrum differed from those reported (Kim *et* al., 1984) only for the following signals, δ: 54.8 (t, C-4), 53.4 (d, C-2), 25.8 (q, C-25); EI MS *m/z*: 401 $[M+H]^+$(1), 383 $[M+H-H_2O]^+$ (2), 319 $[M+H-C_6H_{10}]^+$ (2), 300 $[M-C_6H_{10}-H_2O]^+$ (3), 273 $[M-C_8H_{13}-H_2O]^+$ (3), 164 (40), 107 (100), [*(18)*: EI, *m/z*: 400 $(M)^+$, 382, 273, 176, 165]; ESI MS (+) *m/z*: 401 $[M+H]^+$, 423 $[M+Na]^+$, 439 $[M+K]^+$.

4.1.3. 3-anhydro-6-*epi*-ophiobolin A (38)

3-anhydro-6-*epi*-ophiobolin A, obtained as an amorphous solid had: $[\alpha]^{25}_D$ +7 (*c* 0.1); IR ν_{max} 1685 (α,β unsaturated C=O), 1645 (C=C) cm^1; UV λ_{max} nm (log ε) 225 (3.6), 235 (4.0); ^{1}H NMR spectrum differed from those reported (Canales *et al*., 1988; Sugawara *et al*., 1987) only for the following signals, δ: 2.24 (1H, dd, *J*=6.7 and 3.8 Hz, H-15), 1.99 (1H, dd, *J*=13.2, 2.5 Hz, H-13A), 1.80 (H, m, H-12A), 1.42 and 1.77 (1H each, m H_2C-1); ^{13}C NMR spectrum differed from those reported (Kim *et* al., 1984) only for the following signals, δ: 177.1 (s, C-3), 49.3 (d, C-6), 35.5 (d, C-15), 22.3 (q, C-22), 17.2 (q, C-20). EI MS *m/z*: 383 $[M+H]^+$(27), 301 $[M+H-C_6H_{10}]^+$ (45), 273 $[M-C_8H_{13}]^+$ (3), 175 (100); ESI MS (+) *m/z*: 383 $[M+H]^+$, 405 $[M+Na]^+$, 421 $[M+K]^+$.

4.1.4. Ophiobolin I (39)

Ophiobolin I, obtained as a white crystals, had: $[\alpha]^{25}_D$ +46.7 (*c* 0.2); IR ν_{max}: 3409 (O-H), 1682 (α,β unsaturated C=O), 1619 (C=C) cm^{-1} [(Li *et al*., 1995): $[\alpha]^{25}_D$ +48.6° (*c* 1.0, $CHCl_3$); IR ν_{max} 3450, 1680, 1657, 1613 cm^{-1}]; UV λ_{max} nm (log ε) 225 (4.3) ; ^{1}H NMR spectrum is very similar to those previously reported (Li *et al*., 1995; Sugawara *et al*., 1987; Sugawara *et al*., 1988); ESI MS *m/z*: 385 $[M+H]^+$, 407 $[M+Na]^+$, 423 $[M+K]^+$ [(Sugawara *et al*., 1988): EIHR MS $C_{25}H_{36}O_3$ (M+; obsd *m/z*: 384.2665 $(M)^+$, 366.2559].

4.1.5. Ophiobolin E (40)

Ophiobolin E, obtained as an amorphous solid had : $[\alpha]^{25}_{D}$ +10.4° (*c* 0.16), IR ν_{max} 3435 (O-H), 1682(α,β unsaturated C=O), 1629 (C=C) cm^{-1}; UV λ_{max} nm (log ε) 233 (3.2), 220 (3.11); ^{1}H and ^{13}C NMR spectra: see Table 5.1.1; HRESI MS (+) *m/z* 421$[M + K]^+$, 405.2412 $[M + Na]^+$ (calcd. for $C_{25}H_{34}O_3Na$, 405.2406), 383 $[M+H]^+$; ESI MS (-) *m/z*: 381$[M-H]^-$.

4.2. Production, extraction and purification of ophiobolins from *D. gigantea* solid culture

The fungus was also grown on a solid medium by Dr. M. Vurro, Institute of Food Production Sciences, CNR, Bari, Italy. Steamed and autoclaved wheat kernels placed in 1 l flasks were seeded using a spore suspension of the fungus, and kept at 25 °C for 4 weeks. After incubation and fungal growth, the kernels were dried and finely minced; 1 kg of dried material was extracted with CH_2Cl_2. The organic extracts were combined and evaporated under reduced pressure, affording a brown oily residue. The latter was de-fatted by *n*-hexane extraction and then extracted with CH_2Cl_2. The CH_2Cl_2 extracts were combined, dehydrated by Na_2SO_4 and evaporated under reduced pressure yielding a brown oil (781.3 mg) showing a strong phytotoxic activity when assayed as described below.

This latter was fractionated by column chromatography eluted with $CHCl_3$-*iso*-PrOH (24:1), yielding 10 groups of homogeneous fractions, weighting 2.4, 4.8, 46.0, 5.5, 128.5, 9.7, 27.9, 49.3, 30.0, and 474.2 mg, respectively. The purification of the residue of the third group (46.0 mg) by two successive preparative TLC steps on silica gel ($CHCl_3$-*iso*-PrOH (24:1); EtOAC-*n*-hexane (1.2:1), respectively) gave a very small amount of ophiobolin A (**36**, 1 mg/kg) as an amorphous solid. The residue of the seventh fraction (27.9 mg) was purified by preparative TLC (silica gel, $CHCl_3$-*iso*-PrOH (2.3:1) producing

four bands. The first of them (14.2 mg) was further purified using two successive steps by preparative TLC on reversed-phase [EtOH-H_20 (1.5:1), R_f 0.23] and by silica gel [petrol-Me_2CO (2.3:1)], respectively, yielding a white amorphous solid (R_f 0.30, 1.4 mg/kg) named 8-*epi*-ophiobolin J (**43**). The residue of the eighth fraction (49.3 mg) was purified by preparative TLC on silica gel, [$CHCl_3$-*iso*-PrOH (24:1)] producing six bands. The most polar of them (12.6 mg) was further purified by preparative TLC [silica gel, petrol-Me_2CO (2.3:1)], yielding ophiobolin B (**41**) as a white amorphous solid (R_f 0.49, 1.2 mg/kg). The residue of the ninth fraction (30 mg) was purified by preparative TLC [$CHCl_3$-*iso*-PrOH (24:1)] producing six bands. The first of them (8.9 mg/kg) appeared to be a homogeneous amorphous solid [R_f 0.23 and R_f 0.49, silica gel $CHCl_3$-*iso*-PrOH (24:1) and petrol-Me_2CO (2.3:1)] and was identified as ophiobolin J (**42**).

4.2.1 Ophiobolin B (41)

Ophiobolin B, obtained as an amorphous solid, had: $[\alpha]^{25}_D$ +230° (*c* 0.1), IR ν_{max} 3418 (O-H), 1736 (C=O), 1685 (α,β unsaturated C=O), 1636 (C=C) cm^{-1}, UV λ_{max} nm (log ε) 234 (3.51) [(Li *et al*., 1995): $[\alpha]_D$ +236.4° (*c* 0.1, $CHCl_3$), IR (KBr) ν_{max} 3460, 1720, 1659, 1620 cm^{-1}]; ^1H and ^{13}C NMR spectra were very similar to that already reported (Li *et al*., 1995); ESI MS (+) *m/z*: 441 $[M+K]^+$, 425 $[M+Na]^+$, 403$[M+H]^+$.

4.2.2. Ophiobolin J (42)

Ophiobolin J, obtained as an amorphous solid, had: $[\alpha]^{25}_D$ +46 (*c* 0.14), IR ν_{max} 3408 (O- H), 1688 (α,β unsaturated C=O), 1626 (C=C) cm^{-1}, UV λ_{max} nm (log ε) 260 (3.81) [(Sugawara *et al*., 1988): $[\alpha]_D$ +48° (*c* 1.7, $CHCl_3$)]; IR ν_{max} 3395, 1678, 1614, cm^1; UV λ_{max} nm (log ε)262 (3.96); The ^1H NMR spectrum was integrated in respect to those already reported (Sugawara *et al*., 1988) for the following signals, δ: 2.25 (1H, m H-15), 2.16 and 1.85 (2H, both m, H-9), 1.94 (1H, m. H-10), 1.91 and 1.08 (2H, both m, H-1), 1.77 and 1.54 (2H, both m, H-16), 1.73 (2H, m, H-12), 1.54 and 1.40 (2H, both m, H-13);

The ^{13}C NMR spectrum was very similar to that already reported (Sugawara *et al*., 1988*)*. EI MS *m/z*: 401 $[M+H]^+$(1), 383 $[M+H-H_2O]^+$(9), 365 $[M+H-2xH_2O]^+$(7) 175 (100); ESI MS (+) *m/z*: 439 $[M+K]^+$, 423$[M+Na]^+$.

4.2.3. 8-*epi*-ophiobolin J (43)

8-*epi*-ophiobolin J obtained as an amorphous solid had: $[\alpha]^{25}_D$ +31.1 (*c* 0.1); IR ν_{max}: 3388 (O-H), 1673 (α,β unsaturated C=O), 1614 (C=C)cm^{-1}; UV λ_{max} nm (log ε) 262 (3.64); ^1H and ^{13}C NMR spectra: see Table 5.1.1; HRESI MS (+) *m/z* 439$[M + K]^+$, 423.2515 $[M +Na]^+$ (calcd. for $C_{25}H_{34}O_3Na$, 423.2511), 401 $[M+H]^+$, 383 $[M+H-H_2O]^+$; ESI MS (-) *m/z*: 399 $[M-H]^-$.

4.3. Production of *Ascochyta sonchi* culture filtrates

A conidial suspension for each of the 9 strains (approximately 10^6 conidia ml^{-1}) was prepared and added to 1 l Roux bottles containing 200 ml of M-1 D medium (Pinkerton and Strobel, 1976). The cultures were incubated under static conditions at 25 °C in the dark for 4 weeks, then filtered, lyophilized and stored until determination of the ascosonchine content. Each strain was cultured in triplicate. Strain 240 was also used for a time course experiment of ascosonchine production. M-1 D medium in Roux bottles was prepared, inoculated and incubated as described above, and the culture filtrates were harvested weekly for 8 weeks. Additionally, parallel inoculated medium was cultured on a shaker (100 rpm) at 25 °C in the dark. The culture filtrates were harvested at three-day-intervals for 12 days. Culture filtrates were lyophilized and stored until determination of the ascosonchine content. The growth of fungi was carried out by Dr. M. Vurro, Institute of Food Production Sciences, CNR, Bary, Italy.

4.4. HPLC analysis of *A. sonchi* culture extracts

Aliquots of the samples (20 µl) extracted from the lyophilised *A. sonchi* culture filtrate, were injected for analysis, having the mobile phase of 1:1, v/v methanol and HPLC grade water at a flow rate of 1 ml/min. Detection was performed at 230 nm, corresponding to the maximum ascosonchine absorption. The ascosonchine standard sample was purified and identified from *A. sonchi* culture filtrates as described previously (Evidente *et al.*, 2004). The HPLC calibration curve for quantitative ascosonchine determination was performed with absolute amounts of the toxin standard dissolved in methanol in the range between 7 and 700 µg/ml, in triplicate for each concentration. A HPLC linear regression curve (absolute amount against chromatographic peak area) for ascosonchine was obtained based on weighted values calculated from nine concentrations of the standard in the above range.

The samples were prepared as follows: lyophilised fungal culture filtrates, equivalent to 100 ml liquid culture, were extracted by $CHCl_3$-*iso*-propanol (9:1 v/v) (3x20 ml). The organic phases were combined, filtered through paper and evaporated under reduced pressure. The samples were dissolved in methanol, and aliquots (20 µl) were injected into the HPLC instrument. Each sample was assayed in triplicate. The quantitative determination of the metabolite was calculated interpolating the mean area of their chromatographic peaks with the data of the calibration curves.

4.4.1. Recovery studies

Recovery studies were performed using the lowest ascosonchine producing strain (S-10). Pure ascosonchine was added to the culture filtrate from 0.3 to 2.0 mg/l. The samples were prepared as described above and the extracts analysed by HPLC to determine recovery. Three replicate injections were performed for each concentration. The recovery throughout the range was more than 96 ±2.8%.

4.5. Production, extraction and purification of phytotoxins in *Phoma exigua* var. *exigua* strains C-177 and S-9 solid and liquid cultures

A conidial suspension of the strain C-177 (approximately 10^6 conidia/ml) was prepared and added to 2 l Roux bottles containing 300 ml of M-1 D medium (Pinkerton and Strobel, 1976). The culture (1 l) were incubated under static conditions at 25 °C in the dark for 4 weeks, then filtered and extracted with EtOAc (3x500 ml). The organic extract were combined, dried (Na_2SO_4), filtered and evaporated under reduced pressure to give an oily residue (101.0 mg). For the production of solid culture, the fungi (C-177 and S-9) were grown on autoclaved millet in ten 1000-ml Erlenmeyer flasks (millet 100 g, water 60 ml) for 14 days in the darkness. Fungal metabolites were extracted from dry mycelium accordingly to a protocol described in the paragraph 4.2, which was slightly modified. The dried material (800 g) was extracted with the mixture acetone-water (1:1, 2 l). After evaporation of acetone, NaCl (300 g/l) was added to the aqueous residue, and the latter was extracted with EtOAc (3x500 ml). The organic extracts were combined, dried (Na_2SO_4) and evaporated under reduced pressure yielding brown oily residue 1.43 g and 305 mg for C-177 and S-9 culture, respectively. The growth of fungi as well as the extraction of fungal metabolites was carried out by Dr. A. Berestetskiy, All-Russian Institute of Plant Protection, St. Petersburg, Russia.

The organic extract (1.43 g) obtained from *P. exigua* var. *exigua* strain C-177 solid culture was fractionated by column chromatography eluted with $CHCl_3$-*i*-PrOH (92:8, v/v), yielding ten groups of homogeneous fractions. The residue of the second fraction (103.6 mg) was further fractionated by column chromatography eluted with EtOAc-*n*-hexane (6:4, v/v), yielding seven groups of homogeneous fractions. The residues of the third (329.8 mg) and fourth (244.0 mg) fraction groups of the initial column were crystallized separately twice from EtOAc-*n*-hexane (1:5, v/v) giving white needles of cytochalasin B (**25**, 220 and

200 mg respectively, 525 mg/kg). The mother liquors (77.5 and 22.7 mg, respectively) of cytochalasin B crystallisation were combined and fractionated by column chromatography eluted with EtOAc-*n*-hexane (6:4, v/v), yielding eight groups of homogeneous fractions. The residue of the second fraction (5.2 mg) showed to be a homogeneous amorphous solid identified as *p*-hydroxybenzaldehyde [**44**, EtOAc-*n*-hexane (6:4, v/v), R_f 0.62, 6.5 mg/kg]. The residue of the fifth fraction (32.5 mg) of the last column chromatography was fractionated by preparative TLC [eluent petroleum ether: acetone (65:35, v/v)] yielding three groups of fractions. The less polar of these fractions (4.6 mg) was further purified by preparative TLC [eluent EtOAc-*n*-hexane (6:4, v/v)] affording cytochalasin F as a homogeneous amorphous solid (**28**, R_f 0.43, 1.4 mg, 1.8 mg/kg). The sixth fraction (8.6 mg) of the last column chromatography was purified by preparative TLC [eluent petroleum ether: acetone (65:35)] yielding deoxaphomin as a homogeneous amorphous solid (**30**, R_f 0.31, 4.0 mg, 5.0 mg/kg).

The organic extract (100 mg) obtained from *P. exigua* var. *exigua* strain C-177 liquid culture (1 l of M1-D) was fractionated by column chromatography eluted with $CHCl_3$-*i*-PrOH (92:8, v/v), yielding nine groups of homogeneous fractions. The residue of the second fraction (13.6 mg) was further purified by preparative TLC [eluent EtOAc-*n*-hexane (6:4, v/v)] affording *p*-hydroxybenzaldehyde (R_f 0.62, 1.0 mg) and cytochalasin B (R_f 0.25, 2.2 mg) both as homogeneous amorphous solids.

The organic extracts (305 mg) obtained from *P. exigua* var. *exigua* strain S-9 solid culture was fractionated by column chromatography eluted with $CHCl_3$-*i*-PrOH (92:8, v/v), yielding seven groups of homogeneous fractions. The residue of first fraction (14.4 mg) was purified by preparative TLC [eluent EtOAc-*n*-hexane (6:4, v/v)] yielding cytochalasin B (R_f 0.32, 4.2 mg). The residues of the second (51.6 mg) and third (83.1 mg) fraction groups of the first column chromatography were crystallized separately twice from EtOAc-

n-hexane (1:5 v/v) giving white needles of cytochalasin B (32.3 and 61.1 mg respectively, 122 mg/kg). The mother liquors (18.1 mg) of cytochalasin B crystallisation of the third fraction were purified by preparative TLC [eluent EtOAc-*n*-hexane (6:4, v/v)] affording deoxaphomin (**30**, R_f 0.26, 2.5 mg, 3.1 mg/kg) as a homogeneous amorphous solid. The residue of fourth fraction (11.0 mg) of the first column chromatography was purified by preparative TLC [eluent EtOAc-*n*-hexane (6:4, v/v)] yielding cytochalasin Z2 (**20**, R_f 0.20, 1.6 mg, 2 mg/kg) as a homogeneous amorphous solid. The fifth fraction (10.2 mg) of the first column was purified by preparative TLC with the same solvent yielding cytochalasin Z3 (**21**, R_f 0.11, 1.7 mg, 2.1 mg kg^{-1}) as a homogeneous amorphous solid.

4.6. Production, extraction and purification of nonenolides from *Stagonospora cirsii* solid culture

The fungus was grown on autoclaved millet in 1000-ml Erlenmeyer flasks (millet 100 g, water 60 ml) for 14 days in the darkness, by Dr. A. Berestetskiy, All-Russian Institute of Plant Protection, St. Petersburg, Russia. Fungal metabolites were extracted from dry mycelium accordingly to the protocol reported in the paragraph 4.2.

The organic extract (1 g) obtained from the culture (1 kg) was purified by silica gel column eluted with $CHCl_3$-*i*-PrOH (9:1), obtaining 13 groups of homogeneous fractions. The residues of the second and third fractions were combined (353 mg) and further purified by a column chromatography eluted with EtOAc-*n*-hexane (65:35), yielding 13 groups of homogeneous fractions. The residues (65 mg) of the fourth fraction was purified by preparative TLC on silica gel, eluting with EtOAC-*n*-hexane (7:3), gave four bands, the fourth of them yield a crystalline solid (**51**, R_f 0.27; 18.6 mg) named stagonolide H. The second of them (R_f 0.33, 10.7 mg) was further purified by preparative TLC on reversed-phase, using as eluent MeOH-H_20 (1.5:1), to yield a homogeneous oily compound (R_f 0.31,

1.6 mg), named stagonolide F (**49**), and another band (8.3 mg), which was further purified in the same conditions yielding another homogeneous oily compound (R_f 0.43, 2.9 mg), named stagonolide E (**48**). The residue (49 mg) of the seventh fraction of the same column was further purified by preparative TLC on silica gel, using as eluent $CHCl_3$-*i*-PrOH (93:7) to give four bands. The metabolite associated to the main of them (R_f 0.39, 18.0 mg/kg) was obtained as crystalline solid and named stagonolide D (**47**). The residue (69.8 mg) of the tenth fraction from the initial column was purified by preparative TLC on silica gel, using $CHCl_3$-*i*-PrOH (88:12), to yield six bands. The fifth band (R_f 0.27; 27.0 mg) was further purified by preparative TLC on silica gel, eluted with EtOAc-MeOH (96:4), yielding two homogeneous oily compounds: one was named stagonolide G (**50**, R_f 0.45; 1.5 mg) and the other was indentified as modiolide A (**53**, R_f 0.52; 12 mg). The residue (30.4 mg) of the eleventh fraction of the initial column was purified by preparative TLC on silica gel, using $CHCl_3$-*i*-PrOH (88:12) as eluent, to yield five bands. The fourth band (R_f 0.28; 10.6 mg) was further purified by preparative TLC on silica gel, eluted with EtOAc-MeOH (96:4), yielding a homogeneous oily compound (R_f 0.48; 2.0 mg), named stagonolide I (**52**).

The residue (39.3 mg) of the twelfth fraction of the initial column was purified by preparative TLC on silica gel, using as eluent $CHCl_3$-*i*-PrOH (88:12) to yield six bands. The fifth band (R_f 0.19, 15.2 mg) was further purified by preparative TLC on silica gel, eluted with EtOAC-MeOH (5:5), yielding two homogeneous oily compounds named stagonolides B and C (**45** and **46**, R_f 0.85 and 0.84, 2.0 and 8.0 mg, respectively).

4.6.1. Stagonolide B (45)

Stagonolide B, obtained as a colourless oil had: $[\alpha]^{25}D$: +20 (*c* 0.1); UV λ_{max} nm < 200; IR ν_{max} 3388 (OH), 1710 (C=O), 1595 (C=C), 1232 (O-CO) cm^{-1}; ^1H and ^{13}C NMR

spectra: see Tables 5.8.1 and 5.8.2; HRESI MS (+) *m/z*: 267.2821 $[M+Na]^+$ (calcd for $C_{12}H_{20}NaO_5$, 267.1208).

4.6.2. Stagonolide C (46)

Stagonolide C, obtained as a colourless oil had: $[\alpha]^{25}D$: +48 (*c* 0.2); UV λ_{max} nm < 200; IR ν_{max} 3358 (OH), 1723 (C=O), 1239 (O-CO) cm^{-1}; ^1H and ^{13}C NMR spectra: see Tables 5.8.1 and 5.8.2; HRESI MS (+) *m/z*: 223.2168 $[M+Na]^+$ (calcd for $C_{10}H_{16}NaO_4$, 223.0935), 239 $[M+ K]^+$.

4.6.3. Stagonolide D (47)

Stagonolide D, obtained as a white crystalline solid, had: $[\alpha]^{25}D$: -82 (*c* 0.2); UV λ_{max} nm < 200; IR ν_{max} 3434 (OH), 1732 (C=O), 1643 (C=C), 1221 (O-CO) cm^{-1}; ^1H and ^{13}C NMR spectra: see Tables 5.8.1 and 5.8.2; HRESI MS (+) *m/z*: 221.0781 $[M+Na]^+$ (calcd for $C_{10}H_{14}NaO_4$, 221.0790).

4.6.4. Stagonolide E (48)

Stagonolide E, obtained as a colourless oil had: $[\alpha]^{25}D$: -186 (*c* 0.2); UV λ_{max} nm (log ε): 250 (3.37); IR ν_{max} 3399 (OH), 1718 (C=O), 1651 (C=C), 1605 (C=C), 1254 (O-CO) cm^{-1}; ^1H and ^{13}C NMR spectra: see Tables 5.8.1 and 5.8.2; HRESI MS (+) *m/z*: 205.0852 $[M+Na]^+$ (calcd for $C_{10}H_{14}NaO_3$, 205.0841).

4.6.5. Stagonolide F (49)

Stagonolide F, obtained as a colourless oil had: $[\alpha]^{25}D$: -27 (*c* 0.1); CD $[\Theta]^{25}$ nm: 209.6 (+135165), 254 (+19474) [(Fucsher and Zeeck, 1997), for aspinolide: $[\alpha]^{23}D$= -43.8 (*c*= 0.3 MeOH); CD (MeOH): λ_{extr} $[\Theta]^{23}$ (MeOH)= 209.8 nm (-6800), 283 (+740)]; UV λ_{max} nm < 200; IR ν_{max} 3375, 1729, 1663, 1237 cm^{-1}; ^1H and ^{13}C NMR spectra: see Tables 5.8.1 and 5.8.2; HRESI MS (+) *m/z*: 207.1943 $[M+Na]^+$ (calcd for $C_{10}H_{16}NaO_3$, 207.0997).

4.6.6. Stagonolide G (50)

Stagonolide G, obtained as a colourless oil, had: $[\alpha]^{25}_{D}$ +96 (*c* 0.1); UV λ_{max} < 200 nm; IR ν_{max} 3388 (OH), 1765 (C=O), 1727 (C=C) cm^{-1}; ^{1}H and ^{13}C NMR spectra, see Tables 5.8.5 and 5.8.6; HRESI MS (+) *m/z* 223.2355 $[M+Na]^{+}$ (calcd for $C_{10}H_{16}NaO_4$, 223.2264).

4.6.7. Stagonolide H (51)

Stagonolide H, obtained as a white crystalline solid, had: $[\alpha]^{25}_{D}$ +12 (*c* 0.2); UV λ_{max} < 200 nm; IR ν_{max} 3426 (OH), 1723 (C=O), 1635 (C=C), 1239 (O-CO) cm^{-1}; ^{1}H and ^{13}C NMR spectra, see Tables 5.8.5 and 5.8.6; HRESI MS (+) *m/z* 219.2056 $[M+Na]^{+}$ (calcd for $C_{10}H_{12}NaO_4$, 219.1945)

4.6.8. Stagonolide I (52)

Stagonolide I, obtained as a colourless oil, had: $[\alpha]^{25}_{D}$ +50 (*c* 0.2); UV λ_{max} < 200 nm; IR ν_{max} 3278 (OH), 1713 (C=O), 1640 (C=C), 1217 (O-CO) cm^{-1}; ^{1}H and ^{13}C NMR spectra, see Tables 5.8.5 and 5.8.6; HRESI MS (+) *m/z* 221.2117 $[M+Na]^{+}$ (calcd for $C_{10}H_{14}NaO_4$, 221.2105).

4.6.9. Modiolide A (53)

Modiolide A, obtained as a colourless oil, had: $[\alpha]^{25}_{D}$ +38 (*c* 0.2, MeOH); UV MeOH λ_{max} 204 nm (ε 6400); IR ν_{max} 3436 (OH), 1713, 1280 cm^{-1} [(Tsuda *et al*., 2003): $[\alpha]^{25}_{D}$ +42 (*c* 0.25, MeOH); UV (MeOH) λ_{max} (log) 204 nm (ε 6400)]; ^{1}H and ^{13}C NMR spectra, see Tables 5.8.5 and 5.8.6; HRESI MS (+) *m/z* 205.0852 $[M+Na]^{+}$ (calcd for $C_{10}H_{14}NaO_3$, 205.0841; [(Tsuda *et al*., 2003): EI MS *m/z* 180 $(M-H_2O)^{+}$ and 198 $(M)^{+}$; HREI MS *m/z* 198.0892 (M^{+}, calcd. for $C_{10}H_{14}O_4$, 198.0891)].

4.7. Production, extraction and purification of phyllostictines, phyllostoxin and phyllostin from *Phyllosticta cirsii* culture filtrates.

For the production of phytotoxic metabolites, Roux bottles (1 l) containing a mineral-defined medium (200 ml) (Pinkerton and Strobel, 1976), were seeded with mycelial fragments obtained from colonies actively growing on PDA plates. The cultures were incubated under static conditions at 25 °C in the dark for four weeks, then filtered on filter paper (Whatman n. 4), assayed for phytotoxic activity and lyophilised by Dr. M. Vurro, Institute of Food Production Sciences, CNR, Bari, Italy.

The lyophilised material obtained from the culture filtrates (7.7 l) was dissolved in distilled water (700 ml, final pH 4.4) and extracted with EtOAc (3x700 ml). The organic extracts were combined, dehydrated with Na_2SO_4, filtered and evaporated under reduced pressure. The brown oily residue (1.26 g) proved to be highly phytotoxic when assayed as below described on detached thistle leaves. It was purified by silica gel column eluted with $CHCl_3$-*i*-PrOH (9:1), and 9 groups of homogeneous fractions were obtained. All the fractions were tested for their phytotoxic activity. The residue (74.0 mg) of the second fraction, which proved to be highly phytotoxic, was further purified by a column chromatography eluted with $CHCl_3$-*i*-PrOH (96:4), yielding 10 groups of homogeneous fractions. The residue of the toxic fifth fraction (359 mg) was purified by a preparative TLC on silica gel eluted with EtOEt-EtOAc (9:1) yielding a fraction (R_f 0.38), which proved to be a mixture of at least two metabolites. It was further purified by preparative TLC on reverse phase eluted with EtOH-H_20 (6:4) yielding the main toxin and another metabolite named phyllostictines A and B (**54** and **55**), both as homogeneous oily compounds [R_f 0.36 and R_f 0.58, EtOH-H_20 (6:4), 85 and 7.7 mg, 11.0 and 1.0 mg/l, respectively]. The residues of the sixth (3.6 mg) and seventh (23.2 mg) fractions were combined and purified by preparative TLC on silica gel eluted with $CHCl_3$-*iso*-PrOH (9:1)

yielding a homogeneous solid amorphous compound, which was named phyllostoxin [**62**, R_f 0.7, $CHCl_3$-*iso*-PrOH (9:1), 6.0 mg, 0.78 mg/l]. The residue of third fraction of the first column (64.0 mg), was purified by a preparative TLC on silica gel eluted with $CHCl_3$-*iso*-PrOH (7:3) yielding a crystalline solid compound, which was named phyllostin [**63**, R_f 0.60, $CHCl_3$-*iso*-PrOH (7:3), 7.0 mg, 0.90 mg/l]. The residue of the sixth fraction of the first column (74.7 mg), was further purified by preparative TLC on silica gel eluted with EtOEt-EtOAc (9:1) yielding a homogeneous oily compound [R_f 0.13, EtOEt-AcOEt (9:1), 3.6 mg, 0.5 mg/l] named phyllostictine D (**57**). Finally, the residue of the eight fraction of the first column (25.9 mg) was further purified by a preparative TLC on silica gel eluted with $CHCl_3$-*i*-PrOH (9:1) yielding a homogeneous oily compound [R_f 0.32, $CHCl_3$-*i*-PrOH (9:1), 6.6 mg, 0.9 mg/l] named phyllostictine C (**56**).

4.7.1. Phyllostictine A (54)

Phyllostictine A, obtained as a colourless oil, had: $[\alpha]^{25}D$: -87.5 (*c* 0.2); IR ν_{max} 3394 (OH), 1704 (C=O), 1632 (C=C), 1440 (N-CO) cm^{-1}; UV λ_{max} nm (log ε) 263 (4.07); ^1H and ^{13}C NMR spectra: see Tables 5.11.1 and 5.11.2; HRESI MS (+) *m/z*: 673.3680 [$C_{34}H_{54}N_2NaO_{10}$, calcd. 673.3677, 2M+Na]$^+$, 348.1800 [$C_{17}H_{27}NNaO_5$, calcd. 348.1787, M+Na]$^+$, 326.1962 [$C_{17}H_{28}NO_5$, calcd. 326.1967, M+H]$^+$; HRESI MS (-) *m/z*: 324.1815 [$C_{17}H_{26}NO_5$, calcd. 324.1811, M-H]$^-$, 649.3678 [$C_{34}H_{53}N_2O_{10}$, calcd. 649.3700, 2M-H]$^-$; EI MS *m/z* (rel. int.) 294 [M-MeO]$^+$ (22), 276 [M-MeO-H_2O]$^+$ (5), 251 [M-MeO-CO-Me]$^+$ (2), 71 [Et-N=C=O]$^+$ (100).

4.7.2. Phyllostictine B (55)

Phyllostictine B, obtained as a colourless oil, had: $[\alpha]^{25}D$: -99.8 (*c* 0.07); IR ν_{max} 3407 (OH), 1705 (C=O), 1633 (C=C), 1444 (O-CO) cm^{-1}; UV λ_{max} nm (log ε) 262 (4.13); ^1H and ^{13}C NMR spectra: see Tables 5.11.1 and 5.11.2; HRESI MS (+) *m/z*: 914.4429 [3M+Na]$^+$; 617.2984 [$C_{30}H_{46}N_2NaO_{10}$, calcd. 617.3050, 2M+Na]$^+$, 320.1443

$[C_{15}H_{23}NNaO_5$, calcd. 320.1474, M+Na$]^+$, 298.1628 $[C_{15}H_{24}NO_5$, calcd. 298.1655, M+H$]^+$; HRESI MS (-) *m/z*: 296.1500 $[C_{15}H_{22}NO_5$, calcd. 296.1498, M-H$]^-$; EI MS *m/z* (rel. int.) 298 $[MH]^+$ (8), 280 $[MH\text{-}H_2O]^+$ (4), 266 $[M\text{-}MeO]^+$ (32), 248 $[M\text{-}MeO\text{-}H_2O]^+$ (13), 223 $[M\text{-}MeO\text{-}CO\text{-}Me]^+$ (5), 71 $[Et\text{-}N{=}C{=}O]^+$ (100).

4.7.3. Phyllostictine C (56)

Phyllostictine C, obtained as a colourless oil, had: $[\alpha]^{25}D$: -45.5 (0.1); IR ν_{max} 3395 (OH), 1704 (C=O), 1634 (C=C), 1452 (N-CO) cm^{-1}; UV λ_{max} nm 262 (3.60); ^1H and ^{13}C NMR spectra: see Tables 5.11.1 and 5.11.2; HRESI MS (+) *m/z*: 1046.7240 $[3M+Na]^+$; 705.4676 $[2M+Na]^+$, 364.2303 $[C_{17}H_{27}NNaO_6$, calcd. 364.1736, M+Na$]^+$.

4.7.4. Phyllostictine D (57)

Phyllostictine D, obtained as a colourless oil, had: $[\alpha]^{25}D$: -70.2 (0.2); IR ν_{max} 3409 (OH), 1707 (C=O), 1634 (C=C), 1444 (N-CO) cm^{-1}; UV λ_{max} nm (log ε): 262 (3.25); ^1H and ^{13}C NMR spectra: see Tables 5.11.1 and 5.11.2; HRESI MS (+) *m/z*: 1040.6378 $[3M+Na]^+$; 701.3964 $[2M+Na]^+$, 362.2050 $[C_{17}H_{25}NNaO_6$, calcd. 362.1580, M+Na$]^+$.

4.7.5. Acetylation of phyllostictine A

Phyllostictine A (**54**, 3.7 mg) was acetylated with pyridine (20 μl) and Ac_2O (40 μl) at room temperature overnight. The reaction was stopped by addition of MeOH and the azeotrope formed by addition of C_6H_6 was evaporated by a N_2 stream. The oily residue was purified by preparative TLC [silica gel, $CHCl_3$-*i*-PrOH (96:4)] to give the 15-*O*-acetyl and the 11,15-*O*,*O*'-diacetyl derivatives of phyllostictine A (**58** and **59**) both as homogeneous compounds (R_f 0.48 and 0.77, 2.4 and 0.5 mg). Derivative **58** had: $[\alpha]^{25}D$: -55.6 (0.1); IR ν_{max} 3423 (OH), 1725 (C=O), 1708 (C=O), 1635 (C=C), 1440 (N-CO), 1370 (O-CO), 1225 (O-CO) cm^{-1}; UV λ_{max} nm (log ε): 256 (3.58); ^1H and ^{13}C NMR spectra differed from those of **54** for the following signals, δH: 5.59 (1H, s, H-15), 2.19 (3H, s, MeCO); δC: 172.4 (s, Me<u>C</u>O), 71.1 (d, C-15), 20.9 (q, <u>Me</u>CO) ; ESI MS (+) *m/z*: 757 $[2M+Na]^+$, 390 $[M+Na]^+$.

Derivative **59** had: $[\alpha]^{25}D$: +125 (0.04); IR ν_{max} 1739 (C=O), 1732 (C=O), 1639 (C=C), 1442 (N-CO), 1368 (O-CO), 1218 (O-CO) cm^{-1}; UV λ_{max} nm (log ε): 262 (3.34); ^{1}H and ^{13}C NMR spectra differed from those of **54** for the following signals, δH: 5.59 (1H, s, H-15), 5.20 (1H, d, *J* = 11 Hz, H-11) 2.13 and 1.99 (3H each, s, 2xMeCO); δC: 170.1 and 169.9 (s, 2x MeCO), 81.6 (d, C-11), 68.1 (d, C-15), 22.1 and 20.8 (q, 2xMeCO); ESI MS (+) *m/z*: 841 $[2M+Na]^+$, 432 $[M+Na]^+$.

4.7.6. (S)-α-Methoxy-α-trifluorophenylacetate (MTPA) ester of phyllostictine A (60).

(*R*)-(-)-MPTA-Cl (30 μl) was added to phyllostictine A (**54**, 1.0 mg), dissolved in dry pyridine (50 μl). The mixture was kept at room temperature. After 1 h, the reaction was complete, and MeOH was added. The pyridine was removed by a N_2 stream. The residue was purified by preparative TLC on silica gel [$CHCl_3$-*i*-PrOH (96:4)] yielding **60** as an oil (R_f 0.36, 0.5 mg): $[\alpha]^{25}_D$ - 15.5 (*c* 0.01); UV λ_{max} log (ε) 263 (3.78) nm; IR ν_{max} 3410, 1746, 1718, 1628, 1446, 1272, 1241 cm^{-1}; ^{1}H spectrum differed from that of **54** for the following signals, δ 7.61-7.42 (5H, m, Ph), 5.85 (1H, s, H-15), 4.17 (1H, d, *J*=10.3 Hz, H-11), 3.51 (3H,s, MeO), 1.78 (2H, m, H_2-10), 1.56 and 1.38 (1H each, m, 5.04 H_2-11); ESI MS (+) *m/z* 564 $[M+Na]^+$, 308 $[M+H\text{-}PhC(OMe)CF_3COO]^+$.

4.7.7. *(*R*)*-α-Methoxy-α-trifluorophenylacetate (MTPA) ester of phyllostictine A (61).

(*S*)-(+)-MPTA-Cl (30 μl) was added to phyllostictine A (**54**, 1.0 mg), and dissolved in dry pyridine (50 μl). The reaction was carried out under the same conditions used for preparing **60** from **54**. Purification of the crude residue by preparative TLC on silica gel [R_f 0.36, $CHCl_3$-*i*-PrOH (96:4)] yielded **61** as an oil (0.7 mg): $[\alpha]^{25}_D$ –69.0 (*c* 0.1); UV, IR and EI MS were very similar to those of **61**; ^{1}H spectrum differed from that of **54** for the following signals, δ 7.62-7.42 (5H, m, Ph), 5.79 (1H, s, H-15), 4.10 (1H, d, *J*=10.2 Hz, H-11), 3.62 (3H,s, MeO), 1.61 (2H, m, H_2-10), 1.32 and 1.25 (1H each, m, 5.04 H_2-11) ; ESI MS (+) *m/z* 564 $[M+Na]^+$, 308 $[M+H\text{-}PhC(OMe)CF_3COO]^+$.

4.7.8. Phyllostoxin (62)

Phyllostoxin, obtained as an amorphous solid, had: $[\alpha]^{25}D$: +32.8 (*c* 1.0, $CHCl_3$); IR ν_{max} 1714 (C=O), 1671 (α,β unsaturated C=O), 1658 (OC=O), 1628 (C=C) cm^{-1}; UV λ_{max} (log ε) nm 321 (3.51), 254 (4.21), 242 (4.21) ; ^1H and ^{13}C NMR spectra: see Table 5.11.5; EI MS (rel. int) *m/z*: 232 $[M\text{-}CO]^+$ (58), 217 $[M\text{-}MeCO]^+$(100), 204 $[M\text{-}CH_2{=}C{=}C{=}O]^+$(66), 189 [M-CO-MeCO-]$^+$(64), 175 $[M\text{-}CO\text{-}CH_2{=}C{=}C{=}O]^+$(30), 161 $[M\text{-}MeCO\text{-}CH_2{=}C{=}C{=}O]^+$ (23), 43 $[MeCO]^+$ (76); HRESI MS (+) *m/z*: 487.2070 [$C_{28}H_{32}NaO_6$, calcd. 487.2097, 2xM-CO+Na]$^+$, 465.2254 [$C_{28}H_{33}O_6$, calcd. 465.2277, 2xM-CO+H]$^+$, 255 [M-CO+Na]$^+$.

4.7.9. Phyllostin (63)

Phyllostin, obtained as a white crystal, had: mp 138-142 °C; $[\alpha]^{25}_D$: -29.4 (*c* 0.1, MeOH); IR ν_{max} 3419 (OH), 1715 (C=O), 1628 (C=C), 1303, 1251 (O-CO) cm^{-1} [(Isogai *et al*., 1985): mp: 133-135 °C, $[\alpha]_D$= -188.75° (*c*=2.0 MeOH), IR (nujol) 3410 (OH), 1750 (C=O), 1725 (C=O); (Alberg *et al*., 1992): *R* mp 160-165 °C; *S* mp 136-137 °C; (Muralidharam *et al*., 1990): mp 128-129 °C]; UV λ_{max} nm (log ε) 280 (2.97), 242 (sh); ^1H and ^{13}C NMR spectra: see Table 5.11.5; HREI MS (rel. int) *m/z*: 242.0802 [$C_{11}H_{14}O_6$, calcd. 242.0790, M]$^+$ (0.9), 225 $[M\text{-}OH]^+$(0.4), 214 $[M\text{-}CO]^+$(62), 211 $[M\text{-}MeO]^+$(0.9), 170 $[M\text{-}CO\text{-}CO_2]^+$ (44), 142 $[M\text{-}2XCO\text{-}CO_2]^+$ (66), 95 (100); ESI MS(+), *m/z*: 281 $[M+K]^+$, 265 $[M+Na]^+$.

4.8. Fungal metabolites in the biocontrol of weeds

4.8.1. Fungal metabolites in the suicidal germination of *Orobanche* spp.

Fusicoccin (**35**) was produced by *Fusicoccum amygdali* as reported by Ballio *et al*., (1968a). The crystalline sample of **35** obtained as previously reported (Ballio *et al*., 1968b) preserved at -20 °C under dark for about 26 years showed by TLC [eluent $CHCl_3$-*iso*-

PrOH (9:1)] and ^{1}H-NMR analyses the presence of some minor alteration products, that probably are the well known isomers formed by the shift of the acetyl group from the C-3 to C-2 and C-4 of the glucosyl residue, respectively, (*allo*- and *iso*-FC) (Ballio *et al*., 1972) of the sugar moiety. Therefore, the sample was purified by a column chromatography [eluent $CHCl_3$-*iso*-PrOH (9:1)]. The corresponding dideacetyl derivative (DAF, **64**) was prepared by alkaline hydrolysis of **35** according to the procedure previously reported (Ballio *et al*., 1970) and purified by preparative TLC [eluent $CHCl_3$-*iso*-PrOH (4:1)]. The purity of **35** and **64** were checked by TLC and ^{1}H-NMR analysis.

The other FC derivatives and analogues, whose purity was ascertained by TLC and ^{1}H-NMR, were prepared according to the references listed below: **65** (Evidente *et al*., 1984); **66** (Ballio *et al*., 1981); **67** and 68 (Chiosi *et al*., 1983); **69** (Ballio *et al*., 1968a); **70** (Randazzo *et al*., 1979).

Ophiobolin A (**36**) was obtained from the purification of the ethyl acetate extract of *Drechslera gigantea* as previously reported (see paragraph 4.1).

4.8.2. Fungal metabolites in the management of *C. arvense* and *S. arvensis*

Stagonolide, putaminoxin and pinolidoxin (**34, 1** and **6**) were obtained by purification of the organic extract of *S. cirsii*, *P. putaminum* and *A. pinodes* cultures, respectively, as previously described (Evidente *et al*., 1993; 1995; Yuzikhin *et al*., 2007). Deoxaphomin and cytochalasins A, B, 7-*O*-acetyl-cytochalasin B, cytochalains F, T, Z2 and Z3 (**30** and **25-29**, **20** and **21**) were obtained by the purification of the organic extract of *P. exigua* var. *heteromorpha* solid culture as previously reported (Evidente *et al*., 2003). 7,8-*O,O*'-diacetyl- and 7,8-*O,O*'-isoprophylidene-pinolidoxin (**71** and **72**) were prepared from **6** according to the chemical derivatization previously reported (Evidente *et al*., 1993b) as well as 21,22-dihydro-, 7-O-acetyl- and 7,20-O,O'-diacetyl-cytochalasin B (**73, 27** and **75**), were prepared by chemical modification of **26** as previously reported (Bottalico *et al*., 1990).

4.9. Biological assay

4.9.1. Leaf-puncture assay.

The assessment of toxicity, culture filtrates, organic extracts, chromatographic fractions and pure metabolites were assayed by using a leaf-puncture assay on the suitable host and non host wild or cultivated plants. Pure toxins, as well as extracts and fractions, were first dissolved in a small amount of suitable solvent and then diluted to the desired final concentrations with distilled water. The assays were carried out by Dr. M. Vurro, Institute of Food Production Sciences, CNR, Bari, Italy, and by Dr. A. Berestetskiy All-Russian Institute of Plant Protection, St. Petersburg, Russia.

4.9.1.1. Assay of ophiobolins

Ophiobolin A, 3-anydro-6-*epi*-ophiobolin A, 6-*epi*-ophiobolin A and ophiobolin I, were tested at 50, 100 and 250 µg/ml on 13 weed species (eight mono- and five di-cotyledonous) listed in the Table 5.3.1.

Ophiobolins B, E and J and 8-*epi*-ophiobolin J were assayed for their phytotoxicity on four weedy plants, as reported in the Table 5.3.2. Droplets (8 µl) of the assay solutions were applied to cut segments (length around 5 cm) of leaves detached from young plants grown in greenhouse conditions, on which small circular superficial lesions (0.5 mm) have previously been produced by using a glass capillary. After droplet application, leaf segments were kept on moistened paper filters in Petri dishes, in a growth cabinet at 25 °C under continuous fluorescent lights (10,000 lux). Droplets of DMSO solution (up to 4 %) were applied to leaves as control. Symptoms appearance was observed 2 days after droplet application. Symptoms were evaluated using a visual empiric scale from 0 (no symptoms) to 3 (diameter of the necrotic area: 3 mm or wider).

4.9.1.2. Assays of cytochalasins and nonenolides

Cytochalasins, nonenolides and their derivatives, were tested at 1 mg/ml on *Cirsium arvense* and *Sonchus arvensis* leaves. A drop of test solution (10 µl) was placed in the leaf

disc centre. The discs of 1 cm in diameter were cut out from well expanded leaves of *Cirsium arvense* and *Sonchus arvensis* grown in greenhouse. The discs were placed on moistened filter paper in transparent plastic boxes and wounded with sharp needle in the centre. The treated discs were incubated under alternate artificial light and temperature: 8 h in darkness at 20 °C and 16 h under light at 24 °C. After 48 h of the incubation the leaf disc necrotic area was measured.

4.9.1.3. Assay of phyllostictines, phyllostoxin and phyllostin

Phyllostictines A, B, C and D, phyllostoxin and phyllostin were tested at concentrations of around 6 x 10^{-3} M. Droplets (20 μl) of the assay solutions were applied to punctured detached leaves, that were then kept in moistened chambers under continuous light. Symptoms appearance was observed 3 days after droplet application.

4.9.1.4. Assay of stagonolides and modiolide A

Stagonolides B, C, D, E, F, G, H and I and modiolide A were tested at 1 mg/ml as previously reported (see paragraph 4.9.1.2.)

Additionally, a spectrum of phytoxicity of stagonolide H (**51)** was evaluated at 1 mg/ml on a number of plant species using a leaf disk-puncture bioassay: *Chicorium intybus* L. (chicory), *Aegopodium poagraria* L. (bishop's weed), *Trifolium pretense* L. (red clover), *Raphanus sativus* L. (radish), *Solanum lycopersicum* L. (tomato), *Elytrigia repens* (L.) Desv. ex Nevski (couch-grass), and *Zea mays* L. (corn), as reported in the Table 5.9.2. The plants were produced from seeds in greenhouse and the discs were obtained as previously reported (Yuzikhin *et al*, 2007). The concentration of MeOH was 2% v/v, which is non toxic to leaves of all plants in the control.

4.9.2. Seedlings bioassay of stagonolides G-I and modiolide A

Seedlings of chicory with rootlets of 1-2 mm length were soaked for 1 h in a 1 mg/ml solution of compound **50-53** (concentration of MeOH 2%), and then incubated on a

moistened Petri dish as previously reported (Yuzikhin *et al*, 2007). The length of rootlets in treatment was compared with the control (2% MeOH). The assays were carried out by Dr. A. Berestetskiy, All-Russian Institute of Plant Protection, St. Petersburg, Russia.

4.9.3. Seed germination tests of ophiobolin A and fusicoccin derivatives

The stimulatory activity of ophiobolin, fusicoccin and its derivatives on germination of nine broomrape species was tested *in vitro* at concentration 10^{-4}, 10^{-5}, 10^{-6}, 10^{-7} M. Seeds of *O. aegyptiaca*, *O. crenata*, *O. cumana*, *O. densiflora*, *O. foetida*, *O. gracilis*, *O. hederae*, *O. minor*, *O. ramosa* were sterilised with formaldehyde and spread over 2 cm diameter disc of glass fibber filter paper (GFFP, Whatman GF/A) at a density of 50 seeds/cm^2 (Fernández-Aparicio *et al.,* 2008). Three replicate discs per compound were prepared with each *Orobanche* species. The GFFP discs containing the seeds were individually placed in small Petri dishes (6 cm diameter) and moistened with 250 µl of sterile distilled water. The dishes were placed in the dark at 20 ºC for 10 days to break dormancy of broomrape seeds. For bioassays each compound was dissolved in 0.7% methanol mixed with 125 µl of sterile distilled water and applied to each GFFP disc carrying the conditioned seeds of *Orobanche*. The synthetic germination stimulant GR24 (Johnson *et al*., 1976) was used as a positive control at 10 ppm. In order to allow valid comparisons, 0.7% methanol was also added to GR24 dilution. As negative control sterile distilled water with 0.7% methanol, was included in the experiment. After treatment, dishes containing the discs were maintained in the dark at 20 ºC for seven days. At this stage 100 broomrape seeds per disc were studied under a stereoscopic microscope at 30x magnification to determine the percentage of germination. Seeds with an emerged radicle were scored as germinated. The assays were carried out by Dr. D. Rubiales Olmedo, Istitute for Sustainable Agriculture, CSIC, Cordoba, Spain. Data were approximated to normal frequency distribution by means of angular transformation and analysis of variance

(ANOVA) was conducted using SPSS 15.0 on the percentage of broomrape germination observed, with broomrape species, the inductor effect performed by each compound, concentration at which each compound was applied and their interaction as factors.

4.9.4. Assessment of virulence of *Ascochyta sonchi* strains

For the assessment of fungal virulence clonally propagated plants were used. Underground shoots of *C. arvense* and *S. arvensis* were cut into small pieces (length about 5 cm). The shoot sections were placed in plastic pots (diameter 13 cm, height 11 cm) and covered with soil mixture (sand: peat; 1:3) at a depth of 5 cm. Plants were grown under 16 h artificial light per day at 24 °C day/20 °C night and inoculated at the rosette stage of 5–7 leaves.

Two techniques of inoculation were used. Conidial suspension was applied on 10 mm diameter leaf disks cut from expanded leaves of *C. arvense* and *S. arvensis* (10 µl per disk, 12 disks per treatment). Before inoculation, half of the disks were wounded in the centre with a sharp needle. Leaf disks were incubated in plastic containers at 25 °C under continuous light. Symptoms and disease severity were assessed 7 days after inoculation. Additionally, whole plants were sprayed with a hand atomiser using the same conidial suspension (2 ml per plant, 10 plants per treatment), and they were immediately covered with polyethylene bags to keep high humidity for 48 h. Symptoms and disease severity were assessed 14 days after conidial application. The types of experiments were carried out twice. The assessment of the virulence of *A. sonchi* strains was carried out by Dr. M. Vurro, Institute of Food Production Sciences, CNR, Bari, Italy.

4.9.5. Zootoxic activity

The zootoxic activity was tested on the infusorium, *Colpoda steinii*. (GOST, 1997) or on larvae of *Artemia salina* L. (brine shrimp) (Bottalico *et al*., 1990). The assays were carried out by Dr. A. Berestetskiy, All-Russian Institute of Plant Protection, St. Petersburg,

Russia, and by Dr. M. Vurro, Institute of Food Production Sciences, CNR, Bari, Italy, respectively.

4.9.5.1. Assay of stagonolides B-F

Stagonolides B, C. D, E and F were assayed on *Colpoda steinii*. The standard Lozina-Lozinskogo media (2 ml) was added to the dried infusorium culture containing about 5000 cells per ml and then the resulted suspension was incubated for 24 h at 25 °C before use. The toxin solution in 4% EtOH was added to the infusoria suspension (1:1 v/v) to its final concentration 0.05 mg/ml. After a course of incubation (from 3 to 180 min) the number of immobile cells (%) was counted. In the control treatment *C. steinii* culture was prepared in 4% EtOH. If 100% of the infusoria cells become immobile within 3-min exposure with the toxin, the tested substance demonstrates strong toxicity; if they loose activity in ≥180 min the substance should be evaluated as low toxic.

4.9.5.2. Assay of phyllostictine A-B, phyllostoxin and phyllostin

Phyllostictines A and B, phyllostoxin and phyllostin were tested on larvae of *A. salina* L. (brine shrimp) at concentrations between 10^{-3} and 10^{-4} M, as previously described (Bottalico *et al*, 1990). Brine shrimp eggs were hatched in artificial sea water. Larvae (30-50) were placed in sea water solution (0.5 ml) containing the toxins. After 48 hours larvae mortality was recorded and expressed as a percentage value.

4.9.6. Antimicrobial activity of phyllostictine A-B, phyllostoxin and phyllostin

The antifungal activity of phyllostictines A and B, phyllostoxin and phyllostin was tested up to 100 μg/disk on *G. candidum*, whereas the antibiotic activity was assayed on *Lactobacillus sp.* and *E. coli*, as previously described. (Bottalico *et al*., 1990). The assays were carried out by Dr. M. Vurro, Institute of Food Production Sciences, CNR, Bari, Italy.

4.9.7. Photometric assays of cytochalasin B and stagonolide

Light absorption of leaves treated with phytotoxins was registered *in vivo* with a photometer LAFOT and a spectrophotometer SPEFOT. Both instruments were developed

in St. Petersburg Agrophysical Institute, Russia (Lisker, 1991). LAFOT works at the wave of 632.8 nm. At this wavelength the absorption level closely correlates with the chlorophyll content in plants (Lisker and Dmitriev, 1998; 1999). SPEFOT reads the optical parameters of plant tissue in the spectrum from 450 to 1100 nm and can register relative quantitative changes of a number of plant pigments including chlorophylls and carotenes. The absorption values were expressed as percentage of initial power of radiation. Ten leaf discs per treatment were analysed with LAFOT after 0 (control), 2 and 4 h post toxin application. Photometric assay with SPEFOT at the wavelength range of 450–950 nm was conducted after 24 h post treatment of discs with stagonolide and cytochalasin B. The assays were carried out by Dr. A. Berestetskiy, All-Russian Institute of Plant Protection, St. Petersburg, Russia.

4.9.8. Electrolyte leakage assays of cytochalasin B and stagonolide

Conductivity meter Tercon-04 (Agrophysical Institute, St. Petersburg, Russia) was used for *in vivo* evaluation of the electrical resistivity of leaf tissues of *C. arvense* 24 h post treatment with stagonolide, cytochalasin B, and water (control). The discs boiled in water for several minutes were used as a positive control. For the assay, a treated leaf disc (10 replicate discs per treatment) placed between two copper electrodes was exposed to current at the electric tension of 1 V. Its electric resistivity was measured with determined intervals since 5 to 150 sec after beginning of the current. The resulted data were expressed as a ratio between the first measurement (5 sec post beginning of the current) and following measurements of the resistivity.

Data obtained with the above mentioned technique were compared with observations based on routine electrolyte leakage assay. Treated leaf discs were washed with distilled water, cut into small pieces and soaked for 30 min in water, and electrical conductivity of resulted water extracts was measured by a conductivity meter. The assays were carried out by Dr. A. Berestetskiy, All-Russian Institute of Plant Protection, St. Petersburg, Russia.

5. RESULTS AND DISCUSSION

5.1. Chemical characterization of ophiobolins from *D. gigantea* liquid culture, potential herbicides of weedy grasses

The organic extract of *D. gigantea* culture filtrates, showing a strong phytotoxic activity was purified by column and TLC chromatography as described in the experimental. The main metabolite was isolated as a crystalline white solid (25.0 mg/l) and identified by spectroscopic methods (essentially ^{1}H and ^{13}C NMR and MS techniques) as ophiobolin A (**36**, Fig. 5.1.1). The physical and the spectroscopic data were similar to those previously reported in literature (Nozoe *et al*., 1965; Li *et al*., 1995; Canales *et al*., 1988). This result was also confirmed by a direct X-ray analysis carried out on the natural metabolite in collaboration with Prof. A. Tuzi, Department of Chemistry, University "Federico II" of Naples, Italy. The other three compounds were isolated as amorphous solids but in lower amounts (1.5, 1.1 and 0.3 mg/l) compared to **36** and by preliminary spectroscopic investigation, appeared to be closely related to ophiobolin A. They were identified by comparison of their spectral data, essentially ^{1}H and ^{13}C NMR and MS data, as 6-*epi*-ophiobolin A, 3-anhydro-6-*epi*-ophiobolin A, and ophiobolin I (**37**, **38** and **39**, Fig. 5.1.1). Their physical and spectroscopic data were similar to those reported in literature (Canales *et al*., 1988; Kim *et al*., 1984; Li *et al*., 1995; Suguwara *et al*., 1987; 1988).

The residues of the ophiobolin A mother liquor crystallization were combined and purified as in detail reported in the experimental yielding a further ophiobolin (0.48 mg/l, **40**, Fig. 5.1.1) as a homogeneous compound. This latter had a molecular formula of $C_{25}H_{34}O_3$ as deduced from HRESIMS spectrum consistent with 9 degrees of unsaturations. Compared to ophiobolin A, it showed the significant absence of one oxygen atom and the increase of one unsaturation. The preliminary ^{1}H and ^{13}C NMR (Figg. 5.1.2 and 5.1.3) investigation showed noteworthy differences in respect with the spectra of known

ophiobolins, although the typical systems of the α,β-unsaturated aldehydic group of the octacyclic B ring substantially appeared unaltered (Breitmaier and Volter, 1987; Pretsch *et al*., 2000) as also confirmed by the analysis of the COSY and HSQC (Figg. 5.1.4 and 5.1.5) (Berger and Braun, 2004). Some significant differences seemed present in both the pentacyclic rings A and C. In fact, the ketone group on C-5 and the typical AB system due to the H_2C-4 present in **36** were absent in **40**, with the consequent increase of the multiplicity and complexity of the region of methylene protons of the ^1H NMR spectrum (Table 5.1.1) and due to both H_2C-4 and H_2C-5 resonating between δ 2.45 and 1.50. Furthermore, the broad doublet (J = 6.99 Hz) of H-6 appeared significantly upfield shifted (Δδ 0.36) δ 2.85 (Pretsch *et al*., 2000). However, in the ring A the presence of tertiary hydroxylated quaternary carbon C-3 and the corresponding geminal methyl group appeared evident, as their corresponding signals were observed in the ^{13}C NMR spectrum as a singlet and a quartet at typical chemical shift values of δ 78.9 and 29.2 (Breitmaier and Volter, 1987), while the methyl group appeared as a singlet in the ^1H NMR spectrum at the expected chemical shift value of δ 1.34 (Pretsch *et al*., 2000). These structural features are in agreement with the signal recorded in the IR spectrum (Fig. 5.1.6) for α,β-unsaturated carbonyl and hydroxy groups (Nakanishi and Solomon, 1977), as well as the typical maximum absorption recorded in the UV spectrum (Fig. 5.1.7) at 233 nm (Scott, 1964). Considering the lack of the ketone group at C-5 and the presence of four rings and the double bond of the isoprenyl side [C(17)-C(25)], the remaining two unsaturations of **40** should be located in the ring C. In fact, the ^1H spectrum of **40** showed a broad triplet (J= 5.4 Hz) typical of an olefinic proton (Pretsch *et al*., 2000) at δ 5.08 (H-12) and, compared to the spectrum of ophiobolin A, the absence of the signals of H-10 as well as those of the two methylene groups H_2C-12 and H_2C-13. The comparison of the corresponding ^{13}C NMR spectra showed the absence in **40** of the significant oxygenated quaternary carbon of

C-14, and the methine and the methylene carbons of C-10 and C-12 and C-13, while four olefinic carbons were present at the typical chemical shift values expected for a suitable substituted 1,3-cyclopentadienylic ring (Breitmaier and Voelter, 1987). Of these, the secondary carbon at δ 124.5 was attributed to C-12 while the three remaining quaternary carbons present at δ 159.6, 158.8 and 133.0 were assigned to C-13, C-10 and C-14, respectively, on the basis of the couplings observed in the HMBC spectrum (Fig. 5.1.8, Table 5.1.1) (Berger and Braun, 2004). The 1,3-dienylic nature of the ring C was in agreement with the typical bands observed in both IR (Nakanishi and Solomon, 1987) and UV spectra (Scott, 1964) of **40**. Finally, the ether bridge of D ring should be present between C-17 and C-13, considering the typical chemical shift value of δ 159.6 shown by C-13 in the ^{13}C NMR spectrum (Breitmaier and Voelter, 1987). Consequently, **40** represents the first ophiobolin in which the D ring became a substituted dihydropyran ring, joined with the C ring trough the C(13)-C(14) bond and bearing the secondary methyl group and the 2,2-dimethylvinylidene side chain at 4- and 2-positions in respect to the oxygen atom. The chemical shifts of the secondary methyl group (Me-CH-15) as well as those of the dimethylvinyledene tail at C-17 are very similar to those reported for the ophiobolin A. As expected, substantially different appear to be the signal of H-17 and H-18, both resonating as broad doublets at δ 3.85 and 5.84 in the ^{1}H NMR spectrum (Pretsch *et al*., 2000), as well as those of C-17 downfield shifted (Δδ 14.9) at δ 85.7 in the corresponding ^{13}C NMR spectrum (Breitmaier and Voelter, 1987).

On the basis of the correlations observed in the COSY and HSQC spectra, the chemical shift was attributed to all the protons and the corresponding carbons and reported in Table 5.1.1. The structure of this ophiobolin is depicted in **40**. Considering that in literature the name ophiobolin E appears not to be attributed to any compound (Au *et al*., 2000), we decided to assign this name to **40**.

The structure of ophiobolin E was supported by several $^{1}H,^{13}C$ long-range correlations and the effects recorded for **40** in the HMBC and NOESY (Fig. 5.1.9) spectra (Table 5.1.1 and 5.1.2) (Berger and Braun, 2004), and by data of its HRESI MS spectra. The latter, recorded in positive mode, in addition to the sodium cluster $[M+Na]^{+}$ at *m/z* 405.2416, showed the potassium $[M+K]^{+}$ cluster and the pseudomolecular ions at *m/z* 421and 383, respectively. When recorded in negative modality the ESI MS spectrum showed the significant pseudomolecular ion $[M-H]^{-}$ at *m/z* 381.

5.2. Chemical characterization of other ophiobolins from *D. gigantea* solid culture

Grown on solid culture, *D. gigantea* produced different ophiobolins. The organic extract was purified by a combination of column and preparative TLC, as in details reported in the experimental, giving four ophiobolins, all isolated as amorphous solids. Three of them were identified as ophiobolins A (obtained in very low amounts in respect to the liquid culture of the same fungus), B and J (**41** and **42,** Fig. 5.2.1), by comparison of their spectroscopic properties, essentially ^{1}H and ^{13}C NMR and MS data. Their physical and spectroscopic data were very similar to those reported in the literature (Li *et al*., 1995; Sugawara *et al*., 1988). The fourth ophiobolin appeared to be a new compound closely related to ophiobolin J, as shown by the same molecular formula of $C_{25}H_{34}O_3$ deduced from its HR ESIMS and by the comparison of their IR, UV and ^{1}H and ^{13}C NMR spectra (Figg. 5.2.2-5.2.5). In particular, the only significant difference observed in the ^{1}H NMR spectrum was the signal of H-8 which appears in both compounds as a double doublet at δ 4.68 and 4.70 in **42** and **43**, respectively, but differently coupled with the protons of the adjacent H_2C-9. In fact, the coupling constants measured for H-8 were 10.0 and 9.9 Hz in **43** while the same in **42** were 5.7 and 4.5 Hz respectively. On the basis of these results, the structure of 8-*epi*-ophiobolin J was assigned to **43 (**Fig. 5.2.1**)**. This is the first ophiobolin showing the epimerization of C-8.

The correlations observed in the COSY and the HSQC spectra (Figg. 5.2.6 and 5.2.7) allowed to assign the chemical shifts to all the protons and the corresponding carbons of **43** (Table 5.1.1) which, as expected, were very similar to those of **42** (Sugawara *et al*., 1988).

The structure of 8-*epi*-ophiobolin J (**43**) was supported by several $^{1}H,^{13}C$ long-range correlations and the effects recorded for **43** in the HMBC and NOESY spectra (Figg. 5.2.8 and 5.2.9, Table 5.1.1 and 5.1.2). Particularly significant appeared to be the clear NOE effect observed between H-8, having a β-position, and the Me-22 located on the same side of the molecule.

The structure of **43** was also supported by the data of its HRESI MS spectra (Fig. 5.2.10). The latter, recorded in positive mode, in addition to the sodium cluster $[M+Na]^{+}$ at *m/z* 423.2515, showed the potassium $[M+K]^{+}$ cluster and the pseudomolecular ions at *m/z* 439 and 401, respectively, and the ion at *m/z* 383 generated from this latter by loss of H_2O. When recoded in negative modality the ESI MS spectrum showed the significant pseudomolecular ion $[M-H]^{-}$ at *m/z* 399.

5.3. Biological activity of ophiobolins

Ophiobolin A proved to be highly toxic to almost all the plant species tested (Table 5.3.1), already at the lowest concentration used ($1.25\ 10^{-4}$ M; 3.2 μg $droplet^{-1}$). Among dicotyledons, *Sonchus oleraceus* appeared to be particularly sensitive, whereas almost all of the monocotyledons were very sensitive. On the opposite, even at the highest concentration used, the phytotoxin was almost inactive to *Cynodon dactylon*. Compared to ophiobolin A, 6-*epi*-ophiobolin A proved to have almost the same spectrum of plant sensitivity, but at a lower intensity. With regard to 3-anydro-6-*epi*-ophiobolin A, it was almost inactive to most of the plant tested, with the exception of *Setaria viridis* and *Diplotaxis erucoides*. Ophiobolin I proved to be inactive, even at the highest concentration, to all the plants tested.

Tested on four weedy plants using the leaf-puncture assay only ophiobolins B and J proved to be toxic (Table 5.3.2), whereas the two new ophiobolins, ophiobolin E and 8-*epi*-ophioblin J, appeared to be inactive on all the tested plant species. In particular, ophiobolin B was highly toxic to *Bromus* sp. and *Hordeum marimum* leaves, but less toxic to the other two weed species. The same range of toxicity, but at a lower level, was observed for ophiobolin J.

It is interesting to note a certain level of selectivity of the toxins. In fact, on average ophiobolins proved to be more active to grass weeds in respect to dicotyledonous species. Ophiobolin A proved to be more active to almost all the plant species tested, in comparison with 6-*epi*-ophiobolin A, whereas the 3-anhydro compound was much less toxic, being almost inactive to many of the plant tested, even at the highest concentration used. Furthermore, the ophiobolin I proved to be inactive to all the species tested. On the basis of these results structural features important for the phytotoxicity appear to be the hydroxy group at C-3, the stereochemistry at C-6 and the aldehyde group at C-7. These results are in agreement to the previously reported data (Pena-Rodriguez *et al*., 1989). The modulated activity of ophiobolin B on the different tested plants appears to be similar to that previously reported for ophiobolin A. This result was predictable because the two ophiobolins are structurally closely related. Moreover Ophiobolin J, having reduced or no activity, is related to ophiobolin I, which had proved to be inactive. This activity is in agreement with the phytotoxicity previously observed for the same toxin (Sugawara *et al*., 1988). The different phytotoxicity showed by the two ophiobolins J and I could be attributed to the different conformation that the octacyclic B ring can assume, as a consequence of the different position of the double bond, which is located between C-7 and C-8 in **39**, and between C-6 and C-7 in **42**. Probably, when present, the epimerization of the hydroxy group of C-8, observed for the first time in **43**, imparts the total loss of the activity. The noteworthy structural differences present in the ophiobolin E could justify the

observed inactivity on the tested plants. In fact, this latter ophiobolin showed the conversion of the cyclopentane C ring, present in all the other ophiobolins, into a 1,3-cyclopentadiene joined with the D ring, which in turn is present for the first time as a tetrasubstituted dihydropyran ring. Consequently, the configuration of the octacyclic B ring as well as that of the 2,2-dimethylvinylidene residue at C-17 should be substantially changed. Moreover, as a further difference in respect to the other ophiobolins, **40** showed the lack of the ketone group at C-5, which determines a different A ring conformation.

The ophiobolins are a group of polycyclic sesterterpenoid with a common basic structure. They are secondary phytotoxic metabolites produced by pathogenic fungi attacking several crops, such as rice, maize and sorghum. Ophiobolin A was the first member of the group to be isolated and characterized independently by Canonica (Canonica *et al*., 1966) and Nozoe (Nozoe *et al*., 1966). In addition to ophiobolin A, several analogs were isolated in the late sixties and their structures determined. These include ophiobolin B from *B. oryzae* (Itai *et al*., 1967), ophiobolin C from *B. zizanie* (Nozoe *et al*., 1966), ophiobolin D from *Cephalosporium caerulens* (Itai *et al*., 1967: Nozoe *et al*., 1967), and ophiobolin F *from B. maydis* (Nozoe *et al*., 1968). A wealth of information has been accumulated regarding the biological activities of ophiobolins as well as on their biosynthesis, even if neither the enzymes nor the genes responsible have been identified (Au *et al*., 2000). The isolation of ophiobolins from this strain of *D. gigantea* isolated by *Digitaria sanguinalis* is enough surprising considering Kenfield *et al*. (1989a), had previously studied the metabolites produced by another strain of *D. gigantea* and reported only the isolation of gigantenone as the main toxin. Although being both terpenoids, gigantenone belongs to the chemical subgroup of sesquiterpenes, whereas ophiobolins belong to that of sesterterpenoids. Several biological investigations have also described gigantenone as a promising compound in different areas of research such as pathological physiology, photosynthetic efficiency, senescence, vegetation propagation,

and development of selective herbicides (Kenfield *et al*., 1989a). Many biological properties were reported for ophiobolins, too. For example, they can reduce root and coleoptile growth of wheat seedlings, inhibit seed germination, change cell membrane permeability, stimulate leakage of electrolytes and glucose, or cause respiratory changes (Au *et al*., 2000). In our assays, the necrotic spot lesions on leaves induced by the application of drops of toxins resemble those caused by the pathogen, even if those symptoms are not as specific as the pathogen. For this reason, further studies are in progress to evaluate the possibility of enhancing the efficacy of the promising mycoherbicide *D. gigantea* with the joint application of sublethal doses of the toxins.

Changes in culturing conditions can strongly influence the biosynthetic production of ophiobolins as already reported. For example, *B. maydis* was able to produce ophiobolin A, 3-anhydro-ophiobolin A, ophiobolin B and ophiobolin L when grown in liquid conditions (Li *et al*., 1995), whereas it produced ophiobolin M, 6-*epi*-ophiobolin M, ophiobolin C, 6-*epi*-ophiobolin C, ophiobolin K and 6-*epi*-ophiobolin K when grown on solid media (Tsipouras *et al*., 1996).

Ophiobolins are also toxic to animals. For example, the LD_{50} doses of ophiobolin A for mice are 238 mg/kg when administered subcutaneously, or 73 mg/kg, orally (Nakamura and Ishibashi, 1958). Even if they are much less toxic (as acute toxicity) compared to other powerful mycotoxins [e.g.: oral LD_{50} for T-2 toxin and aflatoxin B_1 is ranging between 0.6 and 6.1 mg/kg, and between 0.4 and 18 mg/kg, respectively, depending on the animal species (Bottalico, 2004)], their real impact in the environment should be evaluated, as well as their effect to non-target organisms, and their fate after the introduction in the environment, if considered as possible natural herbicides.

5.4. Stimolation of seed germination of *Orobanche* spp. by ophiobolin A and fusicoccin derivatives

Ophiobolins share the same carbotryciclic diterpenoid ring with fusicoccins and cotylenins, other two groups of microbial metabolites produced by *Fusicoccum amygdali*, the causal agent of almond and peach disease (Ballio and Graniti, 1991), and by *Clamidiosporum* sp. 501-7W. (Sassa, 1971; Sassa *et al*., 1972).

Fusicoccin (FC) at lower concentration (10^{-6}-10^{-8} M) showed other interesting biological activities as seed germination, stomata opening and hormone like properties. Considering these activities, a structure-activity relationship (SAR) study was carried out using FC and some its derivatives to induce a suicidal germination of *Orobanche ramosa* seeds. The most active compound appeared to be the dideacetyl FC, which being easily prepared in high yield by alkaline hydrolysis from FC, could have a potential practical application (Evidente *et al*., 2006). This prompted to perform further study using fusicoccin derivatives and close related terpenoid as ophiobolin A to evaluate the stimulation of seed germination of different *Orobanche* species.

In this SAR study a total of 9 compounds were used, and 6 of them are FC glucosides, two FC aglycones and ophiobolin A (**36**). In particular, beside FC (**35**, Fig. 5.4.1), the following compounds were tested for their capacity to stimulate the seed germination of *Orobanche* species: the glucoside derivatives **64-68** (Fig. 5.4.1) prepared from FC by "ad hoc" chemical modification; the 8,9-isopropylidene derivative of FC deacetyl aglycone (**69**, Fig. 5.4.1), which was prepared by chemical degradation of the sugar moiety of **35**, and its 19-*O*-trytil-12-oxo derivative (**70**, Fig. 5.4.1); ophiobolin A isolated from liquid culture filtrates of *D. gigantea*.

The *Orobanche* species used were *O. aegyptica, O. crenata*, *O. cumana*, *O. densiflora*, *O. foetida*, *O. gracilis*, *O. hederae*, *O. minor* and *O. ramosa*. A positive germination control was obtained by stimulating the seed germination of all the species

using the synthetic stimulant GR24 (Johnson *et al*., 1976) in the conditions detailed reported in the experimental and by adding 0.7% of methanol, which is the final concentration of this solvent present in the solution of the compound tested. A negative control using sterile distilled water with 0.7% of methanol was also used.

The results reported in Figure 5.4.2 showed that GR24 at the concentrations tested has a high stimulatory activity (inducing 55 to 90% seed germination) of *O. crenata*, *O. cumana*, *O. minor, O. aegyptiaca* and *O. ramosa*, but not of *O. densiflora*, *O. foetida*, *O. gracilis* or *O. hederae*. As expected with the negative control practically all the species did not showed any germination.

The compounds were tested in the concentration range of 10^{-4}-10^{-7} M in the conditions detaily reported in the experimental. The results of the bioassays are reported in Figure 5.4.3. There were significant differences in the broomrape germination due to the broomrape species tested (ANOVA, $p<0.001$), to the compound tested (ANOVA, $p<0.001$), and to the concentration used (ANOVA, $p<0.001$) and their second and third order interaction (ANOVA, $p<0.001$).

Practically, only *O. aegyptiaca*, *O. ramosa, O. cumana* and *O. minor* were stimulated up 50% in the range of the concentration tested but only by the fusicoccin derivative **67** and **68** and by ophiobolin A (**36**). The other fusicoccin derivatives were inactive, except the 8,9-isopropylidene derivative of FC deacetyl aglicone (Fig. 5.4.3 A) that showed a relatively highly stimulation on *O. minor* about 35%. Compound **69** was assayed at higher concentration (10^{-7} M) and on the same species and other ones were practically inactive inducing at maximum a 10% of stimulation against the 55% of stimulation previously observed on *O. ramosa* (Evidente *et al*., 2006).

Our results on response of *O. minor* and *O. ramosa* to fusicoccin and its derivatives differed slightly to previous reports (Yoneyama *et al*., 1998; Evidente *et al*., 2006). We found FC to be little active on *O. minor* and *O. ramosa*, whereas Yoneyama *et al*. (1998),

found high stimulation (56 and 86%) when assayed at 10^{-5} and 10^{-4} on *O. minor* and medium (37 and 25%) on *O. ramosa* (Evidente *et al*., 2006).

The most active FC derivatives **67** and **68**, which are differently acetylated isomers of the 16-*O*-demethyl-de-t-pentenyl-FC, were prepared by chemical modification of fusicoccin by reaction with a Fritz and Schenk reagent normally used for the acetylation of highly hindered hydroxy group (Fritz and Schenk, 1959). The structural modification induced by this reaction was essentially the cleavage of the ether bond and the expansion of the cyclopentane ring A to the cyclohexane or cyclohexene ring as can be observed in **67** and **68**, respectively. Derivative **67** (Fig. 5.4.3 C) showed the same stimulatory effect (about 20%) on *O. aegyptiaca*, *O. cumana* and *O minor* in the concentration range 10^{-4}-10^{-6} M, which rapidly decreased at 10^{-7} M. *O. ramosa* showed a lesser extent germination with a maximum of 10% at 10^{-5} M, that agree with the results previously observed (Evidente *et al*., 2006). Derivative **68** (Fig. 5.4.3 D) showed a modulate activity that is species and concentration dependent. The highest stimulatory effect was observed on *O. aegyptiaca*, whose germination increased from 20% at 10^{-4} M at up 50% at 10^{-5} M and rapidly decreased with the decrease of concentration. *O. cumana* showed a similar 10% of germination at 10^{-4} M and increased up to 40% at 10^{-6} M and then rapidly decreased with the decrease of concentration. *O. minor* showed a similar 10-17% of germination at all the concentrations assayed. Finally, *O. ramosa* was practically not stimulated up to 10^{-5} M and little stimulated (<10%) at higher concentrations. In agreement with this result a low stimulatory effect (10%) was also previously observed testing **68** on the same species.

The results observed with both **67** and **68** are remarkable as the chemical modification induced on the cyclopentane ring A consequently determine a strong modification of the conformation of the carbotricyclic ring that is an important feature to impart activity to FC as previously demonstrated in some SAR study (Ballio and Graniti, 1991; Ballio *et al*., 1991; Pini *et al*., 1979).

Similarly ophiobolin A (**36**) induced (Fig. 5.4.3 B) a stimulation depending from the broomrape species and the concentration. No stimulation was observed at concentration more than 10^{-5} M for *O. aegyptiaca* and *O. cumana*, while for the other two species, *O. minor* and *O. ramosa*, the stimulation started at 10^{-6} M. For the first two species the stimulation increased up to 10^{-6} M and then rapidly decreased with the decrease of concentration for *O. aegyptiaca*, while for *O. cumana* a linear increasing was inversely observed in respect to the concentration. For *O. minor* and *O. ramosa* the stimulation rapidly increased with the decrease of concentration.

5.5. Analysis of ascosonchine content in *A. sonchi* strains, a potential mycoherbicide for biocontrol of *Cirsium arvense* and *Sonchus arvensis*

A simple and sensitive HPLC method was developed for the quantitative analysis of the ascosonchine (**33**, Fig. 1.7) to assess its possible role in the disease induced by *A. sonchi* on both *C. arvense* and *S. arvensis*. Preliminary tests at various elution conditions with standard ascosonchine on reverse phase C-18 and C-8 showed unresolved, asymmetric peaks, which highly delayed the return to baseline. This was due to a strong adsorption on stationary phase. On the basis of earlier positive experience in developing a HPLC method for the analysis of fusaric and 9,10-dehydrofusaric acids (Amalfitano *et al*., 2002), which are pyridilcarboxylic toxins closely related to ascosonchine, the use of a high density C-18 stationary phase drastically reduced this phenomenon. Attempts were made to found the best elution conditions using this stationary phase. The same conditions appropriate for the analysis of fusaric acids with methanol and 1% dipotassium hydrogen phosphate in HPLC grade water adjusted to pH 7.35 with concentrated phosphoric acid (1:1, v/v) as the mobile phase at a flow rate of 1 ml/min and an isocratic gradient over 15 min was used. In these conditions, an asymmetrical broad peak for ascosonchine (Fig. 5.5.1 A) was obtained. The elution with an isocratic gradient of acetonitrile with the same

buffer (1:1, v/v) at a flow rate of 1 ml/min over 15 min yielding a poorer elution profile (Fig. 5.5.1 B) with different peaks, probably due to different tautomeric forms of ascosonchine. Satisfactory shape peak was finally obtained by eluting with an isocratic gradient of methanol and HPLC grade water (1:1, v/v, pH 6.2) at a flow rate of 1 ml/min over 15 min (Fig. 5.5.1 C). The recovery of ascosonchine added to the culture filtrate is near 100%. These results indicated that the simple $CHCl_3$:*iso*-propanol (9:1 v/v) extraction was adequate for quantitative analysis of metabolites in culture filtrates.

These latter conditions were used to quantify the ascosonchine content in the culture filtrates of different *C. arvense* and *S. avernsis* strains (Table 5.5.1). The characteristics of the calibration curves, the absolute range and the detection limits (LOD) of ascosonchine are summarized in Table 5.5.2. Regression analysis suggests that the calibration curves are linear. A representative HPLC chromatogram of the $CHCl_3$-*iso*-propanol soluble culture filtrate of *A. sonchi* (strain C-240) is presented in Figure 5.5.1 D. The metabolite chromatographic peak (a) in the sample was coincident to the 4.6 min retention time of the ascosonchine standard. The retention times were highly reproducible, varying less than 0.50 min. For all strains matrix substances absorbing at 230 nm were eluted within the first 4 minutes. No further peaks appeared when samples were eluted with a higher percentage of water in the mixture, but the retention time increase. This and the high similarity of the features of the metabolite peak in samples with those of the purified standard, suggested other substances were not present that had overlapping peaks. Using the HPLC conditions described, ascosonchine could be quantitatively and reproducibly detected at 10 ng. Poor reproducibility was observed at levels lower than 10 ng.

The ascosonchine content in culture filtrates of seven of the nine strains tested ranged between 0.5 and 2.7 mg/l (strain S-10 and C-240, respectively), whereas two strains (S-9 and C-177) did not produce any measurable ascosonchine (Fig. 5.5.2). The toxin content in the culture of the standard strain (S-7) determined by HPLC (1.4 mg/l) was

higher than that obtained by chemical purification (1.1 mg/l) of the same strain grown in identical conditions (Evidente *et al.*, 2004). This can be probably due to metabolite losses occurred during the complex purification and/or differences in fungal growth.

There were significant differences in virulence (at $p<0.05$) among *C. arvense* strains (Figure 5.5.3) when tested on both intact and wounded leaf disks. The first symptoms, round necrotic lesions, appeared 5 days after inoculation. Generally, disease severity was significantly higher (at $p<0.05$) in wounded leaf disks than in intact ones (Figure 5.5.3) ($r=0.78$ at $p<0.05$). The most virulent strains were C-177, C-216 and C-240, causing necrotic lesions up to 45 % the total leaf surface on wounded leaves, whereas strains S-7 and C-180 were avirulent on intact leaf disks of *C. arvense*, and almost avirulent on wounded leaf disks. None of the strains were virulent to intact or wounded leaf disks of *S. arvensis.*

Although the conditions for the infection were supposed to be very favourable (high inoculum concentration and long period of leaf wetness), all the strains tested on whole plants of *C. arvense* showed a low level of pathogenicity (data not shown), and only in some cases the total lesion size reached 25% of the total leaf area. They were able to infect mainly wounded leaf tissue of the weeds.

Positive relationships between virulence and production of toxins have been found in some cases (Kumar *et al.*, 2002; Reino *et al.*, 2004). In our case, this hypothesis seems not to be supported, considering that strains S-9 and C-177, no *in vitro* ascosonchine producers, and strains S-10 and C-182, low toxin producers, were all able to cause leaf disease. The two best ascosonchine producers, strains C240 and C-208 (2.7 and 1.9 mg/l, respectively) were both isolated from leaves of *C. arvense*, but so were C-177 and C-182, among the worst ascosonchine producers (0 and 0.7 mg/l, respectively). The origin of the host plant (Russia or Norway) does not seem to have any relation with virulence or the ability to produce toxin.

Strain C-240 grown in static conditions synthesized ascosonchine at a linear rate from the first to the fifth week (from 0.15 to 3.1 mg/l), and reached the maximum content at the eighth week (8.30 mg/l) (Fig. 5.5.4). The fungus produced up to almost 1 mg/l, in 12 days in shake culture (Fig. 5.5.5). Considering the variability in ascosonchine production among strains, further studies would be necessary to optimize and maximize toxin production for potential use as a natural herbicide, or in combination with a pathogen, in biological control.

Because the toxin was detected in the later stages of the growth of *A. sonchi* (8 weeks for static culture, and 12 days in shaken conditions), after the stationary phase and when the mycelium started to be senescent, the toxin could be a product of fungal deterioration.

5.6. Taxonomic characterization of *Phoma exigua* var. *exigua in vitro*.

Even though ascosonchine was not in the culture extracts of the strains S-9 and C-177, both proved to be highly toxic when tested using the leaf disk assay (data not shown). Preliminary chemical and spectroscopic (^{1}H and EI- and ESI-MS spectra) analyses of the other main metabolites confirm they were different from ascosonchine and seemed to be closely related to those produced by some other *Phoma* and *Pyrenophora* species (Evidente and Motta, 2001; Evidente and Abouzeid, 2006).

These results suggested studies to ascertain the taxonomy and the nature of phytotoxins produced by this two atypical *Ascochyta* strains.

The strains differed in growth rate significantly ($p<0.05$) on both diagnostic agar media. However, their 7-day old colony dimensions were in accordance to the description of *P. exigua* var. *exigua*. No considerable differences in colony morphology were found in all the strains obtained from both *C. arvense* and *S. arvensis*. All the strains demonstrated E^+ reaction (green following by red staining of the agar media) to a drop of 6 N NaOH

applied to colony margins, which is important species feature of *P. exigua* var. *exigua*. This reaction means presence of antibiotic E in culture media, which is produced only by this species (Boerema *et al*., 2004). Moreover, a comparison of internal trascribed spacer (ITS) sequences from our strains of *P. exigua* var. *exigua* with those uploaded in GenBank showed their identity (G. Múle, M. Vurro, personal communication). These results support the re-classification of S-9 and C-177 strains in the *Phoma exigua* var. *exigua* sp.

5.7. Chemical characterization of phytotoxins from *Phoma exigua* var. *exigua* strains S-9 and C-177 solid and liquid cultures.

Fungal cultures of *P. exigua* var. *exigua* strain C-177 grown on wheat kernels were extracted with water-acetone mixture, evaporated and residual aqueous solution re-extracted with ethyl acetate, then dried to give an abundant brown oil (1.14 g/kg). It was fractionated by silica gel column chromatography as reported in detail in the experimental. The residues of the second and third fractions were combined (for a total of 573.8 mg) and crystallized from EtOAc-*n*-hexane and gave the main metabolite. It was identified as the well known cytochalasin B (**26**, Fig. 5.7.1., 525 g/kg) by comparing its spectroscopic (^{1}H and ^{13}C NMR and ESI MS spectra), physic (melting point) and chromatographic behaviour [R_f 0.32 by TLC, eluent EtOAc-*n*-hexane (6:4, v/v)] with those of a standard sample (Capasso *et al*., 1987). The mother liquors of the cytochalasin B crystallisation were combined and fractionated by silica gel column, as described in detail in the experimental. The residue of the second fraction appeared to be a homogeneous amorphous solid. It was identified as the *p*-hydroxybenzaldehyde (**44**, Fig. 5.7.1, 6.5 mg/kg) by comparing its spectroscopic data (^{1}H and ^{13}C NMR and ESI-MS spectra) and chromatographic behaviour [R_f 0.48 by TLC, eluent $CHCl_3$-Me_2CO-AcOH (90:10:0.3, v/v/v)] with those reported in literature (Shimada *et al*., 1999) and with those of a standard commercial sample. The

residue of the fifth fraction of the same column was further purified by two TLC steps as reported in the experimental yielding a homogeneous amorphous solid. It was identified as cytochalasins F (**27**, Fig. 5.7.1, 1.4 mg/kg) by comparing its spectroscopic (^{1}H and ^{13}C NMR and ESI-MS spectra) and chromatographic behaviour [R_f 0.43 by TLC, eluent EtOAc-*n*-hexane (6:4, v/v)] with those of a standard sample (Capasso *et al*., 1991). The residue of sixth fraction of the cited column purified by TLC as reported in the experimental, gave a homogeneous amorphous solid. It was identified as deoxaphomin (**30**, Fig. 5.7.1, 5.0 mg/kg) by comparing its spectroscopic (^{1}H and ^{13}C NMR and ESI-MS spectra) and chromatographic behaviour [R_f 0.31 by TLC eluent petroleum ether: acetone (65:35, v/v)] with those of a standard sample (Capasso *et al*., 1988).

The ethyl acetate organic extract (101.0 mg/l), obtained by extraction of the culture filtrates of the same strain (C-177) of *P. exigua* var. *exigua*, was fractionated by a silica gel column as in detail reported in the experimental. The residue of the second fraction was further purified by preparative TLC as reported in the experimental yielding *p*-hydroxybenzaldehyde and cytochalasin B (1.0 and 2.2 mg/l, respectively) both as homogeneous amorphous solids.

Finally the organic extract (377.5 mg/kg) of the solid culture of *P. exigua* var. *exigua* strain S-9, obtained as in detail reported in the experimental, was fractionated by silica gel column. The residue of the first fraction was purified by TLC as reported in the experimental giving cytochalasin B as a homogeneous amorphous solid (5.2 mg/kg). The residue of the second and third fraction was independently crystallized from EtOAc-*n*-hexane yielding cytochalasin B as white needles (122 mg/kg). The mother liquors were combined and purified by preparative TLC as reported in the experimental, giving deoxaphomin as a homogeneous amorphous solid (3.1 mg/kg). The residue of the fourth and fifth fraction of the initial column were further purified by TLC as reported in the experimental, giving two homogeneous amorphous solids, which was, in turn, identified as

cytochalasins Z2 and Z3 (**20** and **21**, Fig. 5.7.1, 2.0 and 2.1 mg/kg, respectively) by comparing their spectroscopic (^{1}H and ^{13}C NMR and ESI-MS spectra) and chromatographic behaviour with those of a standard sample (Evidente *et al*., 2002).

The identification of the isolated metabolites was also supported by the extended NMR investigation using bidimensional (COSY, HSQC and HMBC) techniques.

Some of the isolated cytochalasins (B, F and deoxaphomin) are well known metabolites isolated from different fungi (Vurro *et al*., 1997), while cytochalasins Z2 and Z3 were isolated for the first time, together to other well known cytochalsins B, F, T, Z1 and deoxaphomin, from wheat solid culture of *Pyrenophora semeniperda* (Brittlebank & Adam) Shoemaker, a seed-born pathogen proposed as bioherbicide for biological control of grass weed (Evidente *et al*., 2002). These two cytochalasins Z2 and Z3, which showed together to cytochalasin Z1 an originally structure between the 24-oxa[14]cytochalasan subgroup, were biologically characterized testing their capacity to inhibit the germination of wheat and tomato seedlings in comparison to the other above cited cytochalasins and the 21,22-dihydroderivative of cytochalasin B (Evidente *et al*., 2002). Cytochalasins Z2 and Z3 were successively isolated from solid culture of *Phoma exigua* var. *heteromorpha* (Schulzer *et* Sacc.) Noordeloos et Boerema, previously reported as *Ascochyta heteromorpha* (Schulzer *et* Sacc.) Curzi, grown in the same conditions. *P. exigua* var. *heteromorpha* is the causal agent of a foliar disease of oleander (*Nerium oleander* L.), observed in a nursery near Bari, Italy, and was extensively studied for its capacity to produce phytotoxins in liquid cultures. In fact, many already cited cytochalasins were isolated from this culture filtrates as cytochalasins A, B, 7-*O*-acetylcytochalasin B, cytochalasins F, T and deoxaphomin and also new cytochalasins as U, V and W, with the first two belong to the 25,26-dioxa[16]- and the 25-oxa[15] subgroups of cytochalasans, while cytochalasin W is close to cytochalasins B (Vurro *et al*., 1997). When grown on solid culture *P. exigua* var. *heteromorpha* showed an increased capacity to synthesized

cytochalasins. In fact, cytochalasins B was isolated in very large yield together with cytochalasins A, F, T, 7-*O*-acetyl cytochalasin B, Z2 and Z3, as reported in paragraph 1.3.1.

p-Hydroxybenzaldehyde was already known phytotoxic metabolite of fungi pathogenic for some agrarian crops (e.g. apple, stone-leek and onion, and grapewine) (Venkatasuwaiah *et al*., 1991; Guo *et al*., 1996; Tabacchi *et al*., 2000) and forestall plant as a *Ceratocystis* spp., associated with blu stain of pine (Ayer *et al*., 1986). It was also isolated as plant growth metabolites from phytopatogenic *Monilia* spp. (Arinbasarov *et al*., 1988) and as toxin of fungi pathogenic for weeds (*Botryosphearia obtusa*; *Pythium aphanididermatum*) (Capasso et al., 1987; Venkatasuwaiah *et al*., 1991). Assayed on *C. arvense* and *S. arvensis* by leaf disk puncture assay, *p*-hydroxybenzaldehyde was inactive.

A representative culture of *P. exigua* var. *exigua*, the type species of the section *Phyllostictoides* of the genus *Phoma*, was reported to produce both cytochalasins A and B, and antibiotic E (Boerema *et al*., 2004; van der aA *et al*., 2000). A strain of *P. herbarum*, which is type species of the genus *Phoma*, was found to produce cytochalasins C, D and E (El-Kady and Mostafa, 1995). Furthermore, the isolation of cytochalasins from cultures of *Phoma exigua* var. *heteromorpha* (Vurro *et al*., 1997), *P. multipora* (Zhori and Swaber, 1994), and *Phoma spp*. (Wyss *et al*., 1980; Grafa *et al*., 1974) demonstrates these metabolites to be typical for some species or their groups form the genus *Phoma*, whereas they were not found at present time in *Ascochyta* spp.

The production of cytochalasins additionally supports the re-classification of *Ascochyta sonchi*, in particular, strains C-177 and S-9 to *P. exigua* var. *exigua*, which synthesize the above described cytochalasins (B, F, Z2, Z3 and deoxaphomin) and antibiotic E. However, the production of secondary metabolites is not always related to taxonomy. For instance, differentiation between *Phoma foveata* and *P. exigua* both isolated

from potato was inconsistent when it was based only on the production of a secondary metabolite and on the colony morphology (Macdonald *et al.*, 2000).

Several authors proposed *P. exigua* var. *exigua*, in particular strain C-177 (Berestetskiy, 2005; Berestetskiy *et al.*, 2005), a potential mycoherbicide against *C. arvense*. However, this specie was demonstrated to be capable of producing high amounts of known cytochalasins that possess both phytotoxic and cytotoxic activity. Their latter activity restricts usefulness of the fungus as a biocontrol agent.

5.8. Chemical characterization of stagonolides from *Stagonospora cirsii* solid culture, potential herbicides of *C. arvense* and *S. arvensis*

The solid culture of *S. cirsii* (1 kg) was exhaustively extracted as reported in the experimental. The organic extract, showing a high phytotoxic activity, was purified by a combination of column and TLC as described in the experimental giving five metabolites the main of which as crystallized solid and the other ones as four homogenous amorphous solid. Stagonolide (**34,** Fig. 5.8.1) previously isolated from other authors (Yuzikhin *et al.*, 2007), as the main phytotoxin from the culture filtrate of the same fungus was not found. Preliminary ^{1}H and ^{13}C investigations showed that all metabolites have a nonenolide nature, being structurally close themselves and with stagonolide, and consequently were named stagonolides B-F (**45**-**49**, Fig. 5.8.1).

Stagonolide B (**45**) gave a molecular formula of $C_{12}H_{20}O_5$ as deduced from HRESI MS spectrum consistent with 3 unsaturations, two of which are a double bond and a carbonyl lactone group as deduced from the IR spectrum. Preliminary ^{1}H and ^{13}C NMR investigations showed the third one is the nonenolide ring. The IR spectrum (Fig. 5.8.2) also showed bands attributable to hydroxy groups (Nakanishi and Solomon, 1977) while the UV spectrum had no absorption maxima. The ^{1}H and ^{13}C spectra (Figg. 5.8.3 and 5.8.4) showed systems very similar to those herbarumins, the phytotoxins with potential

herbicidal activity isolated from *Phoma herbarum* (Rivero-Cruz *et al*., 2000; 2003). In particular, stagonolide B differs from herbarumin I (Rivero-Cruz *et al*., 2000), for the presence of a further secondary hydroxylated carbons located at C-4 as showed by the broad singlet observed at δ 4.63 in the ^{1}H NMR spectrum, which correlated in the COSY spectrum (Fig. 5.8.5) with H-6, H-5 and H_2-3 at δ 6.00, 5.65 and 2.10 and 1.88, respectively. This proton (H-4) in the HSQC spectrum (Fig. 5.8.6) coupled with the carbon (C-4) present as at the very typical chemical shift value of δ 68.6 (Breitmaier and Voelter, 1987). The couplings observed in the COSY and HSQC spectra allowed to assign the chemical shift to all protons and corresponding carbons (Tables 5.8.1 and 5.8.2, respectively) and to stagonolide B the structure of a 4,7,8-trihydroxy-9-*n*-propyl-5-nonen-9-olide (**45**). This structure was supported by the sodium cluster observed in the HRESI MS spectrum (Fig. 5.8.7) at *m/z* 267.2821 and by the several couplings observed in the HMBC spectrum (Fig. 5.8.8, Table 5.8.3) (Berger and Braun, 2004).

The other four nonenolides C-F (**46-49**) showed in common the lacking of the *n*-propyl group at C-9, which was substituted by a methyl group.

Stagonolide C (**46**) was assigned a molecular formula of $C_{10}H_{16}O_4$ as deduced from HRESI MS spectrum consistent with the same 3 unsaturations of **45** as deduced from IR spectrum and preliminary ^{1}H and ^{13}C NMR investigations. The IR spectrum (Fig. 5.8.9) showed also bands attributable to hydroxy group (Nakanishi and Solomon, 1977) while the UV spectrum had no absorption maxima. The inspection of both ^{1}H and ^{13}C NMR spectra (Figg. 5.8.10 and 5.8.11) showed that **46** in comparison to **45**, beside the substitution of the *n*-propyl at C-9 with a methyl group, differed for the deoxygenation of C-8. In fact, in the ^{1}H NMR spectrum, H-7 appears as a multiplet overlapped to H-4 at δ 4.10 that in the COSY spectrum (Fig. 5.8.12) coupled with the protons of CH_2-8, resonating as a double doublet (*J*=13.8 and 2.6 Hz) and a doublet of double doublets (*J*=13.8, 11.2, 2.6 Hz) at δ

1.88 and 1.77, respectively, which in turn coupled with the double quartet (*J*=11.2 and 6.2 Hz) of H-9 at δ 5.14. This latter coupled with the Me-10, a doublet (*J*=6.2 Hz) resonating at δ 1.22. The two protons of H_2C-8 and those of Me-10 in the HSQC spectrum (Fig. 5.8.13) coupled with the signals present at the typical chemical shift value of δ 43.4 (C-8) and 21.3, respectively (Breitmaier and Voelter, 1987). The couplings observed in the COSY and HSQC spectra allowed to assign the chemical shifts to all protons and corresponding carbons (Tables 5.8.1 and 5.8.2, respectively) and to stagonolide C the structure of 4,7-dihydroxy-9-methyl-5-nonen-9-olide (**46**). This structure was supported by the sodium and potassium clusters observed in the HRESI MS spectrum (Fig. 5.8.14) at *m/z* 223.2168 and 239.2462, respectively, and by the several couplings observed in the HMBC spectrum (Fig. 5.8.15 and Table 5.8.3).

Stagonolide D (**47**) gave a molecular formula of $C_{10}H_{14}O_4$ as deduced from HRESI MS spectrum consistent with 4 unsaturations, with three the same of **45**. The IR spectrum showed bands attributable to a hydroxy group. Both ^{1}H and ^{13}C NMR spectra (Figg. 5.8.16 and 5.8.17) demostrated that **47** in comparison to **45**, beside the substitution of the *n*-propyl at C-9 with a methyl group as in **46**, possessed an epoxy group located between C(7)-C(8). In fact, the ^{1}H NMR spectrum (Table 5.8.1) showed the presence of two double doublets (*J*=4.8 and 3.9 Hz) and (*J*=3.9 and 2.6 Hz) assigned to H-7 and H-8 at δ 3.65 and 3.05, respectively, which are typical chemical shifts value to a 1,2-disubstituted oxiran ring (Batterham, 1972; Pretsch *et al*., 2000). As expected, in the COSY spectrum (Fig. 5.8.18) H-7 coupled with the double doublet (*J*=17.0, 4.8 Hz) of the adjacent olefinic proton (H-6) at δ 5.64 while H-8 coupled with the double quartet (*J*=6.7 and 2.6 Hz) of H-9 at δ 5.34. The two oxiran protons of H-7 and H-8, in the HSQC spectrum (Fig. 5.8.19) coupled with the signals present at the typical chemical shift values of δ 55.4 and 58.2 (C-7 and C-8), (Breitmaier and Voelter, 1987). The coupling observed in the COSY and HSQC spectra

allowed to assign the chemical shift to all protons and corresponding carbons (Tables 5.8.1 and 5.8.2, respectively) and to stagonolide D the structure of 7,8-epoxy-4-hydroxy-9-methyl-5-nonen-9-olide (**47**). This structure was supported by the sodium cluster observed in the HRESI MS spectrum at *m/z* 221.0781 and by the several couplings observed in the HMBC spectrum (Fig. 5.8.20 and Table 5.8.3).

Stagonolide E (**48**) gave a molecular formula of $C_{10}H_{14}O_3$ as deduced from HRESI MS spectrum consistent 4 unsaturations, two of them being a lactone and nonenolide ring as in **45**. The IR spectrum also showed bands attributable to hydroxy and some double bond groups (Nakanishi and Solomon, 1977) while the UV spectrum (Fig. 5.8.21) had an absorption maximum at 250 nm due probably to the extended conjugation of the carbonyl lactone group with one or two double bonds (Scott, 1964). This was confirmed by the inspection of both ^{1}H and ^{13}C NMR spectra (Figg. 5.8.22 and 5.8.23), which when compared to that of **45**, beside the substitution of the *n*-propyl at C-9 with a methyl group as in **46**, showed the presence of signal systems of a 1,4-disubstituted dienyl residue located between C-2 and C-5. In fact, the ^{1}H NMR spectrum (Table 5.8.1) showed the presence of two broad doublets (*J*=11.6 Hz) and (*J*=15.4 Hz), a doublet (*J*=15.4 Hz) and a double doublet (*J*=15.4 and 9.6 Hz) assigned to H-3 and H-4, H-2 and H-5 at the typical chemical shits of δ 6.60 and 6.12, 5.84 and 5.73 (Pretsch *et al*., 2000). In the COSY spectrum (Fig. 5.8.24) besides the coupling between H-2 with H-3 and H-4 with H-5, a very weak coupling (*J*=1.3 Hz) was also observed between H-3 and H-4. Furthermore, H-5 coupled with the proton of an adjacent secondary hydroxylated carbon (HO-CH-6) resonating as a doublet of double doublets (*J*=9.6, 9.0 and 3.8 Hz) at the typical chemical shift values of δ 4.24. In the HSQC spectrum (Fig. 5.8.25), the four protons of the 1,4-dienyl systems and those of the adjacent hydroxylated secondary carbons coupled with the signals observed at the typical chemical shifts values of δ 140.2, 139.6, 126.6 and 125.6

(C-5, C-3, C-4 and C-2) and δ 73.7 (C-6) (Breitmaier and Voelter, 1987). The coupling observed in the COSY and HSQC spectra allowed to assign the chemical shift to all protons and corresponding carbons (Tables 5.8.1 and 5.8.2, respectively) and to stagonolide E the structure of 6-hydroxy-9-methyl-2,4-nonadien-9-olide (**48**). This structure was supported by the sodium cluster observed in the HRESI MS spectrum at *m/z* 205.0852 and by the several couplings observed in the HMBC spectrum (Fig. 5.8.26 and Table 5.8.3).

Stagonolide F (**49**) gave a molecular formula of $C_{10}H_{16}O_3$ as deduced from HRESI MS spectrum consistent with 3 unsaturations. These, as deduced from IR (Fig. 5.8.27), UV spectra and preliminary ^{1}H (Fig. 5.8.28) and ^{13}C NMR investigations, are the same of those observed in putaminoxin, the main phytotoxic nonenolide with potential herbicidal activity isolated from *Phoma putaminum* together some other its congeners (Evidente *et al*., 1995; 1997; 1998a) as reported in the paragraph 1.2. Both ^{1}H and ^{13}C NMR spectra of **49** in comparison to putaminoxin (Evidente *et al*., 1995) showed that the two nonenolides differ only for the substitution of the *n*-propyl at C-9 in putaminoxin with a methyl group in **49**. Accordingly stagonolide F could be formulated as 5-hydroxy-9-methyl-6-nonen-9-olide (**49**). This structure was supported by the sodium cluster observed in the HRESI MS spectrum (Fig. 5.8.29) at *m/z* 207.1943.

As regard the relative stereochemistry of the epoxy group in stagonolide D (**47**) it was assigned by comparison of the $^{3}J_{H,H}$ spin systems with the data reported for suitable 1,2-disubstituted *cis*- and *trans*-oxyrans (Batterham, 1972; Pretsch *et al*., 2000). The stereochemistry of the double bonds of all nonenolides was determined comparing the coupling constants of the olefinic system considered with the value reported in literature (Pretsch *et al*., 2000). The double bonds between C(5)-C(6) in stagonolides B-D (**45**-**47**) and between C(4)-C(5) and C(6)-C(7) in stagonolide E (**48**) and F (**49**) are *trans*, while the

double bond between C(2)-C(3) in **48** is *cis* considering the typical $J_{5,6}$, $J_{4,5}$, and $J_{6,7}$ and $J_{2,3}$ values, respectively (Pretsch *et al*., 2000).

The relative stereochemistry of the chiral carbons of stagonolides B-F (**45**-**49**) was essentially determined by comparison of the $^3J_{H,H}$ spin systems involved with those of herbarumin I and/or putaminoxin of which the absolute stereochemistry was independently determined (Evidente *et al*., 1995; Rivero-Cruz *et al*., 2000). In particular, in stagonolide B (**45**): H-4 is α ($J_{4,5}$=2.6 Hz) while in putaminoxin, in which H-5 is β ($J_{5,6}$=9.4 Hz). In turn, H-7 is β ($J_{5,7}$=2.6 Hz and $J_{7,8}$=$J_{7,9}$=2.4 Hz), as in herbarumin I ($J_{5,7}$=$J_{7,8}$=$J_{7,9}$=2.5 Hz); H-8 is β and H-9 is α ($J_{7,8}$=2.4 Hz and $J_{8,9}$=9.5 Hz) as in herbarumin I ($J_{7,8}$=2.5 Hz and $J_{8,9}$=9.8 Hz).

The relative configuration assigned to stagonolides B-E **(45**-**48**) is in full agreement with the NOE effects observed in the NOESY spectra (Figg. 5.8.30-5.8.33), the main of which were reported in Table 5.8.4, and with the inspection of Dreiding models. Significant NOESY effects were observed: in the spectrum of **45** between H-8 and H-7, and the protons of CH_2-10 and CH_2-11; in the spectrum of **46** between H-7 and H-9; in the spectrum of **47** between H-7 and H-9; and in the spectrum of **48** between H-3 and H-2 and H-4.

Stagonolide F appears to be a diastereomer of aspinolide A, a fungal metabolite isolated together to other nonenolides and polyketides from *Aspergillus ochraceus* and for which any biological activity was reported (Fucsher and Zeeck, 1997). These results were confirmed by the similar spectroscopic data observed for **49** and aspinolides (Fucsher and Zeeck, 1997) and by the different optical properties such as the specific optical rotation and CD data (see experimental).

In conclusion the five new nonenolides could be formulates as following: stagonolide B (**45**): (5*β*,8α,9α,10*β*)-5,8,9-trihydroxy-10-propyl-3,4,5,8,9,10-hexahydro-

oxecin-2-one; stagonolide C (**46**): (5α,8*β*,10*β*)-5,8-dihydroxy-10-methyl-3,4,5,8,9,10-hexahydro-oxecin-2-one; staganolide D (**47**): (1α,2α,7α,10α)-7-hydroxy-2-methyl-3,11-dioaxa-bicyclo[8.1.0]undec-8-en-4-one; stagonolide E (**48**): (7α,10*β*)-7-hydroxy-10-methyl-7,8,9,10-tetrahydro-oxecin-2-one; stagonolide F (**49**): (6α,10*β*)-6-hydroxy-10-methyl-3,4,5,6,9,10-hexahydro-xecin-2-one.

Further purification of the organic extract by a combination of column chromatography and TLC yielding four metabolites (**50-53**, Fig. 5.8.34). Compound **51** was obtained as a solid, and compounds **50**, **52** and **53** as homogenous oils. Preliminary ^{1}H and ^{13}C NMR investigations showed that all metabolites were nonenolides.

Further investigation (essentially 1D and 2D NMR and MS techniques) showed that one of these nonenolides had the same structure as modiolide A (**53**). In particular, the NMR data previously recorded in $CDCl_3$ (Figg. 5.8.35 and 5.8.36 and Tables 5.8.5 and 5.8.6) differed from those reported in CD_3OD because of solvent difference (Tsuda *et al*., 2003). Modiolide A was previously isolated in conjunction with the analogous modiolide B. These were the first two 10-membered macrolides isolated from the culture broth of a fungus separated from the horse mussel *Modiolus auriculatus*, collected at Hedo Cape, Okinawa Island, which was identified as *Paraphaeosphaeria sp.* The antibacterial and antifungal activities of modiolides A and B against *Micrococcus luteus* (MIC value 16.7 mg/ml) and *Neurospora crassa* (MIC value 33.3 mg/ml), respectively, were also reported (Tsuda *et al*., 2003). The first total synthesis of modiolide A, based on the whole-cell yeast catalysed asymmetric reduction of a propargyl ketone, was recently described (Matsuda *et al*., 2007).

The three new nonenolides were structurally similar to stagonolide and stagonolides B-F, previously isolated from the culture filtrates of the same fungus and, consequently, were named stagonolides G-I (**50-53**). All three new stagonolides lacked an *n*-propyl group

at C-9, present in stagonolide and stagonolide B, the *n*-propyl group being substituted in each case by a methyl group, as in stagonolides C-F.

Stagonolide G (**50**) had a molecular formula of $C_{10}H_{16}O_4$ as deduced from HRESI MS data consistent with three degrees of unsaturation, two of which resulted from a double bond and a lactone group as deduced from the IR spectrum and preliminary ^{1}H and ^{13}C NMR investigations. The IR spectrum (Fig. 5.8.37) also showed bands attributable to hydroxy groups (Nakanishi and Solomon, 1977) while the UV spectrum had no absorption maxima. Inspection of the ^{1}H NMR spectrum (Fig. 5.8.38 and Table 5.8.5) showed the presence of a doublet of double doublets (*J*=11.1, 7.7 and 5.2 Hz) and a double doublet (*J*=11.1 and 8.2 Hz) at δ 5.67 and 5.60, typical of two protons (H-6 and H-7, respectively) of a *cis*-1,2-disubstituted olefinic group (Sternhell, 1969; Pretsch *et al*., 2000) and signals of two oxymethine carbons (H-4 and H-8) resonating as a very complex multiplet and a double doublet (*J*=8.2 and 8.2 Hz) at δ 4.54 and 4.11, respectively. H-4 coupled in the COSY spectrum (Fig. 5.8.39) with two doublets of double doublets (*J*=14.5, 7.7, 7.7 and 14.5, 5.2, 5.2 Hz) of CH_2-5 at δ 2.63 and 2.48, and with a multiplet and a doublet of double doublets (*J*=17.7, 10.9 and 9.5 Hz) of CH_2-3 at δ 2.35 and 1.95, respectively. H-8, in turn, coupled with H-7 and with a double quartet (*J*=8.2 and 6.5 Hz) of H-9 at δ 3.67. The ^{13}C NMR spectrum (Fig. 5.8.40 and Table 5.8.6) showed the signals typical of a lactone carbonyl, two secondary olefinic, and three oxymethine carbons at δ 178.0, 132.5, and 127.8, and 79.6, 72.3 and 70.8, which, from the couplings observed in the HSQC spectrum (Fig. 5.8.41), were attributed to C-1, C-7 and C-6, and C-4, C-8 and C-9, respectively (Pretsch *et al*., 2000). The couplings observed in the same spectrum also allowed assignment of the resonances observed in the ^{13}C NMR spectrum at δ 33.7, 28.7, 27.5 and 18.7 to C-5, C-2, C-3, and C-10 (Breitmaier and Voelter, 1987).

The coupling observed in the COSY and HSQC spectra allowed assignment of the chemical shifts to all protons and corresponding carbons (Tables 5.8.5 and 5.8.6, respectively) and for stagonolide G the structure of 4,8-dihydroxy-9-methyl-6-nonen-9-olide (**50**).

This structure was supported by the sodium cluster observed in the HRESI MS spectrum at *m/z* 223.2355 and by the couplings observed in the HMBC spectrum (Fig. 5.8.42 and Table 5.8.7).

Stagonolide H (**51)** had a molecular formula of $C_{10}H_{12}O_4$ as deduced from the HRESI MS spectrum consistent with five degrees of unsaturation, three of which were the same as in **50**. The IR spectrum (Fig. 5.8.43) showed bands attributable to a hydroxy group (Nakanishi and Solomon, 1977), while the UV spectrum had no absorption maxima. Both ^{1}H and ^{13}C NMR spectra (Fig. 5.8.44 and 5.8.45) showed that **51** compared with **50**, differed by the presence of a C(5)-C(6) double bond instead of C(6)-C(7), the presence of an additional C(2)-C(3) double bond, and of a C(7)-C(8) epoxy group as in stagonolide D. In fact, the ^{1}H NMR spectrum (Table 5.8.5) showed the presence of two double doublets (*J*=15.9 and 2.2 Hz and *J*=15.9 and 1.6 Hz), a doublet (*J*=12.0 Hz), and a double doublet (*J*=12.0 and 6.4 Hz) at δ 5.96 and 5.88, and at δ 5.93 and 6.11, typical of two protons (H-5 and H-6) of a *trans*-disubstituted double bond, and two protons (H-2 and H-3) of a *cis*-disubstituted olefinic group (Sternhell, 1969; Pretsch *et al*., 2000). Furthermore, a double doublet (*J*=4.3 and 1.6 Hz) and a broad doublet (*J*=4.3 and < 1.0 Hz), which were assigned to H-7 and H-8, were observed at δ 3.65 and 2.94, respectively, typical chemical shift values for a 1,2-disubstituted oxirane ring (Batterham, 1972; Pretsch *et al*., 2000). As expected, in the COSY spectrum (Fig. 5.8.46) H-7 coupled with the double doublet of the adjacent olefinic proton (H-6), while H-8 coupled with the broad quartet (*J*=6.9 and < 1.0 Hz) of H-9 at δ 5.43. H-3 coupled with H-4 (δ 4.76, brd, *J*=6.4 and 2.2 Hz) oxymethine

that also coupled with the olefinic adjacent H-5. The ^{13}C NMR spectrum (Table 5.8.6) showed, in addition to the lactone carbonyl resonance at δ 167.7 (C-1), the signals typical of four olefinic carbons (δ 133.9, 131.3, 126.1 and 119.7), two oxymethine carbons (δ 66.9 and 65.6), and of an epoxy ring, (δ 56.3 and 55.8). These resonances could be assigned via the HSQC spectrum (Fig. 5.8.47) to C-3, C-5, C-2 and C-6, and C-4 and C-9, and C-8 and C-7, respectively. The same technique also allowed the assignment of the resonance at δ 18.6 to C-10 (Breitmaier and Voelter, 1987).

The coupling observed in the COSY and HSQC spectra permitted the assignment of chemical shifts to all protons and corresponding carbons (Tables 5.8.5 and 5.8.6, respectively), and to stagonolide H the structure 7,8-epoxy-4-hydroxy-9-methyl-2,5-nonadien-9-olide. This structure was supported by the sodium clusters observed in the HRESI MS spectrum at *m/z* 219.2056, and by the couplings observed in the HMBC spectrum (Fig. 5.8.48 and Table 5.8.7).

Stagonolide I (**52**) had a molecular formula $C_{10}H_{14}O_4$ as deduced from the HRESI MS spectrum which was consistent with four degrees of unsaturation, being the same as **51**, as deduced from the IR spectrum and preliminary ^{1}H and ^{13}C NMR results. The IR spectrum (Fig. 5.849) showed also bands attributable to the hydroxy group (Nakanishi and Solomon, 1977), while the UV spectrum had no absorption maxima. Examination of both the ^{1}H and ^{13}C NMR spectra (Figg. 5.8.50 and 5.8.51) showed that **52** in comparison to **51**, differed by the absence of the C(7)-C(8) epoxy group, for the *cis*-configuration of the C(5)-C(6) double bond and the presence of a second oxymethine carbon (C-7). In fact, in the ^{1}H NMR spectrum, H-7 appeared as a broad doublet of double doublets (*J*=9.8, 8.2 and 3.0 Hz) at δ 4.97, which in the COSY spectrum (Fig. 5.8.52) coupled with H-6 (δ 5.50, dd, *J*=10.3 and 8.2 Hz), and with the protons of CH_2-8, (δ 2.24, dd, *J*=13.9, 9.8 and 7.0 Hz) and (δ 1.87, dd, *J*=13.9, 3.9 and 3.0) respectively. The latter, in turn, coupled with the

multiplet of H-9 at δ 5.11. Furthermore, the olefinic H-5 resonated as a double doublet (*J*=10.3 and 9.6 Hz) at δ 5.40 being also coupled with H-4 (δ 5.71, brdd, *J*=9.6, 4.0 and 2.1 Hz) which was also coupled with the adjacent olefinic proton H-3 (δ 6.31, dd, *J*=11.8 and 4.0 Hz), and this, in turn, with H-2 (δ 5.68, dd, *J*=11.8 and 2.1 Hz). The ^{13}C NMR spectrum (Fig. 5.8.51 and Table 5.8.6) showed, apart from the expected signal of the lactone carbonyl at δ 164.8 (C-1), resonances typical of four olefinic carbons (δ 149.1, 134.5, 129.4 and 121.0) as well as those of three oxymethine carbons (δ 68.4, 66.8 and 64.5). These resonances could be assigned via HSQC spectrum (Fig. 5.8.53) to C-3, C-6, C-5 and C-2, and C-9, C-4 and C-7, respectively. The couplings observed in the same spectrum also allowed to assign the signals observed in the ^{13}C NMR spectrum at δ 42.6 and 20.8 to C-8 and C-10, respectively (Breitmaier and Voelter, 1987).

The coupling observed in the COSY and HSQC spectra confirmed the chemical shifts of all protons and corresponding carbons (Tables 5.8.5 and 5.8.6, respectively) and permitted assignment of the structure of stagonolide I as 4,7-dihydroxy-9-methyl-2,5-nonadien-9-olide. This was supported by the sodium cluster observed in the HRESI MS spectrum at *m/z* 221.2117 and by the couplings observed in the HMBC spectrum (Fig. 5.8.54 and Table 5.8.7).

The relative configuration of the epoxy functionality in stagonolide H (**51**), as well the configuration of the double bonds of all nonenolides was determined using the same methods reported above for stagonolides B-F.

The relative configuration of the stereogenic carbons of stagonolides G-I (**50-52**) was essentially determined as previously described for stagonolides B-F using as comparison, modiolide A and herbarumin I, the absolute configuration of which was independently determined by CD, using a suitable derivative, and NOESY and molecular mechanics modelling, respectively (Rivero-Cruz *et al*., 2000; Tsuda *et al*., 2003). In particular, in

stagonolide G (**50**), H-8 is α ($J_{7,8}$=$J_{8,9}$ = 8.2 Hz) as is H-7 in modiolide A ($J_{6,7}$ =7.5 and $J_{7,8}$=11.4 Hz); H-9 is α ($J_{8,9}$=8.2 Hz) as in herbarumin I ($J_{8,9}$=9.8 Hz), H-4 should be β as no effect was observed in the NOESY spectrum (Fig. 5.8.55) between this proton and H-8 and H-9 being both α. In stagonolide H (**51**), H-4 is α ($J_{3,4}$=6.4 and $J_{4,5}$=2.2 Hz) while in modiolide A H-4 is β ($J_{3,4}$=3.5 and $J_{4,5}$=7.3 Hz), H-7 and H-8 both are β ($J_{6,7}$=1.6 and $J_{8,9}$<1.0 Hz) as is stagonolide D in which H-7 and H-8 are both β ($J_{6,7}$=4.8 and $J_{7,8}$=3.9 and $J_{8,9}$=2.6 Hz); H-9 is β ($J_{8,9}$<1.0 Hz), while in herbarumin I H-9 is α ($J_{8,9}$=9.8 and 2.5 Hz). Finally, in stagonolide I (**52**), H-4 is β ($J_{3,4}$=4.0 and $J_{4,5}$=9.6 Hz) as is modiolide A ($J_{3,4}$=3.5 and $J_{4,5}$=7.3 Hz), H-7 is α ($J_{6,7}$=8.2 and $J_{7,8}$=9.8 Hz) as is modiolide A ($J_{6,7}$=7.5 and $J_{7,8}$=11.4 Hz), H-9 is α as ($J_{8,9}$=7.0 and $J_{8,9}$ =3.9 Hz) in modiolide A ($J_{8,9}$=11.4 and $J_{8,9'}$=2.5 Hz).

The relative configuration assigned to stagonolides G-I **(50-52**) is in agreement with the NOE effects observed in the NOESY spectra (Figg. 5.8.55-5.8.57 and Table 5.8.8). In fact, a significant NOE effect was observed in stagonolides G and H between H-8 and H-9, and H-7 and H-8, respectively.

In conclusion the three new nonenolides could be formulates as following: Stagonolide G (**50**): (5α,9β,10β)-5,9-Dihydroxy-10-methyl-3,4,5,6,9,10-hexahydro-oxecin-2-one, Stagonolide H (**51**): (1β,2α,4β,10β)-7-hydroxy-2-methyl-3,11-dioxa-bicyc[8.1.0]undeca-5,8-dien-4-one, Stagonolide I (**52**): (5α,8β,10β)-5,8-dihydroxy-10-methyl-5,8,9,10-tetrahydro-oxecin-2-one.

5.9. Biological activity of stagonolides B-I and modiolide A

Tested by leaf disc-puncture assay at the concentration 1 mg/ml, nonenolides B–F shown no toxicity to *C. arvense* and *S. arvensis* whereas stagonolide was highly toxic to both plants. Stagonolide and stagonolide C were low toxic to *Colpoda steinii* (*Protozoa*) tested at 0.05 mg/ml, other stagonolides were non-toxic.

Stagonolides G-I and modiolide A, tested on *Cirsium arvense* in the same conditions reported above, had different phytotoxic activities. Stagonolide H was the most toxic to the leaves of *C. arvense*, stagonolide I and modiolide A were significantly less active, whereas stagonolide G was inactive (Fig. 5.9.1). The minimum concentration of stagonolide H causing leaf lesions in *C. arvense* was about 30 μg/ml (~$1.5x10^{-4}$ M) (Figure 5.9.2). It is similar to the level of activity of stagonolide (Yuzikhin *et al*., 2007).

At 1 mg/ml only stagonolide H inhibited root growth in chicory seedlings (85% comparing to control), while other compounds were inactive at the concentration used. Stagonolide H appeared to have less inhibitory activity to chicory seedlings than stagonolide, which showed similar activity at 1 μg/ml (Yuzikhin *et al*., 2007).

Leaves of eight plant species were found to have different sensitivities to stagonolide H **(51)**. Leaves of *C. arvense* were significantly more sensitive to **51** (necrotic lesion diameter ~ 7.5 mm, 72 h post application) than other plants tested (necrotic lesion diameter < 4 mm). Tomato leaves were slightly sensitive to the toxin (Figure 5.9.3). Stagonolide H showed both high phytotoxicity and selectively, and this phytotoxin may be considered a potential natural herbicide.

Modiolide A exhibited strong phytotoxicity on radish leaves (necrotic lesion diameter ~ 7 mm, 72 h post application) whereas other plants tested were significantly less sensitive to the toxin (necrotic lesion diameter < 2.5 mm).

The results of biological activity showed that both the functionalization and the conformational freedom of the nonenolide ring appear to be important structural features to impart toxicity. Macrolides, and particularly nonenolides, are common naturally occurring compounds. Structurally close nonenolides appear to be the putaminoxins and the herbarumins, phytotoxins with potential herbicidal activity that were isolated from *Phoma putaminum* (Evidente *et al*., 1995; 1997; 1998a) and *Phoma herbarum* (Rivero-Cruz *et al*., 2000; 2003), respectively. Other phytotoxins are the pinolidoxins and aspinolides A-C

isolated from *Ascochyta pinodes* (Evidente *et al*., 1993a; 1993b) and *A. ochraceus* (Fucsher and Zeeck, 1997), respectively. In addition, the structurally close nonendien-9-olide are modiolide and fusanolide, isolated from *Paraphaesphaeria* sp. (Tsuda *et al*., 2003; Matsuda *et al*., 2007) and *Fusarium* sp. (Shimada *et al*., 2002), respectively.

5.10. Cytochalasins and nonenolides for the management of *C. arvense* and *S. arvensis*

5.10.1. Phytotoxic activity of different fungal toxins on leaves of *C. arvense* and *S. arvensis*

Phoma exigua var. *exigua* and *Stagonospora cirsii* have shown to produce as phytotoxins, cytochalasins and nonenolides. Conseguently, a SAR study was carried out using compounds belonging to both class of natural compounds and some their derivatives (Figg. 5.10.1 and 5.10.2).

Among 15 compounds tested by leaf disc-puncture bioassay, stagonolide (**34**) demonstrated the highest level of toxicity to leaves of *C. arvense* (Fig. 5.10.3). Other nonenolides, putaminoxin (**1**) and 7,8-*O*,*O*'-isopropylidene-pinolidoxin (**72,** Fig. 5.10.1), were significantly less toxic. Among cytochalasins, only cytochalasin A (**25**) was shown to be highly toxic for the weed (Fig. 5.10.3).

Deoxaphomin (**30**) was the most toxic compound for punctured leaf discs of *S. arvensis*. Stagonolide, cytochalasin A and cytochalasin B (**26**) shown high level of phytotoxicity. Other cytochalasins were moderately toxic (Fig. 5.10.3).

Pinolidoxin and 7,8-*O*,*O*'-diacetylpinolidoxin (**6** and **71**) were practically non toxic to leaves of both weeds (Fig. 5.10.3).

The results demonstrated a different behaviour of the two plants (*C. arvense* and *S. arvensis*) in response to the compounds assayed (Fig. 5.10.3). The natural nonenolides were more toxic than cytochalasins on *C. arvense*. Among them the more toxic were

stagonolide and putaminoxin (**34** and **1**) which differ by the location of nucleophilic (hydroxy and double bond) groups on the same fragment between C-5 and C-8 of the macrocyclic ring. Pinolidoxin (**6**), and its two derivatives (**71** and **72**), having a marked modifications in respect to **34** and **1** in both the functional groups and the conformational freedom of the nonenolide ring, showed a strong decrease or practically the total loss of toxicity. These results are in fully agreement with data on a structure activity relationships study performed assaying putaminoxin and pinolidoxin together to their natural and synthetic analogs on several other weeds and cultivated plants (Evidente *et al*, 1998b).

Cytochalasins are more toxic than nonenolide on *S. arvensis*. Among them the more toxic appear to be deoxaphomin, cytochalasins A and B (**30, 25** and **26**), which possess a [13]carbocyclic or a [14]lactonic macrocyclic ring, respectively, joined with an unalterated perihydroisoindolyl residue. In this latter moiety, the presence of the secondary hydroxyl on C-7, which lack in **28, 29** and **20** or was acetylated in **27** and **74**, (Fig. 5.10.1), appear to be an important feature to impart toxicity. Furthermore, the significant decrease of toxicity observed testing the 21,22-dihydroderivative of cytochalasin B (**73**, Fig. 5.10.1) and cytochalasins Z3 (**21**) also indicate the importance of the functionalization on C-20 and the conformational freedom of the macrocyclic ring. These results are in accordance with those previously described in structure activity relationships studies (Bottalico *et al*., 1990; Capasso *et al*., 1991; Vurro *et al*., 1997; Evidente *et al*., 2002).

5.10.2. Effect of selected toxins on photometric properties of *Cirsium arvense* leaves

Five toxins were selected to study their effect on relative chlorophyll content in *C. arvense* leaves by measuring the light absorption at the wavelength of 632.8 nm. The first necroses on leaf discs appeared 6-8 hours post toxin application. Comparing to control, significant changes in the light absorption of leaf discs were caused by cytochalasin A after 2 hours post treatment (Table 5.10.1). The ability of *C. arvense* leaves to absorb light of

the wave 632.8 nm was significantly decreased by stagonolide, putaminoxin and both cytochalasins A and B after 4 hours post treatment. Negative effect of both studied nonenolides on the light absorption and relative chlorophyll content was about 2 times higher than the effect caused by the cytochalasins. The effect of deoxaphomin on relative chlorophyll content was not profound. The changes in the light absorption at the wave 632.8 nm and development of lesions in leaves of *C. arvense* caused by the toxins did not correlate (Table 5.10.1).

Both cytochalasin B and stagonolide caused significant decrease of the light absorption at the wave 450 nm (Table 5.10.2). This observation is most likely connected with the reduction of the content of β-carotene or/and chlorophyll b in leaf tissue of *C. arvense*, because both pigments have a peak of resonant absorption near this wavelength (Britton, 1983).

The increased level of light absorption at 530 and 550 nm was found to be caused by both toxins. However, stagonolide had significantly stronger effect at the wavelength 550 nm than cytochalasin B. It is known that there is the peak of light absorption of cytochrome C in the wavelength range of 530-550 nm. Cytochrome C is a soluble protein with a heme prosthetic group that is involved in mitochondrial electron transport. Possibly, the toxins affected the concentration of cytochrome C in leaf tissue of *C. arvense*.

The reduction of light absorption in the wavelength region of 630-690 nm by *C. arvense* leaves was observed after the treatment of leaf discs by stagonolide only. The peaks of light absorption in this region are characteristic for chlorophyll intermediates, protochlorophyllide and chlorophyllide. Tentoxin (a phytotoxin of several *Alternaria* spp.) and some synthetic herbicides similarly were found to affect chlorophyll synthesis as by *in vitro* spectrometry observations (Duke *et al*., 1991).

Stagonolide also was found to significantly increase light absorption by *C. arvense* leaves in near infrared spectra (Table 5.10.2). Repeated experiments supported the data. At the wavelength more than 700 nm leaves of healthy plants are usually transparent for radiation and the light absorption is minimal or absent. It is known that bacteriochlorophylls, "reduced" forms of plant chlorophyll (without phytol moiety), have absorption maxima from 800 and 875 nm (Britton, 1983).

The results of photometric assays performed with different equipment were in accordance. In fact, the nonenolides, in particular stagonolide and putaminoxin (**34** and **1**), appear to more affect the light absorption at different wavelengths than cytochalasins (cytochalasins A and B, **25** and **26**) and probably the same structural features above discussed for each group of compounds are important to impart this activity.

5.10.3. Effect of selected toxins on conductometric properties of *Cirsium arvense* leaves

In vivo measurement of electrical resistivity in leaf tissues of *C. arvense* showed its growth (up to 100 Ohm) during course of the electrical current in the intact discs (Fig. 5.10.4). Under electrical tension cell ions were accumulated at electrodes and interfered the current. In boiled discs initial increasing of resistivity was changed by its falling to the minimal values (about 10 Ohm) after 150 seconds post the first measurement. Leaf discs treated with cytochalasin B did not expressed considerable changes of resistivity during measurement time. The resistivity dynamics of discs treated with stagonolide was linear and similar to control but with lower angle (Fig. 5.10.4). The results allow to assume that stagonolide practically did not affect the permeability of cellular membranes, while cytochalasin B caused electrolyte leakage from cells of leaf tissues of *C. arvense*.

This observation was supported by another experiment. It was shown that conductivity of water extracts obtained from leaf discs treated with stagonolide was similar

to control treatment and was two times lower than conductivity of the extracts from discs treated with cytochalasin B (Fig. 5.10.5).

These results did not surprise considering the well know effects of cytochalsins, in particular cytochalasins B (**26**), in certain plants. This cytochalasin inhibited cytoplasmatic streaming, organelle movement, cell division, pollen germination, cell wall metabolisms and auxin transport (Natori and Yahara, 1991).

5.11. Chemical characterization of phytotoxins from *Phyllosticta cirsii* culture filtrate, potential herbicides of *C. arvense*

The liquid culture of *P. cirsii* (7.7 l) was exhaustively extracted as reported in the experimental. The organic extract, having high phytotoxicity, was purified by a combination of column chromatography and TLC as described in the experimental. Four metabolites were obtained as homogeneous oily compounds (11.0, 1.0, 0.9 and 0.5 mg/l, respectively), which were named phyllostictine A-D (**54**-**57**, Fig. 5.11.1). Preliminary ^{1}H and ^{13}C investigations allowed to demonstrate that these metabolites have close related structures being, as described below, four novel oxazatricycloalkenones.

Phyllostictine A (**54**) is the main phytotoxic metabolite, and has a molecular formula $C_{17}H_{27}NO_5$, as deduced from HRESI MS spectra, consistent with 5 unsaturations. Two of them were a tetrasubstituted double bond and a carbonyl lactame group, as deduced from the IR spectrum and preliminary ^{1}H and ^{13}C NMR investigations. The IR spectrum (Fig. 5.11.2) also showed bands attributable to hydroxy groups (Nakanishi and Solomon, 1977) while the UV spectrum (Fig. 5.11.3) exhibited an absorption maximum typical of α,β-unsaturated lactames (Scott, 1964). In particular, the ^{1}H NMR spectrum (Fig. 5.11.4 and Table 5.11) of phyllostictine A showed the presence of one broad and two sharp singlets at δ 4.45, 3.91 and 1.27 respectively, attributable to the protons of a secondary hydroxylated carbon (HO-CH-15), to a methoxy and to a tertiary methyl (Me-C-5) group, respectively

(Pretsch *et al*., 2000). H-15 appeared long-range coupled (J<1 Hz) in the COSY spectrum (Fig. 5.11.5) with the broad singlet of a hydroxy group resonating at δ 3.61. A broad singlet attributable to another hydroxy group was also observed at δ 2.80. In the same spectrum, the significant presence of two sharp doublets (J=0.9 Hz), typical of an AB system of an oxygenated methylene group (H_2C-14), as well as, a multiplet due to a proton of another hydroxylated secondary carbon (HO-CH-11), were observed at δ 5.08 and 5.03, and 4.04, respectively. In the COSY spectrum the latter coupled with one or both the protons of the adjacent methylene group (H_2C-10) resonating as complex multiplet at δ 1.80, which were, in turn, coupled with the protons of the successive methylene group (H_2C-9) observed as multiplets at δ 1.58 and 1.37, respectively. The region of the aliphatic protons presented also a very complex multiplet at δ 1.30-1.26 attributable to the protons of three other methylene groups (H_2C-8, H_2C-7 and H_2C-6) (Pretsch *et al*., 2000) which are coupled themselves and with the protons of H_2C-9, as appeared from the COSY spectrum. Furthermore, the triplet (J=7.1 Hz) of the methyl ($\underline{Me}CH_2$-N) of a N-ethyl group resonated at δ 0.83 and in the COSY spectrum coupled with the protons of the adjacent methylene group (Me$\underline{CH_2}$-N) which overlapped at δ 1.30 with the complex signals of the above described methylene groups (H_2C-8, H_2C-7 and H_2C-6) (Pretsch *et al*., 2000). The ^{13}C NMR spectrum (Fig. 5.11.6 and Table 5.11.2) showed the presence of the signals of a lactame carbonyl and those of the α,β-conjugated tetrasubstituted double bond at the typical chemical shifts values of δ 166.6, 156.2 and 136.3 (C-3, C-2 and C-1), respectively (Breitmaier and Voelter, 1987). The oxygenated methylene and two hydroxylated methyne carbons observed at δ 92.7, 86.3 and 68.4 were attributed to C-14, C-11 and C-15 respectively, also based on the coupling observed in the HSQC spectrum (Fig. 5.11.7), as well as the signals at δ 64.5, 17.1 and 14.1 were assigned to the methoxy, the tertiary methyl (Me-C-5) and the methyl group of the N-ethyl residue and those at δ 27.5 and 26.5

to the methylene carbons C-10 and C-9 (Breitmaier and Voelter, 1987). Finally, the two signals at δ 104.3 and 71.8 were assigned to the dioxygenated and nitrogen linked quaternary carbons C-12 and C-5 (Breitmaier and Voelter, 1987). The latter represents the closure of the 3,5-dihydroxy-4-methoxy-11-methylcycloundec-1-ene macrocyclic ring. This hypothesis was confirmed by the typical chemical shifts values of δ 29.7, 29.3 and 22.6 (C-8, C-7 and C-6, respectively) observed for the carbons of the other three methylene groups belonging to the macrocyclic ring (Breitmaier and Voelter, 1987) and the couplings observed in the HMBC spectrum (Fig. 5.11.8 and Table 5.11.3). The correlations observed in this latter spectrum also allowed to locate the tertiary methyl group on C-5, which represents one of the bridge-head carbons of the junction between the macrocyclic and the N-ethyl β-lactame (2-azetidone) rings, while the other one is the olefinic carbon C-1. Based also on the coupling observed in the HMBC spectrum (Table 5.11.3), the remaining unsaturation was attributed to a 2,2,3,4-tetrasubstituted 2,3,5-thrihydrofuran ring which was joined with the macrocyclic ring through two bridge-head carbons, namely the other quaternary olefinic (C-2) and the deoxygenated quaternary (C-12) carbons. On the basis of these results phyllostictine A appears to be a new oxazatricycloalkenones, to which the structure of a 4-ethyl-11,15-dihydroxy-12-methoxy-5-methyl-13-oxa-4-aza-tricyclo [10.2.1.0*2,5*]pentadec-1-en-3-one (**54**) can be assigned. This structure was confirmed by the results observed in the ESI and EI mass spectra. In fact, the HRESI MS spectrum (Fig. 5.11.9) recorded in positive modality showed sodium clusters formed by the toxin itself and the corresponding dimmer at *m/z* 348.1800, $[M+Na]^+$ and 673.3680 $[2M+Na]^+$, respectively, as well as the pseudomolecular ion $[M+H]^+$ at *m/z* 326.1962. The same spectrum, recorded in negative modality, showed the pseudomolecular ion $[M-H]^-$ and that of the corresponding dimmer $[2M-H]^-$ at *m/z* 324.1815 and 649.3678, respectively. Significant were the data of the EIMS spectrum which did not show the molecular ion but

peaks due to fragmentation typical of the presence both a β-lactame and a suitable substituted trihydrofuran ring, methoxy, hydroxy and tertiary methyl groups (Porter, 1985; Pretsch *et al*., 2000). In fact, the molecular ion losing in succession the methoxy group and H_2O generated the ions at *m/z* 294 and 276. Alternatively, the molecular ion losing in succession the methoxy group followed by CO and Me residues yielded the ion at *m/z* and 251. Significant for the presence of the β-lactame residue is the most abundant ion $[Et\text{-}N{=}C{=}O]^+$ observed at *m/z* 71 (Porter, 1985).

The structure assigned to phyllostictine A was further supported by converting the toxin into the mono- and di-acetyl derivatives (**58** and **59**) by the usual reaction with pyridine and acetic anhydride. The spectroscopic data of both derivatives were full consistent with the structure **54** assigned to the toxin. In particular, the IR spectrum of the 15-*O*-acetylphyllostictine A (**58**) still showed the presence of hydroxy groups, which are obviously absent in that of the 11,15-diaceyl derivative (**59**). The ^1H and ^{13}C NMR spectra of **58** differed from those of **54** for the significant downfield shift (Δδ 1.14) of H-15 at δ 5.59 and for the presence of the singlet of the acetyl group ad δ 2.19, respectively (Pretsch *et al*., 2000), and for the presence of the signals of the acetyl group observed at δ 172.4 (Me<u>C</u>O) and 20.9 <u>Me</u>CO), (Breitmaier and Voelter, 1987). Similarly, the same spectra of **59**, compared to those of **54**, showed, respectively, the downfiled shift of both H-15 and H-11 (Δδ 1.14 and 1.16) at δ 5.59 and 5.20 and the presence of the singlets of two acetyl groups at δ 2.13 and 1.99 (Pretsch *et al*., 2000), and the signals of the two acetyl groups at δ 170.1 and 169.9 (two Me<u>C</u>O) and δ 22.1 and 20.8 (two <u>Me</u>CO), (Breitmaier and Voelter, 1987).

The other three phyllostictines B-D (**55-57**) appear to be very closely related to phyllostictine A and each other.

Phyllostictine B (**55**) has a molecular formula of $C_{15}H_{23}NO_5$ as deduced from HRESI MS spectra consistent with the same 5 unsaturations of **54**, which are in agreement with the IR bands and the preliminary ^{1}H and ^{13}C NMR investigations, but differed for the lack of two CH_2 groups. As expected, the IR and UV spectra (Figg. 5.11.10 and 5.11.11) were very similar to those of **54.** The investigation of the ^{1}H and ^{13}C NMR spectra (Figg. 5.11.12 and 5.11.13, and Tables 5.11.1 and 5.11.2) confirmed that the two toxins differed for the size of the macrocyclic ring, which is a 3,5-dihydroxy-4-methoxy-11-methylcycloundec-1-ene in **54**, while is a 3,5-dihydroxy-4-methoxy-9-methyl-cyclonon-1-ene in **55**. The couplings observed in the COSY and HSQC spectra (Figg. 5.11.14 and 5.11.15) allowed to assign the chemical shifts to all the protons and the corresponding carbons (Tables 5.11.1 and 5.11.2, respectively) and to phyllostictine B the structure of 4-ethyl-9,13-dihydroxy-10-methoxy-5-methyl-11-oxa-4-aza-tricyclo[8.2.1.0*2,5*]tridec-1-en-3-one (**55**). This structure was supported by the several couplings observed in the HMBC spectrum (Fig. 5.11.16 and Table 5.11.3) and by the pseudomolecular ion and sodium clusters observed in the HRESI MS spectrum (Fig. 5.11.17) for the toxin itself and its dimmer and trimmer at *m/z* 298.1628 $[M+H]^+$ and 320.1443 $[M+Na]^+$, 617.2984 $[2M+Na]^+$, 914 $[3M+Na]^+$, respectively. Furthermore, the same spectrum recorded in negative modality showed the pseudolmolecular ion $[M-H]^-$ at *m/z* 296.1500. The stucture **55** was further supported by the data of its EIMS spectrum, which showed, beside the pseudomolecular ion $[MH]^+$ at *m/z* 298, ions produced by fragmentation mechanisms similar to those observed in **54**. In fact, the pseudomolecular ion by loss of H_2O generated the ion at *m/z* 280, as well as the molecular ion $[M]^+$ produced the ions at *m/z* 266, 248 and 223 by successive loss of methoxy, H_2O and Me residues, respectively. Finally, the most abundant ion $[Et\text{-}N{=}C{=}O]^+$, which is significantly due to the presence of the β-lactame residue, was observed at *m/z* 71 (Porter, 1985; Pretsch *et al.*, 2000).

Phyllostictine C (**56**) has a molecular formula of $C_{17}H_{27}NO_6$ as deduced from HRESI MS spectrum consistent with the same 5 unsaturations of **54**, which are in agreement with the IR bands (Fig. 5.11.18) and the preliminary ^{1}H and ^{13}C NMR investigation. A comparison of both ^{1}H and ^{13}C NMR spectra (Figg. 5.11.19 and 5.11.20) of phyllostictine C with those of **54** showed that the two toxins differed for the substituent at C-5 and for the macrocyclic ring size, which in **56** is a 3,5-dihydroxy-4-methoxy-10-(1-hyroxyethyl)-cyclodec-1-ene. In fact, in the region of the aliphatic methylene group of both spectra of **56** signals accounting for only four methylene protons are present, and lacked the signal of the tertiary methyl group, which in **54** is linked to C-5. On the contrary, the significant presence of the signals of 1-hydroyethyl group was observed (Breitmaier and Voelter, 1987; Pretsch *et al*., 2000). In particular, the ^{1}H NMR spectrum (Fig. 5.11.19) showed presence of the multiplet due to the proton of a further secondary hydroxylated carbon (Me<u>CH</u>-OH), the doublet (J = 6.2 Hz) of the adjacent terminal methyl group (<u>Me</u>-CH-OH), and the broad singlet of a further hydroxy group at δ 3.80, 1.18 and 1.61, respectively (Pretsch *et al*., 2000). The ^{13}C NMR spectrum (Fig. 5.11.20) showed the signals of the corresponding secondary hydroxylated carbon (Me<u>CH</u>-OH) and methyl group (<u>Me</u>CH-OH) at δ 68.1 and 23.6 (Breitmaier and Voelter, 1987). The couplings observed in the COSY and HSQC spectra (Figg. 5.11.21 and 5.11.22) allowed to assign the chemical shifts to all the protons and the corresponding carbons (Tables 5.11.1 and 5.11.2, respectively) and to phyllostictine C the structure of 4-ethyl-10,14-dihydroxy-5-(1-hydroxyethyl)-11-methoxy-12-oxa-4-aza-tricyclo[9.2.1.0*2,5*]tetradec-1-en-3-one (**56**). This structure was supported by the several couplings observed in the HMBC spectrum (Fig. 5.11.23 and Table 5.11.3) and by the sodium clusters observed in the HRESI MS spectrum (Fig. 5.11.24) for the toxin itself and its dimmer and trimmer at *m/z* 364.1707 $[M+Na]^+$, 705 $[2M+Na]^+$ and 1046 $[3M+Na]^+$, respectively.

Phyllostictine D (**57**) has a molecular formula of $C_{17}H_{25}NO_6$ as deduced from HRESI MS spectrum consistent with 5 unsaturations, four of which were the same observed **54** and in agreement with the IR bands (Fig. 5.11.25) and preliminary ^{1}H and ^{13}C NMR investigations. A comparison of both ^{1}H and ^{13}C NMR spectra (Figg. 5.11.26 and 5.11.27) of phyllostictine D with those of **54** showed that the two toxins differed for the size and the functionalization of both the lactame and macrocyclic rings. In **57** the lactame appears to be an N-methyl-δ-lactame (2-piperidone) always joined, through the same two bridge-head carbons to the macrocyclic ring, which in **57** is 3,5-dihydroxy-4-methoxy-10-methyl-9-oxo-cyclodec-1-ene. In fact, the region of the aliphatic methylene and methyl groups of both ^{1}H and ^{13}C NMR spectra of **57,** compared to those of **54**, showed substantial differences. Complex multiplets and one singlet accounting for only three methylene groups belong to the macrocyclic ring and the methyl group bonded to the bridge-head quaternary carbon (C-7) were observed in the ^{1}H NMR spectrum. In addition, the triplet (J=7.3 Hz) and the singlet of a methylene (CH_2-5) and methyl (N-Me) bonded to a nitrogen atom were observed at the typical chemical shifts values of δ 2.44 and 2.14 respectively (Pretsch *et al*., 2000), while the protons of the other methylene (CH_2-6) group of the δ-lactame ring adjacent to CH_2-5 resonated as two complex multiplets at δ 1.61 and 1.36. In the ^{13}C NMR spectrum the carbons of these two methylene groups and that of N-methyl group appeared at the very typical chemical shifts values of δ 43.6, 23.6 and 29.9 (C-5, C-6 and Me-N), respectively (Breitmaier and Voelter, 1987). In addition, the signal of a saturated ketone group (O=C-8) was observed at the expected chemical shift value of δ 210.0 (Breitmaier and Voelter, 1987). The couplings observed in the COSY and HSQC spectra (Figg. 5.11.28 and 5.11.29) allowed to assign the chemical shifts to all the protons and the corresponding carbons (Tables 5.11.1 and 5.11.2, respectively) and to phyllostictine D the structure of 12,16-dihydroxy-13-methoxy-4,7-dimethyl-14-oxa-4-aza-

tricyclo[11.2.1.0*2,7*]hexadec-1-en-3,8-dione (**57**). This structure was supported by the several couplings observed in the HMBC spectrum (Fig. 5.11.30 and Table 5.11.3) and by the sodium clusters observed in the HRESI MS spectrum (Fig. 5.11.31) for the toxin itself and its dimmer and trimmer at *m/z* 362.1548 $[M+Na]^+$, 701 $[2M+Na]^+$ and 1040 $[3M+Na]^+$, respectively.

The absolute stereochemistry of the secondary hydroxylated carbon C-15 of phyllostictine A (**54**) was determined applying the Mosher's method (Dale *et al*., 1969; Dale and Mosher, 1973; Ohtani *et al*., 1991). By reaction with the *R*-(-)-α-methoxy-α-trifluorophenylacetate (MTPA) and *S*-(+)MTPA chlorides, phyllostictine A was converted in the corresponding diastereomeric *S*-MTPA and *R*-MTPA esters (**60** and **61** respectively), whose spectroscopic data were consistent with the structure assigned to **54**. The comparison between the ^{1}H NMR data (see experimental) of the *S*-MTPA ester (**60**) and those of the *R*-MTPA ester (**61**) of **54** [Δδ (**60**-**61**): H-11 +0.07; H_2-10 +0.17; H-9 +0.24; H-9' +0.13] allowed to assign an *S*-configuration at C-15. The significant effects observed in the NOESY spectrum (Table 5.11.4) allowed to assign the relative configuration to C-12, C-11 and C-5 being the MeO, H-11 and Me-C(5) at the same side of the molecule, while the double bond appeared to have an *E*-configuration (Pretsch *et al*., 2000). Considering the absolute *S*-stereochemistry determined for C-15, the absolute stereochemistry of C-5, C-11 and C-12 should be *R*, *S* and *S*, respectively.

On the basis of the similar spectroscopic properties of phyllosticitines B-D with those of phyllostictine A and the NOESY effects recorded for these toxins (Figg. 5.11.32 and 5.11.33 and Table 5.11.4), the absolute stereochemistry of the chiral centres of **55**-**57** could be assigned as that observed in **54** and as depicted in their structural formulae with the exception of C-7 of **57,** which should be *S* as the substituent priority is opposite in respect to that of **54**.

Besides phyllostictine A-D, two other compounds were obtained as an amorphous and crystalline solid, respectively, which were named phyllostoxin and phyllostin (**62** and **63,** 0.78 and 0.90 mg/l, Fig. 5.11.34).

Preliminary ^{1}H and ^{13}C NMR investigation showed that the two metabolites were considerably different from phyllostictines A-D.

Phyllostoxin (**62**), the most phytotoxic metabolite, together with phyllostictine A, has a molecular formula of $C_{15}H_{16}O_4$ as deduced from HRESI MS spectrum, consistent with 8 unsaturations four of which were attributed to a tetra-substituted benzene ring, and the other four to a ketone, an ester and a conjugated carbonyl group in agreement with the typical bands and absorption maxima observed in both IR (Fig. 5.11.35) and UV spectra.

The ^{1}H spectrum (Fig. 5.11.36 and Table 5.10.5) showed the doublets (J=9.9 Hz) of two *ortho*-coupled aromatic protons at the typical chemical shift values of δ 7.88 and 6.15 (H-5 and H-4) (Pretsch *et al*., 2000). Furthermore, the singlets typical of an aromatic and acetyl methyl group were observed at δ 2.36 (Me-11) and 2.00 (Me-10) respectively, together with the triplet (J=7.5 Hz) of the methyl (Me-14) of a propionyl residue resonating at δ 0.66. In the COSY spectrum the latter coupled with the two double quartets (J=14.8 and 7.5) of the protons of the adjacent methylene group (CH_2-13), which, in turn, resulted also bonded to the saturated ketone group (O=C-12) by the correlations observed in the HMBC spectrum (Fig. 5.11.37 and Table 5.11.5). The couplings observed in the same spectrum allowed assignment the remaining methyl group (Me-15), resonating as singlet at δ 1.42, at the quaternary carbon C-7 (Pretsch *et al*., 2000). In the ^{13}C NMR spectrum (Fig. 5.11.38 and Table 5.11.5) C-7 appeared at the typical chemical shift value of δ 53.6 (Breitmaier and Voelter, 1987) and on the basis of the correlation observed in the HMBC spectrum (Table 5.11.5), it appeared also bonded to the propionyl residue. C-7 represents the fourth carbon of a disubstituted cyclobutanone ring, which accounted for the

remaining unsaturation of **62**. In the HMBC spectrum this latter ketone group (O=C-8), resonating at δ 170.0, coupled with H-5, and with the quaternary methyl group Me-15. The disubstituted cyclobutanone ring joined the benzene ring through its bridge-head quaternary carbons C-1 and C-6, appearing in the ^{13}C NMR spectrum at the typical chemical shifts values of δ 115.8 and 121.1 (Breitmaier and Voelter, 1987). In the same spectrum, the acetyloxy and the aromatic methyl carbons, appeared at δ 175.0 (O=C-9), 10.6 (Me-10) and 17.8 (Me-11), and were assigned, on the basis of the coupling observed in the HMBC spectrum, on C-2 and C-3 of the benzene ring, respectively. The latter two carbons were observed at typical chemical shift values of δ 161.0 and 130.0 (C-2 and C-3) as well as the signals at δ 138.0 and 124.0 were assigned to C-5 and C-4, respectively (Breitmaier and Voelter, 1987), also on the coupling observed in the HSQC spectrum (Fig. 5.11.39). The signals of the propionyl and the tertiary methyl group were observed at δ 201.0 (O=C-12), 33.0 (C-13) and 9.6 (C-14) and 24.0 (C-15), respectively and were attributed also on the basis of the couplings observed in the HSQC spectrum. On the basis of these results phyllostoxin proved to be a new fungal metabolite having the structure of acetic acid 3,7-dimethyl-8-oxo-7-propionyl-bicyclo[4.2.0]octa-1,3,5-trien-2-yl ester (**62**). This structure was confirmed by the results observed in the ESI and EI MS spectra. In fact, the HRESI MS spectrum, recorded in positive modality, showed sodium clusters formed by the molecular ion after the loss of C=O and those of the corresponding dimmer at *m/z* 255 and 487.2070, together with the protonated ion of the cited dimmer at *m/z* 465.2254. Furthermore, the EIMS spectrum did not show the molecular ion, but ions produced by a fragmentation mechanism typical of the functionalities present in **62** (Pretsch *et al*., 2000). In fact, the molecular ion by loss of CO produced the ion at *m/z* 232 and this, in turn, by alternatively loss of MeCO or CH_2=C=C=O residues yielded the ions at *m/* 189 and 175, respectively. The most abundant ion at *m/z* 217 was formed from the molecular ion by loss

of the acetyl residue and this, in turn, by the loss of CH_2=C=C=O residue generated the ion at *m/z* 161. When the molecular ion lost the CH_2=C=C=O residue yielded the ion at *m/z* 204. Finally, also the significant acetyl ion was observed at *m/z* 43.

The structure of phyllostoxin appears quite rigid as observed by the inspection of its Deriding model. The NOE effects observed in the NOESY spectrum (Table 5.11.6) showed the expected proximity of both the aromatic protons (H-4 and H-5), that of the protons of the methylene (CH_2-13) with both the terminal methyl (Me-14) groups of the propionyl residue and the quaternary methyl group (Me-15), as well as that of the aromatic methyl (Me-11) and the methyl (Me-10) of the acetyloxy groups. These results confirmed the structure assigned to **62**.

Phyllostin (**63**) has a molecular formula of $C_{11}H_{14}O_6$ as deduced from HRESI MS spectrum, consistent with 5 unsaturations, three of which were attributed to the two ester carbonyl groups and to a trisubstituted conjugated double bond, as also in agreement with the typical bands and absorption maxima observed in both IR (Fig. 5.11.40) and UV spectra.

The ^{1}H NMR spectrum (Fig. 5.11.41 and Table 5.11.7) showed the presence of a broad singlet typical of an olefinic proton (H-7) at δ 6.75, which in the COSY spectrum coupled with both the proton (H-8) of a secondary hydroxylated carbon and one proton of the methylene group (CH_2-5), resonating as a broad doublet (*J*=8.4) and a doublet of double doublets (*J*=17.5, 9.9, 3.3) at the expected chemical shift values of δ 4.54 and 2.40 respectively (Pretsch *et al*., 2000). The latter (H-5'), in turn, coupled both with the double doublet (*J*=17.5 and 6.1 Hz) of the geminal proton (H-5) at δ 2.99, and with the proton of the adjacent secondary oxygenated carbon (CH-4a), which resonated at δ 3.76 as a doublet of double doublets (*J*=9.9, 8.6 and 6.1), being also coupled with the double doublet (*J*=8.6

and 8.4 Hz) at δ 4.34 due to the proton of the adjacent secondary oxygenated carbon (CH-8a). The latter also coupled with the proton H-8 above described.

These results showed in **63** the presence of a tetrasubstituted cyclohexene ring joined to a trisubstituted 2-oxo-1,4-dioxan ring. In fact, the ^{1}H NMR spectrum also showed the quartet (*J*=7.0) of a secondary oxygenated carbon belonging to this latter ring, which coupled, in the COSY spectrum, with the doublet (*J*=7.0 Hz) of the adjacent methyl group (Me-9), and the singlet of an ester methoxy group (Me-11) at δ 3.78 (*16*). The ^{13}C NMR spectrum of **63** (Fig. 5.11.42 and Table 5.11.7) showed the expected presence of two ester carbonyl groups, the quaternary olefinic carbon and the methoxy group at δ 169.0, 167.0, 132.0 and 52.4 and were assigned also based on the HMBC correlations (Fig. 5.11.43 and Table 5.11.7) to C-2, C-10, C-6 and C-11, respectively (Breitmaier and Voelter, 1987). The signals of the secondary olefinic carbon and those of four oxygenated methine carbons were observed at typical chemical shift values of δ 137.0, 84.3, 73.1, 70.3 and 70.2 and, were assigned to C-7, C-8a, C-3, C-4a and C-8, respectively, on the basis of the HSQC couplings (Fig. 5.11.44). Furthermore, the signals of the methylene and the secondary methyl groups at δ 29.8 and 17.9 were assigned to C-5 and C-9, respectively (Breitmaier and Voelter, 1987). The several interesting correlations observed in the HMBC spectrum (Table 5.11.7) joined the tetrasubstituted cyclohexene ring to the trisubstituted 2-oxo-1,4-dioxan ring through the bridge-head carbons C-4a and C-8a, and to locate the carboxymethyl and the methyl groups at C-6 and C-3, respectively. On the basis of these results phyllostin is assigned the structure of a 8-hydroxy-3-methyl-2-oxo-2,3,4a,5,8,8a-hexahydro-benzo[1,4]dioxine-6-carboxylic acid methyl ester (**63**).

This structure (**63**) was confirmed by the data obtained from the EI and ESI MS spectra. In fact the HRESI MS spectrum showed the molecular ion at *m/z* 242.0802 and ions formed by fragmentation mechanisms typical of the ring nature and functionalities

present in **63** (Porter, 1985; Pretsch *et al*., 2000). The molecular ion losing in succession CO, CO_2 and CO residues produced ions at *m/z* 214, 170 and 142, respectively. Alternatively, the molecular ion yielded the ions at *m/z* 225 and 211, by loss of OH or MeO residues, respectively. The ESI MS spectrum showed the potassium and sodium clusters at *m/z* 281 and 265.

On the basis of above NMR data and the several NOE couplings observed in the NOESY spectrum (Table 5.11.6) the relative stereochemistry of junction between the two rings and the four chiral carbons was assigned as depicted in **63**. As deduced from a Dreiding model inspection, the tetrasubstituted cyclohexene and the trisubstituted 2-oxo-1,4-dioxan rings assume a half-chair and a like-chair conformation, respectively. They appeared *trans* joined considering the typical axial-axial values (*J*=8.6 Hz) measured for the coupling between H-4a and H-8a (Pretsch *et al*., 2000). This conformation and the relative stereochemistry of all the chiral centres were definitively assigned by an X-ray diffrattometric analysis of **63,** and resulted to be: 3*R*,4a*S*,8*R*,8a*S* or its enantiomer 3*S*,4a*R*,8*S*,8a*R*.

5.12. Biological activity of phyllostictine A-D, phyllostoxin and phyllostin

When tested at concentration around 6 x 10^{-3} M by the leaf puncture assay on *C. arvense*, phyllostictines had different toxicity. Phyllostictine A was particularly active, causing the fast appearance of large necrotic spots (about 6-7 mm of diameter). Phyllostictines B and D were slightly less toxic compared to the main metabolite, whereas phyllostictine C was almost not toxic (Table 5.11.8). These results showed a clear structure-activity relationship between the phytotoxic activity and the structural feature characterizing the phyllostictine group. In fact, the most toxic compound appeared to be phyllostictine A (**54**) in which the 3,5-dihydroxy-4-methoxy-11-methylcycloundec-1-ene macrocyclic ring is joined with both the N-ethyl β-lactame and the 2,2,3,4-tetrasubstituted-2,3,5-thrihydrofuran rings. The phytotoxicity decreases in phyllostictines B and D, in

which the dimension and the conformational freedom of the macrocyclic ring are changed but its functionalization remains unalterated. When also this latter changes in combination with the size and the conformational freedom, as in phyllostictine C (**56**), which showed a higher steric hindered 1-hydroethyl group at C-5 instead of the methyl group as in **54**, the toxicity was completely lost. The N-ethyl β-lactame ring appears to be less important for the activity as phyllostictine D (**57**), in which it became an N-methyl δ-lactame, showed the same level of toxicity of **55**. The importance of the 2,2,3,4-tetrasubstituted-2,3,5-trihydrofuran rings remains to be ascertained, by assaying derivatives showing modifications of this moiety prepared from phyllostictine A.

The antimicrobial and the zootoxic activities were assayed only for phyllostictines A and B, being phyllostictines C and D isolated in very low amounts.

In the antifungal assay on *Geotrichum candidum*, phyllostictines A and B, were completely inactive assayed up to 100 μg/disk. Assayed against bacteria, only phyllostictine A was active against *Lactobacillus* sp. (Gram+) species, already at 5μg/disk, whereas both compounds were completely inactive against *Escherichia coli* (Gram-) even when tested up to 100 μg/disk.

When tested on brine shrimp (*Artemia salina* L.) larvae only phyllostictine A caused the total larval mortality when assayed at 10^{-3} M, and a still noticeable mortality at 10^{-4} M (24%), whereas phyllostiine B proved to have a negligible activity.

In both antimicrobial and zootoxic activities, the integrity of the oxazatricycloalkenone system present in phyllostictine A appears an important feature to preserve the activity.

When tested on punctured *C. arvense* leaves at concentration of 10^{-3} M (20μl/droplet) phyllostoxin proved to be phytotoxic, causing the rapid appearance of large necrosis, similar to those caused by phyllostictine A. On the contrary phyllostin, assayed at

the same concentration, proved to be no phytotoxic. Both phyllostoxin and phyllostin, when assayed at concentrations up to 100 μg/disk did not show antimicrobial activity towards *Geotrichum candidum* and Gram- and Gram+ bacteria *Escherichia coli* and *Lactobacillus sp*., respectively. No toxicity was caused by both toxins to brine shrimps (*Artemia salina* L.) larvae when assayed up to 10^{-3} M.

Phyllostictines A-D are the first four fungal metabolites described to belong to an oxazatricicloalchenone group and to occur for the first time as natural compounds with interesting biological activity. In particular the main fungal metabolite, phyllostictine A, showed potentially strong herbicidal properties not associated to antifungal and zootoxic activities, while a selective antibiosis was exhibited against Gram+ bacteria. Compounds containing macrocyclic rings as well as furan derivatives are quite common as naturally occurring compounds and some of them are biologically active (Turner and Aldrige, 1983; Tringali, 2001), while compounds containing β-lactame (2-azetidone) are only known as synthetic substances and some of them have pharmacological application as hypocholesterolemic agents (Williams, 2006; Vaccaro *et al*., 1996). 2-Piperidones are known as naturally occurring compounds and essentially as metabolites of plants (Nagarajan *et al*., 2005) and animals (Wood, 2002).

Phyllostoxin appeared to be a new bicyclooctatrienyl derivative with a strong phytotoxic activity not associated to antimicrobial or zootoxic activities. Therefore this toxin could represent a potential new natural herbicides. Further studies are in progress in order to produce the active compound in larger amounts, allowing a more accurate biological characterization. Phyllostoxin appeared to be the first bicyclooctatrienyl derivative naturally occurring, being the other reported, synthetic or intermediate compounds (Grieco *et al*., 1980; Kobayashi *et al*., 1992a; 1992b).

Phyllostin, which proved to have no toxicity in any of the assays performed, is one of the possible sixteen stereoisomers having the same structure, of which one is a fungal

metabolite (Isogai *et al*., 1985) while the others are all synthetic compounds (Chen and Low, 1966; Alberg *et al*., 1992). Phyllostin appeared to be the diastereomer of the 5-lactyl shikimate lactone previously isolated from a *Penicillium* sp. (Isogai *et al*., 1985) for which the absolute stereostructure 3*S*,4a*R*,8*R*,8a*R* was established by two independent enantioselective synthesis (Muralidharam *et al*., 1990; Alberg *et al*., 1992). In the same paper, Alberg *et al*. (1992), also described the preparation of the 3*R*,4a*R*,8*R*,8a*R* diastereomer of **63**. As expected, the spectroscopic (IR, ^{1}H and ^{13}C NMR and MS) data of phyllostin were similar to those described in literature for the natural (Isogai *et al*., 1985; Muralidharam *et al*., 1990) and synthetic (Alberg *et al*., 1992) diastereomers but the physic (melting point and specific optical rotation) properties appeared quite different as reported in the experimental. Furthermore, the data of the crystalline cells are also quite different in respect to those reported (Chen and Low, 1966) of an unidentified diastereomer of **63,** previously synthesized by Sprecher and Sprinson (1962).

6. CONCLUSIONS

i) From *D. gigantea*, a mycoherbicide proposed for the biocontrol of grass weeds, were isolated some well know sesterterpenoids, as ophiobolin A, (the main metabolite), 6-*epi*-, 3-anhydro-6-*epi*-ophiobolin A, and ophiobolins B, J and I.

Two further new ophiobolins were isolated and named ophiobolin E and 8-*epi*-ophiobolin J. These two latter are the first ophiobolins which present, a diidropyran ring joined to ring C and the epimerization at C-8, respectively.

Considering the biological activity showed by ophiobolin A, it could be proposed as potential natural herbicide alone or in combination with the fungus for the management of grass weeds.

ii) Ophiobolin A and close related fusicoccin, the main diterpenoid phytotoxin produced by *Fusicoccum amygdaly* and some its derivatives assayed at lower concentration they are phytotoxic, appeared to induce the germination of different *Orobanche* spp. The results showed that this stimulation is specie and concentration dependent. However this one represents an alternative method, called "suicidal germination" for the biocontrol of *Orobanche* spp.

iii) Phytopathogenic fungi belonging to different genera were proposed for the biocontrol of *C. arvense* and *S. arvensis* as *Ascochyta*, *Stagonospora* and *Phyllosticta*.

The investigation on the toxins produced by nine *A. sonchi* strains with different origin showed that two of them were atypical isolates. The latter were reclassified, on the basis of biochemical, molecular and chemical studies as *Phoma exigua* var. *exigua* species. This classification was confirmed by the isolation from their cultures of several well known cytochalasins which are typical toxic metabolites produced by *Phoma* species.

iv) From *S. cirsii* were isolated ten new nonenolides, nine of which are new naturally occurring compounds. Among them only stagonolide and stagonolide H appeared to have a

significant phytotoxic activity and could be proposed for their practical application in agriculture for the management of the two *Asteracee*.

v). A structure-activity relationship study, carried out using 15 compounds among cytochalasins, nonenolides and their derivatives, showed that the most phytotoxic compound on *C. arvense* was stagonolide, while deoxaphomin appeared to be the most toxic on *S. arvensis*. The conformational freedom is an important factor to impart the toxicity of the nonenolides, while the presence of the two hydroxy groups at C-7 and C-20, and the conformational freedom of the macrocyclic ring, for the cytochalasins.

Stagonolide was a strong inhibitor of photosynthesis on *C. arvense* leaves, while cytochalain B showed a strong effect on cell membrane permeability.

vi). *P. cirsii* showed to produce four phytotoxins with a very original carbon skeleton. These named phyllostictines A-D, are the first natural oxazatricicloalchenones. The most phytotoxic compound appeared to be phyllostictine A, whose phytotoxicity was dependent for the size and functionalization of the macrocyclic ring. The β-lactame ring appeared to be not essential.

Lacking zootoxic and antimicrobial activity, phyllostictine A appear to be an ideal potential natural herbicide.

Furthermore, two new metabolites were isolated and named phyllostoxin, which is a new pentasubstituted bycicloctatrienyl acetic acid ester, showing a strong phytotoxicity at same level of phyllostictine A, and phyllostin, a new pentasubstituted hexahydrobenzodioxine carboxylic acid methyl ester showing no activity.

7. REFERENCES

Abate, D., Abraham, W.R., Meyer, H. (1997). Cytochalasins and phytotoxins from the fungus *Xylaria obovata*. *Phytochemistry*, 44: 1443-1448.

Abbasher, A. A., Sauerborn, J. (1992). *Fusarium nygamai*, a potential bioherbicide for *Striga hermontica* control in sorghum. *Journal of Biological Control*, 2: 291-296.

Abebe, G., Sahile, G., Tawaha, A. (2005). Evaluation of potential trap crops on *Orobanche* soil seed bank and tomato yield in the Central Rift Valley of Ethiopia. *World Journal of Agricultural Science*, 1: 148-151.

Abouzeid, A. M., Boari, A., Zonno, M. C., Vurro, M., Evidente, A. (2004). Toxicity profiles of potential biocontrol agents of *Orobanche ramosa*. *Weed Science*, 52: 326-332.

Abraham, W. R. and Hensenn, H. P. (1992). Fusoxysporone - a new type of diterpene from *Fusarium oxysporum*. *Tetrahedron*, 48: 10559-10562.

Alberg, G. D., Lauhon, C. T., Nyfeler, R., Fässler, A., Bartlett, P. A. (1992). Inhibition of EPSP synthase by analogue of tetrahedral intermediate and EPSP. *Journal of American Chemical Society,* 114: 335-354.

Amalfitano, C., Pengue, R., Andolfi, A., Vurro, M., Zonno, M. C., Evidente, A. (2002). HPLC analysis of fusaric acid, 9,10-dehydrofusaric acid and their methyl esters, toxic metabolites from weed pathogenic *Fusarium* species. *Phytochememical Analysis,* 13: 277-282.

Andolfi, A., Boari, A., Evidente, A., Vurro, M. (2005). Metabolites inhibiting germination of *Orobanche ramosa* seeds produced by *Myrothecium verrucaria* and *Fusarium compactum*. *Journal of Agricultural and Food Chemistry*, 53: 1598-1603.

Arai, K., Rawlings, B. J., Yoshizawa, Y., Vederas, C. (1989). Biosynthesis of antibiotic A26771B by *Penicillium turbatum* and dehydrocurvularin by *Alternaria cinerariae*. Comparison of stereochemistry of polyketide and fatty acid enoyl thiol ester reductase. *Journal of American Chemical Society*, 111: 3391-3399.

Arinbasarov, M. U., Murygina, V. P., Adamin, V. M., Sakharovskii, V. G., Nefedova M. Y. U., Gerasimova, N. M., Kozlovskii, A. G. (1988). Growth-regulating metabolites of the fungus *Monilia* sp. *Priklad. Biok. Mikrobiol*., 24: 754-759.

Au, T. K., Chick, W. S. H., Leung, P. C. (2000). The biology of ophiobolins. *Life Science*, 67: 733-742 (and reference therein cited).

Aviv, D., Amsellem, Z., Gressel, J. (2002). Transformation of carrots with mutant acetolactate synthase for *Orobanche* (broomrape) control. *Plant Science,* 18: 1187-1193.

Ayer, W. A., Brawne, L. M. Feng, M. C., Orszanska, H., Saeedi-Ghomi, H. (1986). The chemistry of the blue stain fungi. Part 1. Some metabolites of *Ceratocystis* species associated with mountain pine beetle infected lodgepole pine. *Canadian Journal of Chemistry,* 64: 904-909.

Bach, E., Christiansen, S., Dalgaard, L., Larse, P. O., Olsen, P. E., Smedergard-Peterson, V. (1979). Structures, properties and relationship to the aspergillomarasmines of toxins produced by *Pyrenophora teres*. *Physiological Plant Pathology*, 14: 41-46.

Bakheit, Br., Allam, A. Y., Galal, A. H. (2002). Intercropping faba bean with some legume crops for control of *Orobanche crenata*. *Acta Agronomica Hungarica*, 50: 1-6.

Bailey, K. L., Boyetchko, S. M., Derby, J., Hall, W., Sawchyn, K., Nelson, T. (2000). Evaluation of fungal and bacterial agents for biological control of *Cirsium arvense*.

In: Proceeding X International Symposyum Biological Control Weeds. Spencer, N. R. (Ed.). Montana State Univ., Bozeman, Montana, USA, 4–14 July, pp. 203-208.

Ballio, A., Brufani, M., Casinovi, C. G., Cerrini, S., Fedeli, W., Pellicciari, R., Santurbano, B., Vaciago, A. (1968a). Structure of fusicoccin A. *Experientia,* 24: 631-635.

Ballio, A., Carilli, A., Santurbano B., Tuttobello, L. (1968b). Produzione di fusicoccina in scala pilota. *Annuale Istituto Superiore Sanità*, 4: 317-332.

Ballio, A., Casinovi, C. G., Capasso, R., Ferrara, A., Randazzo, G. (1981). Structure revision of the ketone formed by Jones oxidation of fusicoccin triacetate and preparation of 9-*epi*-fusicoccin. *Gazzetta Chimica Italiana,* 111: 129-132.

Ballio, A., Casinovi, C. G., Framondino, M., Grandolini, G., Randazzo, G., Rossi, C. (1972). Structure of three isomers of monodeacetylfusicoccin. *Experientia,* 28: 1150-1151.

Ballio, A., Casinovi, C. G., Randazzo, G., Rossi, C. (1970). Characterization of by-products of fusicoccin in culture filtrates of *Fusicoccum amygdali. Experientia*, 26: 349-351.

Ballio, A., Castellano, S., Cerrini, S., Evidente, A., Randazzo, G., Segre, A. L. (1991). ^{1}H NMR conformational study of fusicoccin and related compounds: molecular comformation and biological activity. *Phytochemistry*, 30: 137-146.

Ballio, A., Chain, E. B., De Leo, P., Erlanger, B. F., Mauri, M., Tonolo, A. (1964). Fusicoccin: a new wilting toxin produced by *Fusicoccum amygdali*. *Nature*, 203-297.

Ballio, A., Graniti, A. (1991). Phytotoxins and their involvement in plant diseases. *Experientia*, 47: 751-864.

Barrow, K. D., Barton, D. H. R., Chain, E., Ohnsorge, U. F. W., Thomas, R. (1998). The constitution of fusicoccin. *Chemical Commununication*, 1198-1200.

Batterham, T. J. (1972). NMR Spectra of Simple Heterocycles. J. Wiley & Sons, New York, pp. 365-419.

Bassarello, C., Bifulco, G., Zampella, A. D'Auria, M. V., Riccio, R., Gomez-Paloma, L. (2001). Stereochemical studies on auscalitoxin: Extension of the J-based NMR configuration analysis of a nitrogen substituted system. *Tetrahedron Letters,* 42: 8611-8613.

Berestetsky, A. (1997). Mycobiota of *Cirsium arvense* and allied species over the territory of the European part of Russia. *Mikologiya i Fitopatologiya* 31: 39-45. (in Russian).

Berestetskiy, A. (2005). Efficacy of strains of different fungal species and their application techniques for biological control of *Cirsium arvense*. *In*: Proceedings of 2nd Conference on Plant Protection, Saint-Petersburg, Pushkin, Russia, December 5–10, pp. 136–138.

Berestetskiy, A., Gagkaeva, T. Y., Gannibal, P. B., Gasich, E. L., Kungurtseva, O. V., Mitina, G. V., Yuzikhin, O. S., Bilder, I. V., Levitin, M. M. (2005). Evaluation of fungal pathogens for biocontrol of *Cirsium arvense*. *In*: Proceedings of 13th European Weed Research Society Symposium. Bàrberi, P., Bastiaans, L., Christensen, S. et al. (Eds.). Bari, Italy, June 19-23.

Berestetski, A., Smolyaninova, N. V. **(**1998). Study of the mycobiota of *Sonchus arvensis* for developing a bioherbicide. *In*: Proceedings 4th International Bioherbicide Workshop. Glasgow, England, 6-7 August, p. 27**.**

Berger, S., Braun, S. (2004). 200 and More Basic NMR Experiments: a Practical Course, 1st Ed. Wiley-VCH, Weinheim.

Betina, V. (1992). Biological effects of the antibiotic brefeldin A (decumbin, cyanein, ascotoxin, synergisidin): a retrospective. *Folia Microbiology*, 37: 3-11.

Boerema, G. H., de Gruyter, J., Noordeloos, M. E., Hamers, M. E. C. (2004). *Phoma* identification manual: differentiation of specific and infraspecific Taxa in culture. CABI publishing, Wallingford, Oxon, UK.

Bottalico, A. (2004). Micotossine. *In*: Chimica degli alimenti. Cabras, P., Martelli, A. (Eds). Piccin, Padova, Italy, Chapter 27.

Bottalico, A., Capasso, R., Evidente, A., Randazzo, G., Vurro, M. (1990). Cytochalasins: structure-activity relantionships. *Phytochemistry*, 29: 93-96.

Bottiglieri, A., Zonno, M. C., Vurro, M. (2000). I bioerbicidi contro le piante infestanti. *L'informatore agrario*, 13: 69-73.

Breitmaier, E., Voelter, W. (1987). Carbon-13 NMR Spectroscopy. VCH, Weinheim, pp. 183-280.

Britton, G. (1983). Biochemistry of Natural Pigments. Univ. Press, Cambridge.

Campbell, M. A., Medd, R. W., and Brown, J. F. (1996). Cultural and infection studies on *Pyrenophora semeniperda*, a possible bioherbicide for annual grass weeds. *In*: Proceedings of the 9th International Symposium on Biological Control of Weeds, Stellenbosch, South Africa, pp. 519-523.

Canales, M. W., Gray, G. R. (1988). 6-*epi*-ophiobolin A and 3-anhydro-6-*epi*-ophiobolin A, host specific phytotoxins of *Drechslera maydis* (race T). *Phytochemistry*, 27: 1653-1663.

Canonica, L., Fiecchi, A., Galli Kienle, M., Scala, A. (1966). Isolation and constitution of cochliobolin. *Tetrahedron Letters*, 13: 1329-1333.

Capasso, R., Evidente, A., Cutignano, A., Vurro, M., Zonno, M. C. and Bottalico, A. (1996). Fusaric and 9,10-dehydrofusaric acids and their methyl esters from *Fusarium nygamai*. *Phytochemistry*, 41: 1035-1039.

Capasso, R., Evidente, A., Randazzo, G., Ritieni, A., Bottalico, A., Vurro, M., Logrieco, A. (1987). Isolation of cytochalasins A and B from *Ascochyta heteromorpha*. *Journal of Natural Products,* 50: 989-990.

Capasso, R., Evidente, A., Ritieni, A., Randazzo, G., Vurro, M., Bottalico, A. (1988). Ascochalasin, a new cytochalasin from *Ascochyta heteromorpha*. *Journal of Natural Products,* 51: 567-571.

Capasso, R., Evidente, A., Vurro, M. (1991). Cytochalasins from *Phoma exigua* var. *heteromorpha*. *Phytochemistry*, 30: 3945-3950.

Caputo, O., Viola, F. (1977). Isolation of α,β-dehydrocurvularin from *Aspergillus aureofulgens*. *Planta Medica*, 31: 31-32.

Chandramohan, S., Charudattan, R. (2001). Control of seven grasses with a mixture of three fungal pathogens with restricted host range. *Biological Control*, 22: 246-255.

Chandramohan, S., Charudattan, R., Sonoda, R., Singh, M. (2002). Field evaluation of a fungal pathogen mixture for the control of seven weedy grasses. *Weed Science*, 50: 204-213.

Chen, C. H., Low, B. W. (1966). Preliminary X-ray crystallopgraphic data for methyl 3-O-(1-carboxyethyl) shikimate δ-lactone. *Acta Crystallographica*, 20: 917.

Chiosi, S., Evidente, A., Randazzo, G., Casinovi, C. G., Segre, A. L., Ballio, A. (1983). The reaction of fusicoccin with Fritz and Schenk reagent. *Gazzetta Chimica Italiana*, 113: 717-720.

Cole, J. C., Cox, R. H. (1981). Handbook of toxic fungal metabolites. Academic Press, New York.

Comstock, J. C., Martinson, C. A., Gengenbach, B. G. (1973). Host specificity of a toxin from *Phyllostycta maydis* for Texas cytoplasmically male-sterile maize. *Phytopathology*, 63: 1357-1361.

Cook, C. E., Whichard, L. P., Wall, M. E., Egley, G. H., Coggon, P., Luhan, P. A., McPhail, A. T. (1972). Germination stimulants II. The structure of strigol, a potent seed germination stimulant for wichweed (*Striga lutea* Lour.). *Journal of American Chemical Society*, 94: 6198-6199.

Coombe, R. R., Jacobs, J. J., Watson, T. R. (1968). Costituents of some *Curvularia* species. *Australian Journal of Chemistry,* 21: 783-788

Dale, J. A., Dull, D. L., Mosher, H. S. (1969). alpha-Methoxy-alpha-trifluoromethylphenylacetic acid, a versatile reagent for the determination of enantiomeric composition of alcohols and amines. *Journal of Organic Chemistry,* 34: 2543-2549.

Dale, J. A., Mosher, H. S. (1973). Nuclear magnetic resonance enantiomer regents. Configurational correlations via nuclear magnetic resonance chemical shifts of diastereomeric mandelate, O-methylmandelate, and alpha-methoxy-alpha-trifluoromethylphenylacetate (MTPA) esters. *Journal of American Chemical Society,* 95: 512-519.

Delfosse, E.S. (1990). Proceedings of the VII International Symposium on Biological Control of Weeds, Roma, Italy, March 6-11**.**

Donald, W.W. (1990). Management and control of Canada thistle (*Cirsium arvense*). *Reviews of Weed Science,* 5: 193-250.

Duke, S. O., Duke, M. V., Sherman, T. D., Nandihalli, U. B. (1991). Spectrometric and spectrofluorimetric methods in weed science. *Weed Science*, 39: 505-513.

El-Kady, I. A., Mostafa, M. (1995). Production of cytochalasins C, D, and E from dematiaceous hyphomycetes. *Folia Microbiologica*, 40: 301-303.

Entwistle, I. D.; Howard, C. C.; Johnstone, R. A. W. (1974). Isolation of brefeldin A from *Phyllosticta medicaginis*. *Phytochemistry*, 13: 173-274.

Evidente, A. (1997). Bioactive metabolites from phytopathogenic fungi and bacteria. *In:* Recent Research Developments in Phytochemistry, Ed. Pandalai, S.G., Research Signpost, Trivandrum (India), pp. 255-292.

Evidente, A. (2006). Chemical and biological characterization of toxins produced by weed pathogenic fungi as potential natural herbicides. *In:* Natural Products for Pest Management, ACS Sympossium Series 927. Rimando, A. M., Duke, S. O. (Eds.). ACS Division of Agricultural and Food Chemistry, Inc., Washington, USA, pp. 62-75.

Evidente, A., Abouzeid, M. A. (2006). Characterization of phytotoxins from phytopathogenic fungi and their potential use as herbicides in integrated crop management. *In:* Handbook of Sustainable Weed Management. Singh, P. H., Batish, D. R., Kohli, R. K. (Eds.). The Harworth Press Inc., New York, pp. 507-532.

Evidente, A., Andolfi, A., Abouzeid, M. A., Vurro, M., Zonno, M. C. , Motta, A. (2004). Ascosonchine, the enol tautomer of 4-pyridylpyruvic acid with herbicidal activity produced by *Ascochyta sonchi*. *Phytochemistry,* 65: 475-480.

Evidente, A., Andolfi, A., Fiore, M., Boari, A., Vurro, M. (2006). Stimulation of *Orobanche ramosa* seed germination by fusicoccin derivatives: A structure-activity relationships study. *Phytochemisty*, 67: 19-26.

Evidente, A., Andolfi, A., Vurro, M., Fracchiolla, M., Zonno, M.C. and Motta, A. (2005) Drazepinone, a trisubstituted tetrahydronaphthofuroazepinone with herbicidal activity produced by *Drechslera siccans*. *Phytochemistry*, 66: 715-721.

Evidente, A., Andolfi, A., Vurro, M., Zonno, M. C. (2001). Determination of *Ascochyta caulina* phytotoxins by high-performance anion exchange chromatography and pulsed amperometric detection. *Phytochemical analysis,* 12: 383-387.

Evidente, A., Andolfi, A., Vurro, M., Zonno, M. C., Motta, A. (2000). *Trans*-4-aminoproline, a phytotoxic metabolite with herbicidal activity produced by *Ascochyta caulina*. *Phytochemistry,* 53: 231-237.

Evidente, A., Andolfi, A., Vurro, M., Zonno, M. C., Motta, A. (2002). Cytochalasins Z1, Z2 and Z3, three 24-oxa[14]cytochalasans produced by *Pyrenophora semeniperda*. *Phytochemistry,* 60: 45-53.

Evidente, A., Andolfi, A., Vurro, M., Zonno, M. C., Motta, A. (2003). Cytochalasins Z4, Z4 and Z5, three new 24-oxa[14]cytochalasans produced by *Phoma exigua* var. *heteromorpha. Journal of Natural Products*, 66: 1540-1544.

Evidente, A., Capasso, R., Abouzeid, M. A., Lanzetta, R., Vurro, M., Bottalico, A. (1993a). Three new pinolidoxins from *Ascochyta pinodes*. *Journal of Natural Products,* 56: 1937-1943.

Evidente, A., Capasso, R., Andolfi, A., Vurro, M. and Zonno, M.C. (1998a). Putaminoxins D and E from *Phoma putaminum*. *Phytochemistry*, 48: 941-945.

Evidente, A., Capasso, R., Andolfi, A., Vurro, M. and Zonno, M.C. (1998b). Structure-activity relationship studies of putaminoxins and pinolidoxins, phytotoxic nonenolides produced by phytopathogenic *Phoma* and *Ascochyta* species. *Natural Toxins*, 6: 183-188.

Evidente, A., Capasso, R., Cutignano, A., Taglialatela-Scafati, O., Vurro, M., Zonno, M. C., Motta, A. (1998c). Ascaulitoxin, a phytotoxic *bis*-amino acid *N*-glucoside from *Ascochyta caulina*. *Phytochemistry,* 48: 1131-1137.

Evidente, A., Fernández-Aparicio, M., Andolfi, A., Rubiales, D., Motta, A. (2007). Trigoxazonane, a monosubstituted trioxazonane by *Trigonella foenum-graecum* root exudates, inhibiting agent of *Orobanche crenata* seed germination. *Phytochemistry*, 68: 2487-2492.

Evidente, A., Lanzetta, R., Capasso, R., Andolfi, A., Bottalico, A., Vurro, M. and Zonno, M.C. (1995). Putaminoxin, a phytotoxic nonenolide from *Phoma putaminum*. *Phytochemistry*, 40: 1637-1641.

Evidente, A., Lanzetta, R., Capasso, R., Vurro, M., Bottalico, A. (1993b). Pinolidoxin, a phytotoxic nonenolide from *Ascochyta pinodes*. *Phytochemistry,* 34: 999-1003.

Evidente, A., Lanzetta, R., Capasso, R., Andolfi, A., Vurro, M. and Zonno, M.C. (1997). Putaminoxins B and C from *Phoma putaminum*. *Phytochemistry*, 44: 1041-1045.

Evidente, A., Motta, A. (2001). Phytotoxins from fungi, pathogenic for agrarian, forestall and weedy plants. *In*: Bioactive Compounds from Natural Products, Tringali, C. (Ed.). Taylor & Francis, London, pp. 473-526.

Evidente, A., Randazzo, G., Casinovi, C. G., Ballio, A. (1984). Catalytic hydrogenation of fusicoccin. *Gazzetta Chimica Italiana*, 114: 61-64.

Farr, D. F., Bills, G. F., Chamuris, G. P., Rossman, A. Y.(1989). Fungi on Plants and Plant Products in the United States. APS Press, St. Paul, MN, USA, pp. 1252.

Fernández-Aparicio, M., Andolfi, A., Evidente, A., Pérez-De-Luque, A., Rubiales, D. (2008). Fenugreek root exudates with *Orobanche* species specific seed germination stimulatory activity. *Weed Research,* 48: 163 -168.

Fucsher, J., Zeeck, A. (1997). Secondary Metabolites by Chemical Screening, 34. Aspinolides and aspinonene/aspyrone co-metabolites, new pentaketides produced by *Aspergillus ochraceus. Liebigs Annalen*, 87-95.

Fracchiolla, M., (2003). Biological control of grass weeds by using bioherbicides. Ph.D. Thesis University of Bari, Italy (in Italian).

Friis, P., Olsen, C. E., and Moller, B. G. (1991). Toxin production in *Pyrenophora teres* the ascomycete causing the net-spot blotch disease of barley (*Hordeum vulgare* L.). *Journal of Biological Chemistry*, 266: 13329-13335.

Fritz, J. S., Schenk, G. H. (1959). Acid-catalyzed acetylation of organic hydroxyl group. *Analitical Chem*istry, 31: 1808-1812.

GOST 13496.7-97. (1997). *In*: Methods for the determination of toxicity. Standards Publishing House, Moscow, Russia.

Grafa, W., Robert, J., Vederas, J. C., Tamm, C., Solomon, P. H., Moiura, I., Nakanishi, K. (1974). Biosynthesis of the cytochalasins. III. Carbon-13 NMR of cytochalasin B (phomin) and cytochalasin D. Incorporation of sodium acetate-1-13C and sodium acetate 2-13C. *Helvetica Chimica Acta*, 57: 1801-1815.

Graniti, A., Durbin, R. D. and Ballio, A. (1989). Phytotoxins and Plant Pathogenesis. NATO ASI Series, Series H, Vol 27, Springer-Verlag, Berlin.

Grekul, C. W., Cole, D. E., Bork, E. W. (2005). Canada thistle (*Cirsium arvense*) and pasture forage responses to wiping with various herbicides. *Weed Technology*, 19: 298–306.

Grieco, P.A., Tahikawa, T., Schillinger, W. J. (1980). Bicyclo[2.2.1]heptanes as intermediates in the synthesis of steroids. Total synthesis of estrone. *Journal of Organic Chemistry,* 45: 2247-2251.

Guo, Y., Morikawa, Y., Nita, S., Ohnishi, K., Yamashita, M. (1996). Isolation and HPLC determination of *p*-hydroxybenzaldehyde from *Alternaria porri*. *Science Engineering Review, Doshisha University*, 36: 252-259.

Hallock, Y. F., Clardy, J., Kenfield, D. S., and Strobel, G. (1988). De-*O*-methyldiaporthine, a phytotoxin from *Dreschslera siccans*. *Phytochemistry*, 27: 3123-3125.

Harlan, J. R., deWelt, J. M. J. (1965). Some thoughts about weeds. *Economic Botany* 19: 16-24.

Hauck, C., Múller, S., Schildtknecht, H. (1992). A germination stimulant for parasitic flowering plants from *Sorghum bicolour*, a genuine host plant. *Journal Plant Physiology*, 139**:** 474-478.

Holm, L. G., Pluckett, D. L., Pancho, J. V., Herberger, J. P. (1977). The World's Worst Weeds (Distribution and Biology). University Press of Hawaii, Honoloulou, pp. 84-91.

Holm, L., Doll, J., Holm, E., Pancho, J., Herberger, J. (1997). World Weeds: Natural Histories and Distribution. John Wiley & Sons, Inc., New York.

Hoppe H. H., (1998). Fungal phytotoxins. *In*: Resistance of Crop Plants Against Fungi. Hartleb, H., Heitefuss, R., Hoppe, H. H. (Eds.). G. Fischer, Stuttgart, pp. 54-82.

Humphrey, A. J., Galster, A. M., Beale, M. H. (2006). Strigolactones in chemical ecology: waste products or vital allelochemicals? *Natural Products Report,* 23: 592-614.

Isogai, A., Washizu, M., Murakoshi, S., Suzuki, A. (1985).A new shikimate derivative, methyl 5-lactyl shikimate lactone, from *Penicillium* sp. *Agricultural and Biolological Chemistry*, 49: 167-169

Itai, A., Nozoe, S., Tsuda, K., Okuda, S., Iitaka, Y., Makayama, Y. (1967). Structure of cephalonic acid, a pentaprenyl terpenoid. *Tetraedron Letters*, 42: 4111-4112.

Joel, D. M., Kleifeld, Y., Losner-Goshen, D., Herzlinger, G., Gressel, J. (1995). Transgenic crops against parasites. *Nature,* 374: 220-221.

Joel, D. M., Hershenhorn, Y., Eizenberg H., Aly, R., Ejeta, G., Rich P. J., Ranson, J. K., Sauerborn, J., Rubiales, D. (2007). Biology and management of weedy root parasites. *In:* Horticultural Review. Janik, J., **(**Ed.). Wiley, New York, USA, pp. 267-350.

Johnson, A., Rosebery, G., Parker, C. (1976). A novel approach to Striga and Orobanche control using synthetic germination stimulants. *Weed Research*, 16: 223-227.

Kastanias, M. A., Tokousbalides, M. C. (2000). Herbicidal potential of pyrenophorol isolated from a *Drechslera avenae* pathotype. *Pest Management Science*, 56: 227-232.

Kempenaar, C. (1995). Studies on the biological control of *Chenopodium album* by *Ascochyta caulina*. Thesis. Wageningen, the Netherlands.

Kenfield, D., Bunkers, G., Wu, Y. H., Strobel, G., Sugawara, F., Hallock, Y., and Clardy, J. (1989a). Gigantenone, a novel sesquiterpene phytormone mimic. *Experientia*, 45: 900-902.

Kenfield, D., Hallock, Y., Clardy, J., and Strobel, G. (1989b). Curvulin and *o*-methylcurvulinic acid: phytotoxic metabolites of *Drechslera indica* which cause necroses on purslane and spiny amaranth. *Plant Science*, 60: 123-127.

Kharrat, M., Halila, M. H., Linke, K. H., Haddar, T. (1992). First report of *Orobanche foetida* Poiret on faba bean in Tunisia. *FABIS Newsletter*, 30: 46-47.

Kim, J. M., Hyeon, S. B., Isobai, A., Suzuki, A. (1984). Isolation of ophiobolin A and its analogs to photosynthesis. *Agricultural and Biological Chemistry,* 48: 803-805.

Kloppenburg, D. J., Hall, J. C. (1990). Efficacy of five different formulations of clopyralid on *Cirsium arvense* (L.) Scop. and *Polygonum convolvulus* L. *Weed Research*, 30: 227-234.

Kobayashi, K., Kanno, Y., Seko, S., Suginome, H. (1992). Photoinduced molecular transformation. Part 135. New synthesis of taiwanin C and justicin E based on a radical cascade process involving β-scission of alkoxy radicals generated from 3- and 8-aryl-1-ehtyl-1,2-dihydrocyclobuta[b]naphthalen-1-ols prepared by thermolysis of (*Z*)-*tert*-butyl-3-amino-3-(bicyclo[4.2.0]octa-1,3,5-trienyl)propenoates. J. Chem. Soc. Perkin Trans. 1 22, 3111-3117.

Kobayashi, K., Kanno, Y., Seko, S., Suginome, H. (1992b). New general synthesis of *tert*-butyl-3-amino-2-naphthalenecarboxylate by an electrocyclic reaction of *o*-quinonedimethides generated from *tert*-butyl (*Z*)-3-amino-3-(bicyclo[4.2.0]0cta-1,3,5,trienyl-7-yl)prop-2-enoates. J. Chem. Soc. Chem. Commun. 780-781.

Kohli, R. K., Batish, D. R. and Singh, H. P. (2006). Weeds and their management: rationale and approaches. *In*: Handbook of Sustainable Weed Management. Singh, P. H., Batish, D. R., Kohli, R. K. (Eds). The Harworth Press Inc., New York, pp. 1-19.

Kumar, J., Schäfer, P., Hückelhoven, R., Langen, G., Baltruschat, H., Stein, E., Nagarajan, S., Kogel, K. H. (2002). *Bipolaris sorokiniana*, a cereal pathogen of global concern: cytological and molecular approaches towards better control. *Molecular Plant Pathology*, 3: 185–195.

Lai, S., Shizuri, Y., Yamamura, S., Kawai, K., Terada, Y., Furukawa, H. (1989). Novel curvularin-type metabolites of a hybrid strain me 0005 derived from *Penicillium citreo-viride* B. IFO 6200 and 4692. *Tetrahedron Letters*, 30: 2241-2244.

Lemna, W. K., Messersmith, C. G. (1990). The biology of Canadian weeds. 94. *Sonchus arvensis* L. *Canadian Journal Plant Science*, 70: 509–532.

Leth, V., Andreasen, C. (1999). *Septoria*, *Ramularia* and *Phomopsis cirsii* as potential control agents of *Cirsium arvense* (L.) Scop. *In:* Workshop on Biological Weed Control EWRS/COST-816. Hatcher, P. (Ed.). Basel, Schwitzerland, p. 16.

Li, E., Clark, A. M., Rotella, D. P., Hufford C. D. (1995). Microbial metabolites of ophiobolin A and antimicrobial evaluation of ophiobolins. *Journal of Natural Products,* 58: 74-81.

Lim, C. H., Miyagawa, H., Ueno, T., Takenaka, H., Sung, N. D. (1996). Siccanol: sesterterpene isolated from pathogenic fungus *Drechslera siccans*. *Han'guk Nonghwa Hakhoechi*, 39**:** 241-244. From C.A.126: 131654 (1996).

Lisker, I. S. (1991). Equipment for determination of light reflection and transmission characters of objects. Patent of Russian Federation N. 1673928.

Lisker, I. S., Dmitriev, A. P. (1998). The optico-physiological method of fungi phytotoxicity determination. *Mikologiya i Fitopatologyia*, 32: 79-82 (in Russian).

Lisker, I. S., Dmitriev, A. P. (1999). Laser-optical methods for earlier diagnostics of plant and seeds diseases in various habitant media taken into consideration anthropogenic and biological pollution. *In*: Environ. and Industr. Sensing. SPIE International Symposium, Boston, USA, p. 44-53**.**

Luz, J. M., Paterson, R. R. M. and Brayford, D. (1990). Fusaric acid and other metabolite production in *Fusarium oxysporum* f. sp. *vasinfectum*. *Letters in Applied Microbiology*, 11: 141-144.

Macdonald, J. E., White, G. P., Côté, M. J. (2000). Differentiation of *Phoma foveata* from *Phoma exigua* using a RAPD generated PCR-RFLP marker. *Europan Journal Plant Pathology*, 106: 67–65.

Marré, E. (1979). Fusicoccin: a tool in plant physiology. *Annual Review Plant Physiol*ogy, 30: 273-288.

Matsuda, M., Yamazaki, T., Fuhshuku, K., Sugai, T. (2007). First total synthesis of modiolide A, based on whole-cell yeast-catalyzed asymetric reduction of a propargyl ketone. *Tetrahedron*, 63: 8752-8760.

Matsumori, N., Kaneno, D., Murata, M., Nakamura, H., Tachibana, K. (1999). Stereochemical determination of acyclic structures based on carbon-proton spins coupling constants: A method of configuration analysis for natural products. *Journal of Organic Chemistry,* 64: 866-876.

Matsumori, N., Murata, M., Tachibana, K. (1995). Conformational analysis of natural products using long range carbon-proton coupling constants: Three-dimensional structure of okadaic acid solution. *Tetrahedron*, 51: 12229-12238.

Matsumori, N., Nonomura, T., Sasaki, M., Murata, M., Tachibana, K., Satake, M., Yasumoto, T. (1996). Long-range carbon-proton coupling for stereochemical assigment of acyclic structures in natural products: Configuration of the C5-C9 portion of maitotoxin. *Tetrahedron Letters*, 37: 1269-1272.

Mel'nik, V. A. (1971). Taxonomy of the genus *Ascochyta* Lib. *Mikologiya Fitopatologiya,* 5: 15-22.

Mel'nik VA. (2000). Key to the fungi of the genus *Ascochyta* Lib. (Coelomycetes). *In*: Hrsg. von der Biologischen Bundesanstalt für Land- und Forstwirtschaft, H. 379, Mel'nik, V. A, Braun, U., Hagedorn, G. (Eds). Berlin und Brauscheig. Parey: Berlin. (Mittteilungen aus der Biol. Bund. für Land- und Forstwirtschaft Berlin-Dahlem).

Medd, R. H. (1992). A review of the world distribution and host range of *Pyrenophora semeniperda*. *Review of Plant Pathology*, 71: 891-901

Mitina, G. V., Yuzikhin, O. S., Kozlov, I. D., Berestetskiy, A. (2005). *In*: Proceedings of 13th European Weed Research Society Symposium. Bari, Italy, 19-23 June, Abstr. 217.

Morin, L., Auld, B. A., Brown, J. F., Cholili, M. A. (1994). Pathogenic fungi occurring on the Noogoora burr complex in Australia. Proceedings Linnean Society NSW114, pp. 133-148.

Müller, S., Hauck, C., Schildknecht, H. (1992). Germination stimulants produced by *Vigna unguiculata* Waalp cv Saunders Upright. *Journal Plant Growth Regulator,* 11: 77-84.

Muralidharam, V. B., Wood, H. B., Ganem, B. (1990). Enantioselective synthesis of (-)-methyl 5-lactylshikimate lactone. *Tetrahedron Letters,* 31: 185-188.

Nagarajan, N. S., Rao, R. P., Manjo, C. N., Sethuraman, M. G. (2005). Piperidone derivatives from *Dalbergia sympatetica*. *Magnetic Resonance in Chemistry*, 43: 264-265.

Nakanishi, K., Solomon, P. H. (1977). Infrared Absorption Spectroscopy, 2nd edition. Holden Day, Oakland, pp. 17-44.

Nakamura, M., Ishibashi, K. (1958). New antibiotic ophiobolin, produced by *Ophiobolus miybeanus*. *Journal Agricultural Chemistry Soc. Japan,* 32: 739-744.

Natori, S., Yahara, I. (1991). Cytochalasins. *In*: Mycotoxins and Phytoalexins, Chapter 12, Sharma, R. P., Salunke, D. K. (Eds). CRC Press, Boca Raton, pp. 291-336.

Naylor, R. E. (2002). Weed Management Handbook. Blackwell Publishing, Oxford.

Neergard, P. (1979). Seed Pathology, Vol. 1. The Macmillan Press, London.

Netland, J., Dutton, L. C., Greaves, M. B., Baldwin, M., Vurro, M., Evidente, A., Einhorn, G., Scheepens, P. C. (2001). Biological control of *Chenopodium album* L. in Europe. *BioControl,* 46: 211-228.

Nozoe, S., Hirai, K., Tsuda, K. (1966). The structure of zizanin-A and –B, C_{25}-terpenoids isolated from *Helminthosporium zizaniae*. *Tetraedron Letters*, 20: 2211-2216.

Nozoe, S., Itai, A., Tsuda, K., Okuda, S. (1967). Chemical trasformation of cephalonic acid. *Tetraedron Letters*, 42: 4113-4117

Nozoe, S., Morisaki, M., Fukushima, K., Okuda, S. (1968). The isolation of an acyclic C25-isoprenoid alcohol, geranylnerolidol, and a new ophiobolin *Tetraedron Letters,* 42: 4457-4458.

Nozoe, S., Morisaki, M., Tsuda, K., Iitaka, Y., Tokahashi, N., Tamura, S., Ishibashi, K., Shirasaka, M. (1965). Structure of ophiobolin, a C25 terpenoid having a novel skeleton. *Journal of American Chemical Society*, 87: 4968-4970.

Ohtani, I., Kusumi, T., Kashman, Y., Kakisawa, H. (1991). *Journal of American Chemical Society*, 113: 4092-4096.

Padmanabhan, S. Y. (1973). The great Bengal famine. *Annual Review of Phytopathology*, 11: 11-26.

Parker, C., Riches, C. R. (1993). *Parasitic Weeds of the World; Biology and Control*. CAB International, Wallinford, UK. 1993.

Parker, C. (1994). The present state of the *Orobanche* problem. *In*: Biology and Management of Orobanche. Pieterse, A. H., Verkleij, J. A. C., ter Borg S. J.(Eds.). Proceedings of the Third International Workshop on Orobanche and Related Striga Research, Amsterdam, The Netherlands. The Netherlands Royal Tropical Institute: Amsterdam, The Netherlands, pp 17-26.

Pena-Rodriguez, L. M., Chilton, W. S. (1989). 3-anhydro-ophiobolin A and 3-anhydro-6-*epi*-ophiobolin A, phytotoxic metabolites of the johnson grass pathogen *Bipolaris sorghicola*. *Journal of Natural Products*, 52: 1170-1172.

Pini, C., Vicari, G., Ballio, A., Federico, R., Evidente, A., Randazzo, G. (1979). Antibodies specific for fusicoccin. *Plant Sciences Letters*, 16: 343-353.

Pinkerton, F., Strobel, G. A. (1976). Serinol as an activator of toxin production in attenuate cultures of *Helminthosporium sacchari*. *Proceeding of the National Academy of Science U.S.A.*, 73: 4007-4011.

Porter, Q. N. (1985). Mass spectrometry of heterocyclic compounds; John Wiley & Sons: New York, pp. 46-55, 480-486.

Pretsch, E., Bühlmann, P., Affolter, C. (2000). Structure Determination of Organic Compounds – Tables of Spectral Data. Springer-Verlag, Berlin, pp. 161-244.

Pujadas-Salvá, A. (2002). Orobanchaceae. *In*: Plantas Parásitas de la Península Ibérica e Islas Baleares. López-Sánchez, J. A., Catalán, P., Sáez, L. (Eds.). Mundi-Prensa, Madrid, Spain, pp. 345-452.

Randazzo, G., Evidente, A., Capasso, R., Colantuoni, F., Tuttobello, L., Ballio, A. (1979). Further experiments on the biosynthesis of fusicoccin. *Gazzetta Chimica Italiana*, 109: 101-104.

Reino, J. L., Hernández-Galán, R., Durán-Patrón, R., Collado, I. G. (2004). Virulence–toxin production relationship in isolates of the plant pathogenic fungus *Botrytis cinerea*. *Journal of Phytopathology*, 152: 563–566.

Rimando, A., Duke, S. O. (2006). Natural products for pest management. *In:* Natural Products for Pest Management, ACS Sympossium Series 927. Rimando, A. M., Duke, S. O. (Eds.). ACS Division of Agricultural and Food Chemistry, Inc., Washington, USA, pp. 2-21.

Rivero-Cruz, J. F., García-Aguirre, G., Cerda-García-Rojas, C. M., Mata, R. (2000). Conformational behaviour and absolute stereostructure of two phytotoxic nonenolides from the fungus *Phoma herbarum*. *Tetrahedron*, 56: 5337-5344.

Rivero-Cruz, J. F., Macías, M., Cerda-García-Rojas, C. M., Mata, R. (2003). A new phytotoxic nonenolides from *Phoma herbarum. Journal of Natural Products*, 66: 511–514.

Robenson, D. J., Strobel, G. A. (1985). The identification of a major phytotoxic component from *Alternaria macrospora* as α,β-dehydrocurvularin. *Journal of Natural Products*, 48: 139-141.

Rubiales, D., Sadiki, M., Román, B. (2005). First Report of *Orobanche foetida* on common vetch (*Vicia sativa*) in Morocco. *Plant Disease*, 89: 528-528.

Sakamura, S., Niki, H., Obata, Y., Sakai, R., Matsumoto, T. (1969). Isolation and structure of phytotoxic compounds produced by *Phyllosticta* sp. *Agricultural and Biological Chemistry*, 33: 698-703.

Sato, D., Awad, A. A., Chae, S. H., Yokota, T., Sugimoto, Y., Takeuchi, Y., Yoneyama, K. (2003). Analysis of strigolactones, germination stimulants for *Striga* and *Orobanche*, by high-performance liquid chromatography/tandem mass spectrometry. *Journal of Agricultural and Food Chemistry*, 51: 1162-1168

Sassa, T. (1971). Cotylenines, leaf growth substances produced by fungus. Part I. Isolation and characterization of cotylenins. *Agricultural and Biological Chemistry*, 35: 1415-1418.

Sassa, T., Neguro, T., Ueki, H. (1972). Production and characterization of a new fungal metabolite, cotylenol. *Agricultural and. Biological Chemistry*, 36: 2281-2285.

Sauerborn, J. (1991). Parasitic Flowering Plants: Ecology and Management. Weikersheim, Germany,Verlag Josef Margraf.

Schneeweiss, G. M., Colwell, A., Park, J. M., Jang, C. G., Stuessy, T. F. (2004). Phylogeny of holoparasitic Orobanche (Orobanchaceae) inferred from nuclear ITS-sequences. *Molecular Phylogenetics and Evolution*, 30: 465-478.

Scott, A. I. (1964). Interpretation of the Ultraviolet Spectra of Natural Compounds. Pergamon Press, Oxford, pp. 45-88.

Shimada, A., Takeuchi, S., Nakajima, A., Tanaka, S., Kawano, T., Kimura, Y. (1999). Phytotoxicity of indole-3-acetic acid produced by the fungus *Pythium aphanidermatum*. *Bioscience Biotechnology and Biochemistry*, 63: 187-189.

Shimada, A., Kusano, M., Matsumoto, K., Nishibe, M., Kawano, T., Rimura, Y. Z. (2002). Pollen growth regulator, fusanolide A, and a related metabolite from *Fusarium* sp. *Verlag der Zeitschrift fur Naturforschung*, 57b: 239-242.

Siame, B. A., Weerasuriya, Y., Wood, K., Ejeta, G., Butler, L. G. 1993). Isolation of strigol, a germination stimulant for *Striga asiatica*, from host plants. *Journal of Agricultural and Food Chemistry*, 41**:** 1486-1491.

Sivanesan, A. (1992). IMI description of fungi and bacteria no. 1123. *Drechslera gigantea*. *Mycopathologia*, 119: 40-50.

Sprecher, M., Sprinson, D. B. 1(962). Private communication

Strange, R. N. (1997). Phytotoxins associated *Ascochyta species*. *In*: Toxin in Plant Disease Development and Evolving Biotechnology. Upadhyay, R. K,. Mukherji, K. G. (Eds.). Oxford & IBH Publishing Co. Pvt., Ltd. New Delhi, India.

Sternhell, S. (1969). Correlation of interproton spin-spin coupling constants with structure. *Quarterly Review*, 23: 237-269

Strobel, G.A. (1982). Phytotoxins. *Annual Review of Biochemistry*, 51: 309-333.

Strobel, G.A. (1991). Il controllo biologico delle erbe infestanti. *Le Scienze*, 277: 56-63. Italian edition of Scientific American, New York: Scientific American Inc.

Strobel, G.A., Kenfield, D., Bunkers, G., Sugawara, F., Clardy, J. (1991). Phytotoxins as potential herbicides. *In*: Phytotoxins and Their Involvement in Plant Disease. Ballio, A., Graniti, A. (Eds.). *Experientia*, 47: 819-826.

Strobel, G., Kenfield, D., Sugawara, F. (1988). The incredible fungal genus *Drechslera* and its phytotoxic ophiobolins. *Phytoparasitica*, 16: 145-152.

Sugawara, F., Strobel, G., Stange, N. R., Siedow, J. N., Van Duyne G. D., Clardy, J. (1987). Phytotoxins from the pathogenic fungi *Drechslera maydis* and *Drechslera sorghicola*. *Proceeding of the National Academy of Sciences U.S.A.*, 84: 3081-3085.

Sugawara, F., Takahashi, N., Strobel, G., Yun, C. H., Gray, G., Fu, Y., Clardy, J. (1988). Some new phytotoxic ophiobolins produced by *Drechslera oryzae*. *Journal of Organic Chemistry*, 53: 2170-2172.

Surov, T., Aviv, D., Aly, R., Joel, D. M., Golman,-Guaez, T., Gressel, J. (1997). Generation of transgenic adulan-resistant potatoes to facilitate eradication of parasitic bromrapes (*Orobanche* spp.) *Theoretical and Applied Genetics*, 96: 132-137.

Suzuki, Y., Tanaka, H., Aoki, H., Tamura, T. (1970). Ascotoxin (decumbin), a metabolite of *Ascochyta imperfecta* Peck. *Agricultural and Biological Chemistry*, 34: 395-413.

Tabacchi, R., Fkyerat, A., Poliart, C., Dubin, G. M. (2000). Phytotoxins from fungi of esca of grapevine. *Phytopathologia Mediterranea*, 39: 156-161.

Tatum, L. A. (1971). The Southern corn leaf blight. *Science*, 171: 1113-1115.

Tetjen, K. G., Shaller, E., Matern, U. (1983). Phytotoxins from *Alternaria cartami* Chowdhuri: structural identification and physiological significance. *Physiology and Plant Pathology*, 23: 387-400.

Tringali, C. (2001). Bioactive Compounds from Natural Sources; Taylor & Francis: London.

Tsipouras, A., Adefarati, A. A., Tkacz, J. S., Frazier, E. G., Rohrer, S. P., Birzin, E., Rosegay, A., Zink, D. L., Goetz, M. A., Singh, S. B., Schaeffer, J. M. (1996). Ophiobolin M and analogues, noncompetitive inhibitors of ivermectin binding with nematocidal activity. *Bioorganic & Medicinal Chemistry*, 4: 531-536.

Tsuda, M., Mugishima, T., Komatsu, K., Sone, T., Tanaka, M., Mikami, Y., Kobayashi, J. (2003). Modiolides A and B, two new 10-membered macrolides from a marine-derived fungus. *Journal of Natural Products*, 66: 412-415.

Turner, W. B. (1971). *Fungal Metabolites*. London, Academic Press, p. 312.

Turner, W. B., Aldridge, D. C. (1983). *Fungal Metabolites II*. London, Academic Press, pp. 228-280, 370-383,398-399, 468-484, 505, 530-532, 631.

Upadhyay, R. K., Kenfield, D., Strobelm G. A, Hess, W. M. (1991). *Ascochyta cypericola* sp. *nov*. causing leaf blight of purple nutsedge (*Cyperus rotundus*). *Canadian Journal of Botany*, 69: 797-802.

Upadhyay, R. K., Maker, K. G. (1997). Toxins in Plant Disease Development and Evolving Biotechnology, Oxford & IBH Publishing Co. Pvt. Ltd, New Delhi India.

Vaccaro, W. D., Burnett, D. A, Clader, J. W. (1996). U.S. Patent WO 95-US16007 19951218.

van der aA, H. A.;, Boerema, G. A., de Gruyter, J. (2000). Contribution towards a monography of *Phoma* (Coelomycetes) VI – 1. Section Phyllostictictoides: characteristics and nomenclature of its type species *Phoma exigua*. *Personia*, 17: 435-456.

Venkatasuwaiah, P., Sutton, T. B., Chilton, W. S. (1991). Effect of phytototoxins produced by *Botryosphaeria obtusa*, the cause of black rot of apple fruit and frogeye leaf spot. *Phytopathology*, 81: 243-247.

Vurro, M., Bottalico, A., Capasso, R., Evidente, A. (1997). Cytochalasins from phytopatogenic *Ascochyta* and *Phoma* species. *In:* Toxins in Plant Disease Development and Evolving Biotechnology. Upadhyay, R. K., Mukerji, K. G. (Eds.). Oxford & IBH Publishing Co, New Delhi, India, pp. 127-147.

Vurro, M., Ellis, B. E. (1997). Effect of fungal toxins on induction of phenylalanine ammonia-lyase activity in elicited cultures of hybrid poplar. *Plant Science*, 126: 29-38.

Vurro, M., Evidente, A., Andolfi, A., Zonno, M. C., Giordano, F., Motta, A. (1998). Brefeldin A and α,β-dehydrocurvularin, two phytotoxins from *Alternaria zinniae*, a biocontrol agent of *Xanthium occidentale*. *Plant Science*, 138: 67-79.

Vurro, M., Zonno, M. C., Evidente A., Andolfi, A., Montemurro, P. (2001). Enhancement of efficacy of *Ascochyta caulina* to control *Chenopodium album* by use of phytotoxins and reduced rate of herbicides. *Biological Control*, 21: 182-190.

Williams, C. K. (2006). *Abstracts of Papers* 223nd National Meeting of the American Chemical Society, San Francisco, CA, September 10-14, American Chemical Society, Washington, DC, 2007, INOR-1000.

Wood, W. F. (2002). 2-Pyrrolidinone, a putative alerting pheromone from rump glands of pronghorn, *Antilocapra americana. Biochemical Systematics Ecology*, 30: 361-363.

Wu, M., Okino, T., Nogle, L. M., Marquez, B. L., Williamson, R. T., Sitachitta, N., Berman, F. W., Murray, T. F., McGough, K., Jacobs, R., Colsen, K., Asano, T., Yokokawa, F., Shioiri, T.,Gerwick, W. H. (2000). Structure, synthesis, and biological properties of kalkitoxin, a novel neurotoxin from the marine cyanobacterium Lyngbya majuscula *Journal of American Chemical Society*, 122: 12041-12042.

Wyss, R., Tamm, C., Vederas, J. C. (1980). Differential hydrogen exchange during biosynthesis of cytochalasins B and D. *Croatica Chemica Acta* , 58: 537-546.

Yokota, T., Sakai, H., Okuno, K., Yoneyama, K., Takeuchi, Y. (1998). Alectrol and orobanchol. Germination stimulants for *Orobanche minor*, from its host red clover. *Phytochemistry*, 49: 1967-1973.

Yoneyama, K., Sato, D., Takeuchi, Y., Sekimoto, H., Yokota, T., Sassa, T. (2006). Search for germination stimulants and inhibitors for root parasitic weeds. *In*: Natural Products for Pest Management. Duke, S. O., Rimando, A. (Eds.). American Chemical Society, Washington, DC, USA, 2006, pp. 88-98.

Yoneyama, K., Takeuchi, Y., Ogasawara, M., Konnai, M., Sugimoto, Y., Sassa, T. (1998). Cotylenins and fusicoccins stimulate seed germination of *Striga hermonthica* (Del.) Benth and *Orobanche minor* Smith. *Journal of Agricultural and Food Chemistry,* 46: 1583-1586.

Yoneyama, K., Takeuchi, Y., Sato, D., Sekimoto, H., Yokota, T. (2004). Determination and quantification of strigolactones. *In*: Proceedings of the 8th International Parasitic Weed Symposium; Joel, D. M., (Ed.). International Parasitic Plant Society, Amsterdam, p 9.

Yuzikhin, O., Mitina, G., Beretstetskiy, A. (2007). Herbicidal potential of stagonolide, a new phytotoxic nonenolide from *Stagonospora cirsii*. *Journal of Agricultural and Food Chemistry*, 55: 7707-7711.

Zhan, W. M., Watson, A. K. (1997). Host range of *Exserohilum monoceras,* a potential bioherbicide for the control of *Echinocloa* species. *Canadian Journal of Botany*, 75: 685–692.

Zhori, A. A., Swaber, S. M. (1994). Cytochalasins A and B of dematiaceous hypomycetes. *Letters in Applied Microbiology*, 19: 37-39.

Zonno, M. C., Vurro, M., Capasso, R., Evidente, A., Cutignano, A., Suaerborn, J., Thomas, H. (1996). Phytotoxic metabolites produced by *Fusarium nygamai* from *Striga hermontica*. *In*: Proceedings of the IX International Symposium on Biological Control of Weeds. Moran, V. C., Hoffmann, J. H. (Eds). Stellenbosh, South Africa, January 21-26, pp. 223-226.

Photo 1. *Digitaria sanguinalis*

Photo 2. *Cirsium arvense*

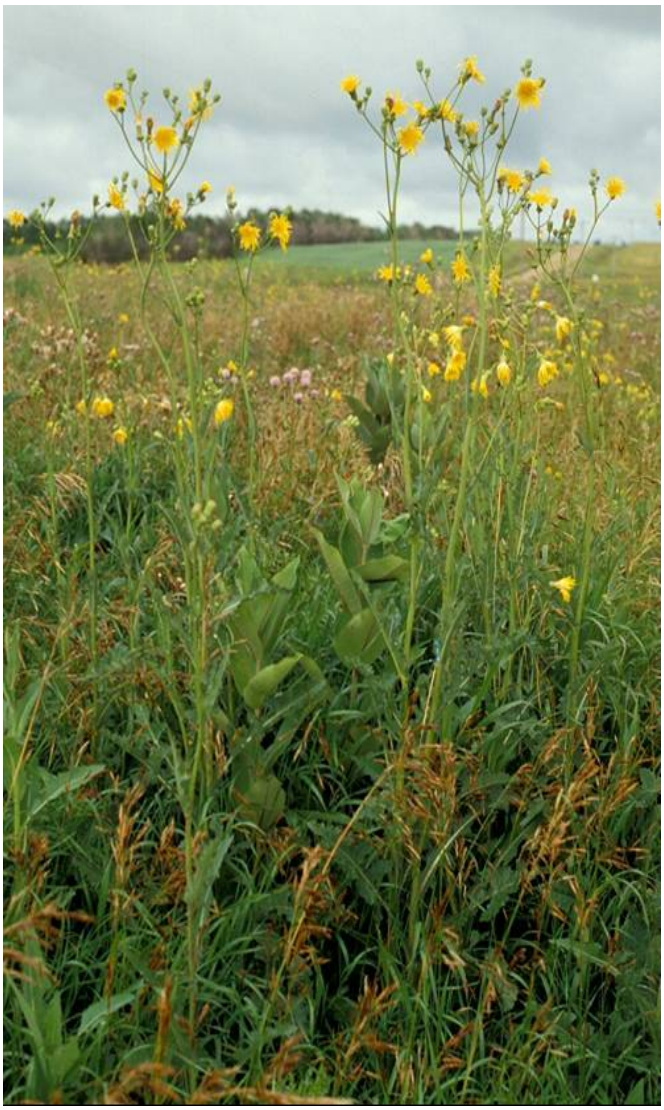

Photo 3. *Sonchus arvens*

Photo 4. *Orobanche ramosa* infesting cabbage field

Photo 5. *Orobanche ramosa* infested tomato field

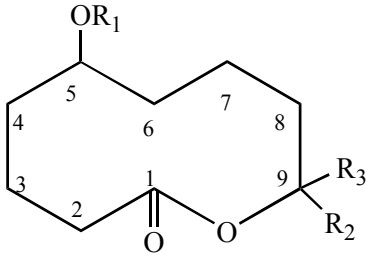

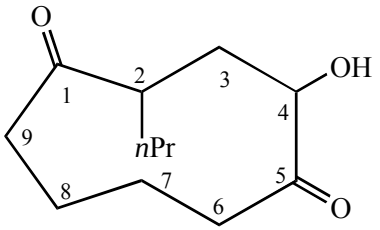

3

1 R_1=H, R_2=$CH_2CH_2CH_3$, R_3=H

2 R_1=H, R_2=$CH_2CH_2CH_2CH_2CH_3$, R_3=H

4 R_1=H, R_2=H, R_3=$CH_2CH_2CH_2CH_2CH_3$

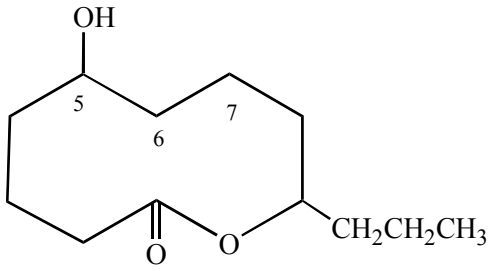

5

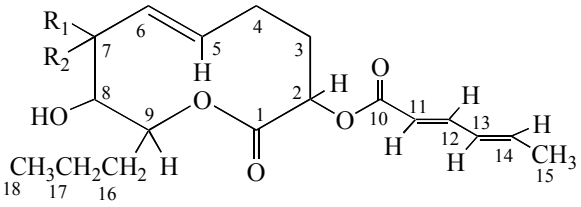

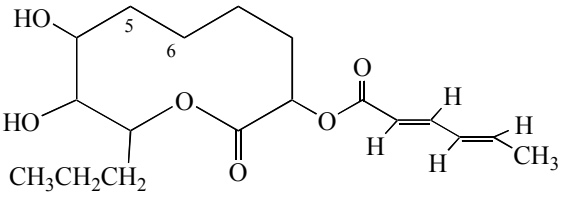

6 R_1=OH R_2=H

7 R_1=H R_2=OH

8

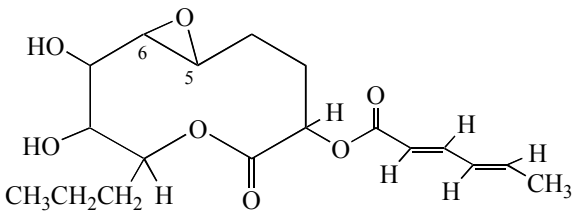

9

Figure 1.1. Structure of putaminoxin (**1**), pinolidoxin (**6**) and some their analogues (**2-5** and **7-9**) isolated from *Phoma putaminum* and *Ascochyta pinodes* culture filtrates, respectively

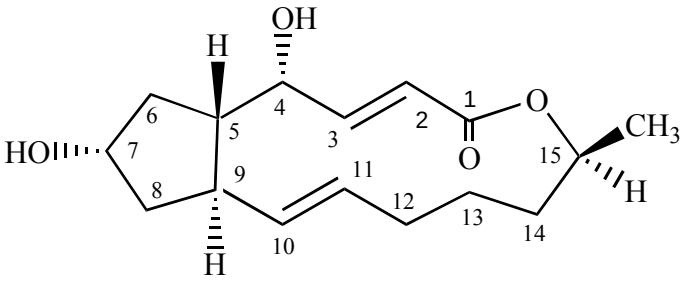

10

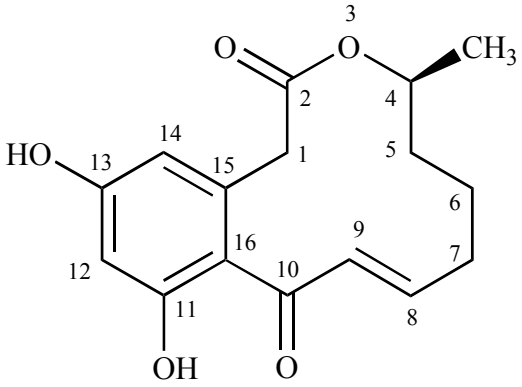

11

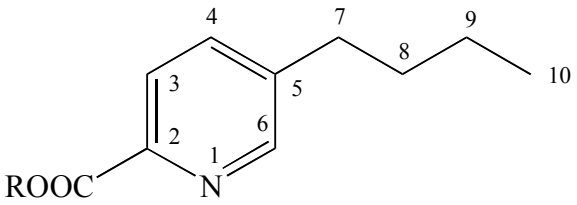

12 R=H **13** R=CH_3

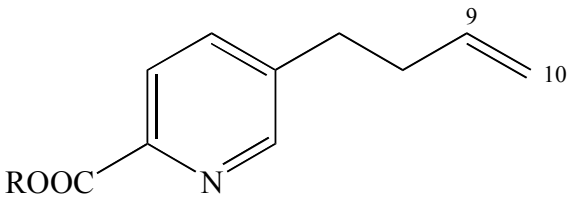

14 R=H **15** R=CH_3

Figure 1.2. Structure of brefeldin A (**10**) and α,β-dehydrocurvularin (**11**) isolated from *Alternaria zinniae* culture filtrates and fusaric acid (**12**), 9,10 dehydrofusaric acid (**14**) and corresponding methyl esther (**13** and **15**) isolated from *Fusarium nygamai* culture filtrates

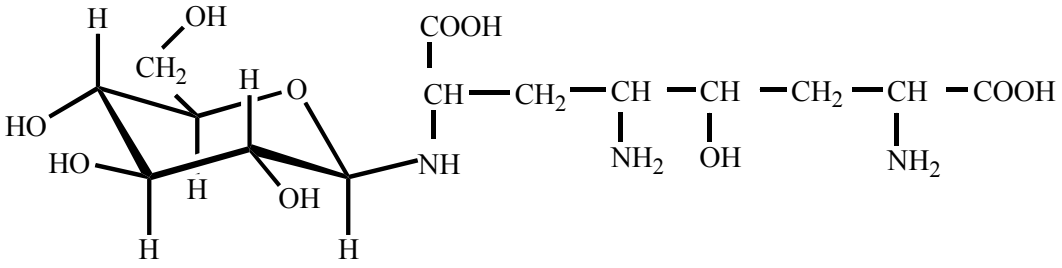

16

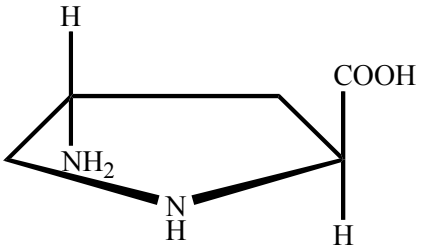

17

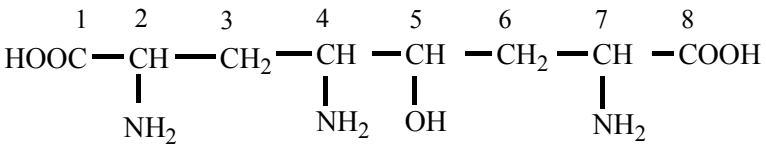

18

Figure 1.3. Structure of ascaulitoxin (**16**), *trans*-4-aminoproline (**17**) and the ascaulitoxin aglycone (**18**) isolated from *Ascochyta caulina* culture filtrates

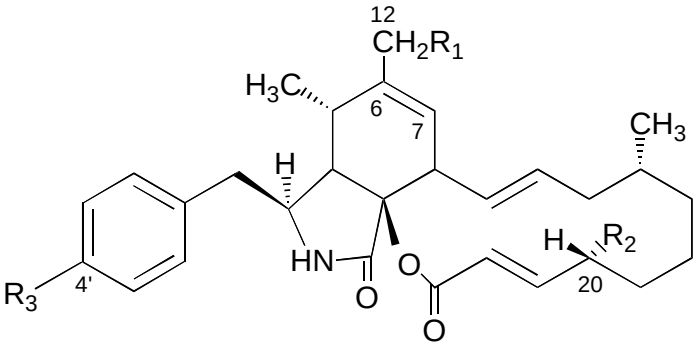

19 $R_1=R_2=H$, $R_3=OH$

20 $R_1=R_2=OH$, $R_3=H$

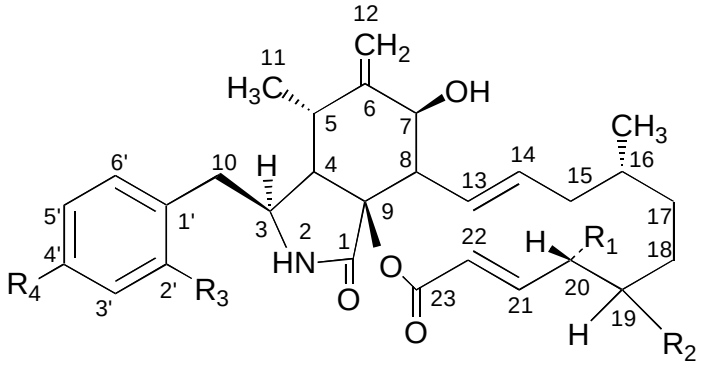

21 $R_1=R_3=R_4=H$, $R_2=OH$

22 $R_1=R_3=OH$, $R_2=R_4=H$,

23 $R_1=R_4=OH$, $R_2=R_3=H$

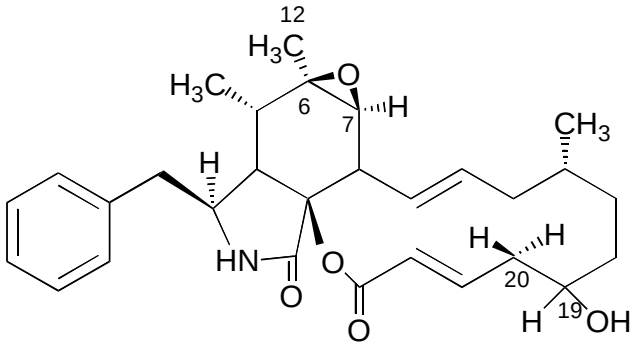

24

Figure 1.4. Structure of cytochalasins produced by *Pyrenospora seminiperda* (**19-21**) and *Phoma exigua* var. *heteromorpha* (**20-24**)

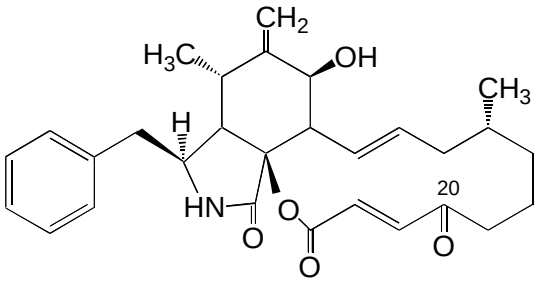

25

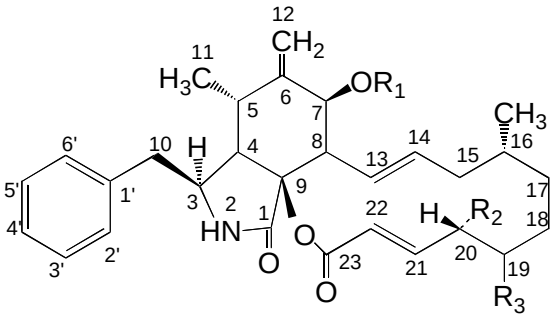

26 $R_1=R_3=H$, $R_2=O$
27 $R_1=Ac$,
$R_2=OH$, $R_3=H$

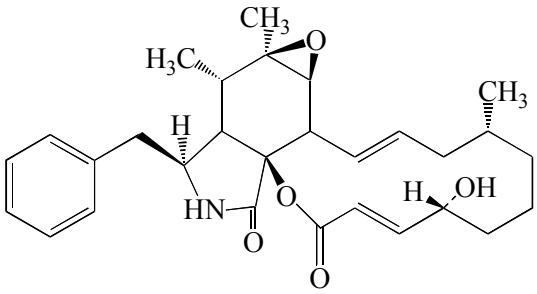

28

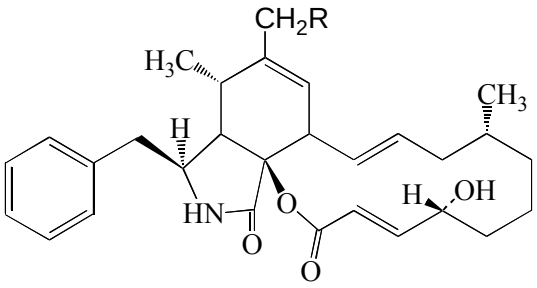

29 R=H

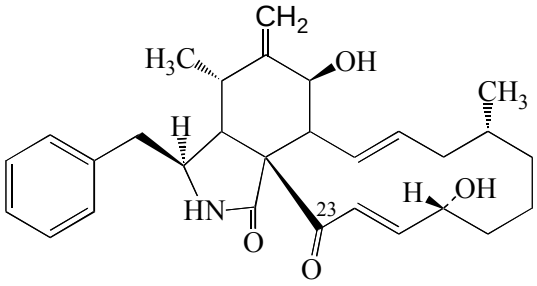

30

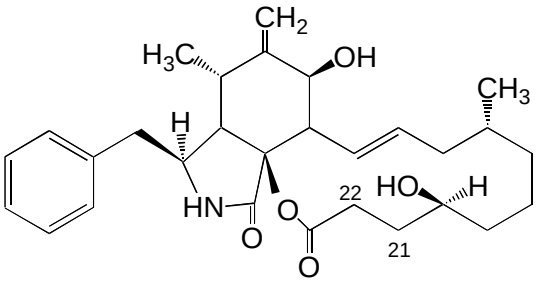

31

Figure 1.5. Structure of cytochalasins isolated from *Phoma exigua* var. *heteromorpha* culture filtrates and some their derivatives

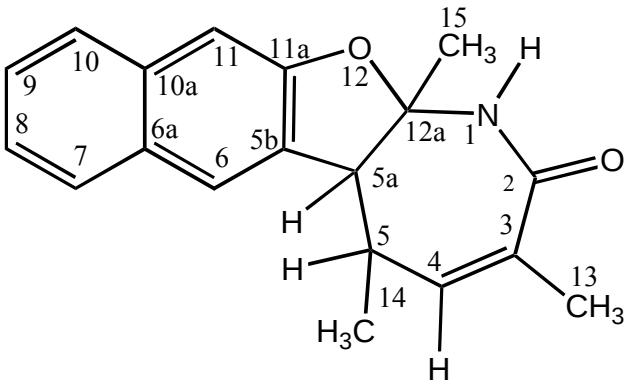

32a

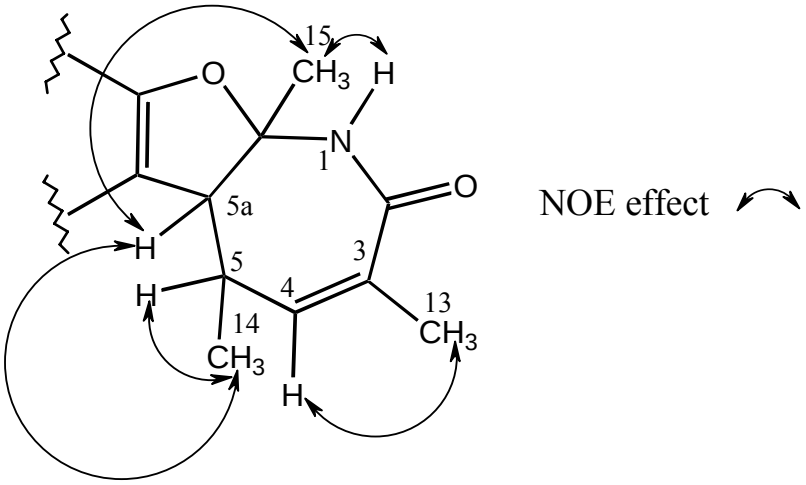

32b

Figure 1.6. Structure of drazepinone isolated from *Dreschlera siccans* culture filtrates

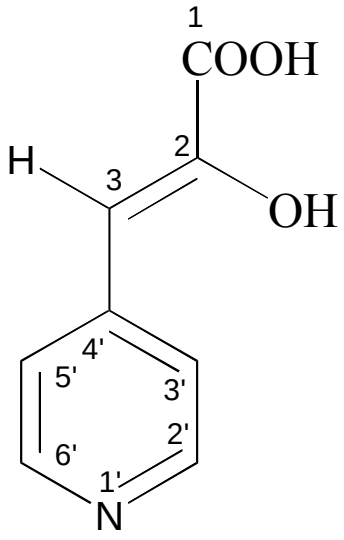

33

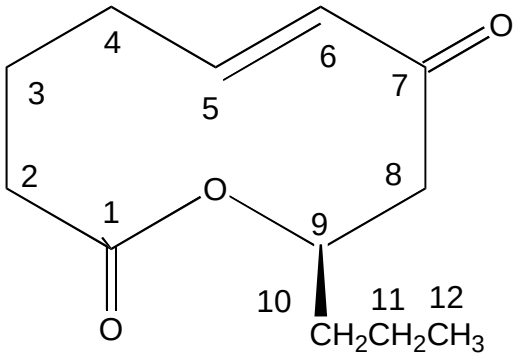

34

Figure 1.7. Structure of ascosonchine (**33**) and stagonolide (**34**) isolated from *A. sonchi* and *Stagonospora cirsii* culture filtrates, respectively

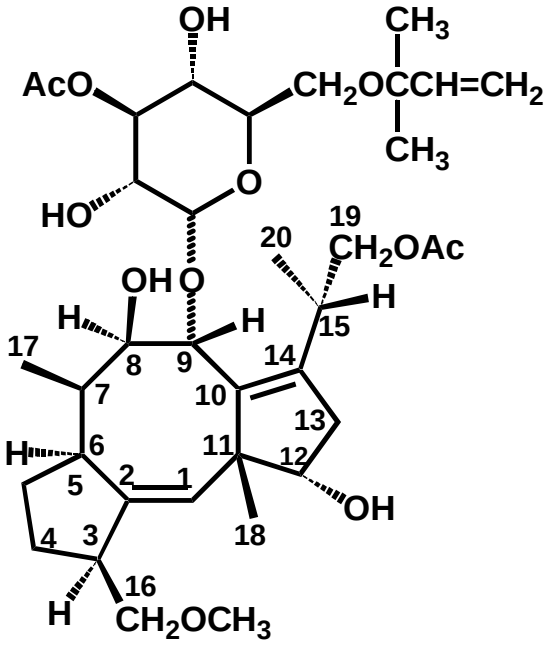

35

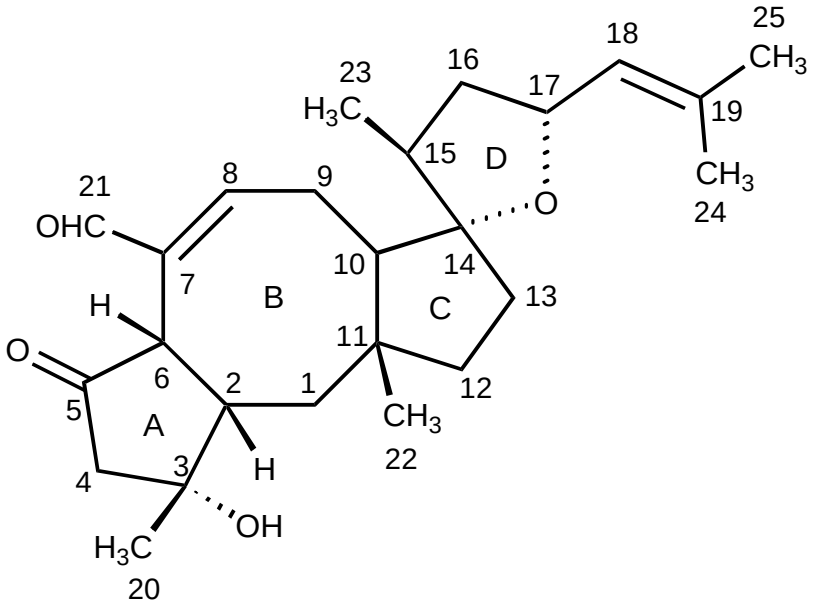

36

Figure 1.8. Structure of fusicoccin (**35**) and ophiobolin A (**36**)

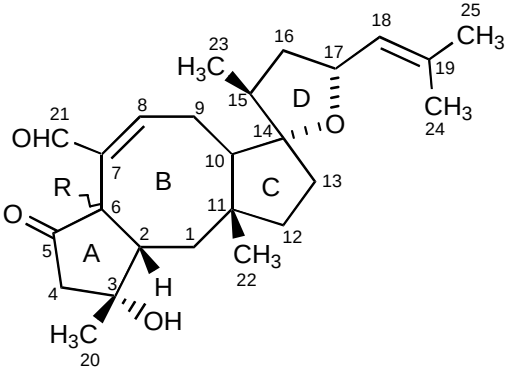

36 R=βH
37 R=αH

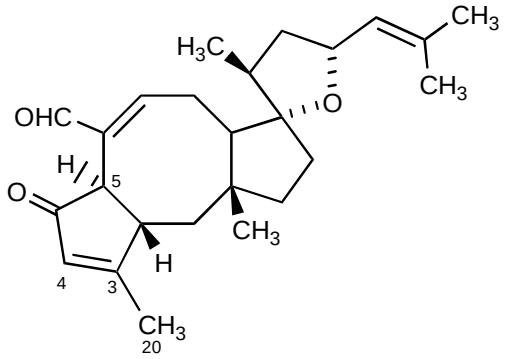

38

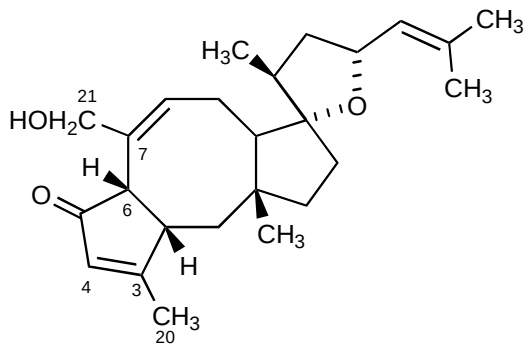

39

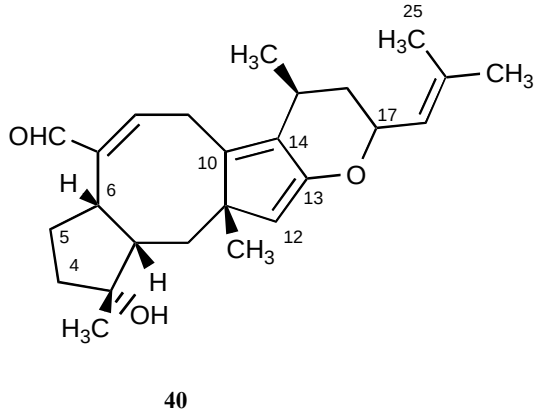

40

Figure 5.1.1. Structure of ophiobolins isolated from *D. gigantea* culture filtrates

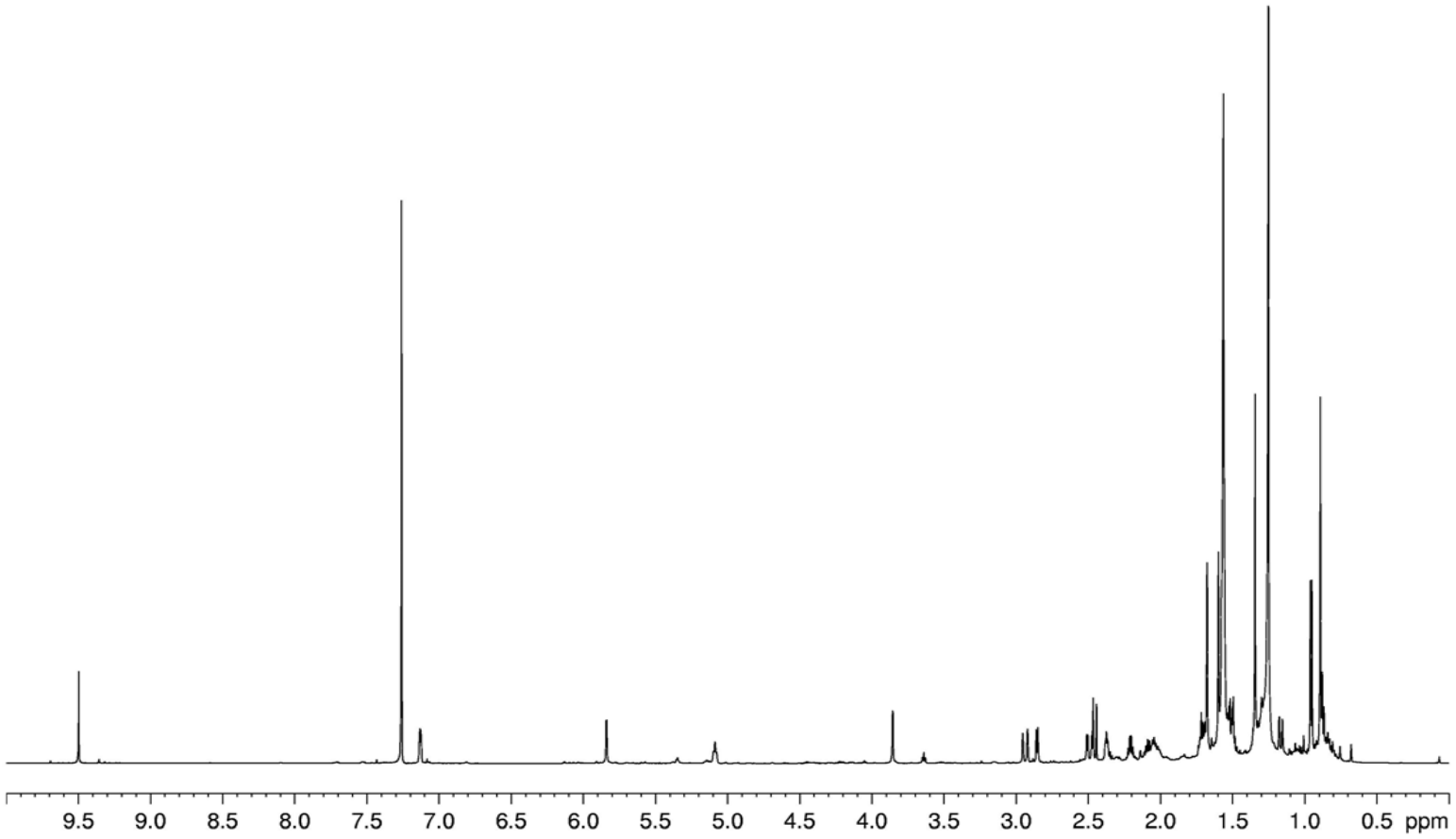

Figure 5.1.2. ^{1}H NMR spectrum of ophiobolin E, isolated from *D. gigantea* culture filtrates, recorded at 600 MHz

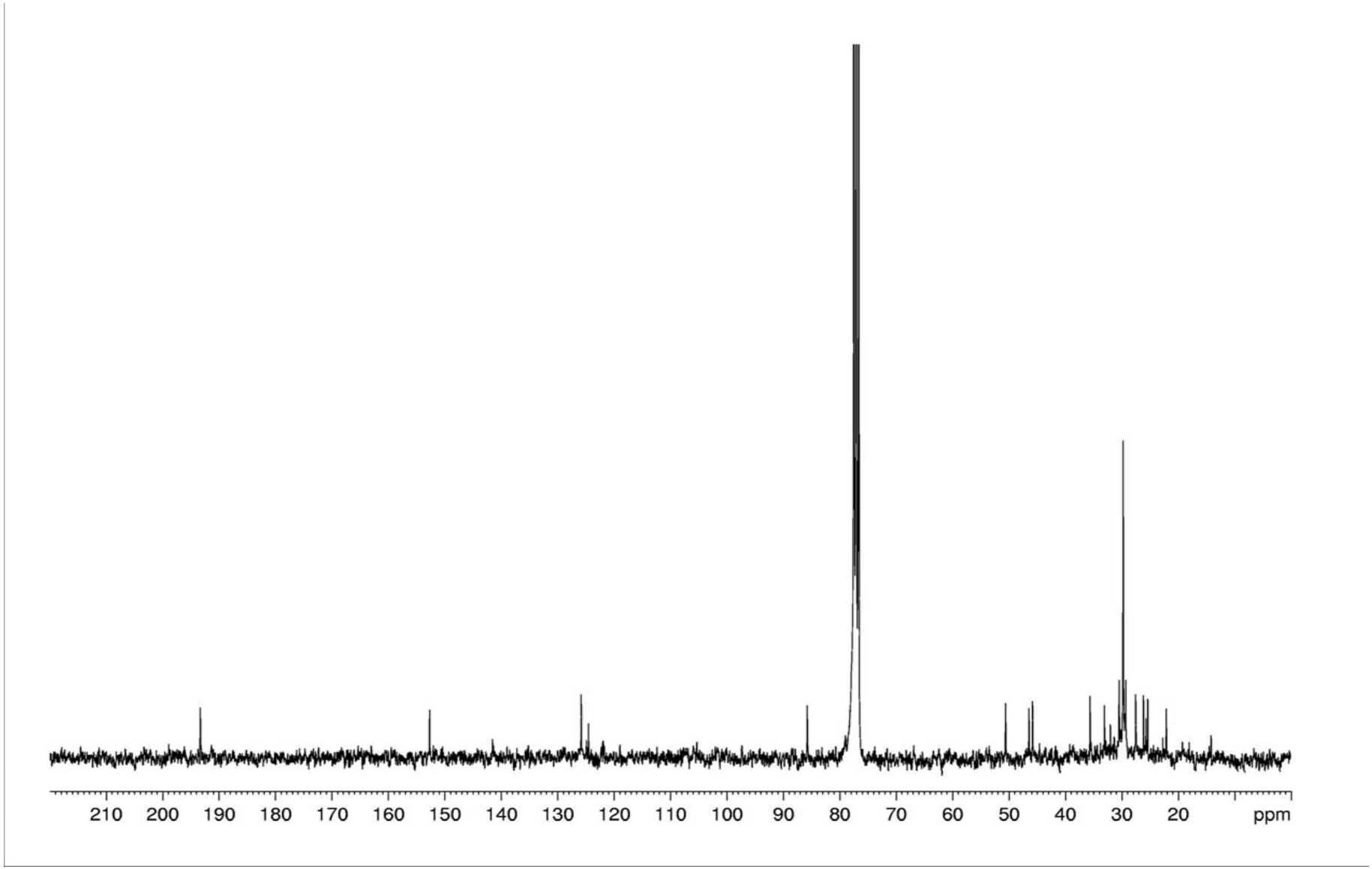

Figure 5.1.3. ^{13}C NMR spectrum of ophiobolin E, isolated from *D. gigantea* culture filtrates, recorded at 300 MHz

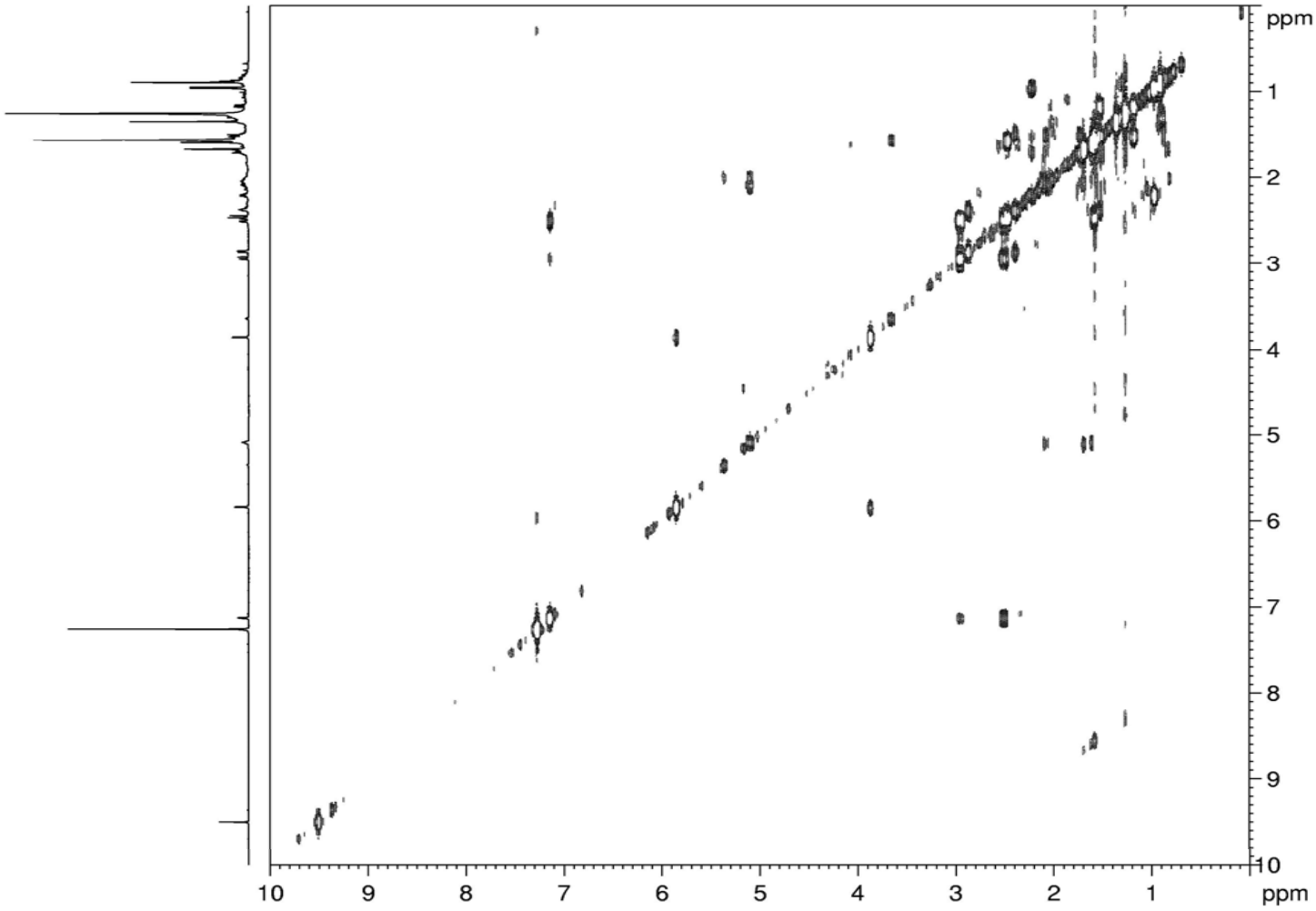

Figure 5.1.4. COSY spectrum of ophiobolin E, isolated from *D. gigantea* culture filtrates, recorded at 600 MHz

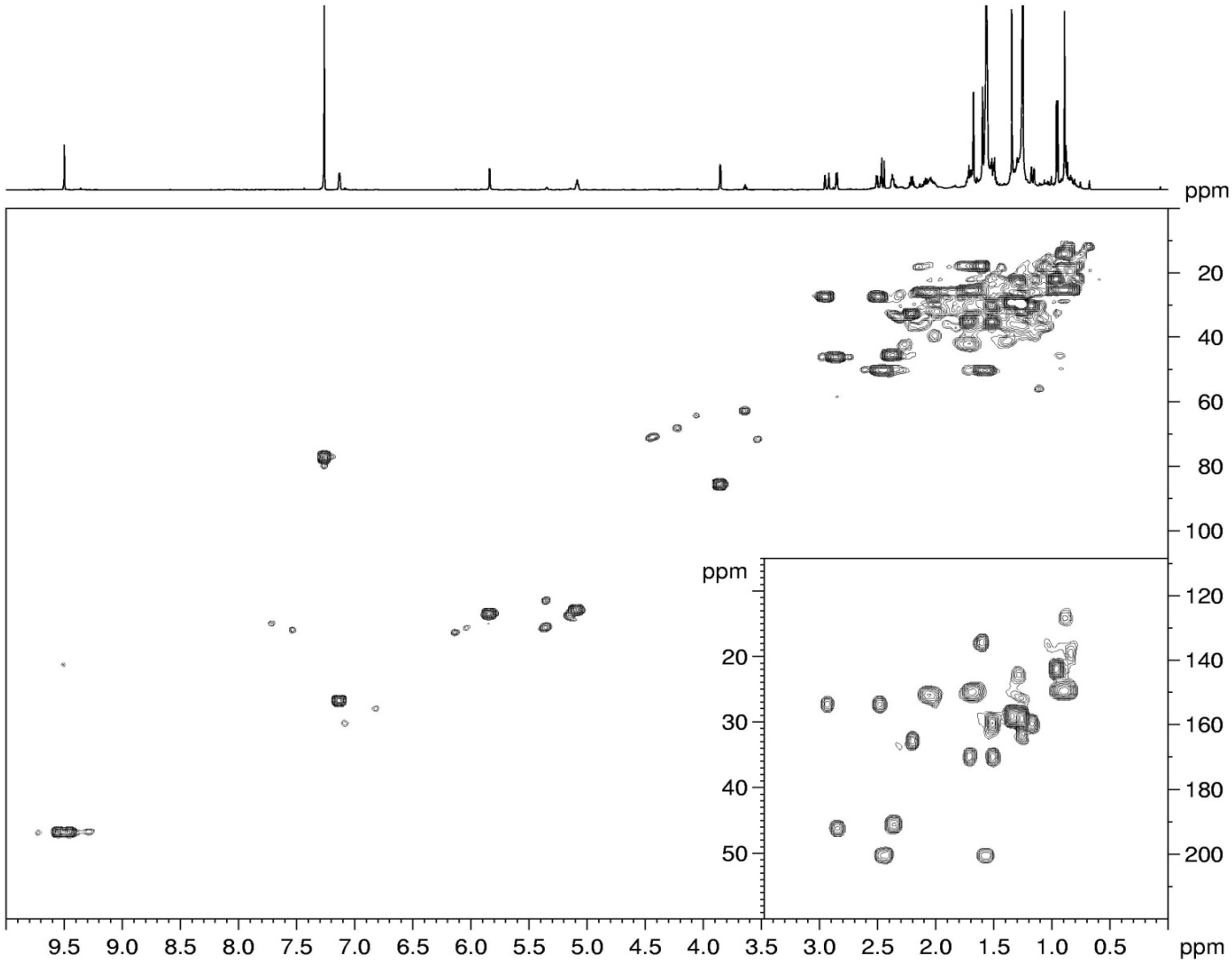

Figure 5.1.5. HSQC spectrum of ophiobolin E, isolated from *D. gigantea* culture filtrates, recorded at 600 MHz

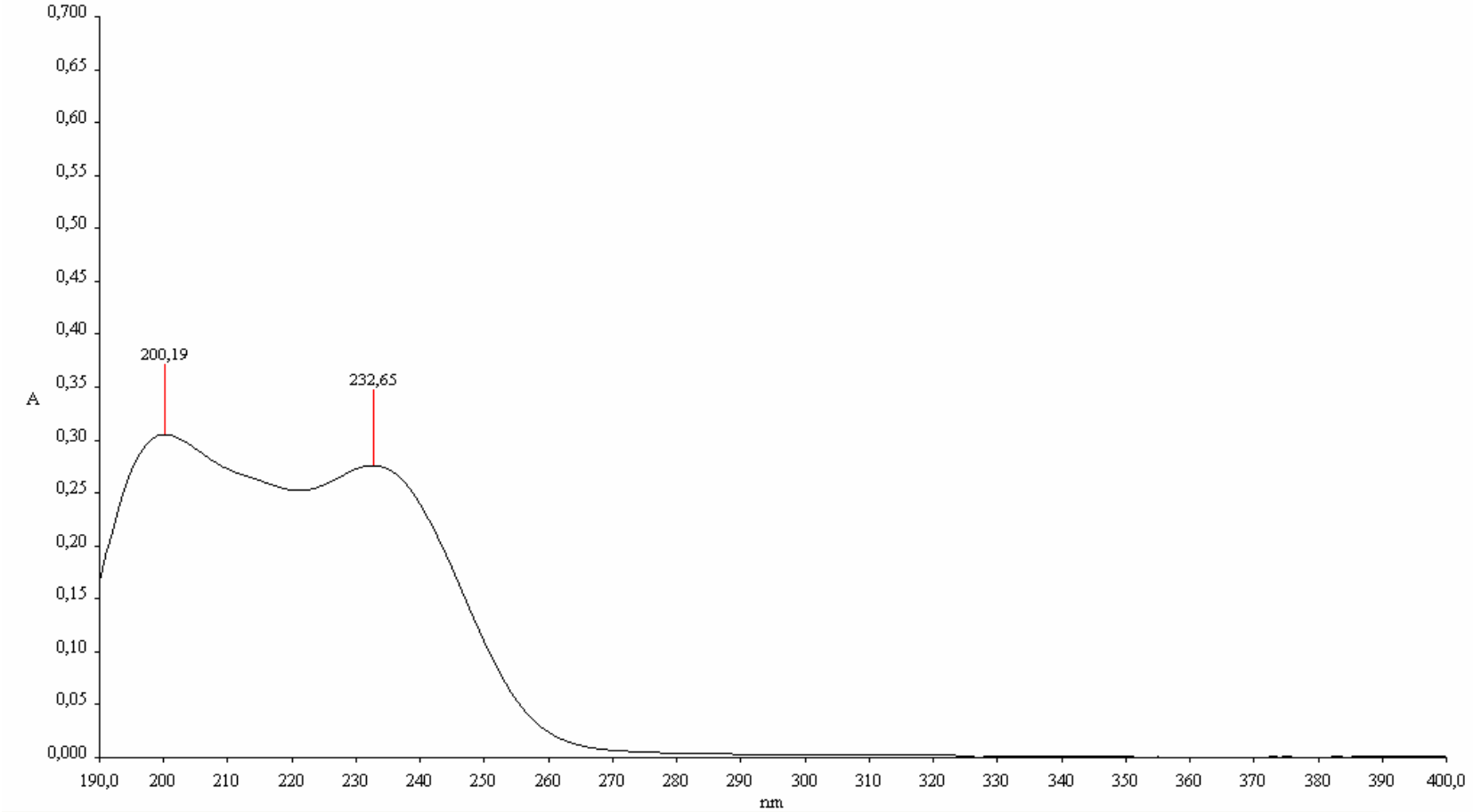

Figure 5.1.6. UV spectrum of ophiobolin E, isolated from *D. gigantea* culture filtrates, recorded in MeCN solution

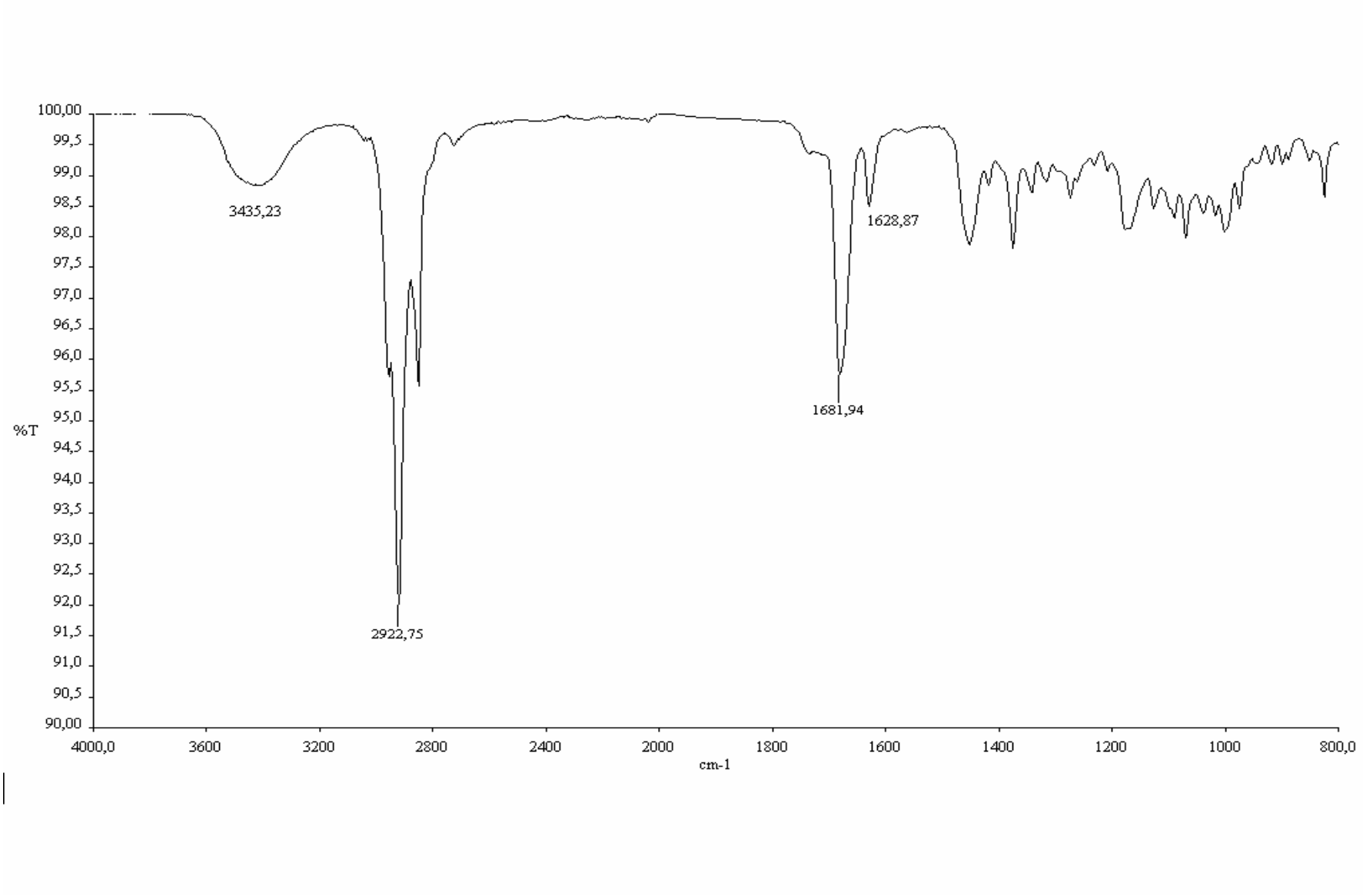

Figure 5.1.7. IR spectrum of ophiobolin E, isolated from *D. gigantea* culture filtrates, recorded as neat

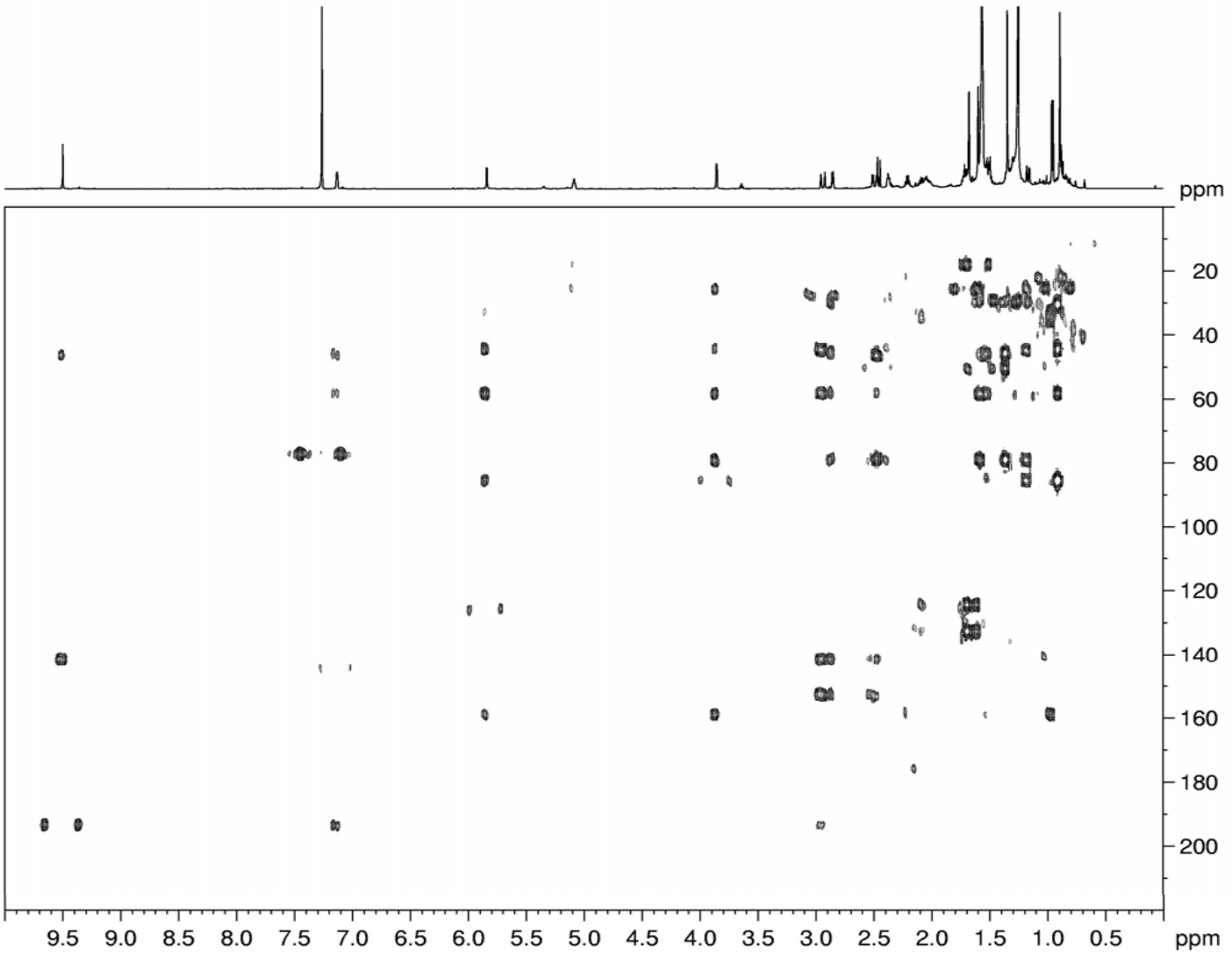

Figure 5.1.8. HMBC spectrum of ophiobolin E, isolated from *D. gigantea* culture filtrates, recorded at 600 MHz

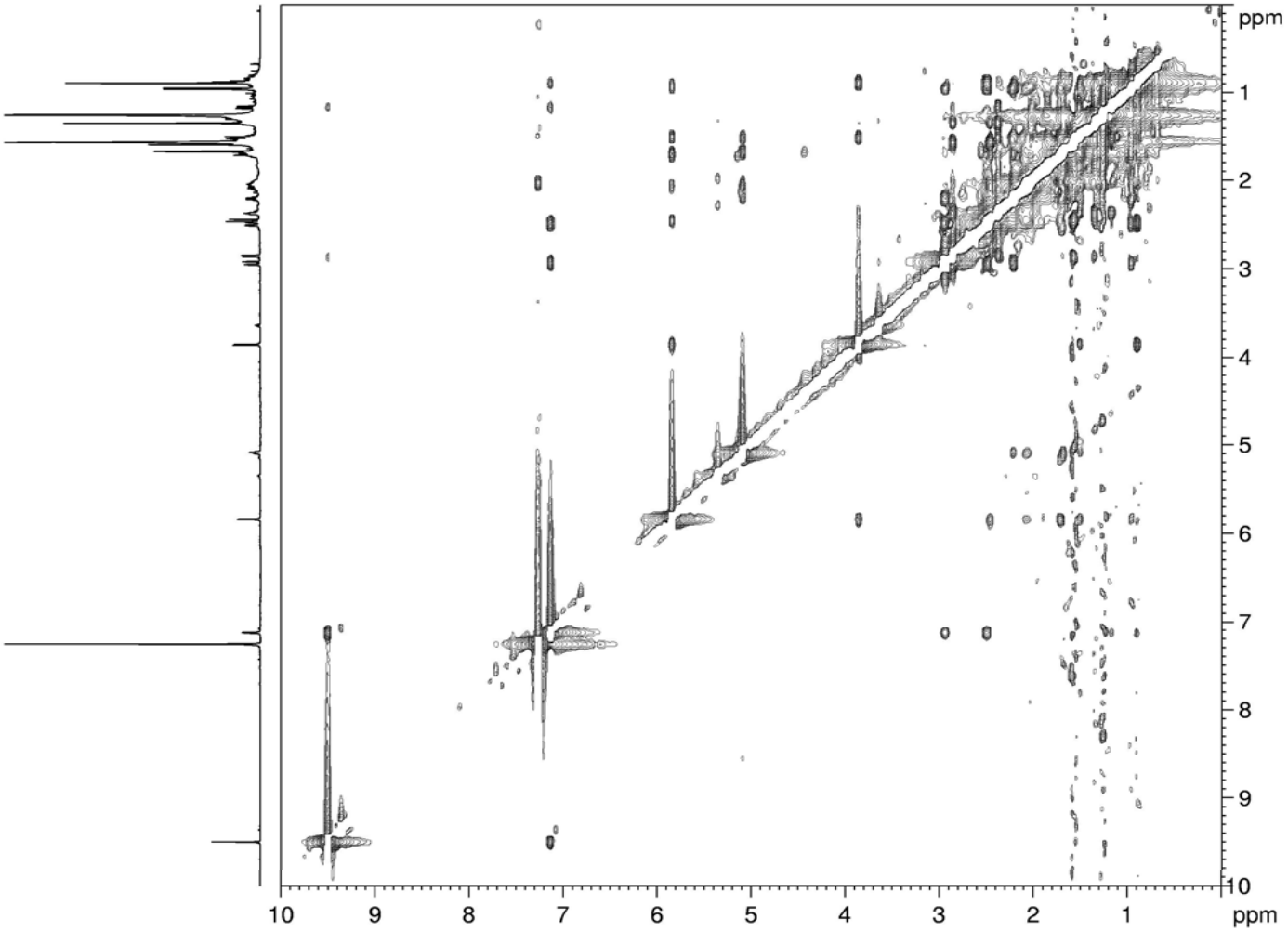

Figure 5.1.9. NOESY spectrum of ophiobolin E, isolated from *D. gigantea* culture filtrates, recorded at 600 MHz

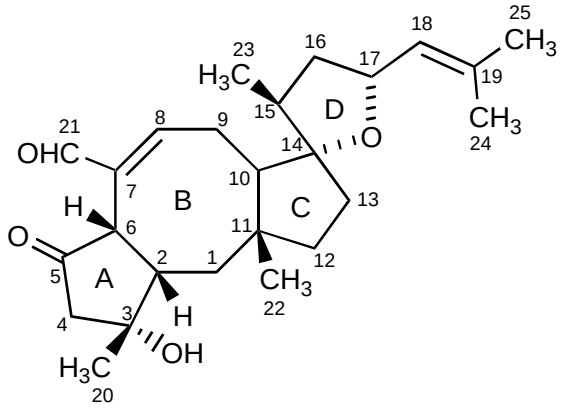

36

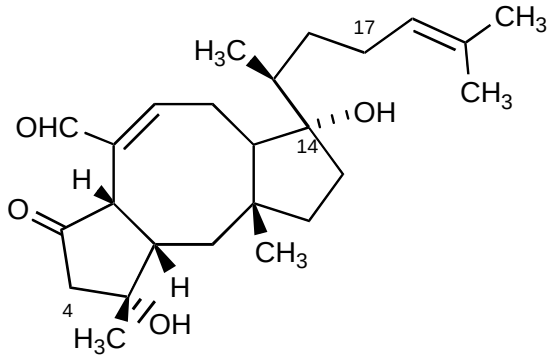

41

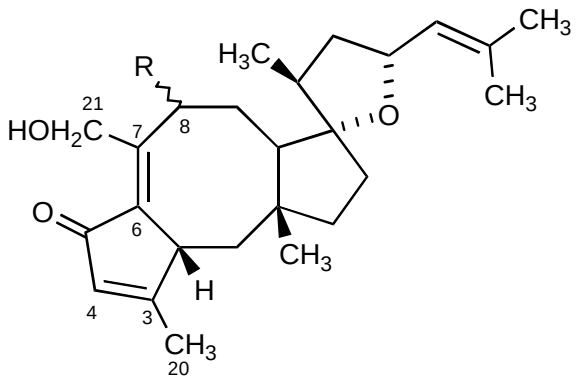

42 R=βOH
43 R=αOH

Figure 5.2.2. Ophiobolins isolated from *D. gigantea* solid culture

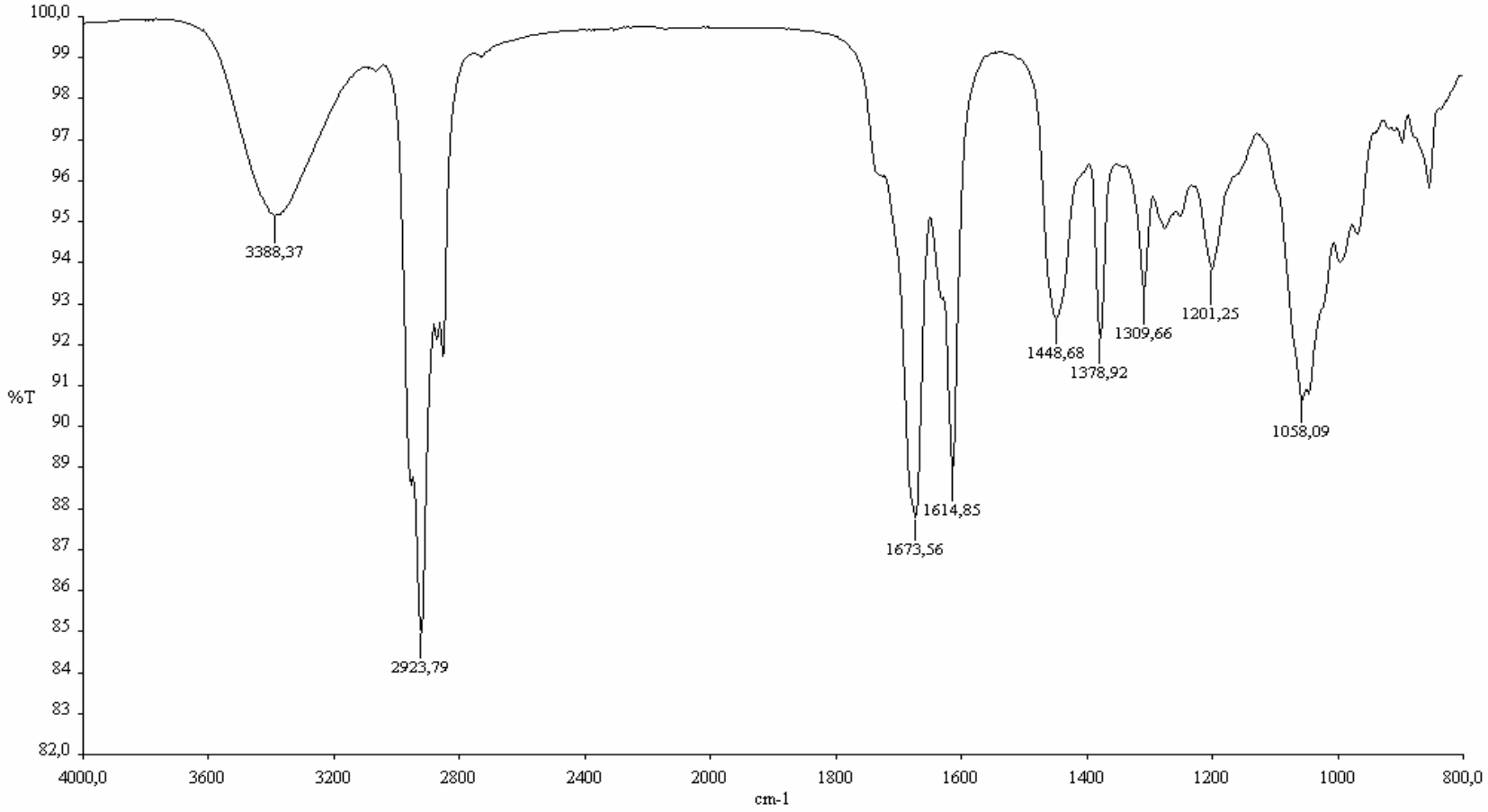

Figure 5.2.2. IR spectrum of 8-*epi*-ophiobolin J, isolated from *D. gigantea* solid culture, recorded as neat

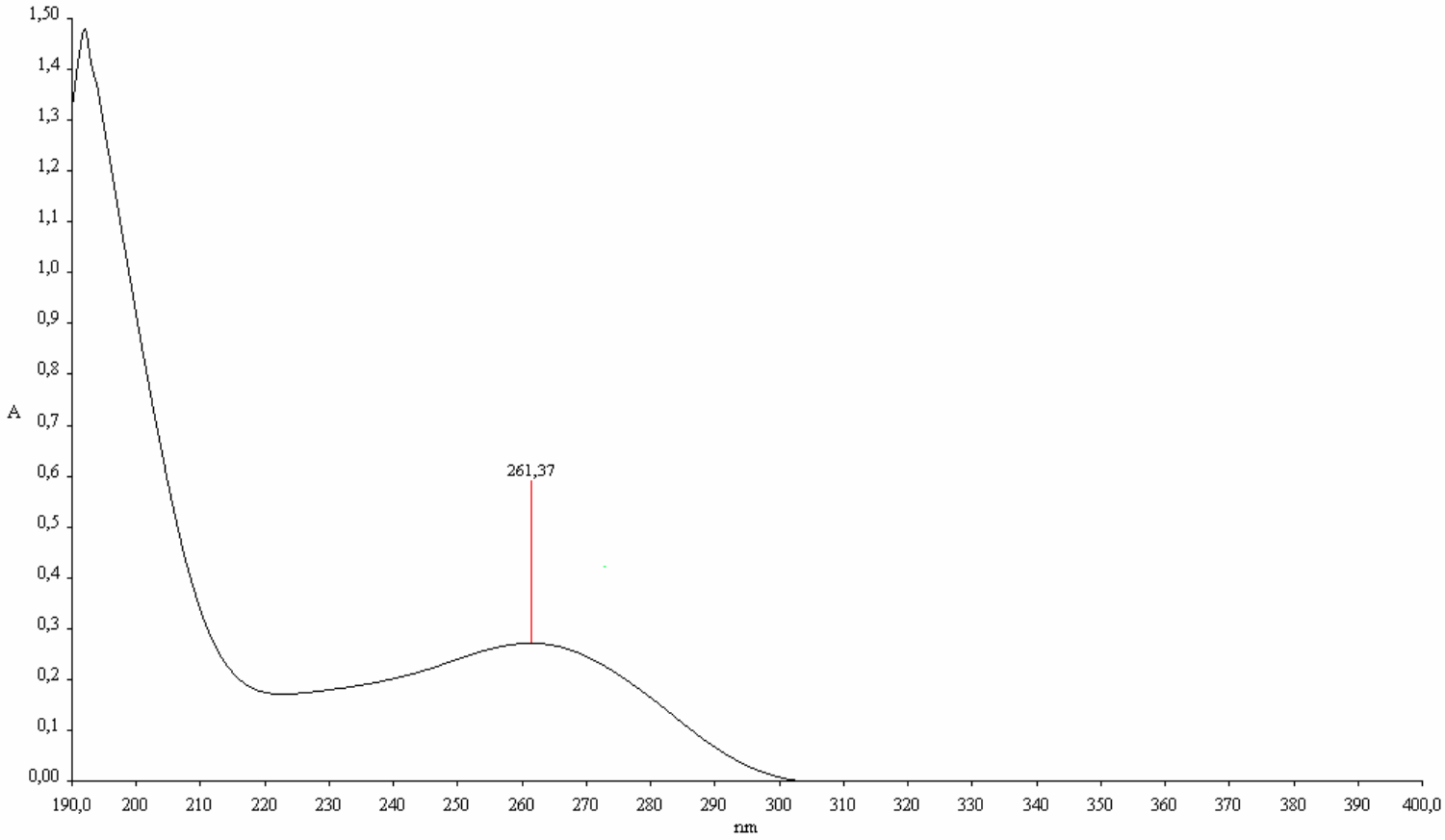

Figure 5.2.3. UV spectrum of 8-*epi*-ophiobolin J, isolated from *D. gigantea* solid culture, recorded in MeCN solution

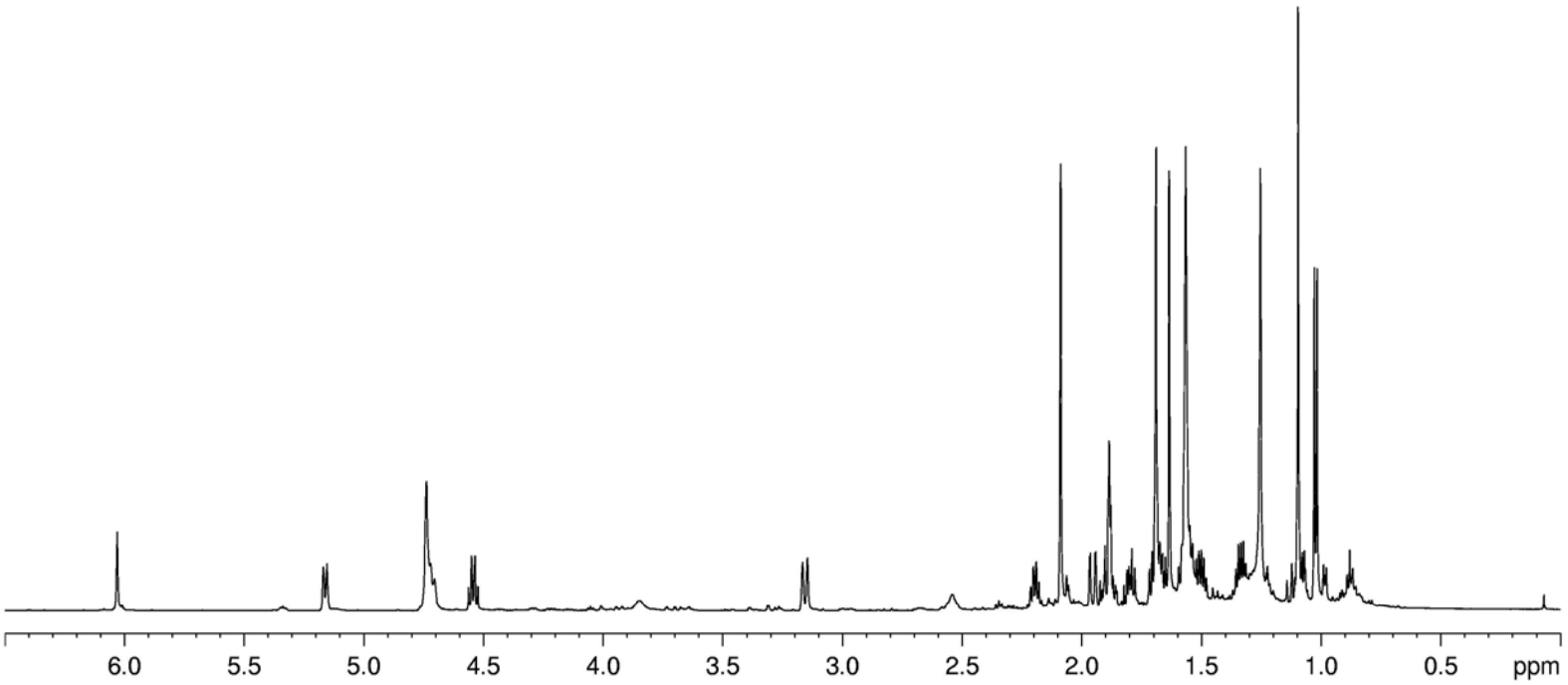

Figure 5.2.4. ^{1}H NMR spectrum of 8-*epi*-ophiobolin J, isolated from *D. gigantea* solid culture, recorded at 600 MHz

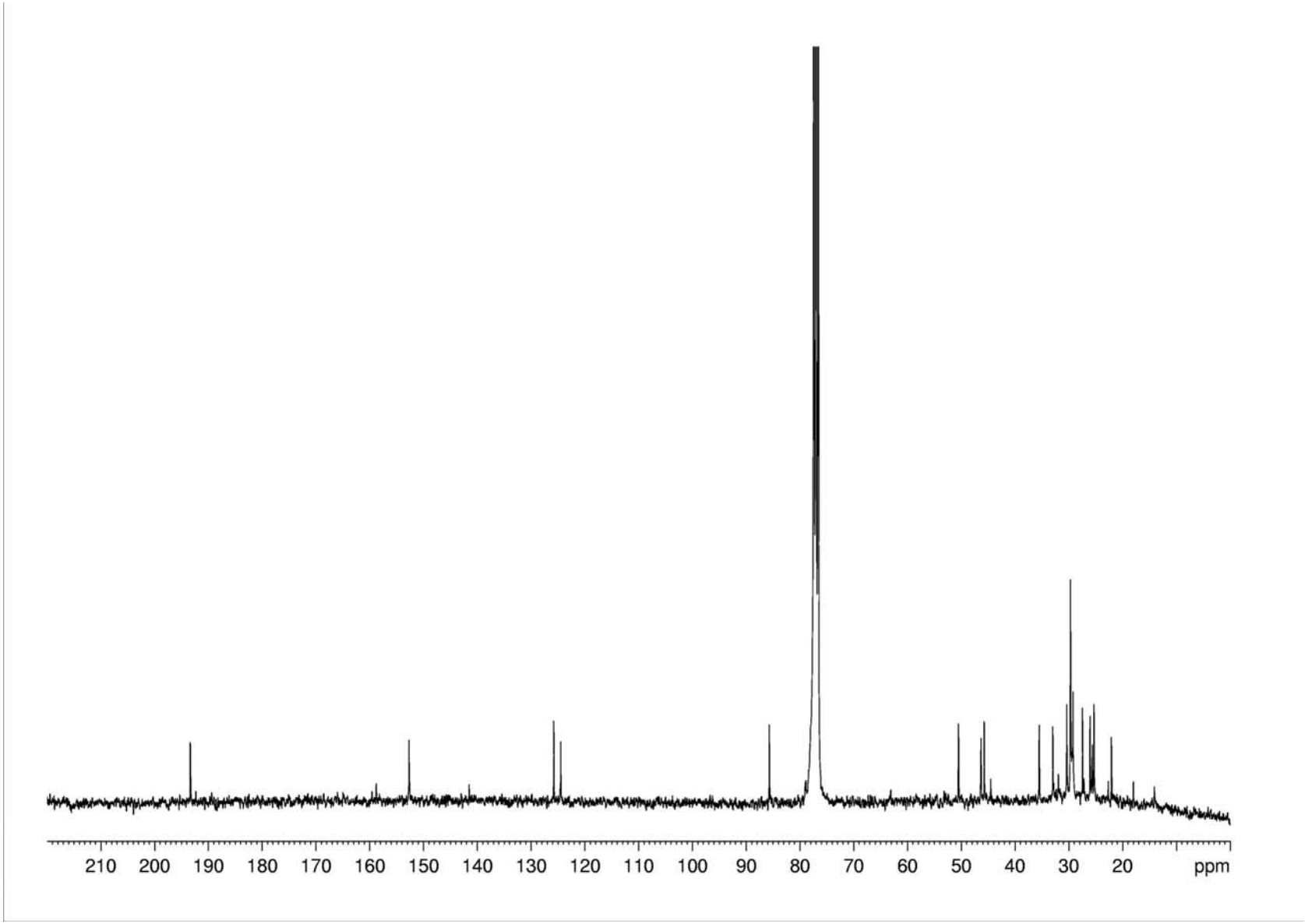

Figure 5.2.5. ^{13}C-NMR spectrum of 8-*epi*-ophiobolin J, isolated from *D. gigantea* solid culture, recorded at 300 MHz

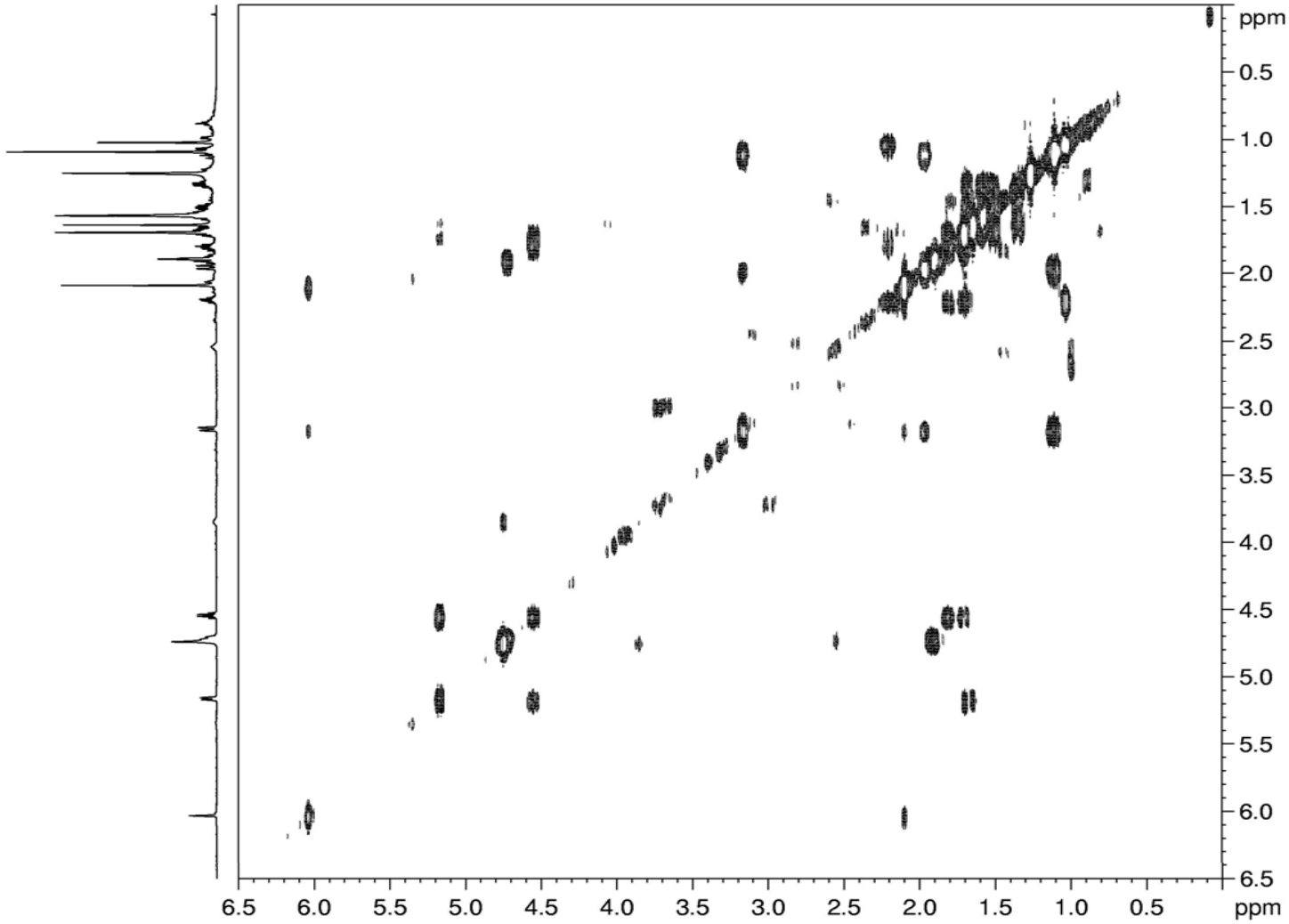

Figure 5.2.6. COSY spectrum of 8-*epi*-ophiobolin J, isolated from *D. gigantea* solid culture, recorded at 600 MHz

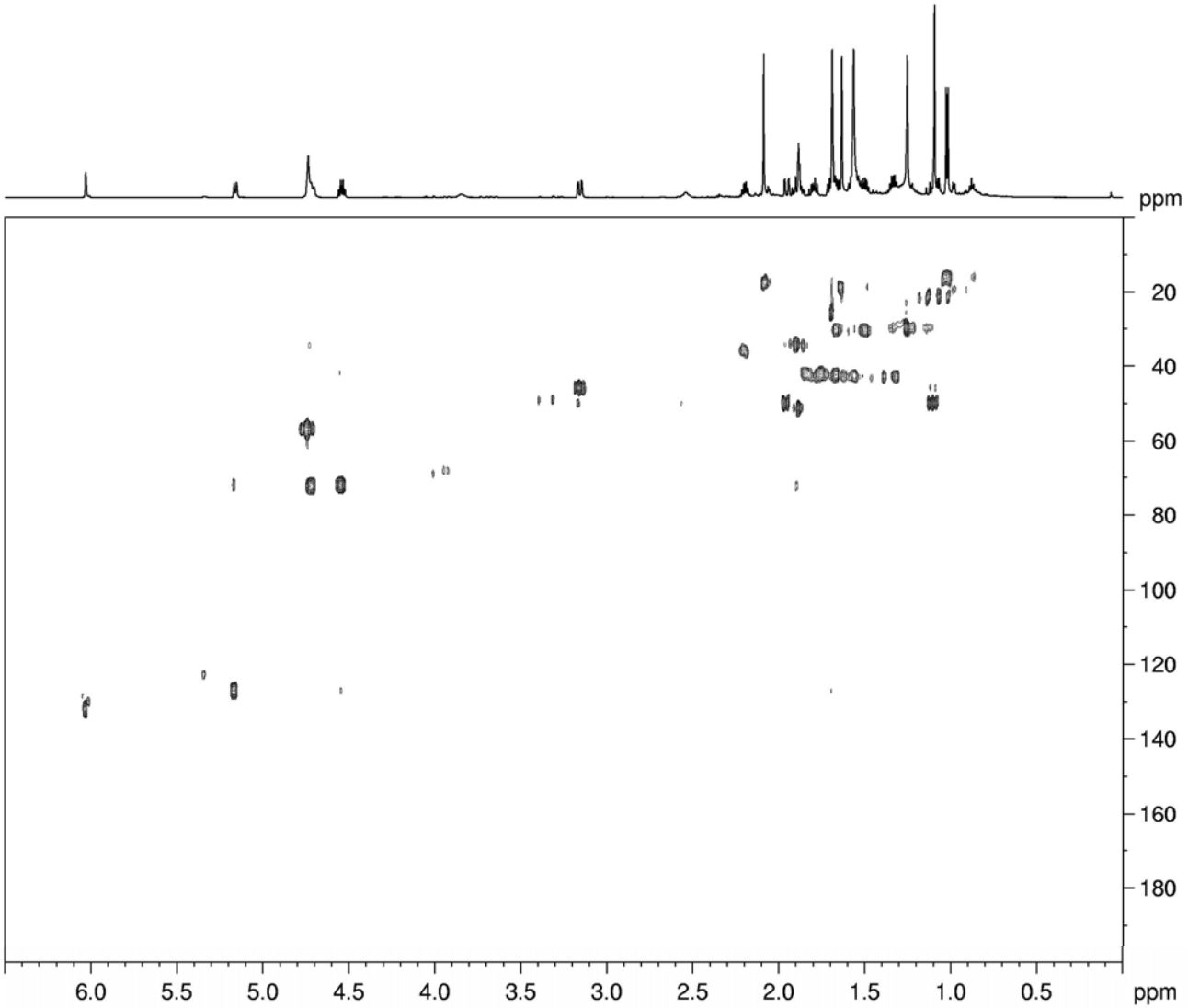

Figure 5.2.7. HSQC spectrum of 8-*epi*-ophiobolin J, isolated from *D. gigantea* solid culture, recorded at 600 MHz

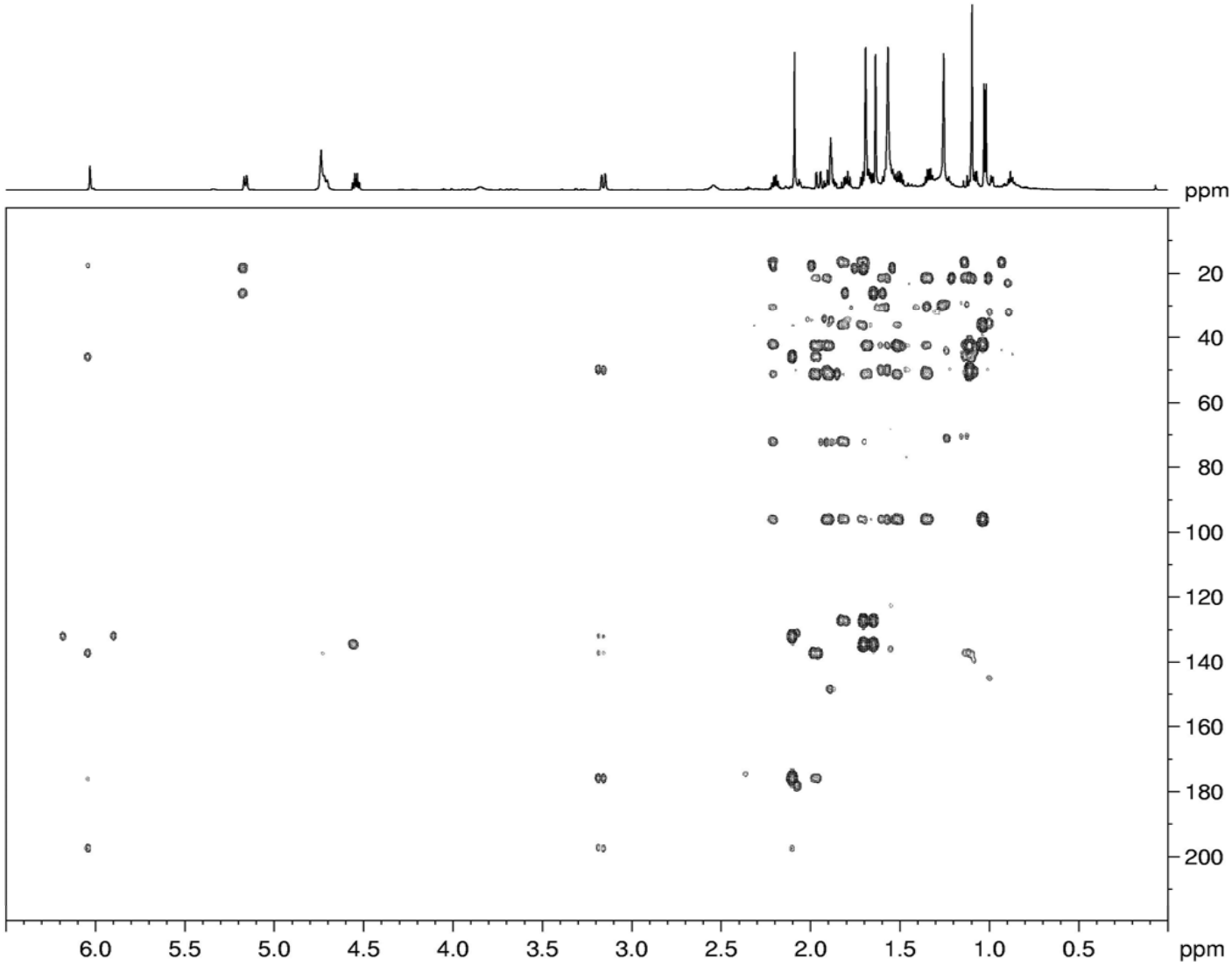

Figure 5.2.8. HMBC spectrum of 8-*epi*-ophiobolin J, isolated from *D. gigantea* solid culture, recorded at 600 MHz

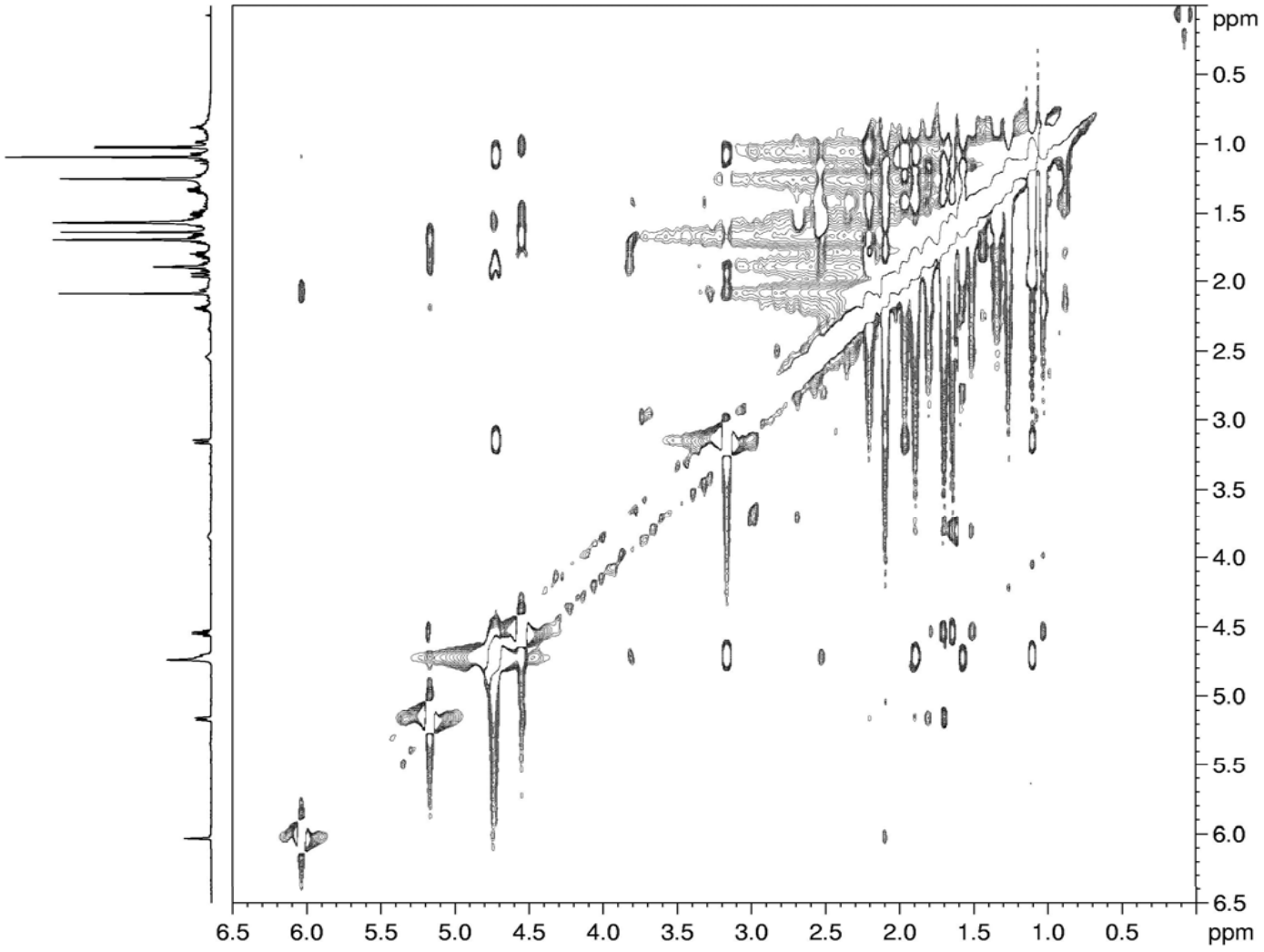

Figure 5.2.9. NOESY spectrum of 8-*epi*-ophiobolin J, isolated from *D. gigantea* solid culture, recorded at 600 MHz

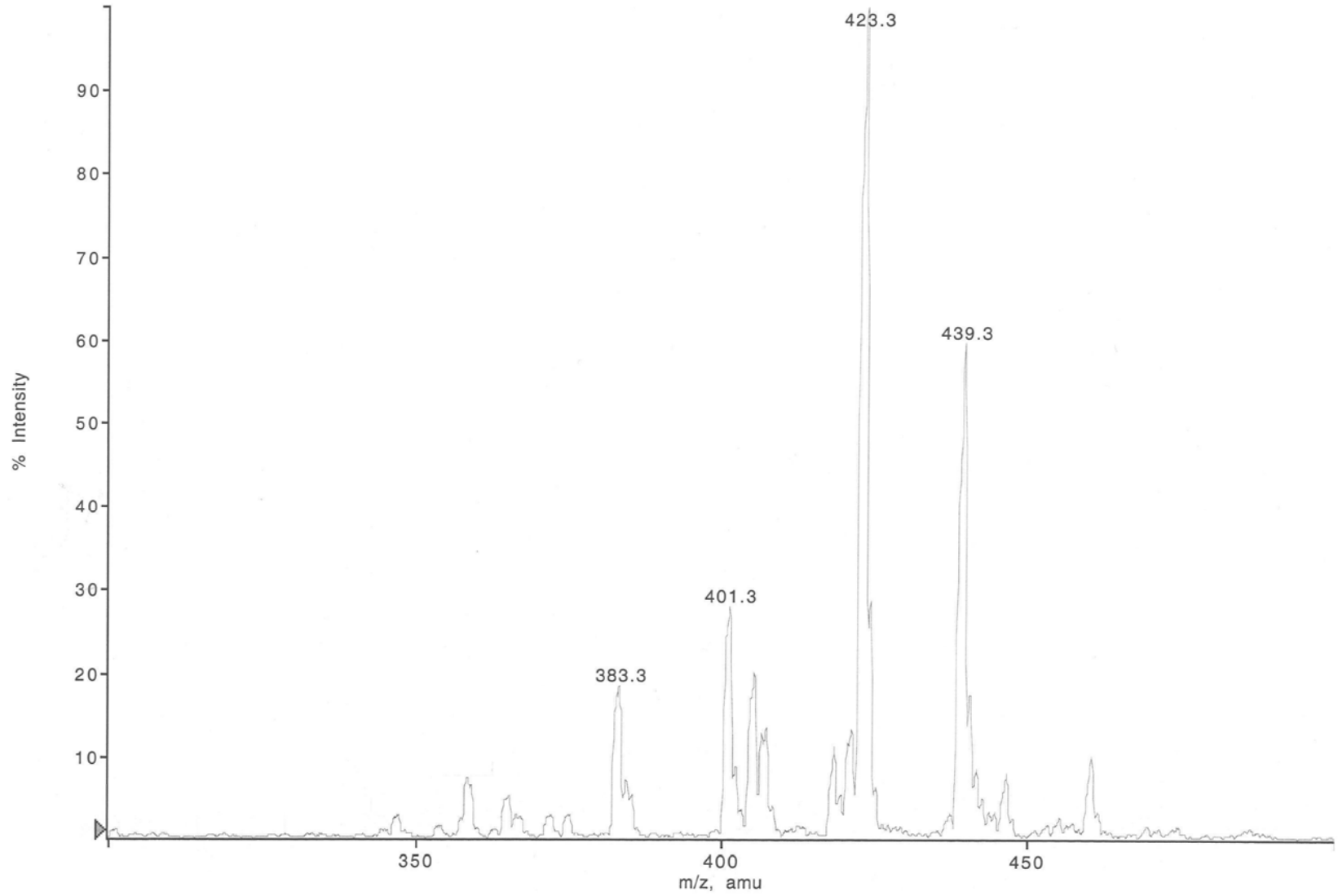

Figure 5.2.10. ESI MS spectrum of 8-*epi*-ophiobolin J, isolated from *D. gigantea* solid culture, recorded in positive modality

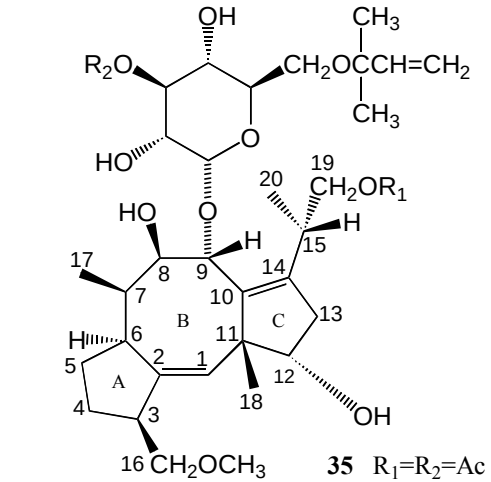

35 R_1=R_2=Ac

64 R_1= R_2=H

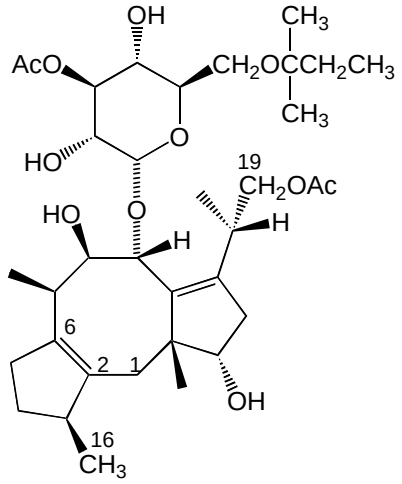

65

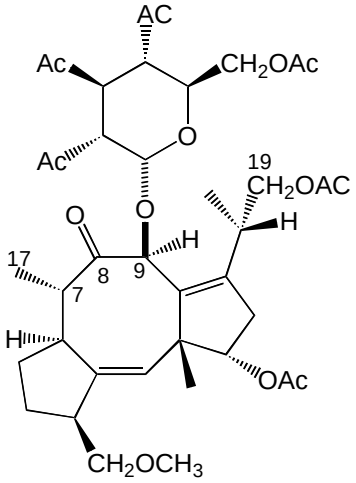

66

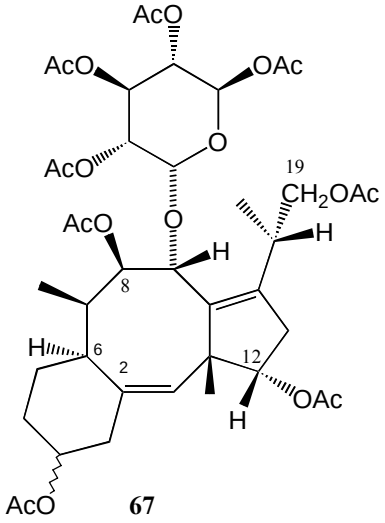

67

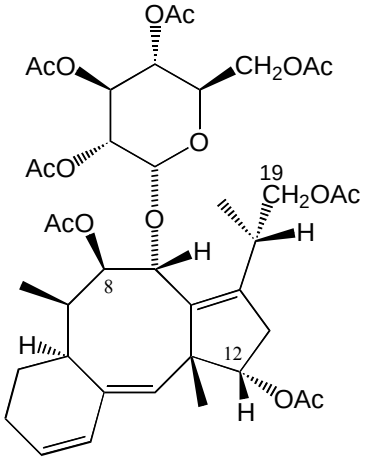

68

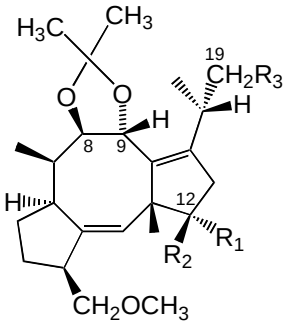

69 R1=OH, R2=H, R3=OH

70 R1+R2=O, R3= OC(Ph)3

Figure 5.4.1. Structures of fusicoccin (**35**), some of its derivatives (**64**-**68**), and fusicoccin deacetyl aglycone derivatives (**69** and **70**)

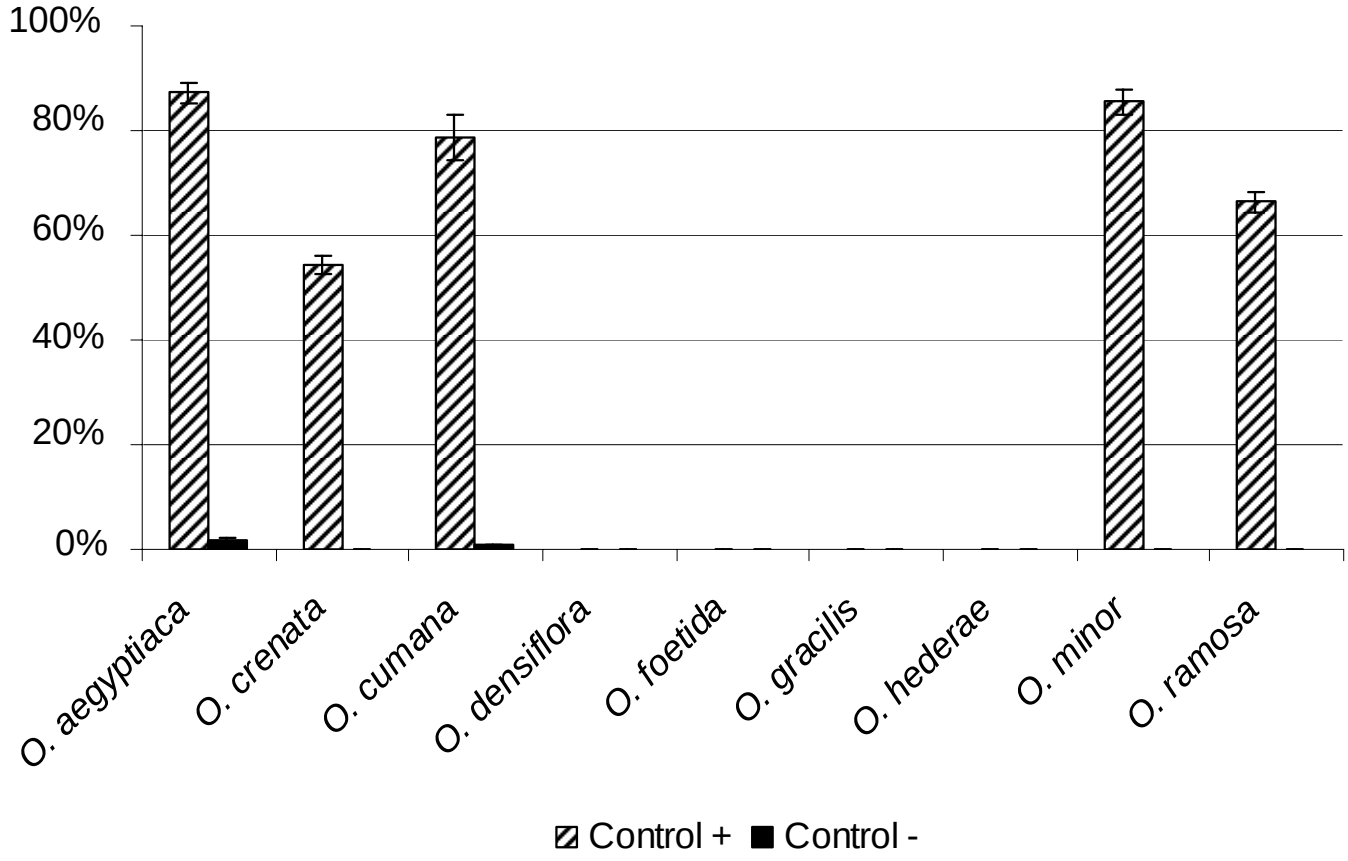

Figure 5.4.2. Percentage of germination of *O. aegyptiaca, O. crenata, O. cumana, O. densiflora, O. foetida, O. gracilis, O. hederae, O. minor, O. ramosa* seeds induced by the positive treatment control (GR24) and the negative treatment control (sterile distilled water). Error bars represent +/-2 SE

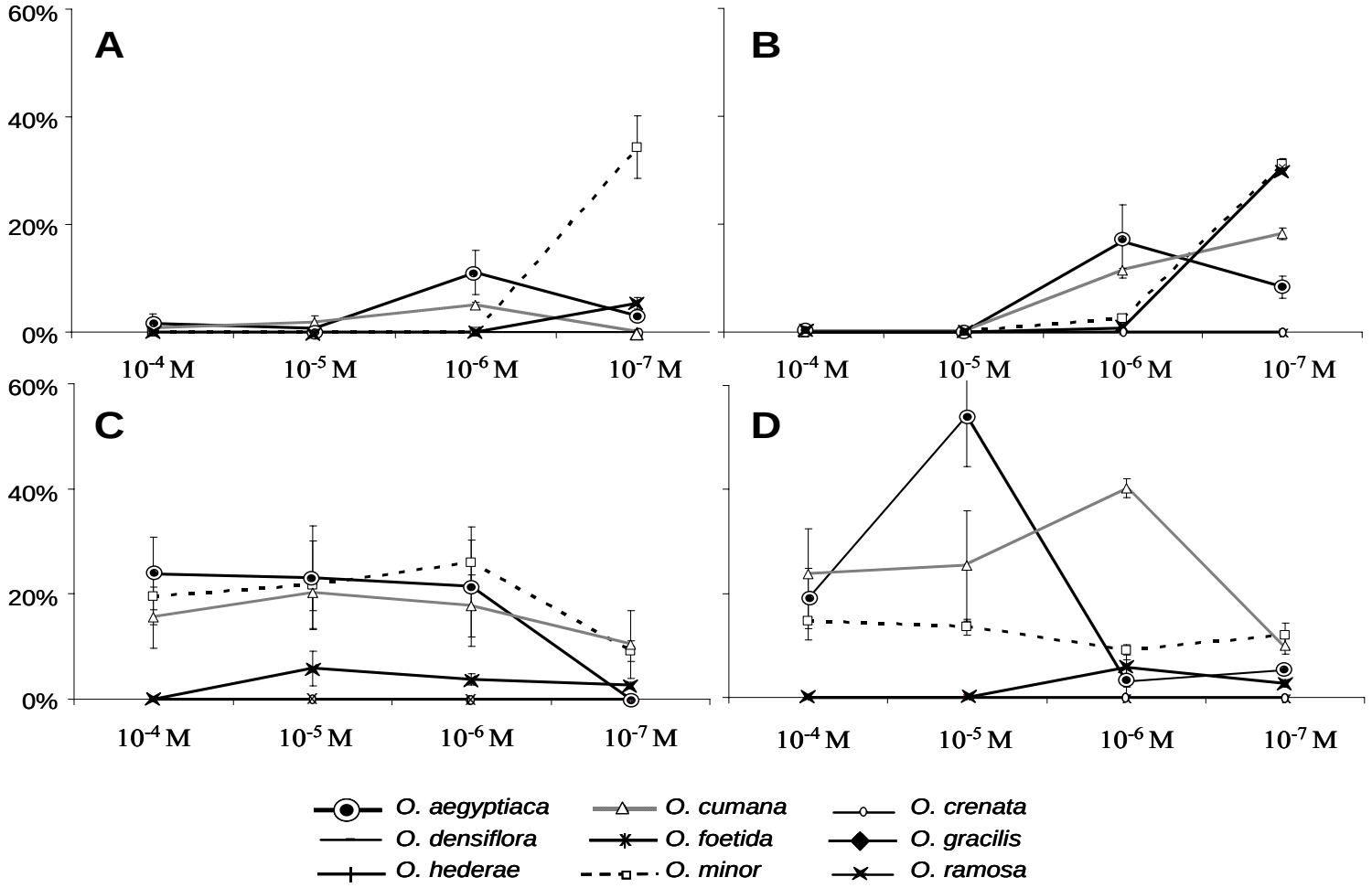

Figure 5.4.3. Percentage of germination of *O. aegyptiaca, O. crenata*, *O. cumana*, *O. densiflora*, *O. foetida*, *O. gracilis*, *O. hederae*, *O. minor* and *O. ramosa* seeds induced by A) 8,9-isopropylidene derivative of FC aglycone (**69**) B); Ophiobolin A (**36**); C) FC derivative **67;** D) FC derivative **68.** Error bars represent +/-2 SE

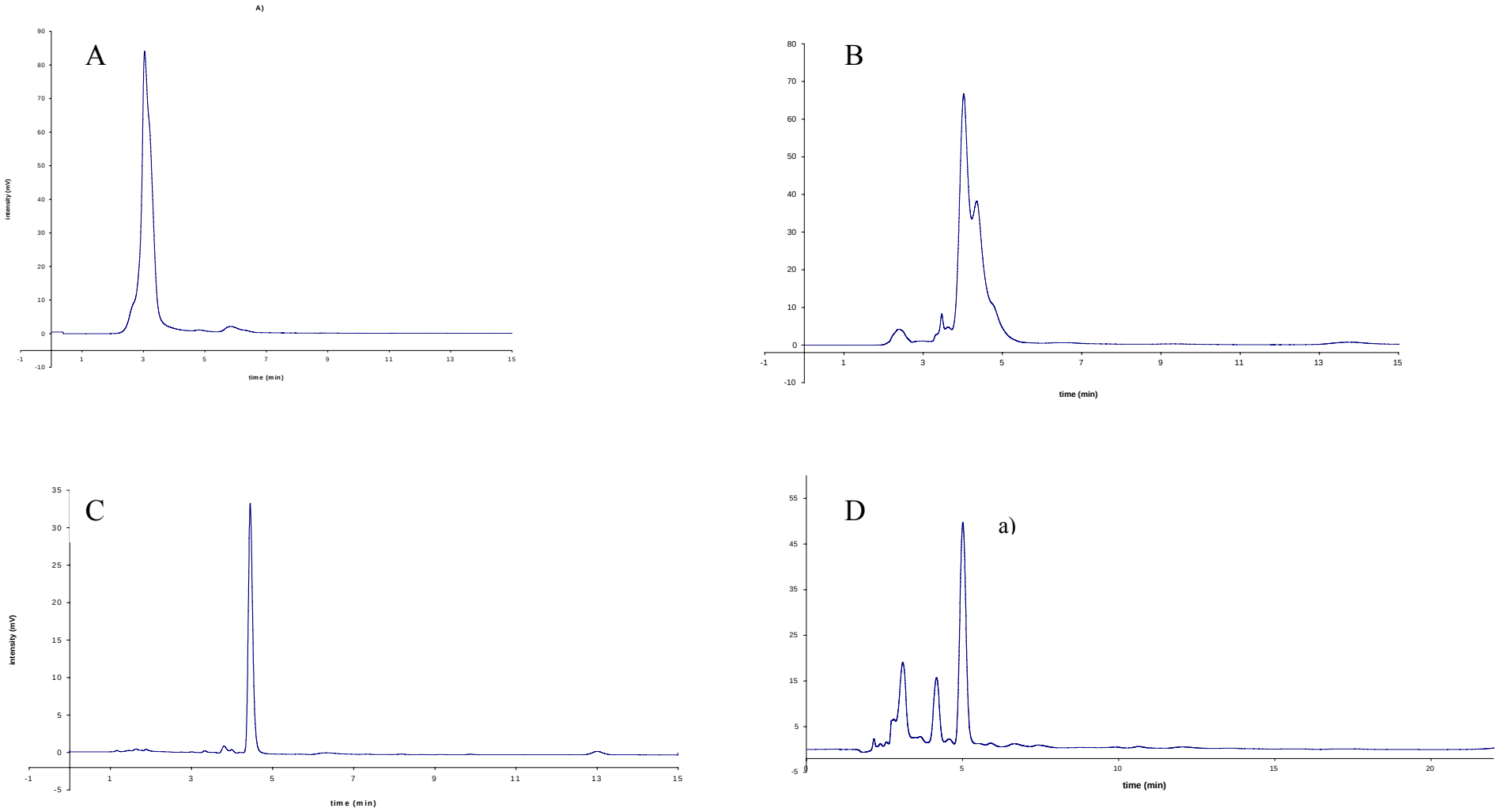

Figure 5.5.1. HPLC profiles with a flow rate of 1 ml/min. **A-C**: ascosonchine standard; **D**: Culture extract of *A. sonchi* strain C-240 **A**) isocratic gradient of methanol and 1% dipotassium hydrogen phosphate in water adjusted to pH 7.35 with concentrated phosphoric acid (1:1, v/v). **B**) isocratic gradient of acetonitrile with the same buffer (1:1, v/v). **C**) isocratic gradient of methanol and HPLC grade water (1:1, v/v). **D**) isocratic gradient of methanol and HPLC grade water (1:1, v/v).

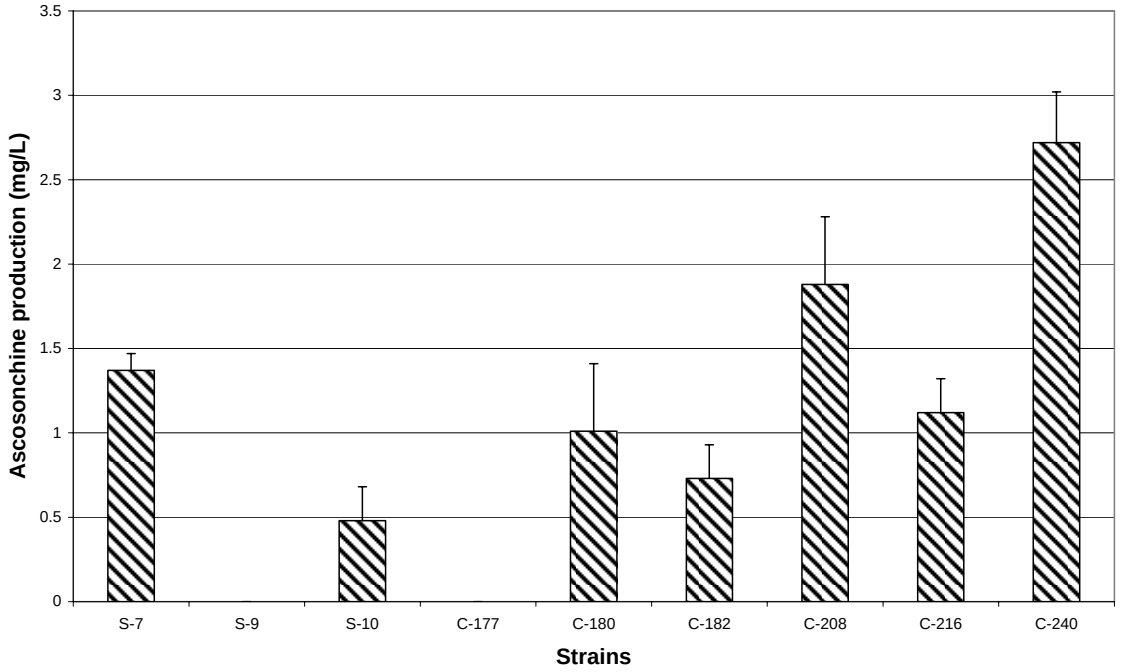

Figure 5.5.2. Content of ascosonchine in the culture filtrates of *A. sonchi* strains

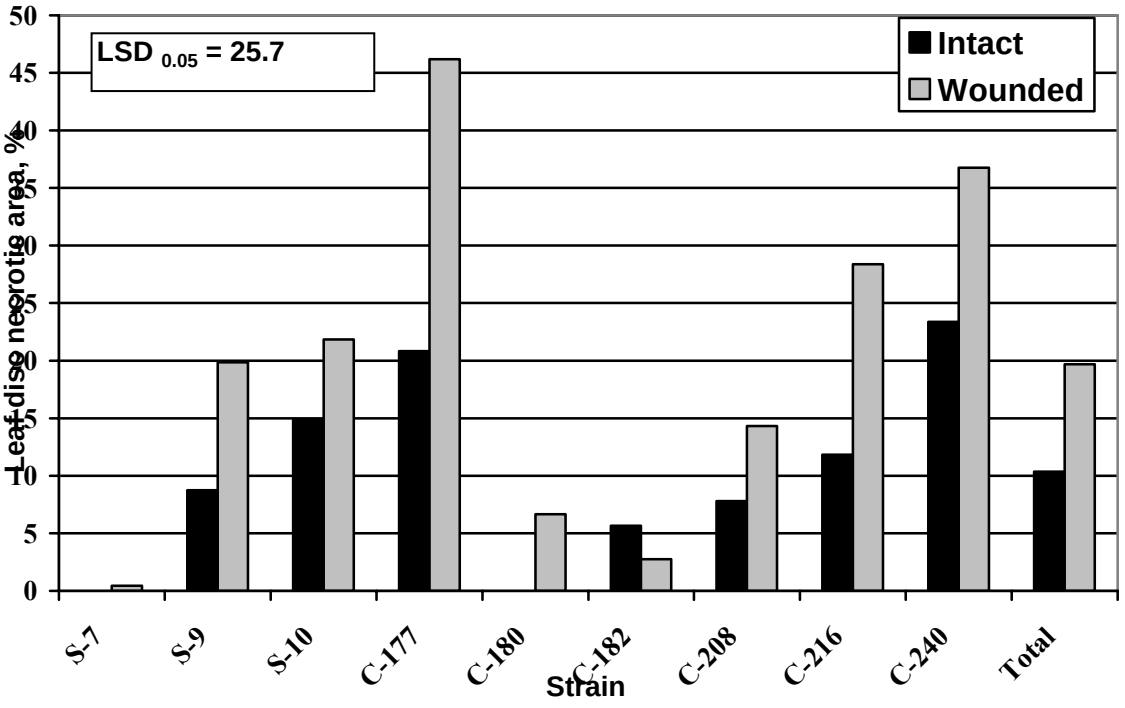

Figure 5.5.3. Virulence of *A. sonchi* strains to intact and wounded leaf disks of *C. arvense*

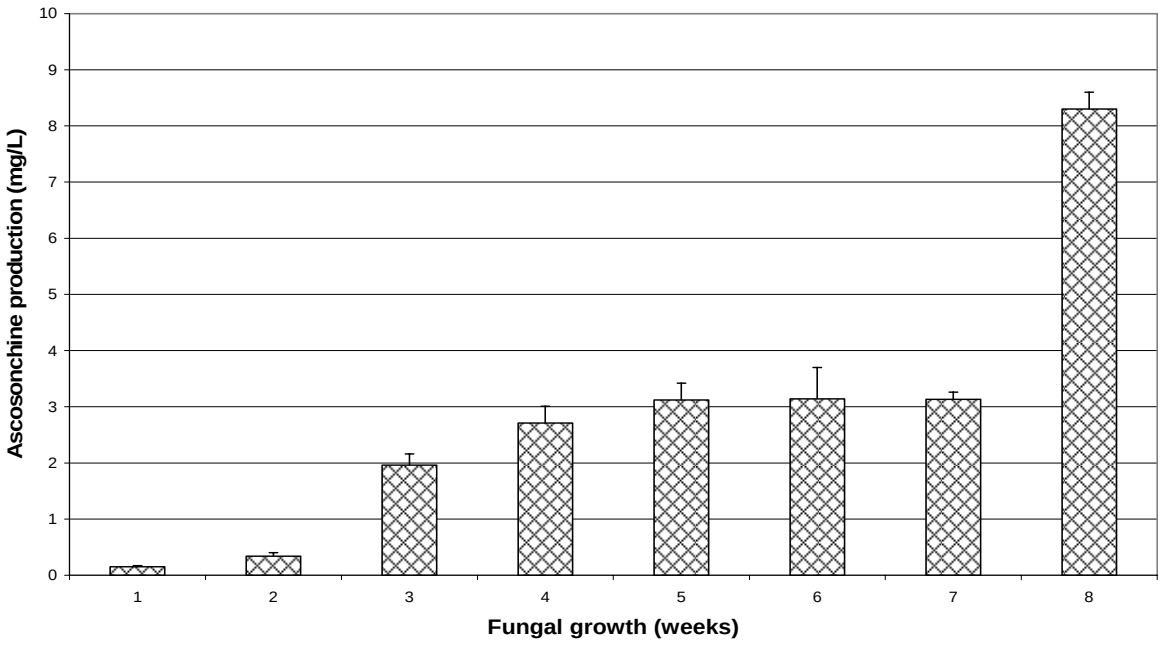

Figure 5.5.4. Time course of ascosonchine production in static cultures of *A. sonchi* strain C-240

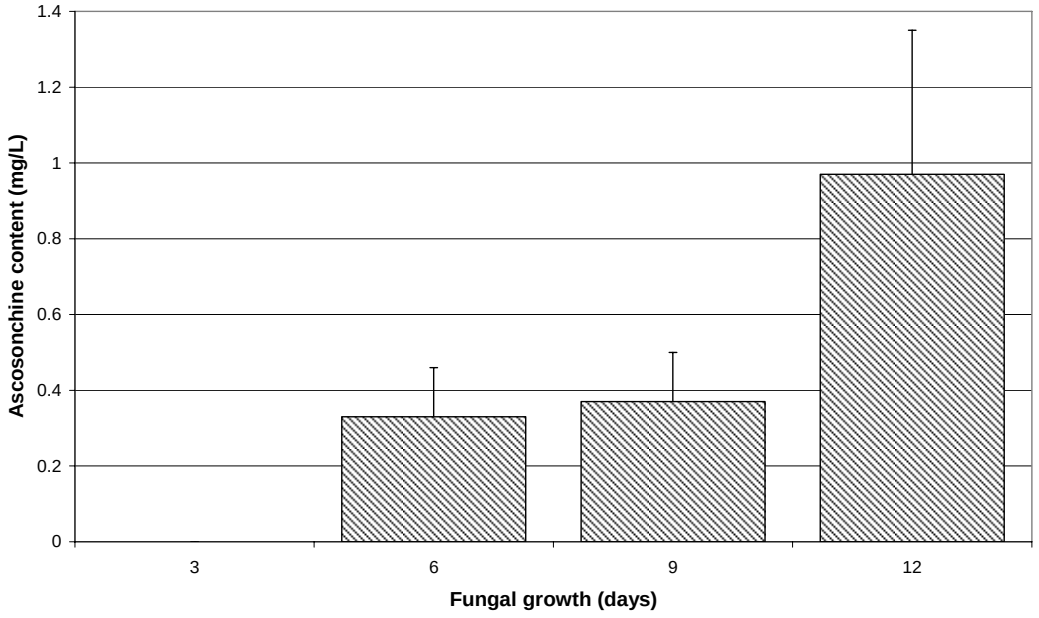

Figure 5.5.5. Time course of ascosonchine production in shaken cultures of *A. sonchi* strain C-240

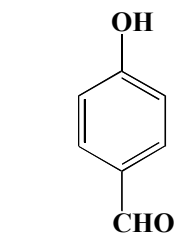

44

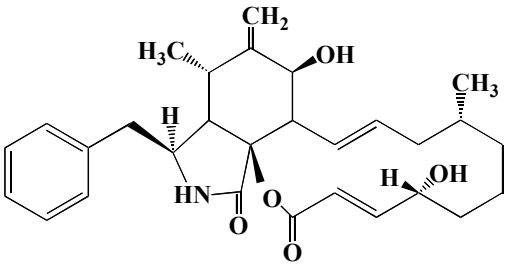

26

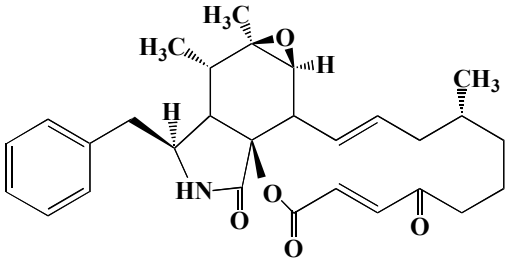

27

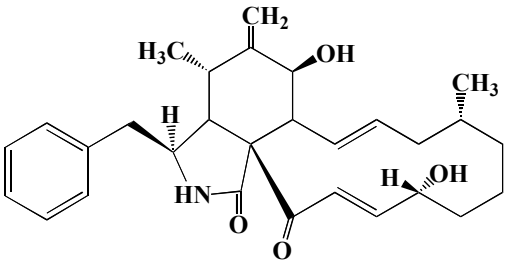

30

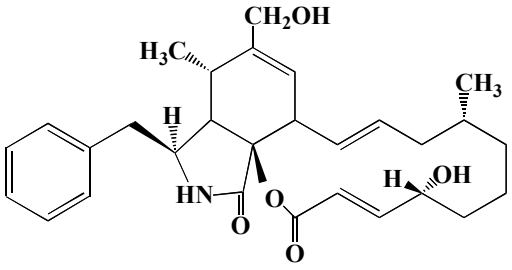

20

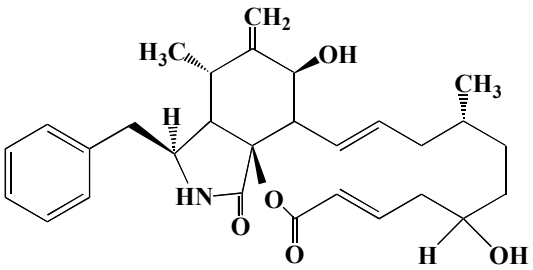

21

Figure 5.7.1. Phytotoxins isolated from *Phoma exigua var. exigua* strains C-177 and S-9 liquid and solid cultures

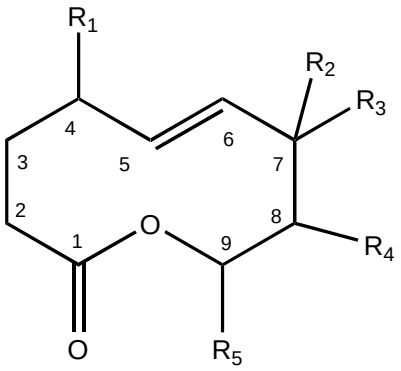

34 R_1=H, R_2+R_3=O, R_4=α-OH, R_5=$CH_2CH_2CH_3$

45 R_1=β-OH, R_2=β-H, R_3=α-OH, R_4=α–OH, R_5=β-$CH_2CH_2CH_3$

46 R_1=α-OH, R_2=α-H, R_3=β–OH, R_4=H, R_5=β-CH_3

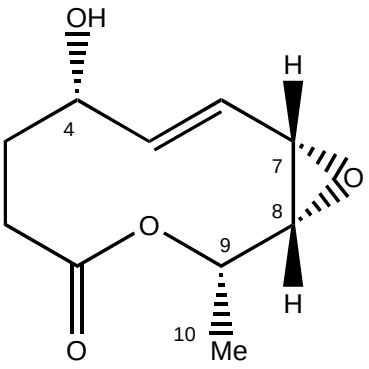

47

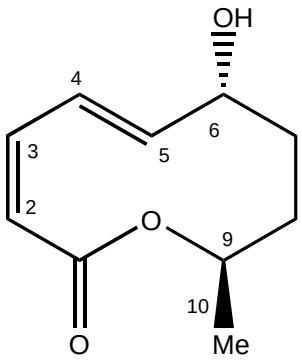

48

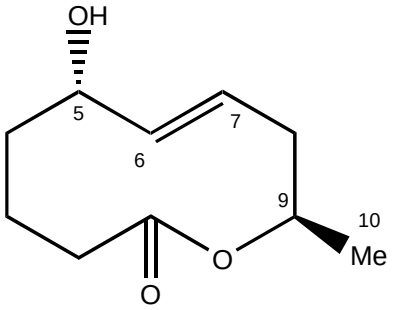

49

Figure 5.8.1. Stagonolides B-F (**45-49**) isolated from *S. cirsii* solid culture

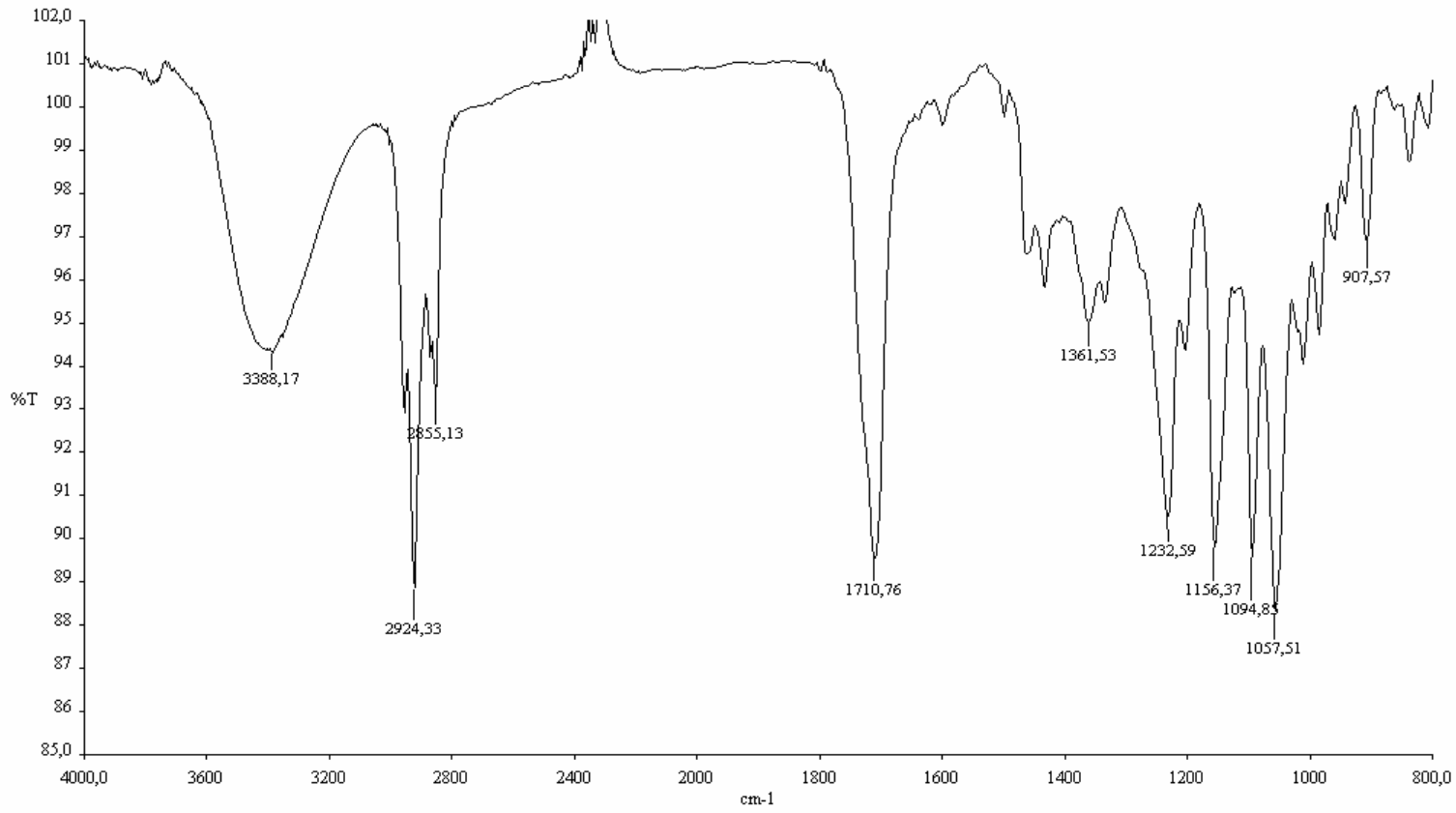

Figure 5.8.2. IR spectrum of stagonolide B, isolated from *S. cirsii* solid culture, recorded as neat

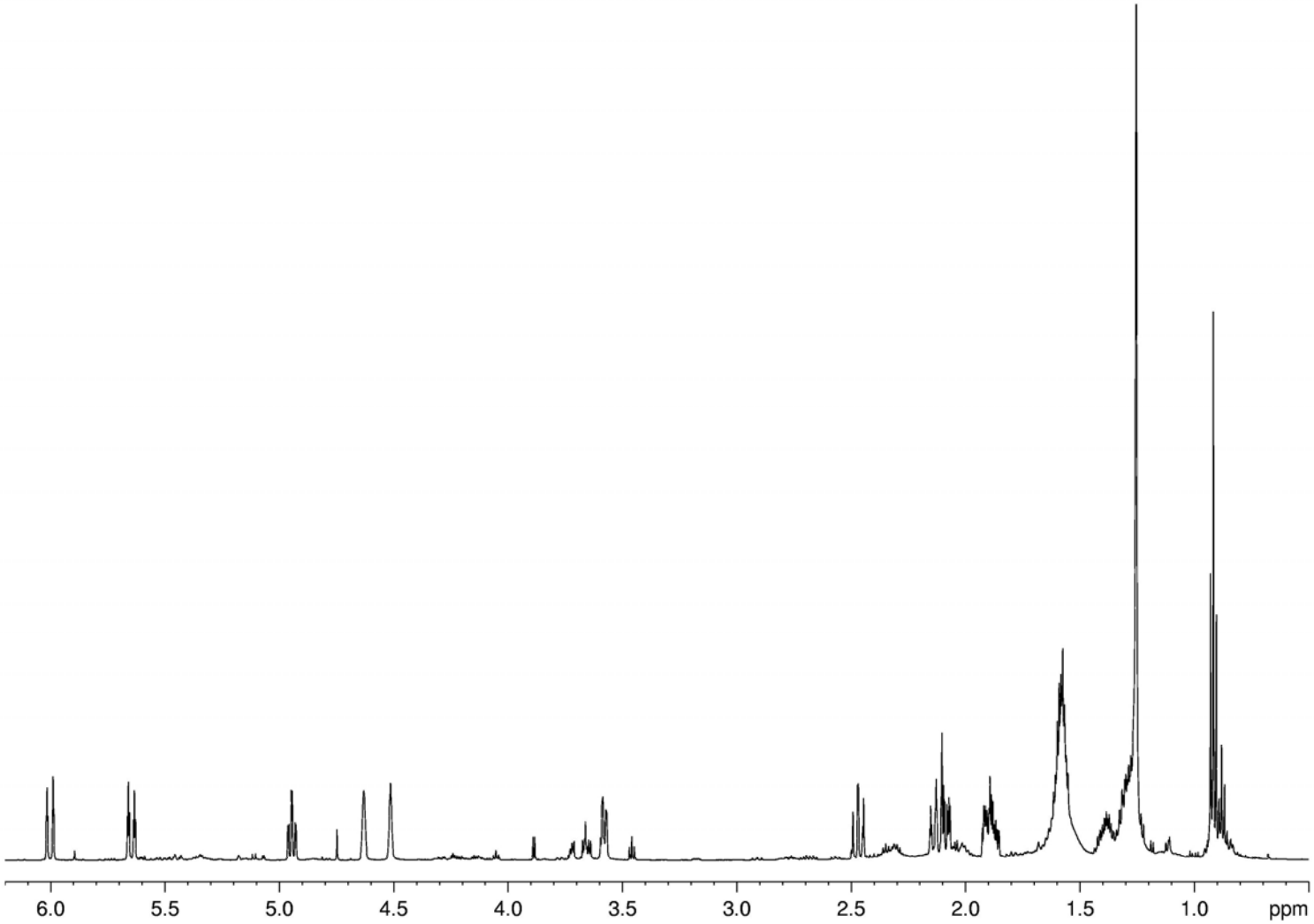

Figure 5.8.3. ^{1}H NMR spectrum of stagonolide B, isolated from *S. cirsii* solid culture, recorded at 600 MHz

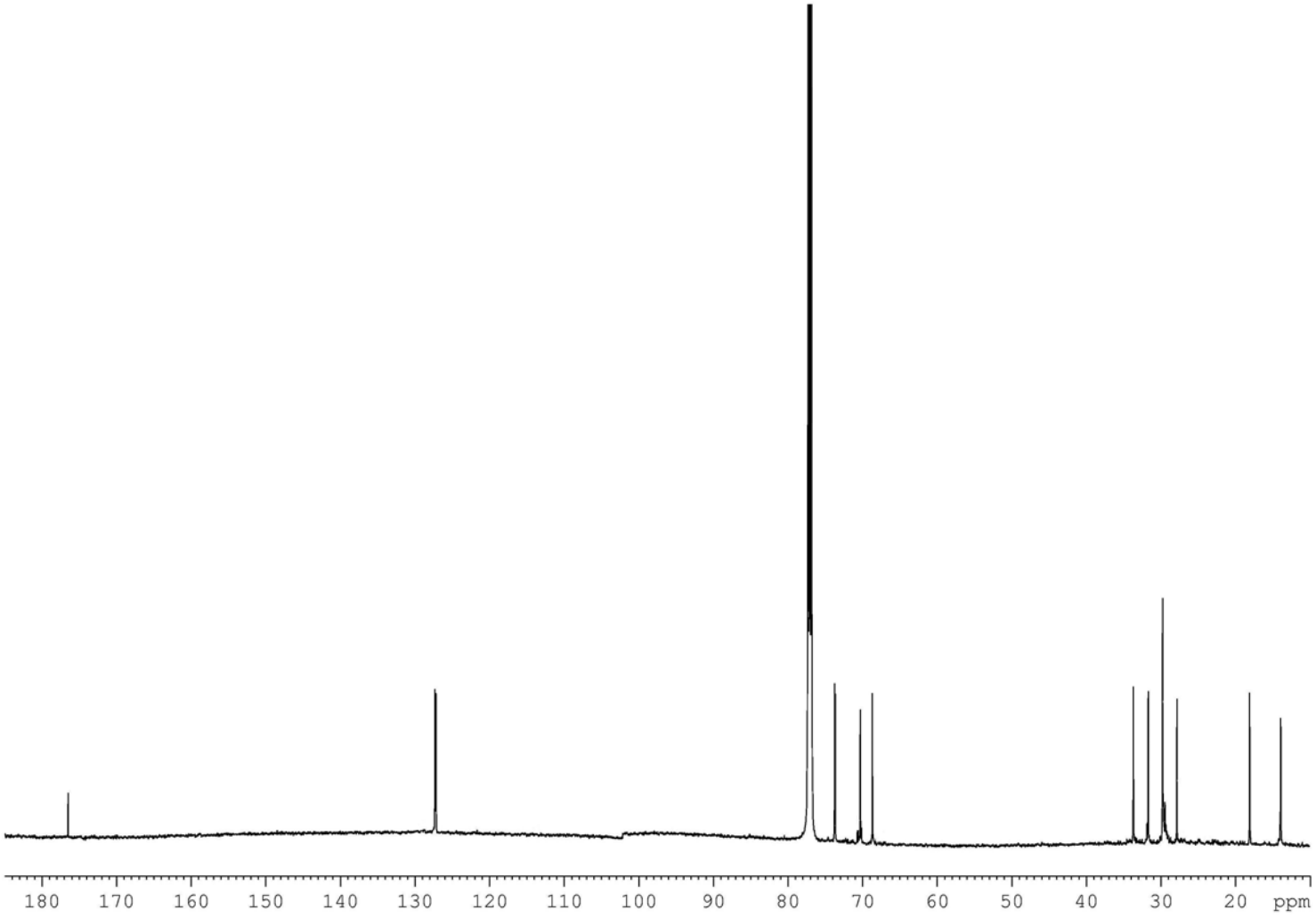

Figure 5.8.4. ^{13}C NMR spectrum of stagonolide B, isolated from *S. cirsii* solid culture, recorded at 600 MHz

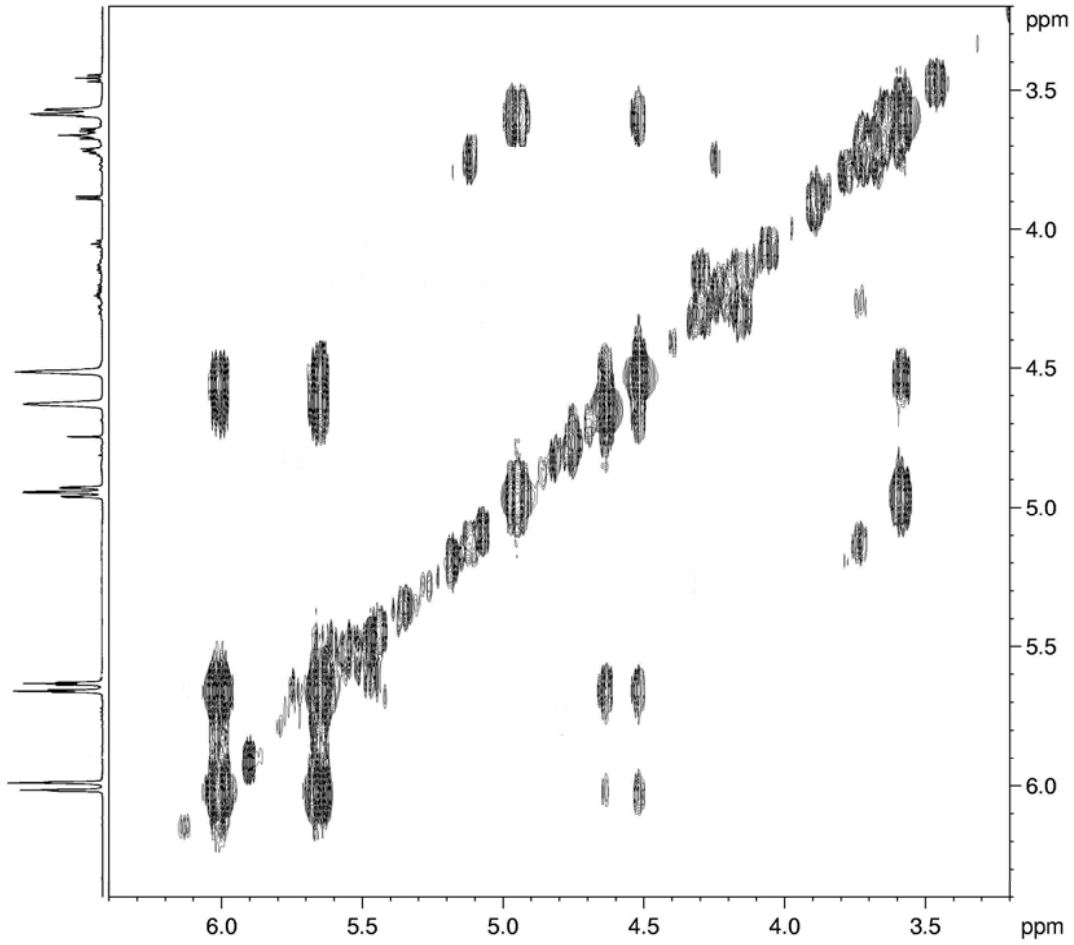

Figure 5.8.5. COSY spectrum of stagonolide B, isolated from *S. cirsii* solid culture, recorded at 600 MHz

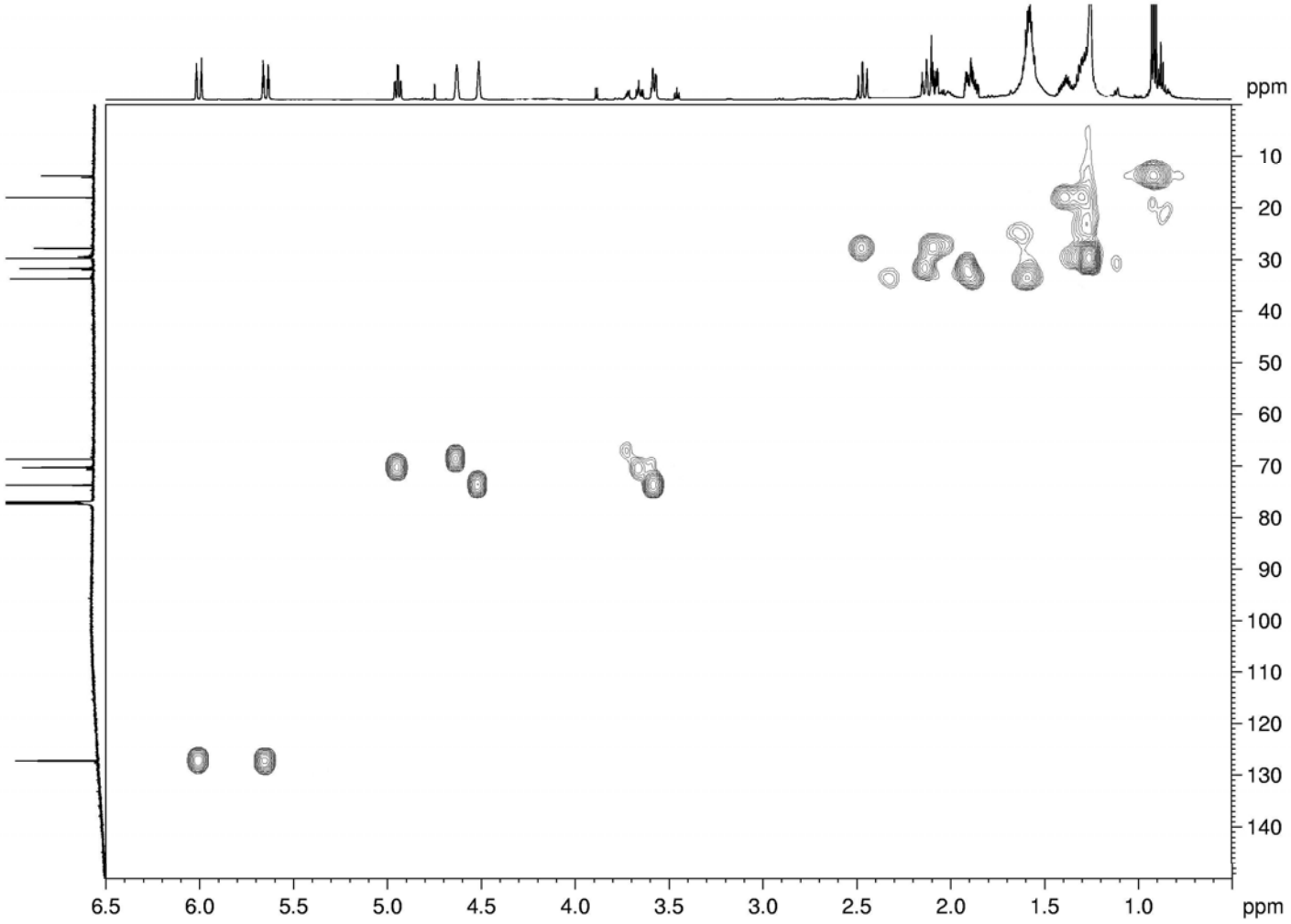

Figure 5.8.6. HSQC spectrum of stagonolide B, isolated from *S. cirsii* solid culture, recorded at 600 MHz

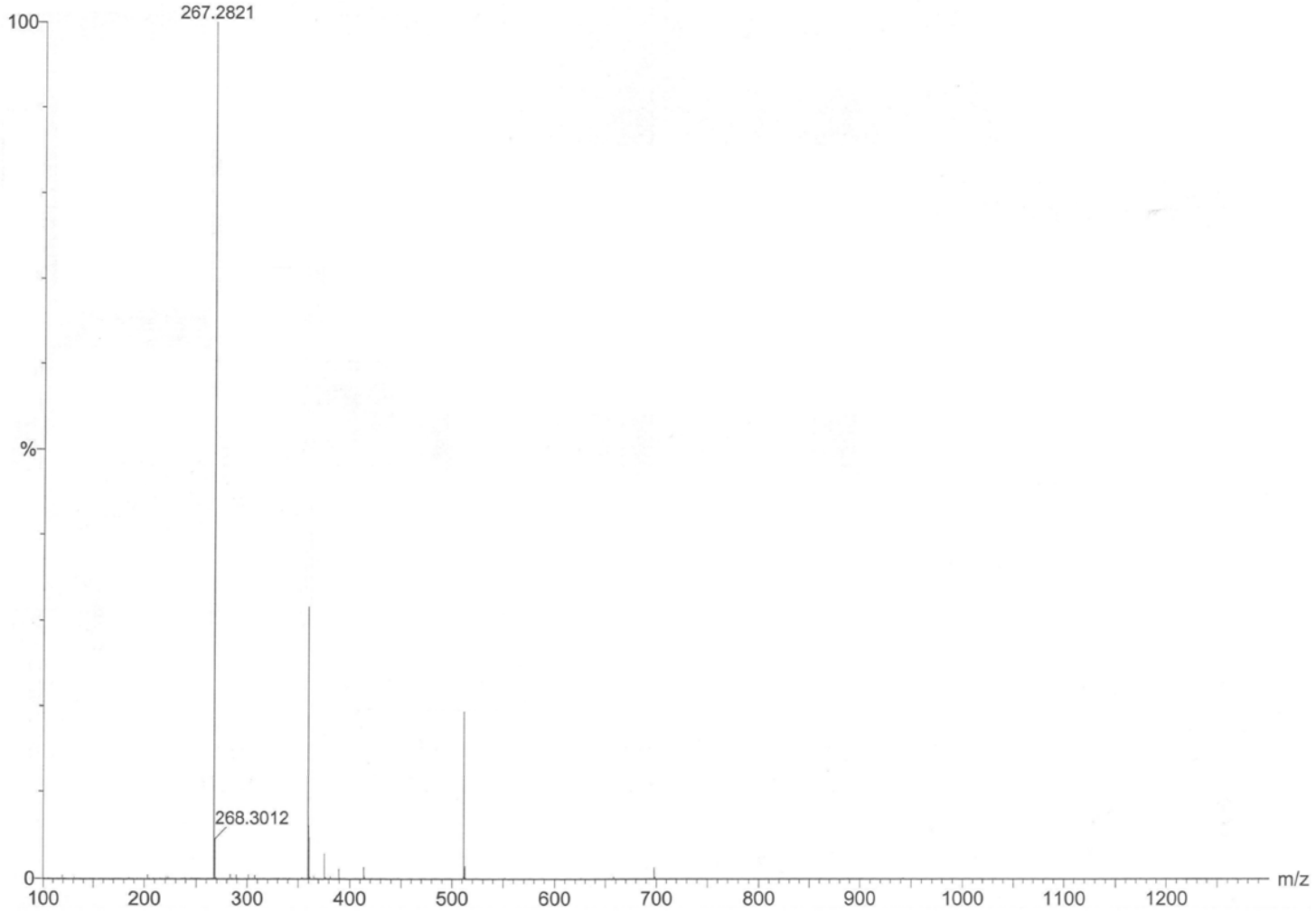

Figure 5.8.7. ESI MS spectrum of stagonolide B, isolated from *S. cirsii* solid culture, recorded in positive modality

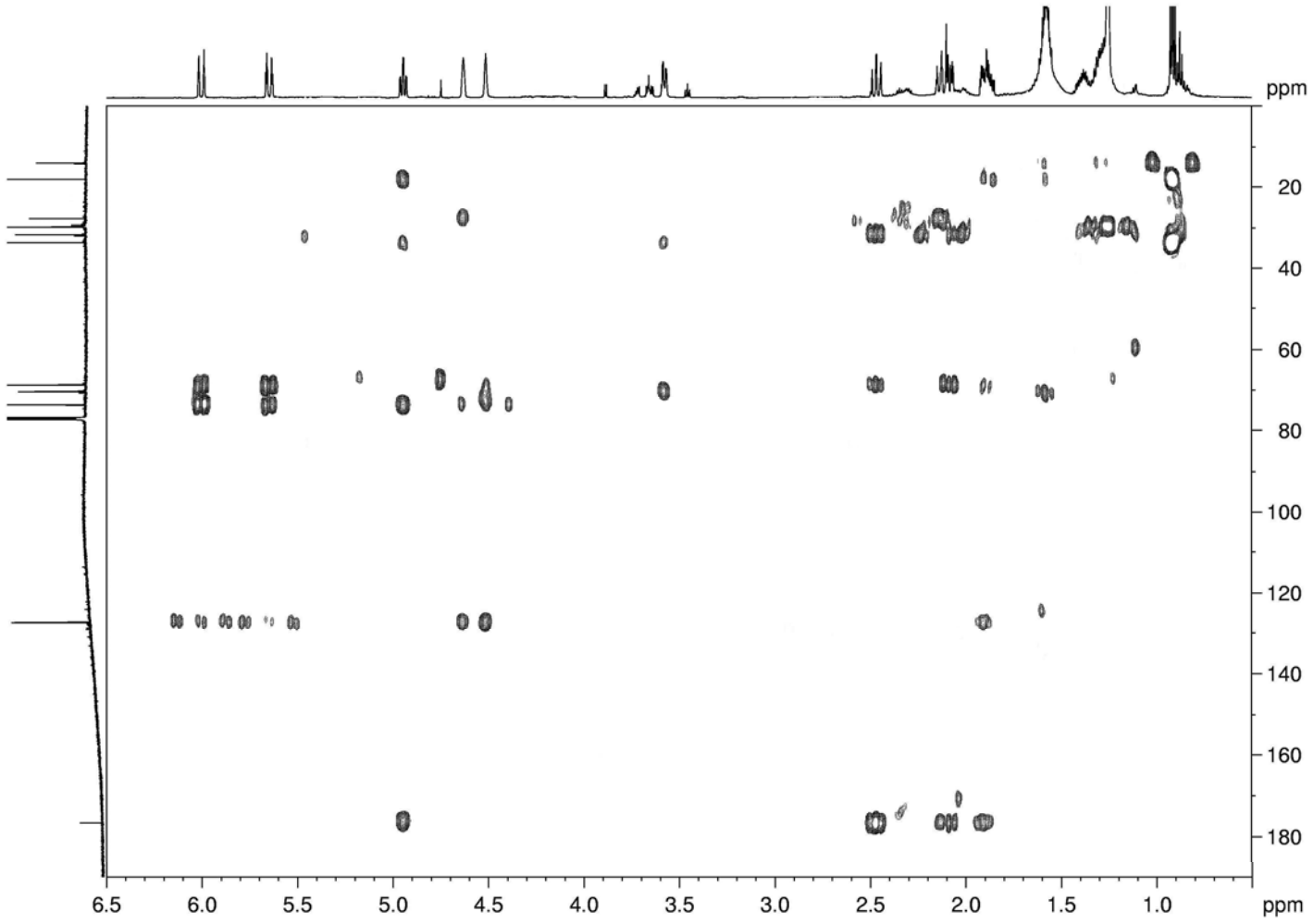

Figure 5.8.8. HMBC spectrum of stagonolide B, isolated from *S. cirsii* solid culture, recorded at 600 MHz

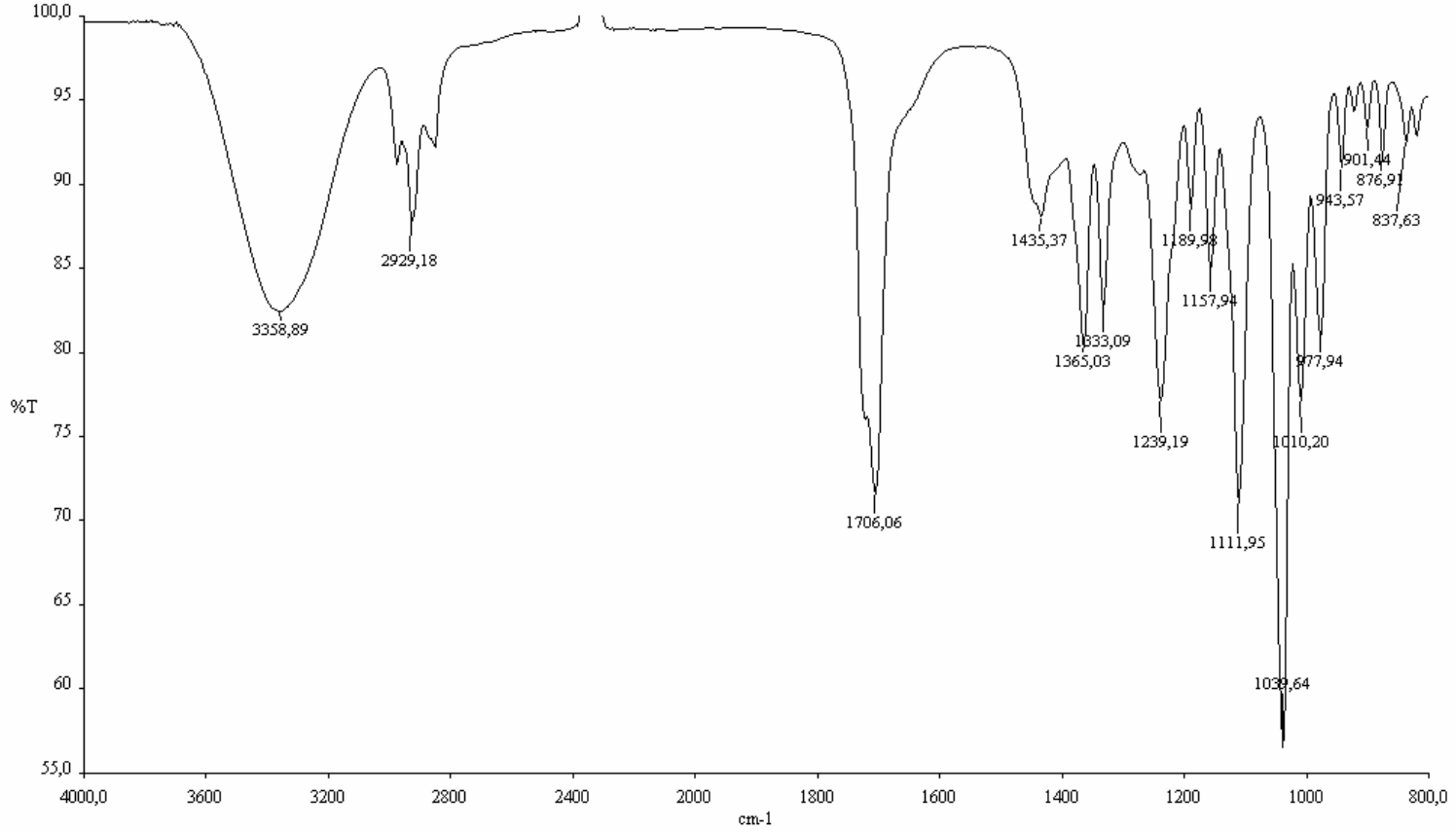

Figure 5.8.9. IR spectrum of stagonolide C, isolated from *S. cirsii* solid culture, recorded as neat

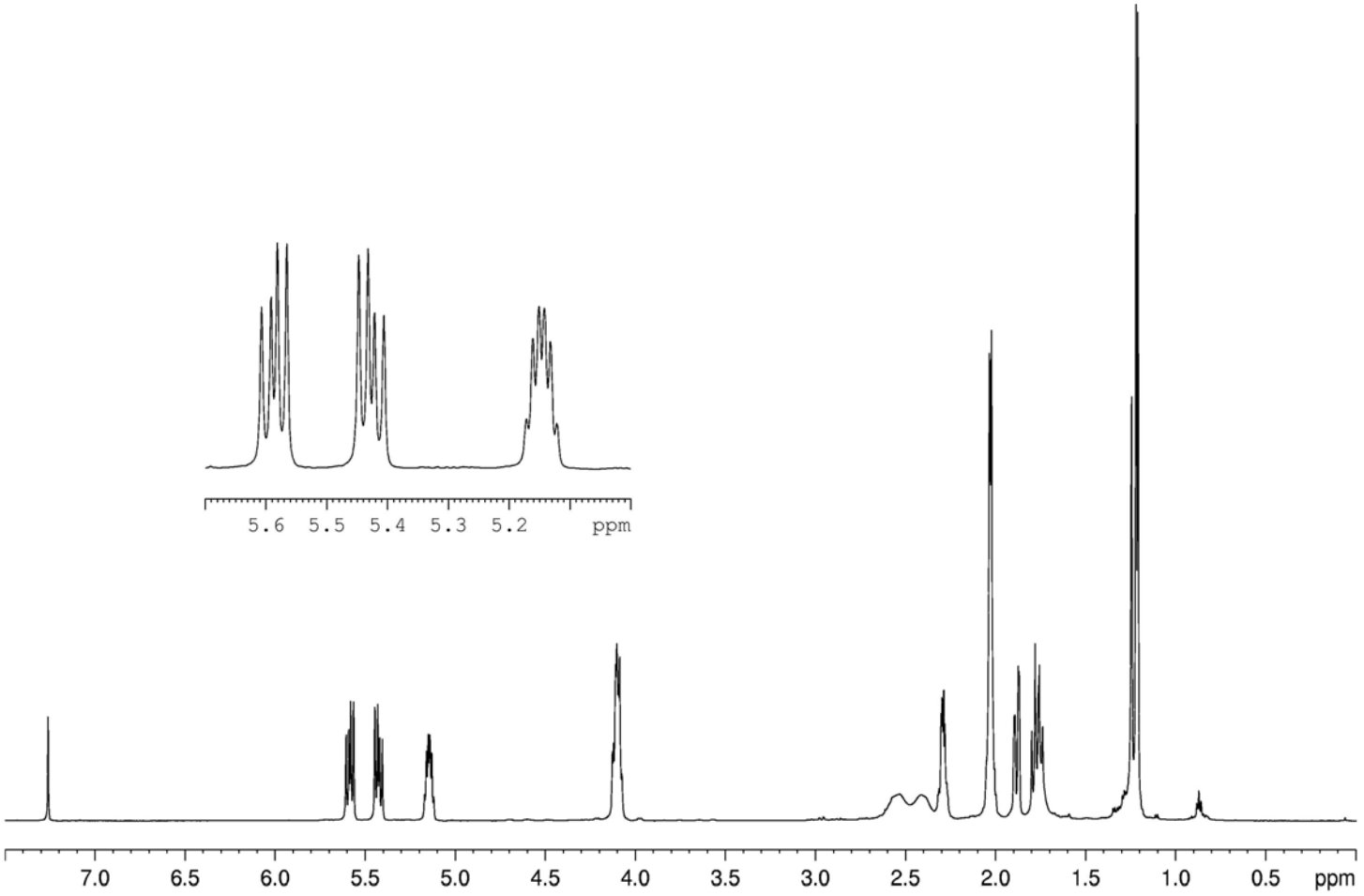

Figure 5.8.10. ^{1}H NMR spectrum of stagonolide C, isolated from *S. cirsii* solid culture, recorded at 600 MHz

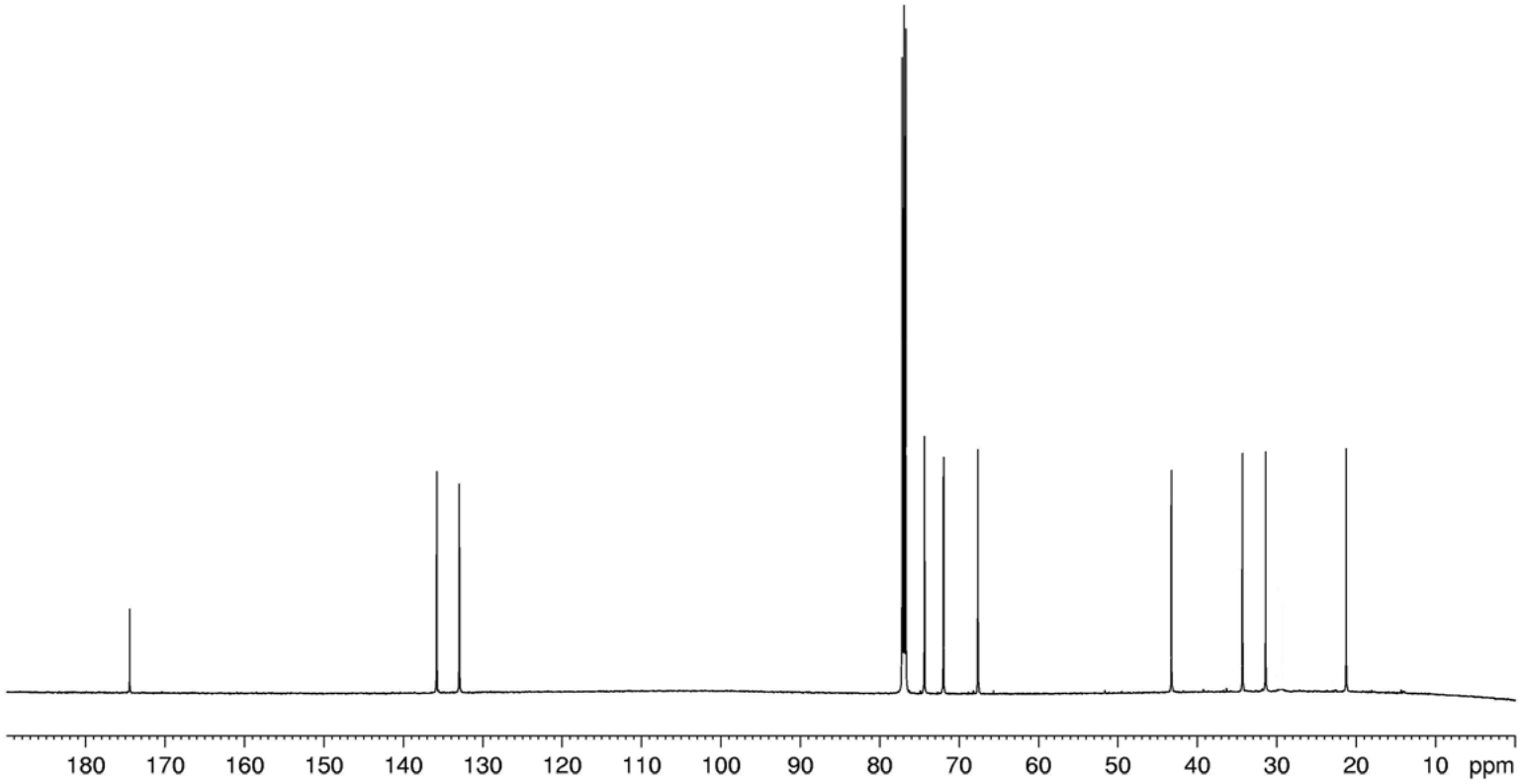

Figure 5.8.11. ^{13}C NMR spectrum of stagonolide C, isolated from *S. cirsii* solid culture, recorded at 600 MHz

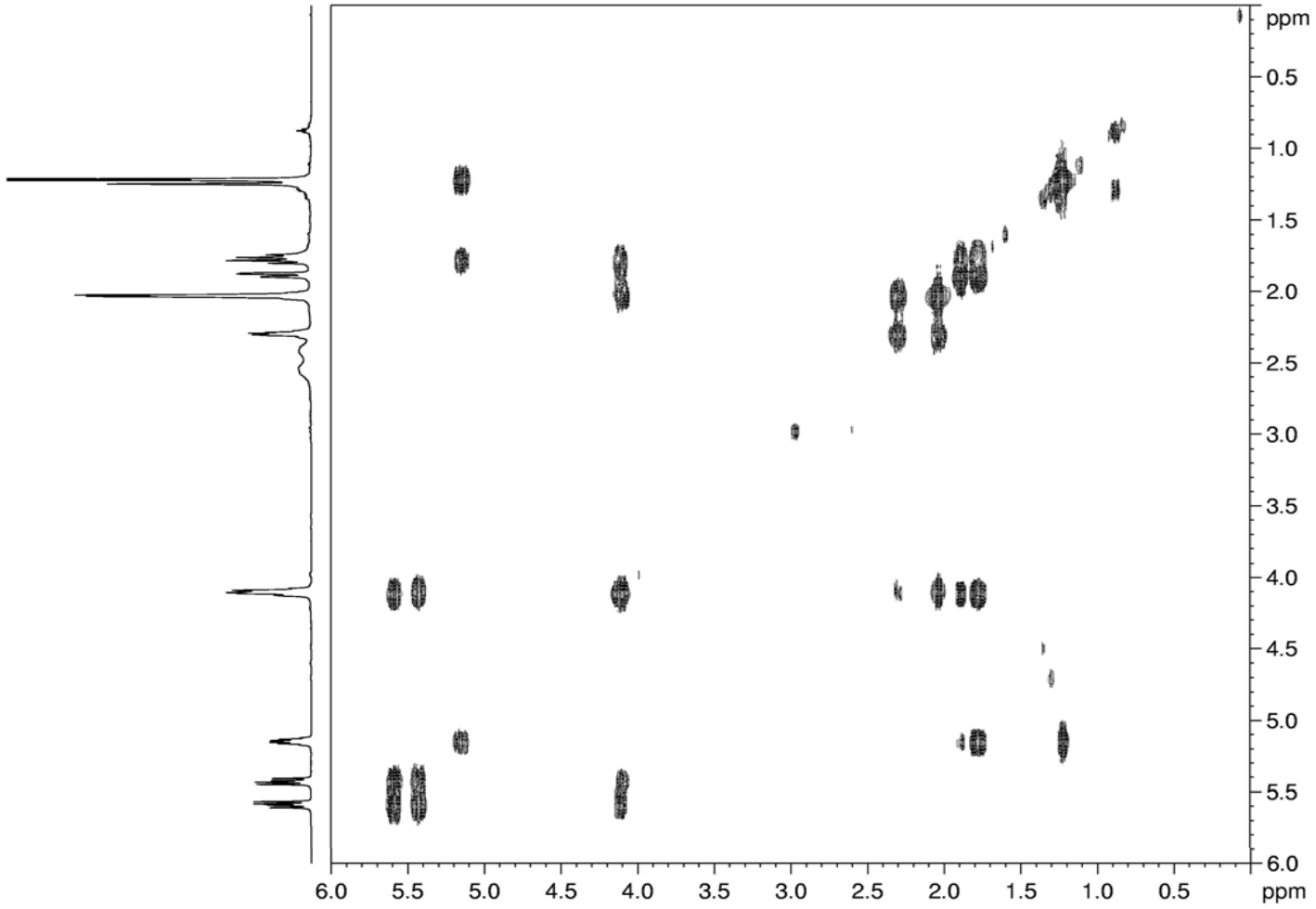

Figure 5.8.12. COSY spectrum of stagonolide C, isolated from *S. cirsii* solid culture, recorded at 600 MHz

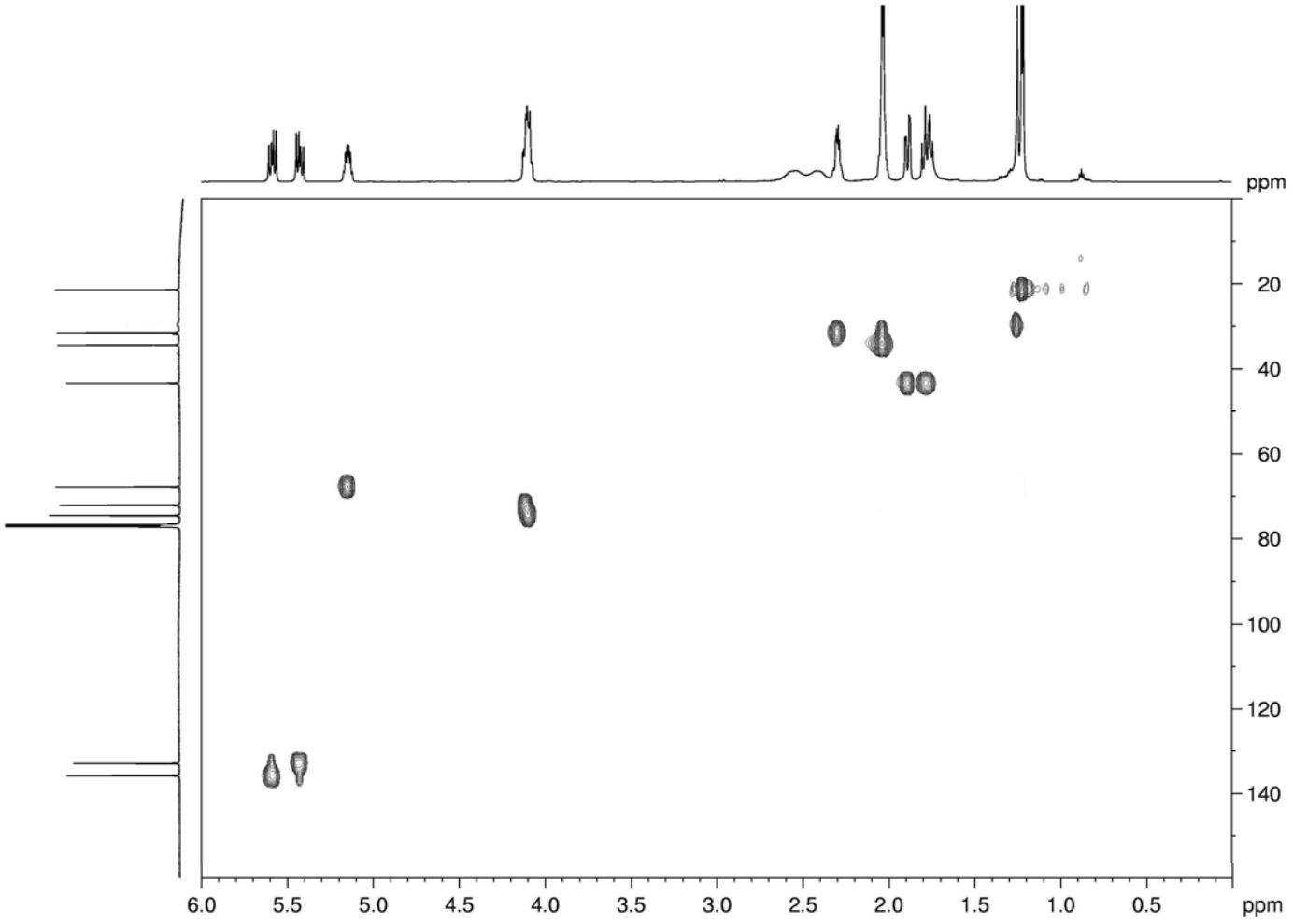

Figure 5.8.13. HSQC spectrum of stagonolide C, isolated from *S. cirsii* solid culture, recorded at 600 MHz

Figure 5.8.14. ESI MS spectrum of stagonolide C, isolated from *S. cirsii* solid culture, recorded in positive modality

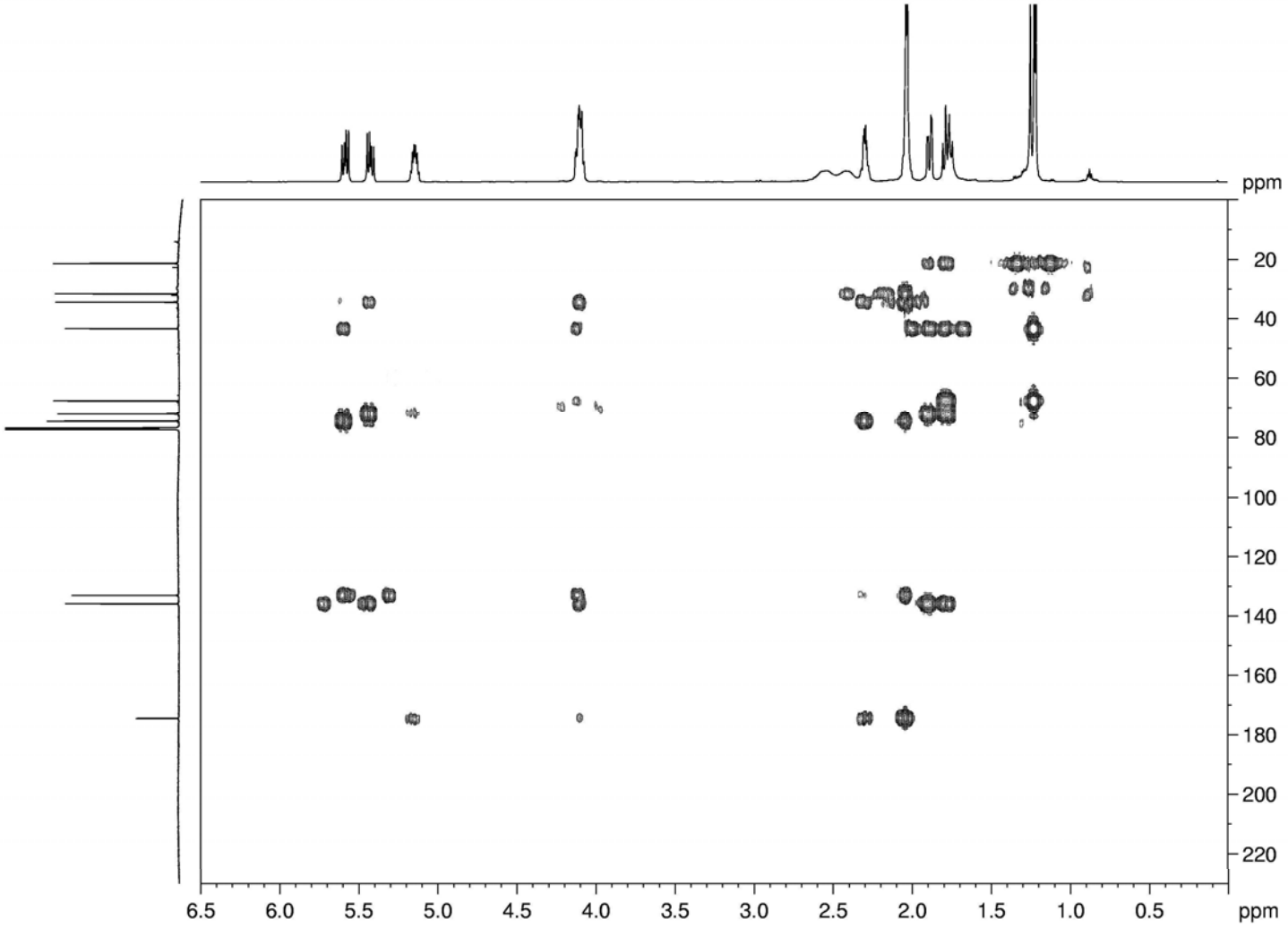

Figure 5.8.15. HMBC spectrum of stagonolide C, isolated from *S. cirsii* solid culture, recorded at 600 MHz

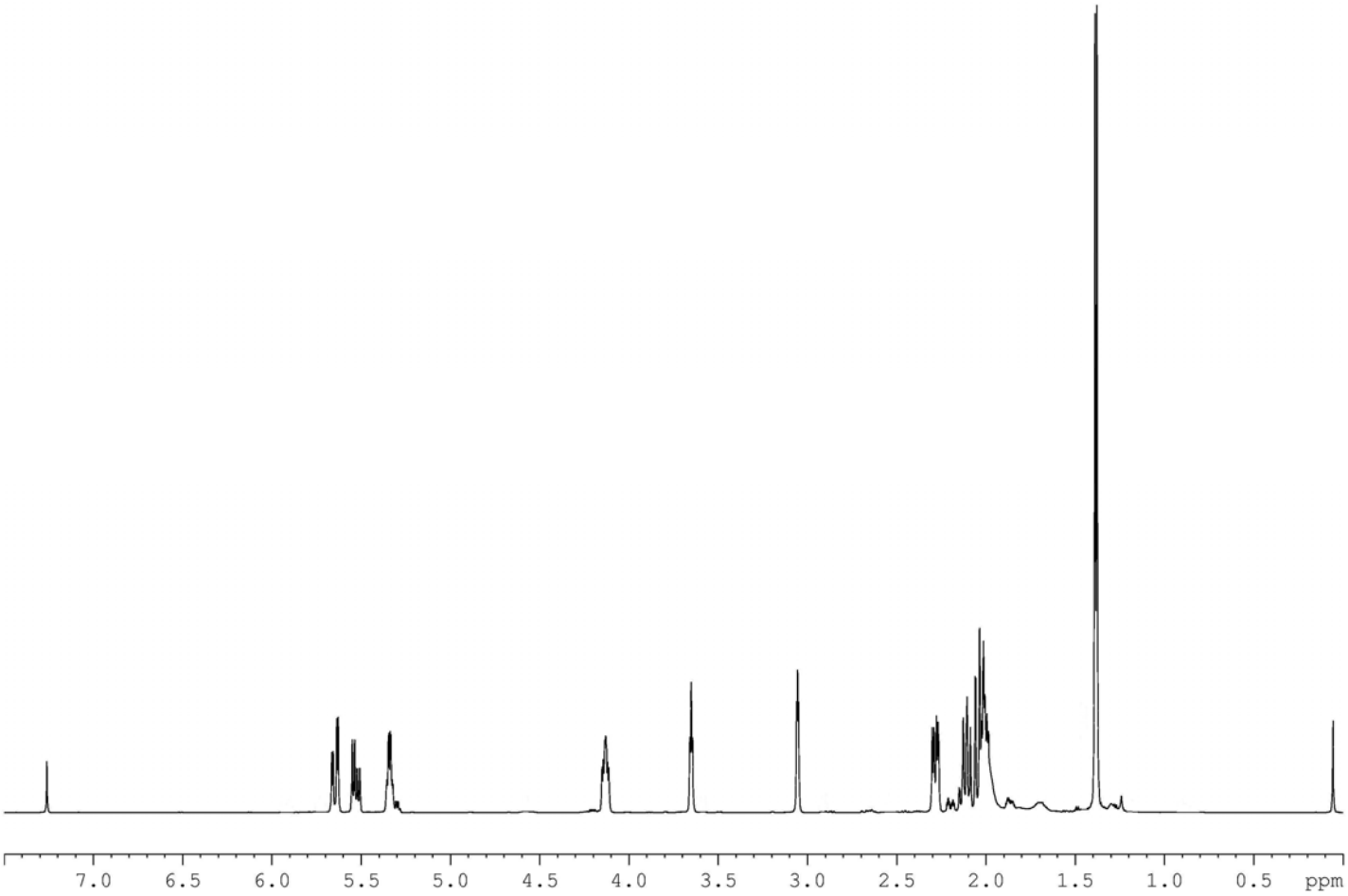

Figure 5.8.16. ^{1}H NMR spectrum of stagonolide D, isolated from *S. cirsii* solid culture, recorded at 600 MHz

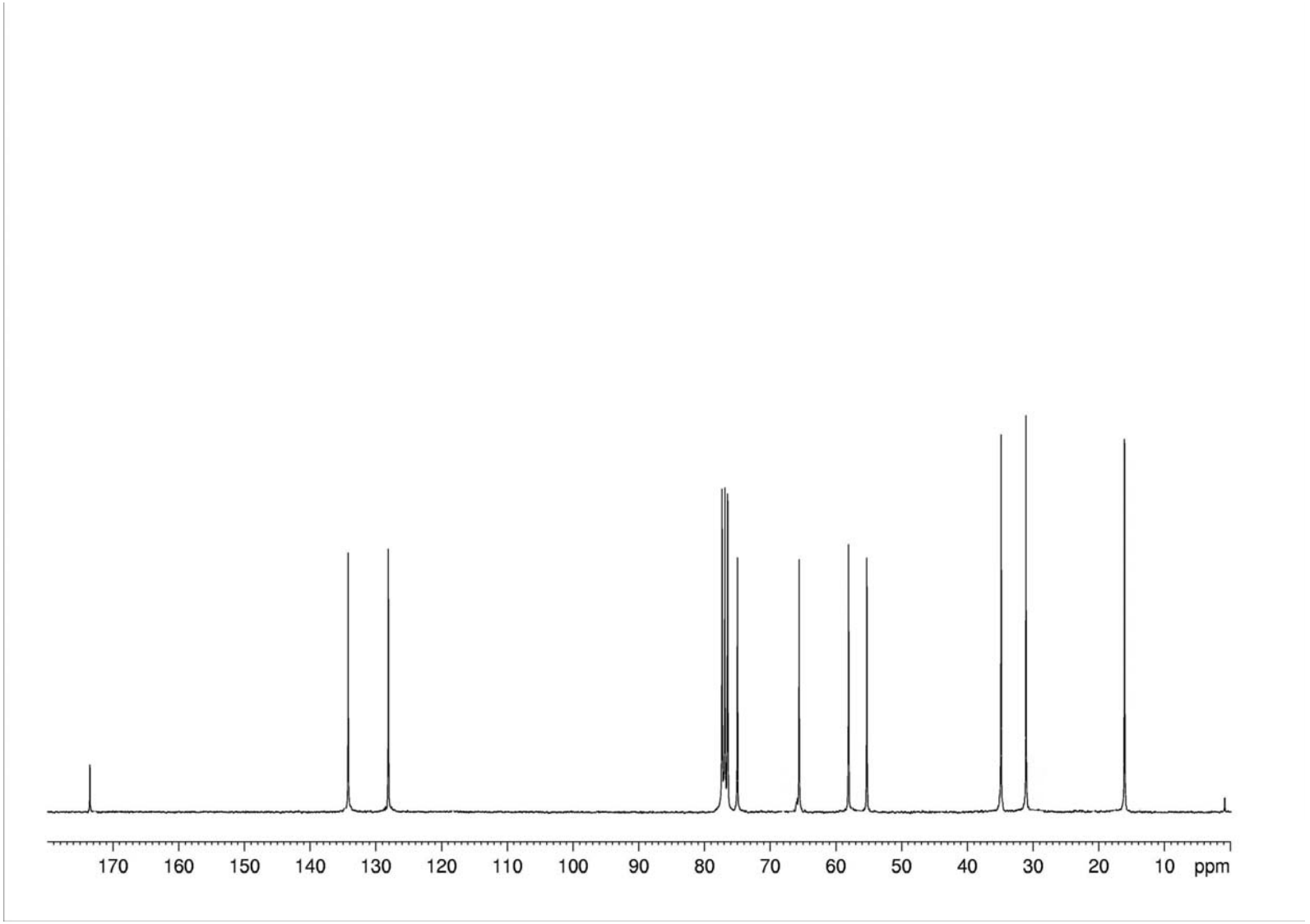

Figure 5.8.17. ^{13}C NMR spectrum of stagonolide D isolated from *S. cirsii* solid culture recorded at 300 MHz

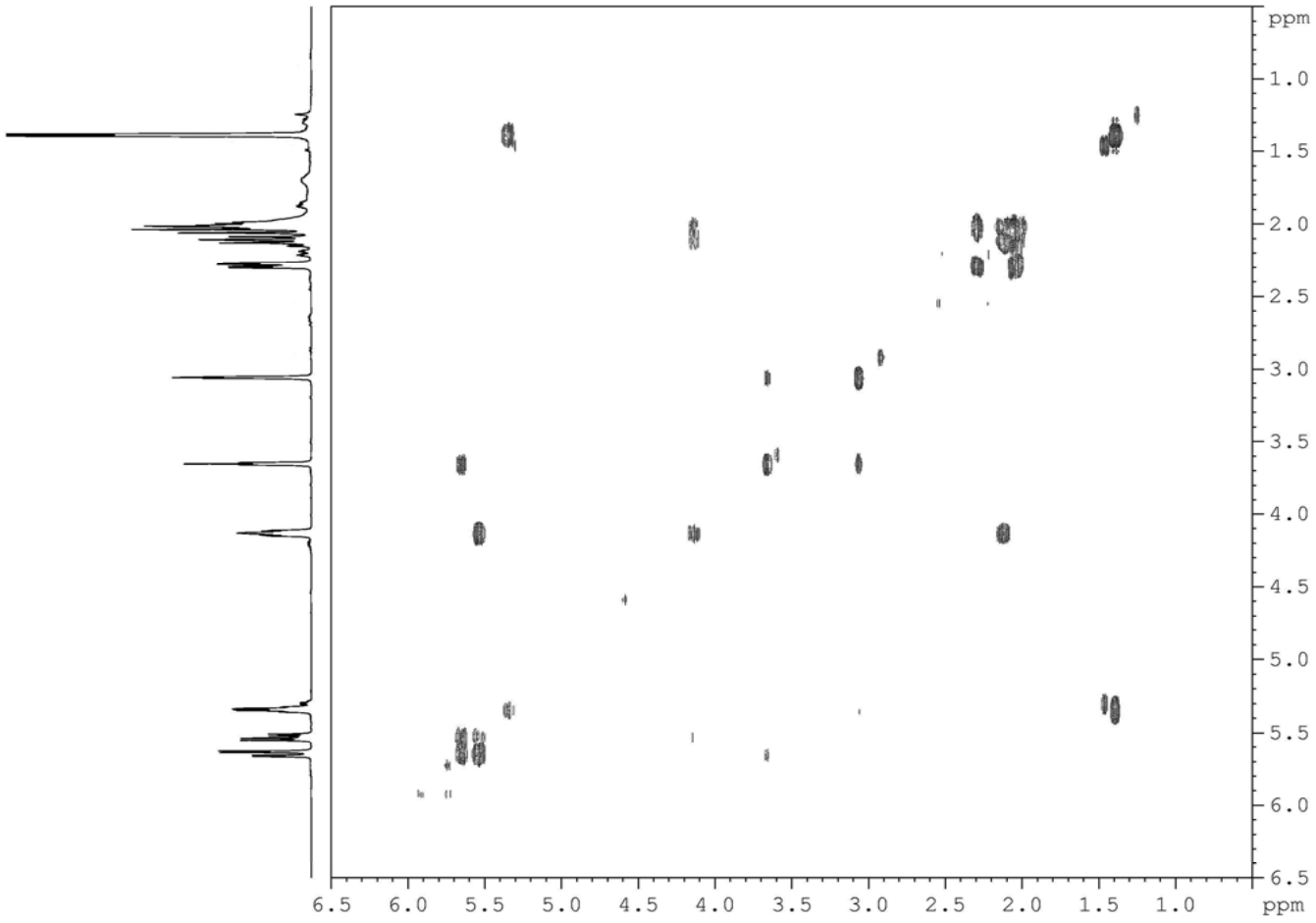

Figure 5.8.18. COSY spectrum of stagonolide D, isolated from *S. cirsii* solid culture, recorded at 600 MHz

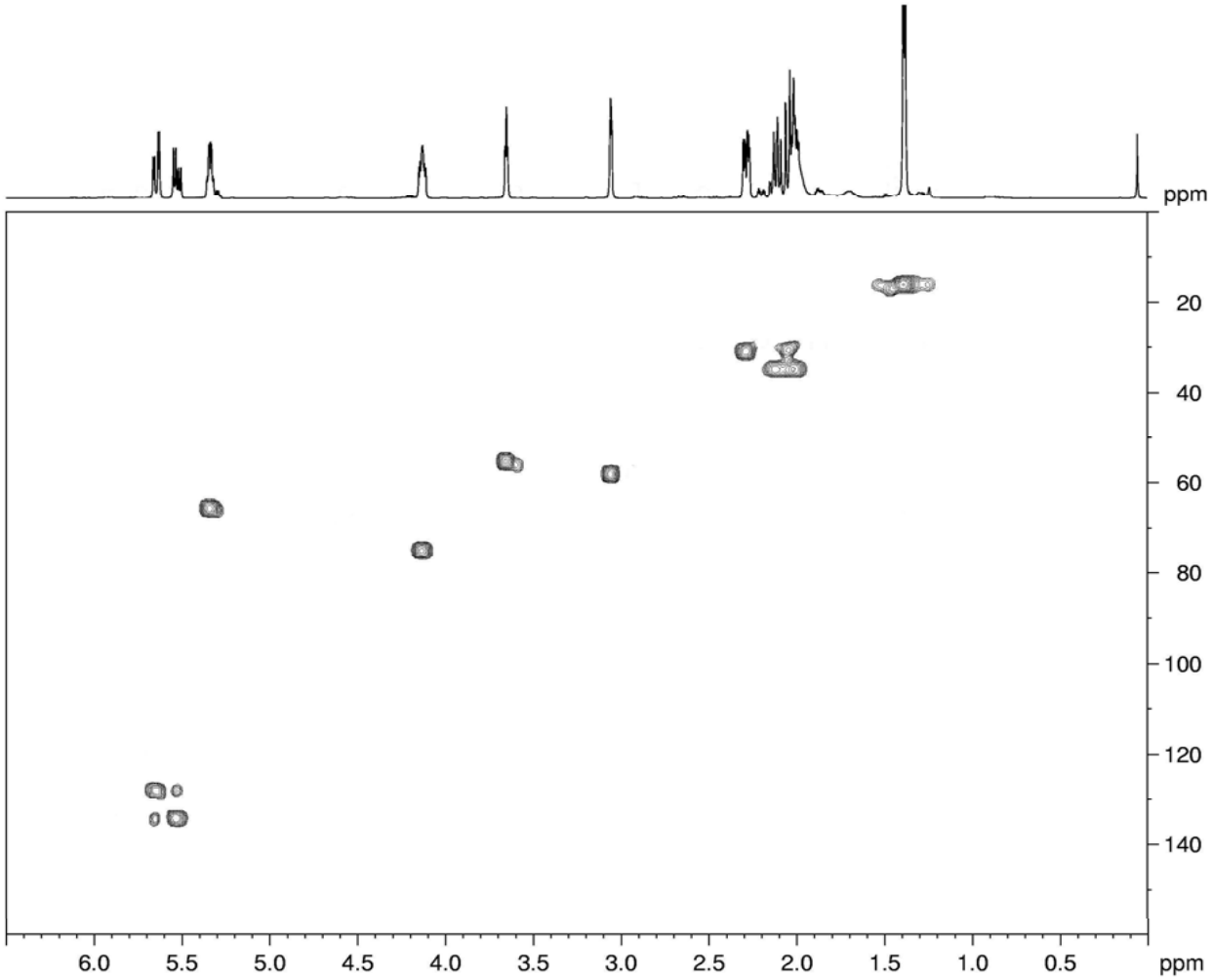

Figure 5.8.19. HSQC spectrum of stagonolide D, isolated from *S. cirsii* solid culture, recorded at 600 MHz

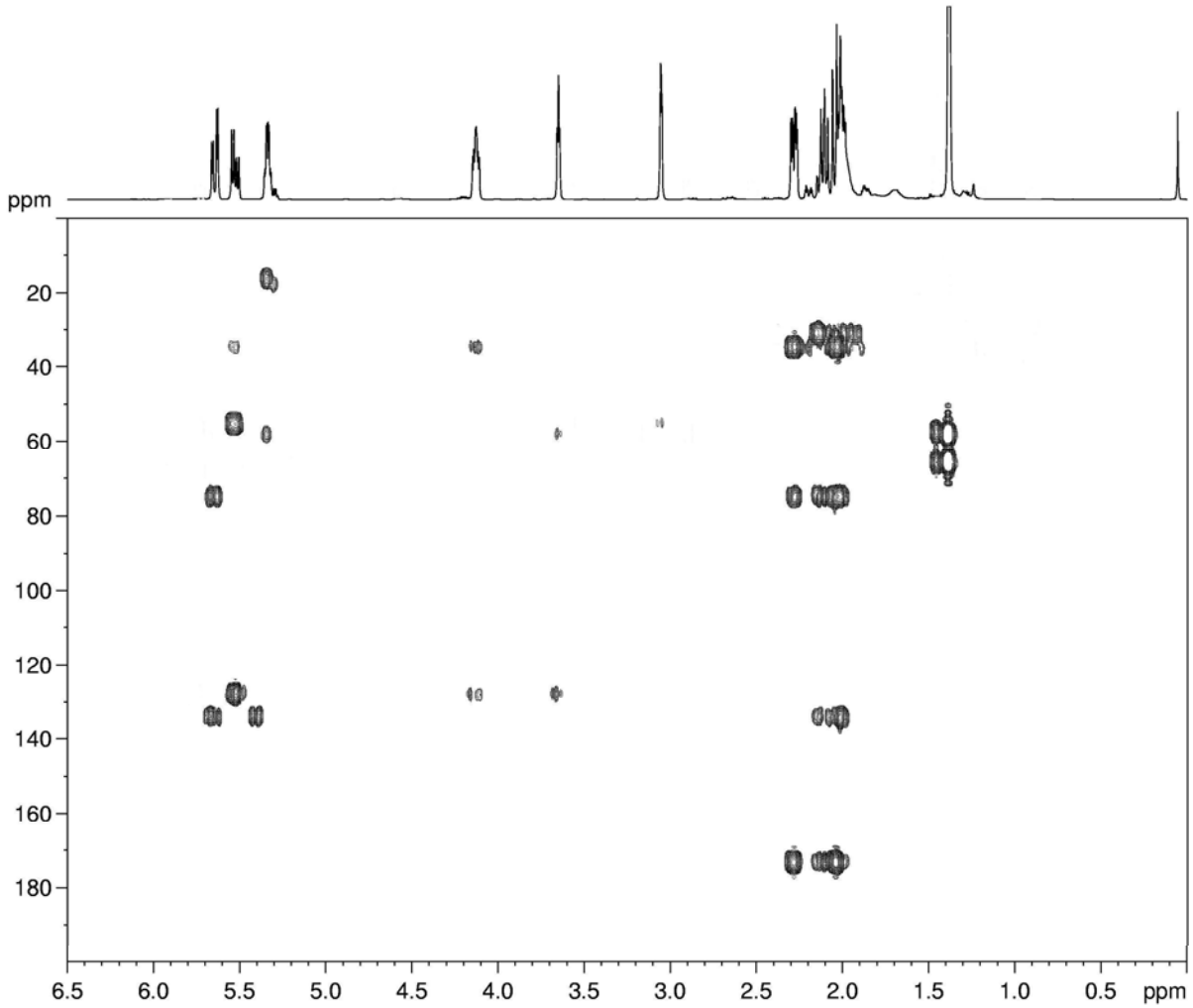

Figure 5.8.20. HMBC spectrum of stagonolide D, isolated from *S. cirsii* solid culture, recorded at 600 MHz

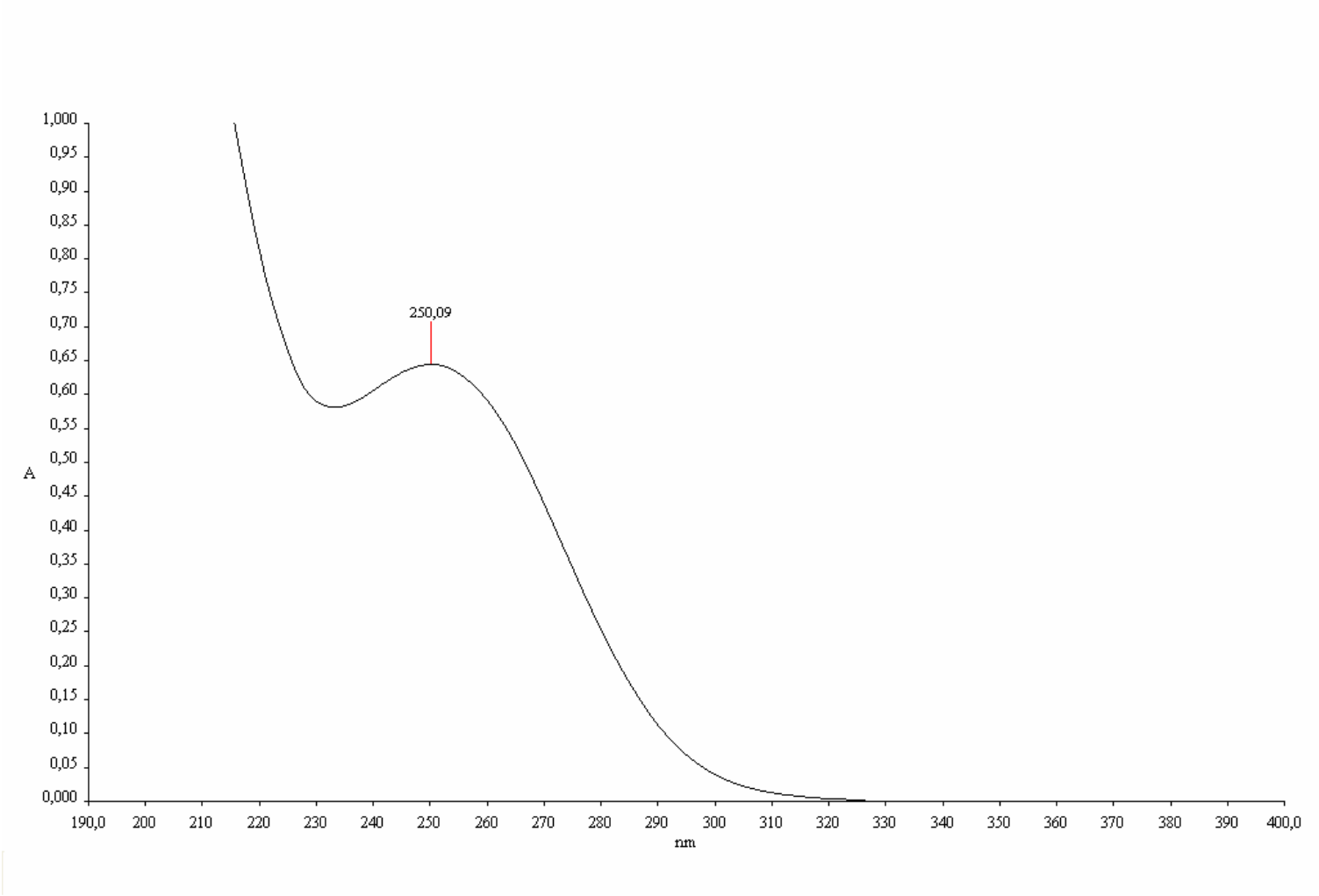

Figure 5.8.21. UV spectrum of stagonolide E, isolated from *S. cirsii* solid culture, recorded in MeCN solution

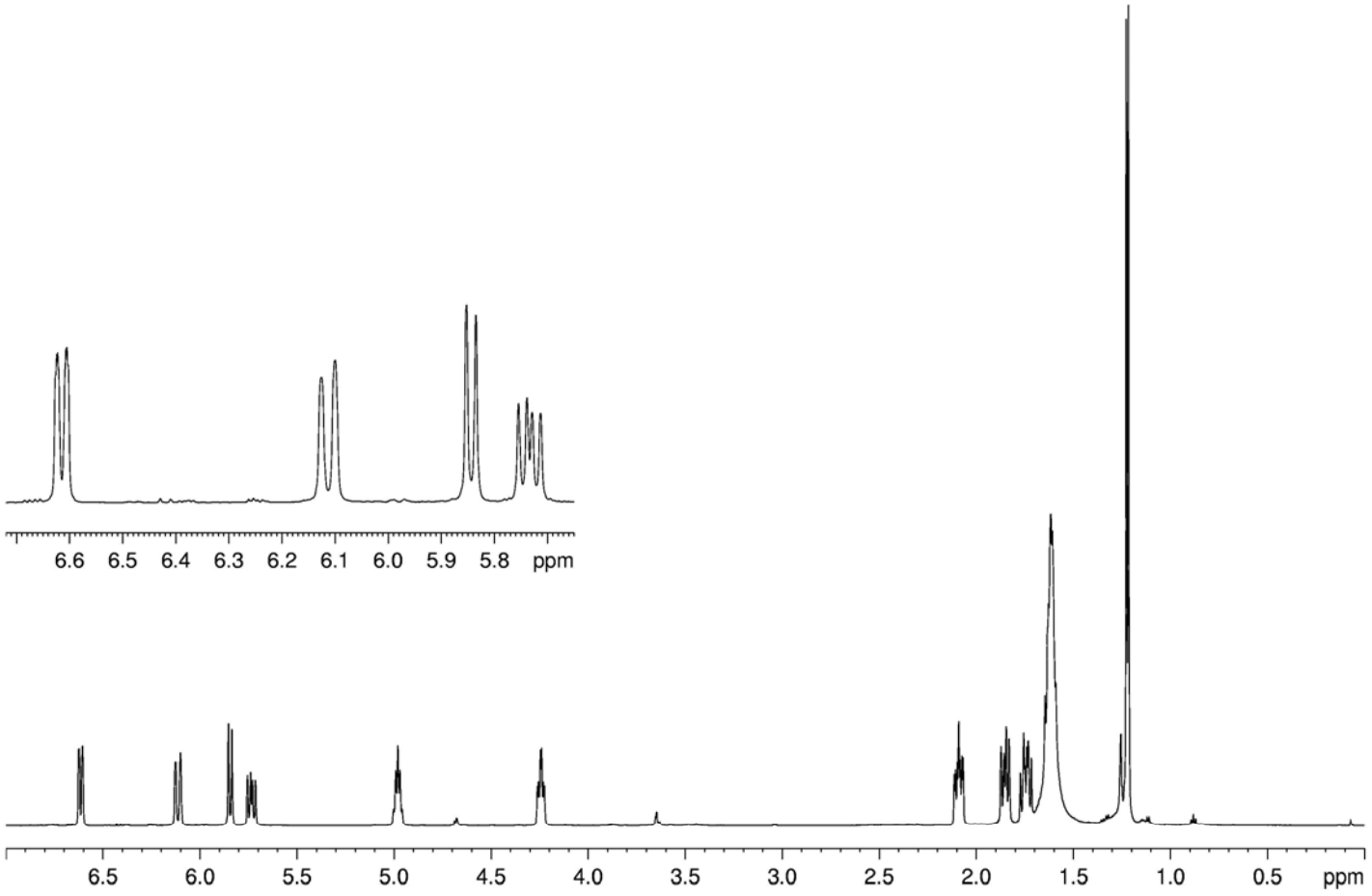

Figure 5.8.22. ^{1}H NMR spectrum of stagonolide E, isolated from *S. cirsii* solid culture, recorded at 600 MHz

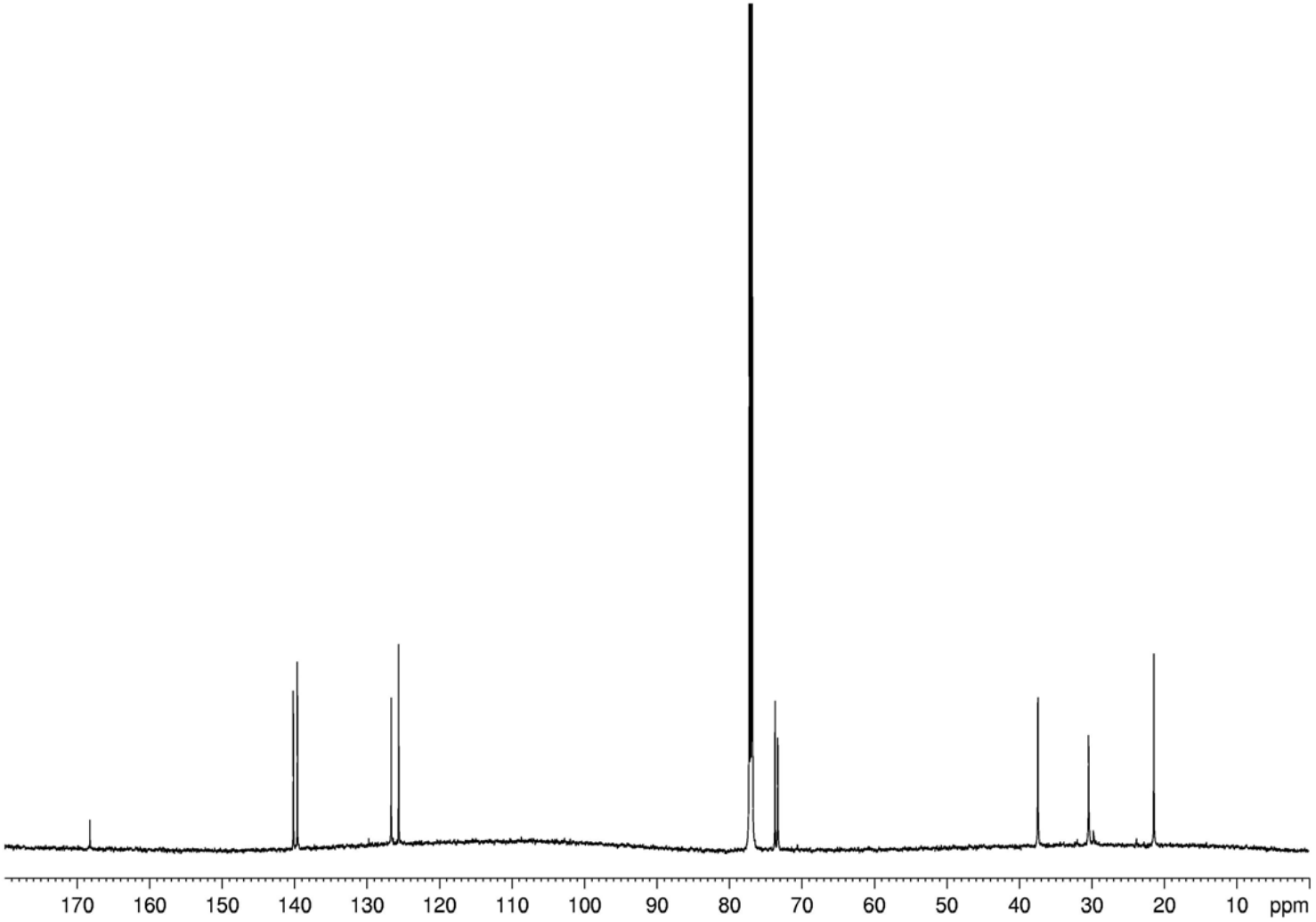

Figure 5.8.23. ^{13}C NMR spectrum of stagonolide E, isolated from *S. cirsii* solid culture, recorded at 600 MHz

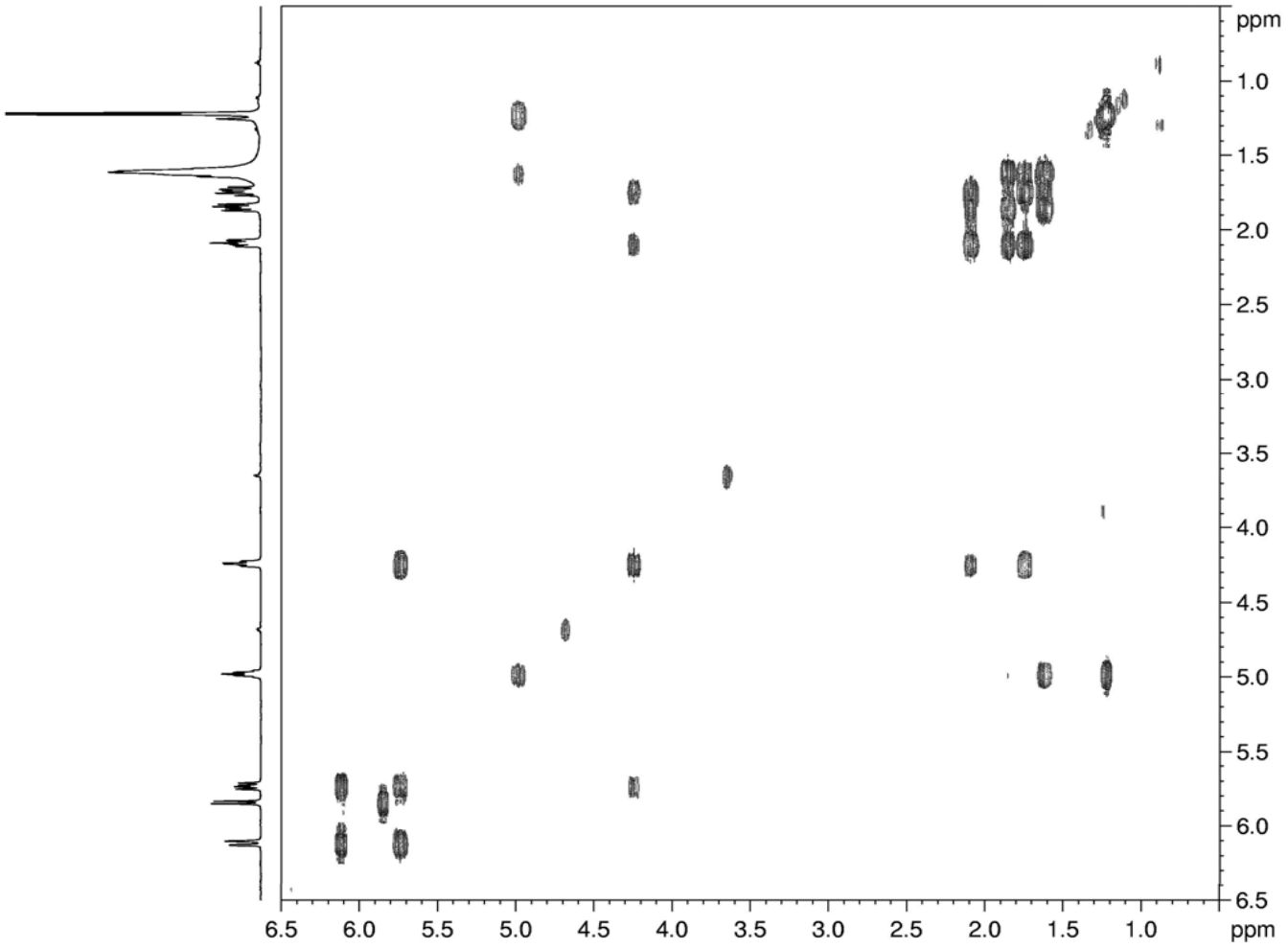

Figure 5.8.24. COSY spectrum of stagonolide E, isolated from *S. cirsii* solid culture, recorded at 600 MHz

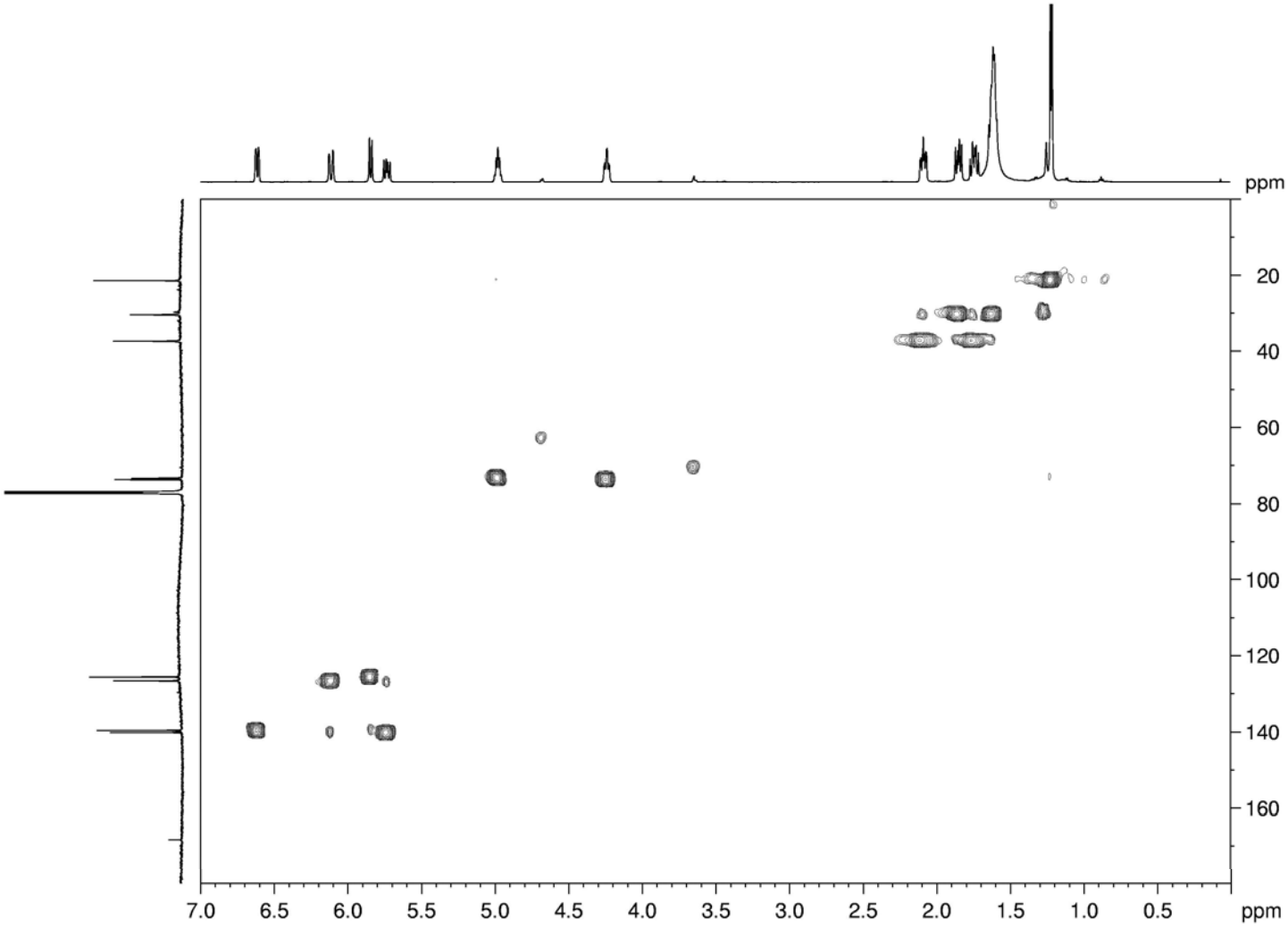

Figure 5.8.25. HSQC spectrum of stagonolide E, isolated from *S. cirsii* solid culture, recorded at 600 MHz

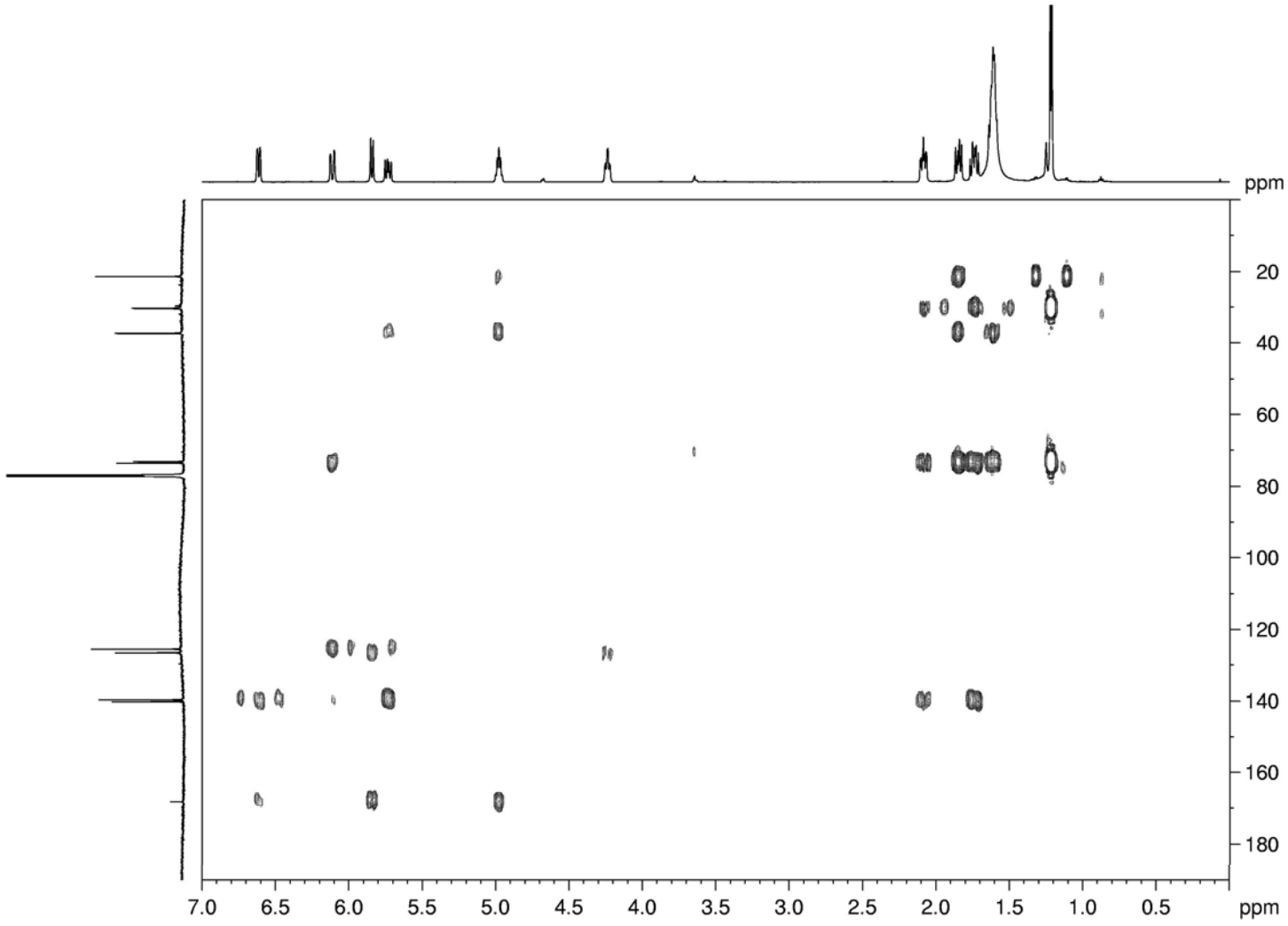

Figure 5.8.26. HMBC spectrum of stagonolide E, isolated from *S. cirsii* solid culture, recorded at 600 MHz

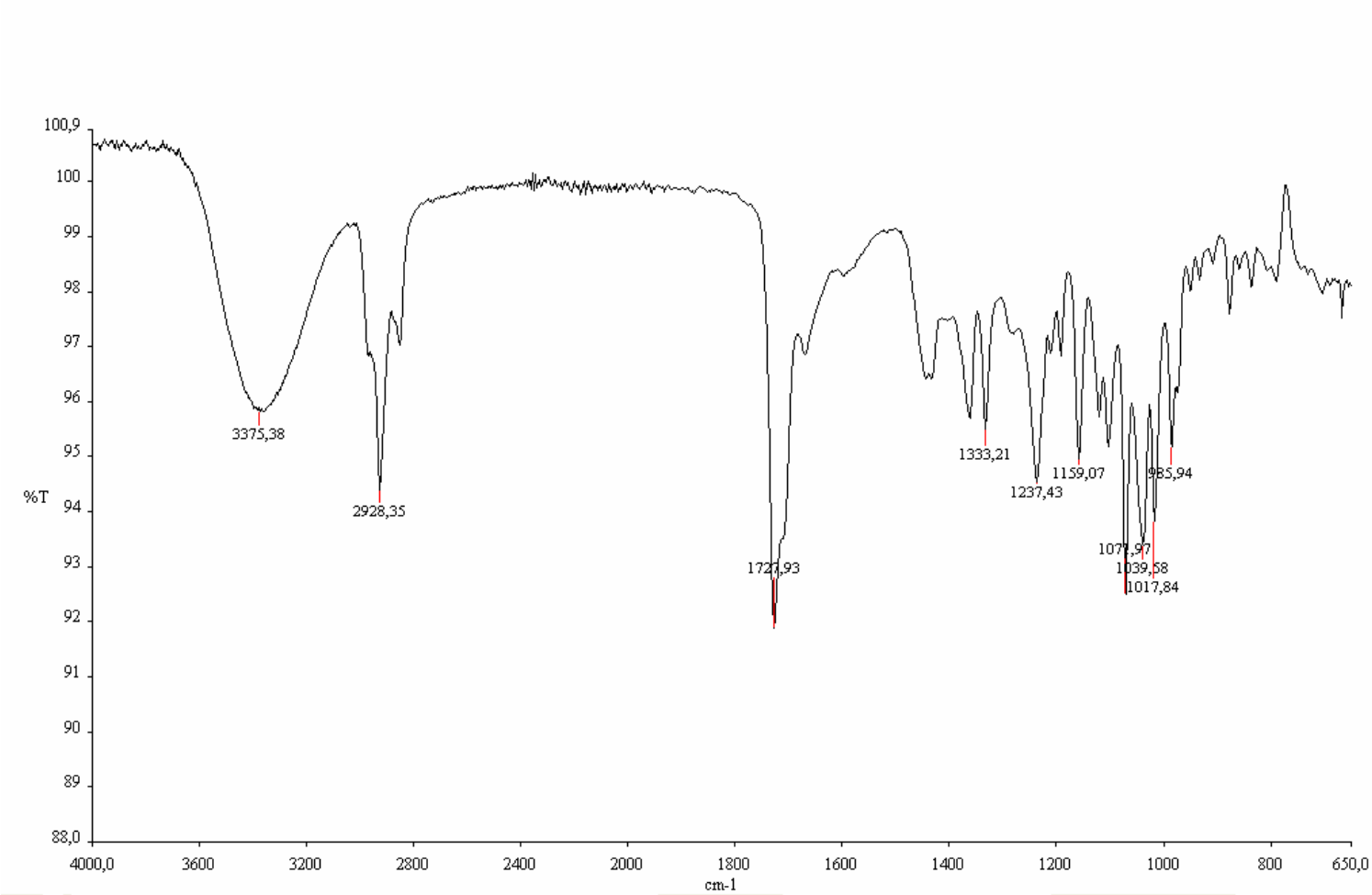

Figure 5.8.27. IR spectrum of stagonolide F, isolated from *S. cirsii* solid culture, recorded as neat

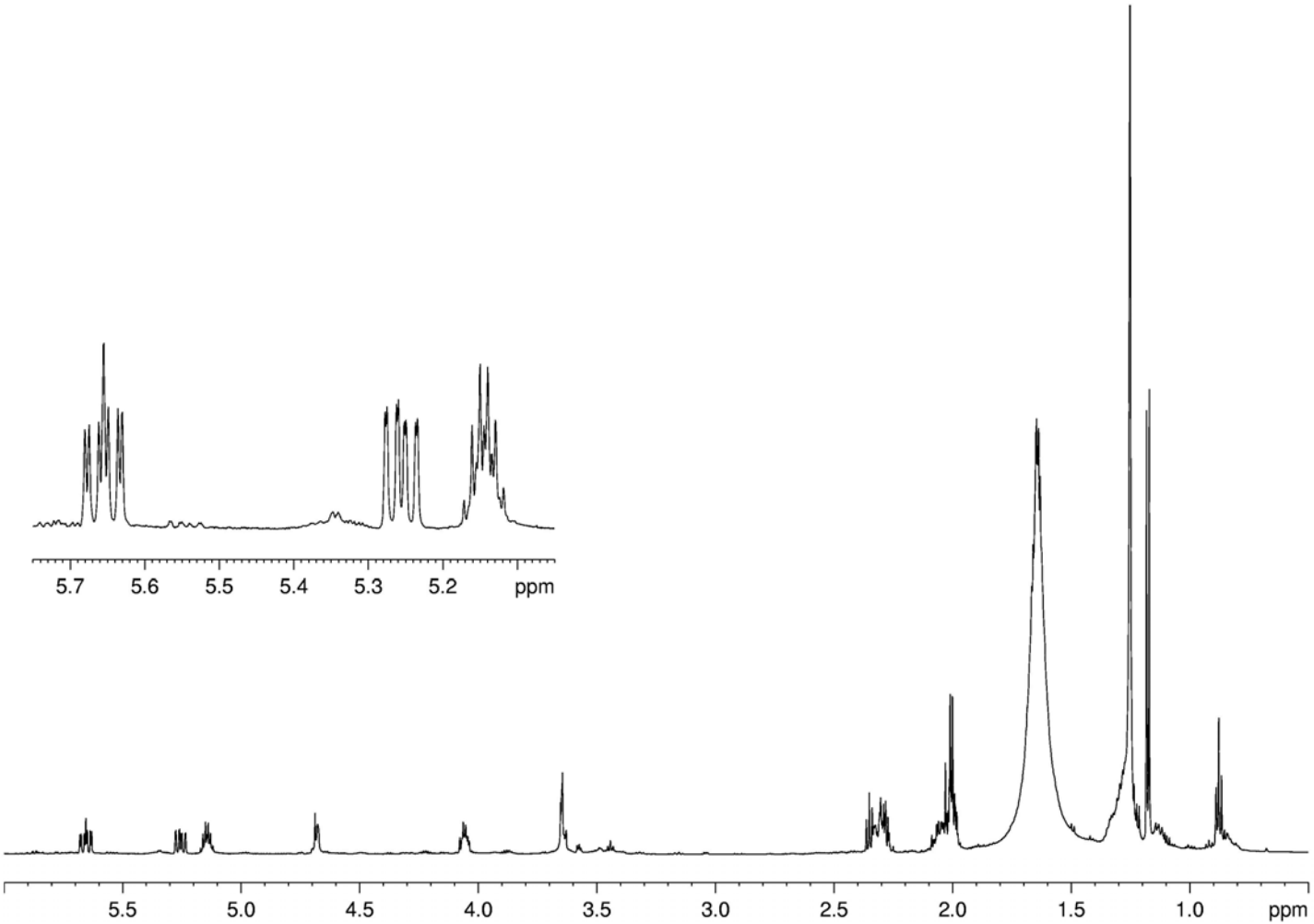

Figure 5.8.28. ^{1}H NMR spectrum of stagonolide F, isolated from *S. cirsii* solid culture, recorded at 600 MHz

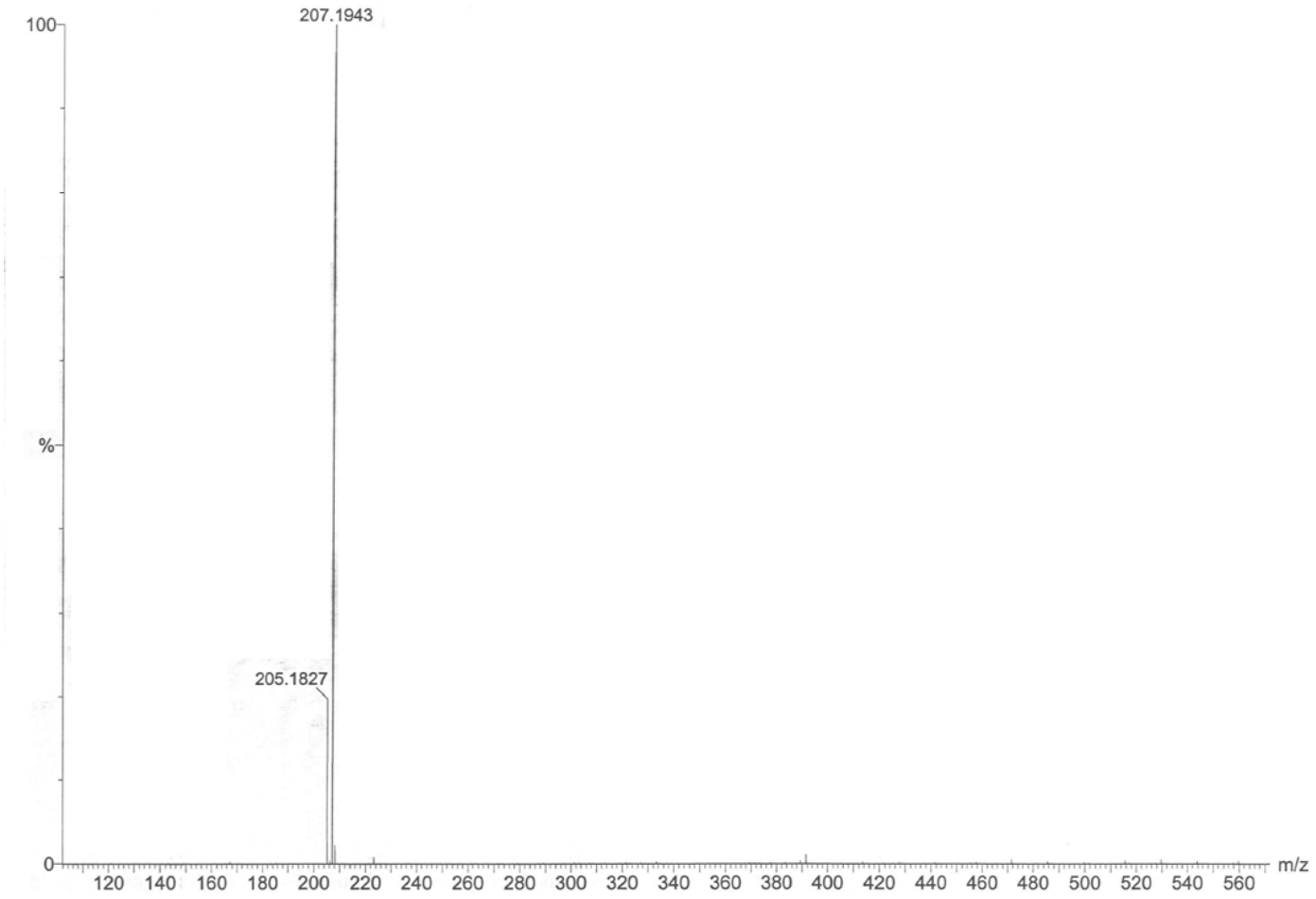

Figure 5.8.29. ESI MS spectrum of stagonolide F isolated from S. cirsii solid culture recorded in positive modality

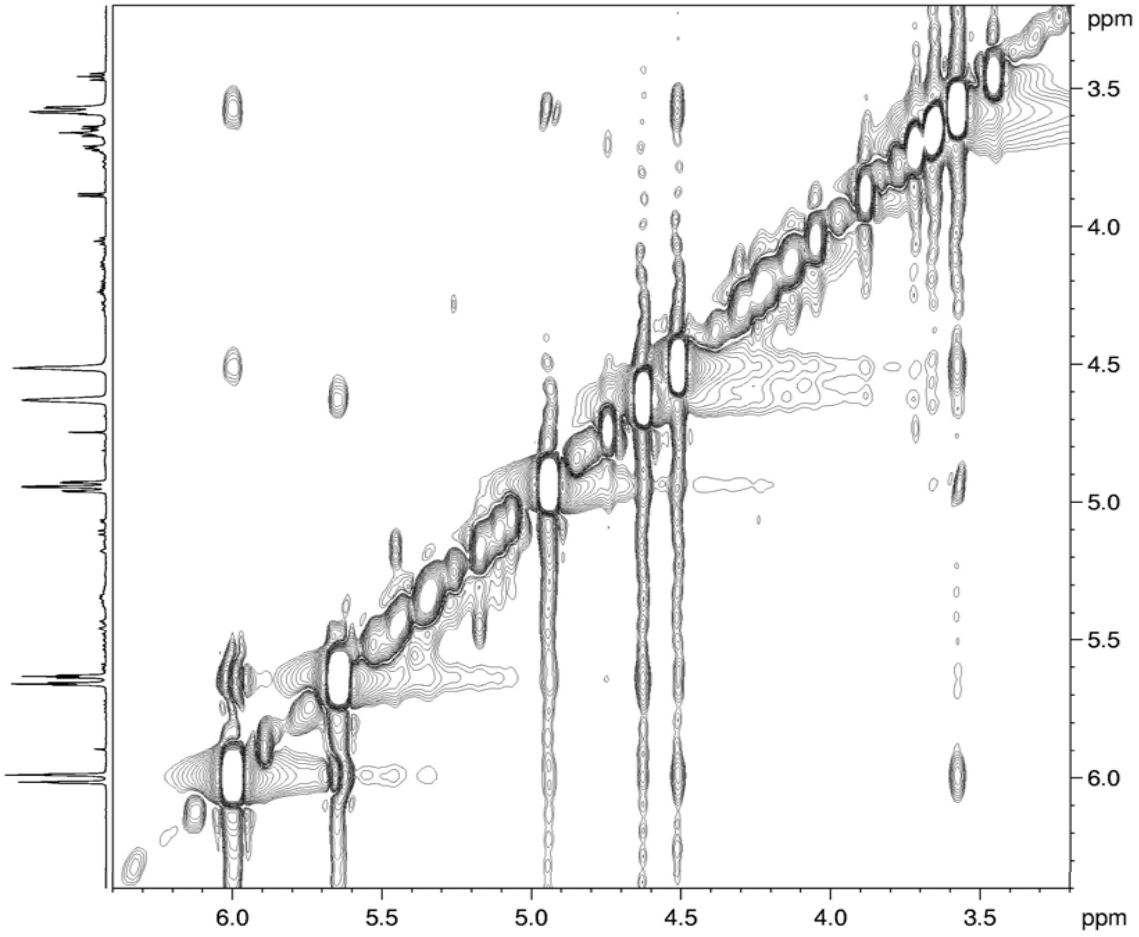

Figure 5.8.30. NOESY spectrum of stagonolide B, isolated from *S. cirsii* solid culture, recorded at 600 MHz

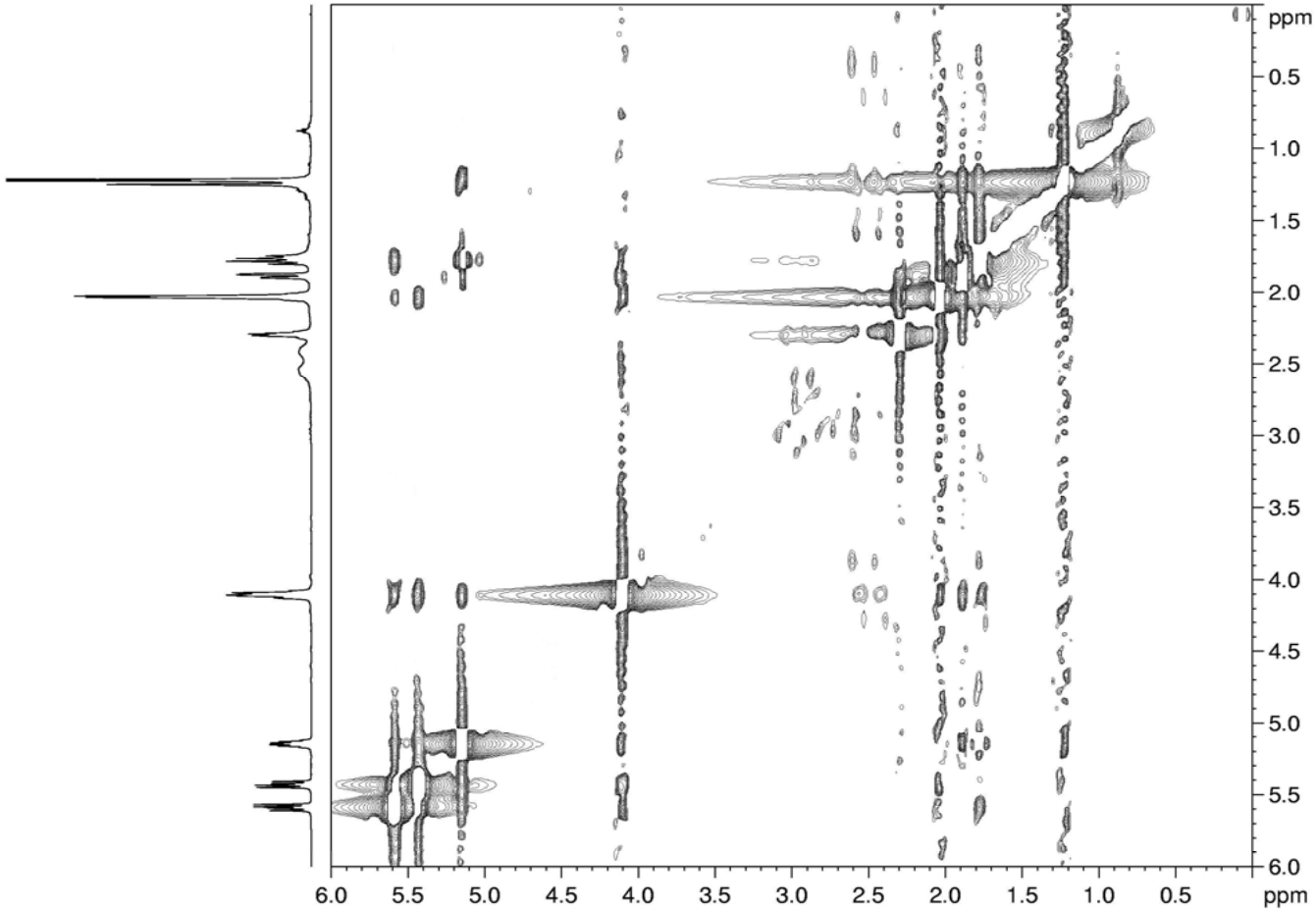

Figure 5.8.31. NOESY spectrum of stagonolide C, isolated from *S. cirsii* solid culture, recorded at 600 MHz

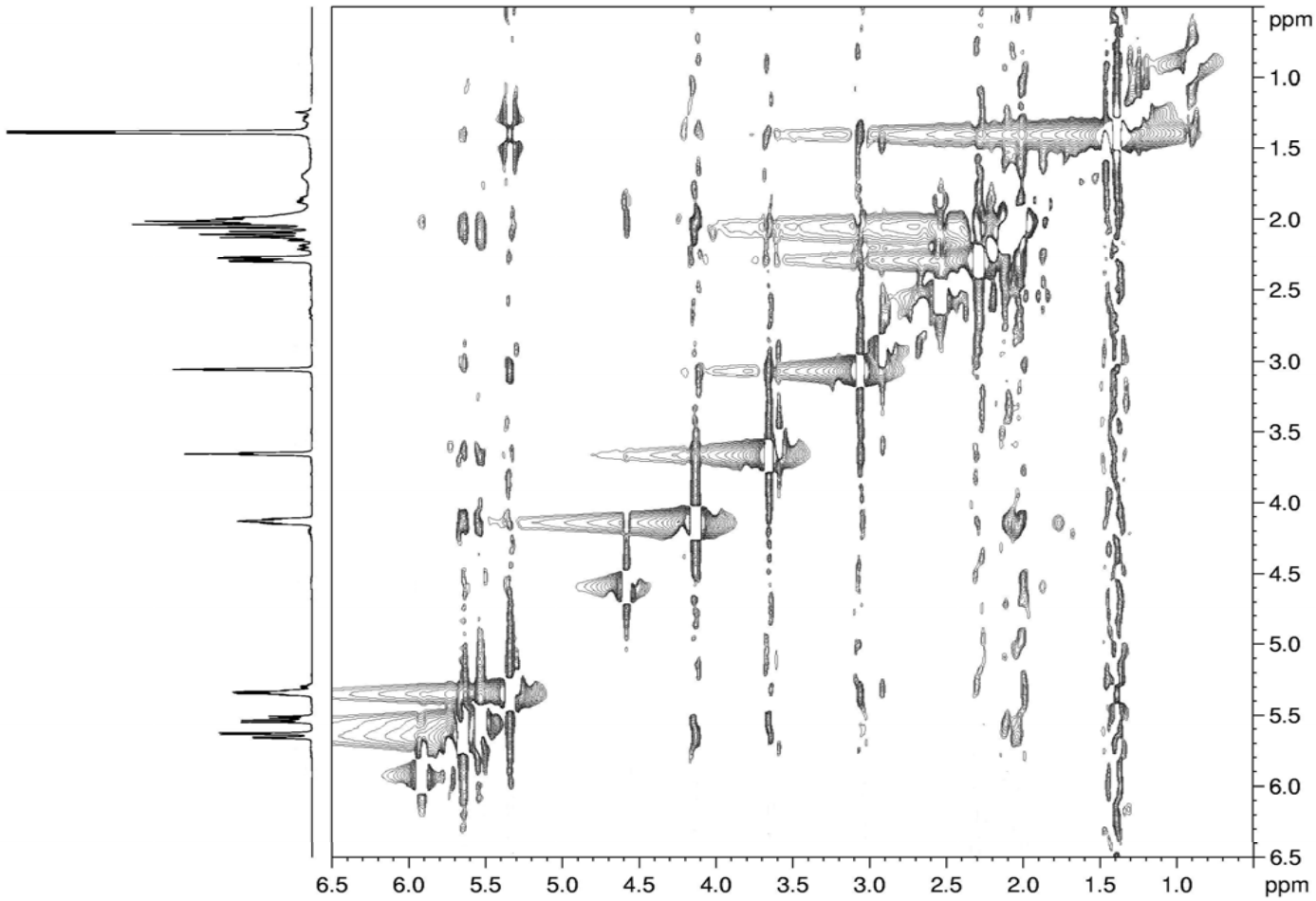

Figure 5.8.32. NOESY spectrum of stagonolide D, isolated from *S. cirsii* solid culture, recorded at 600 MHz

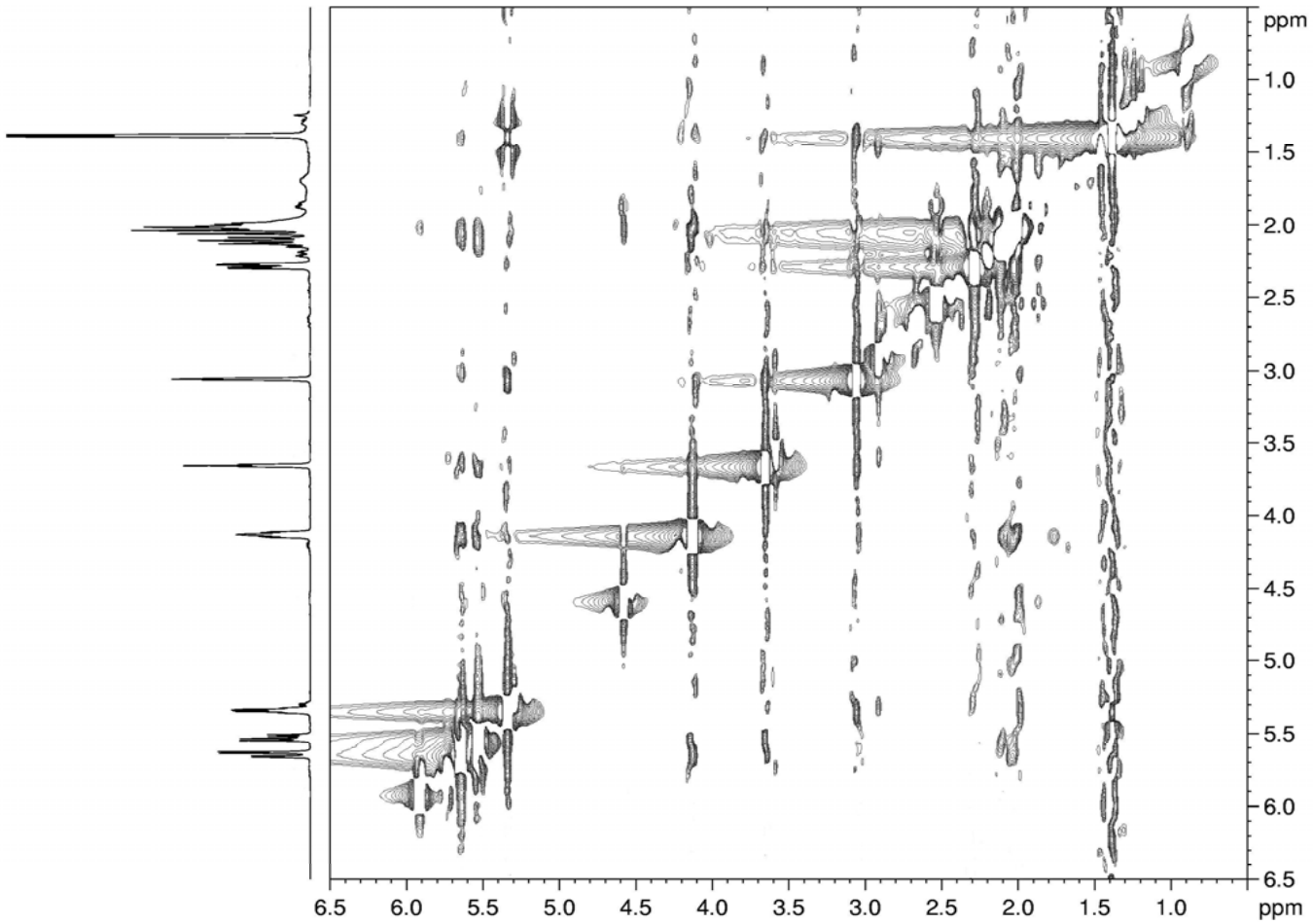

Figure 5.8.32. NOESY spectrum of stagonolide D, isolated from *S. cirsii* solid culture, recorded at 600 MHz

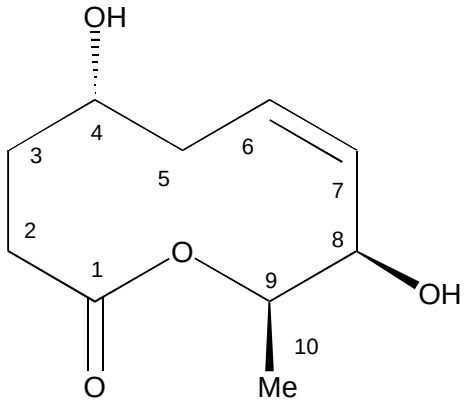

50

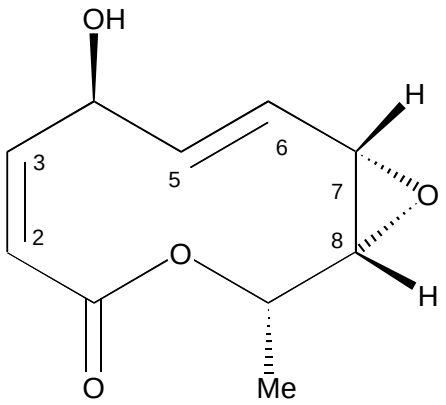

51

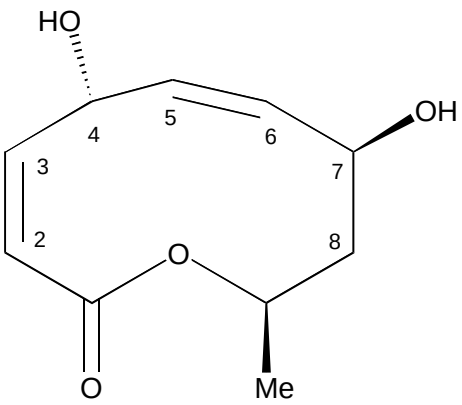

5**2**

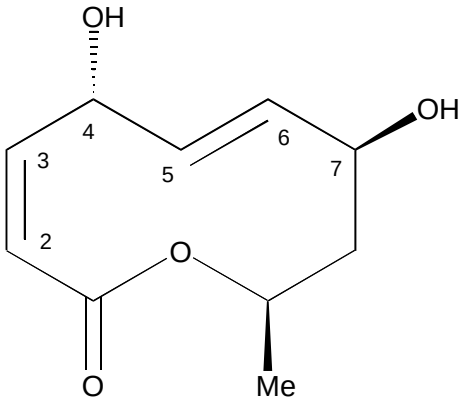

53

Figure 5.8.34. Structures of stagonolide G-I and modiolide A, isolated from *S. cirsii* solid culture

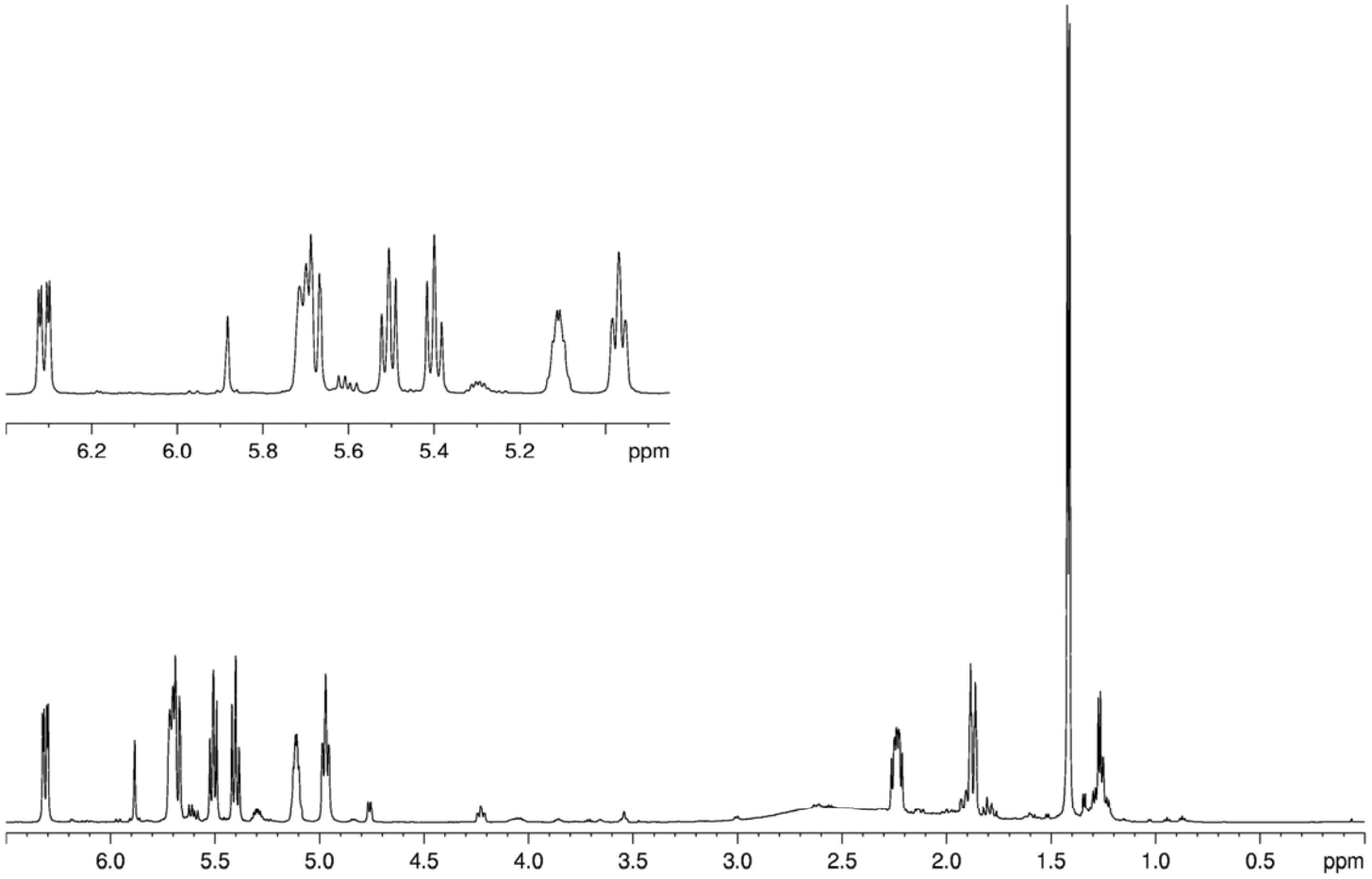

Figure 5.8.35. ^{1}H NMR spectrum of modiolide A, isolated from *S. cirsii* solid culture, recorded at 600 MHz

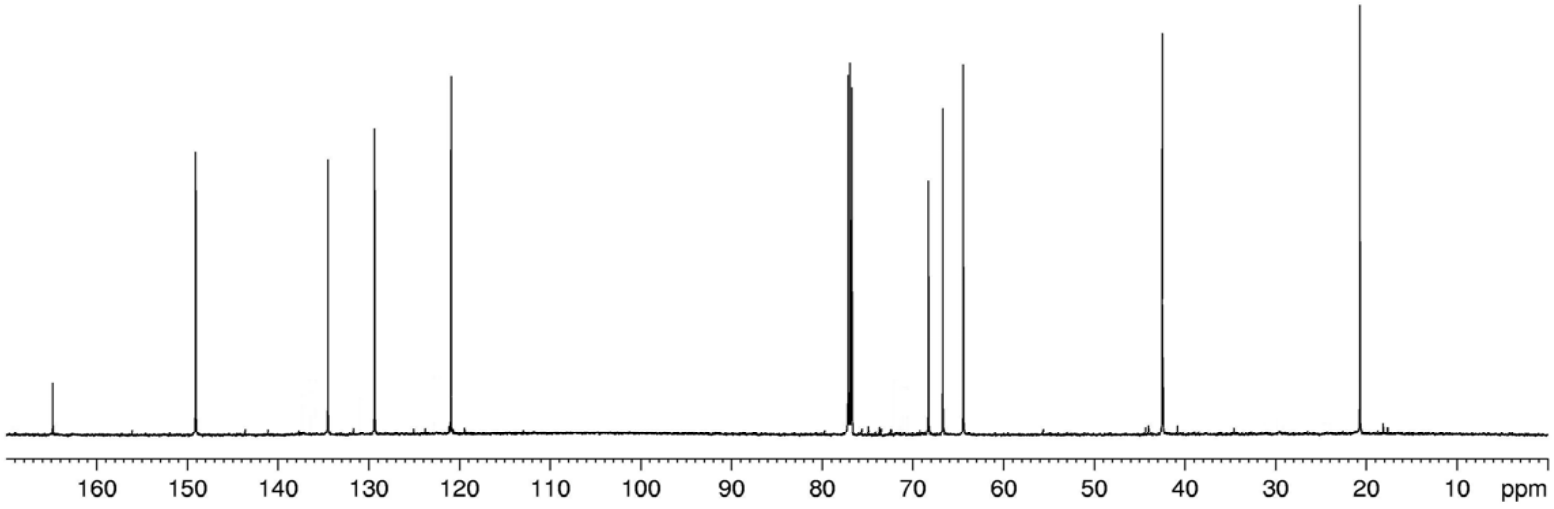

Figure 5.8.36. ^{13}C NMR spectrum of modiolide A, isolated from *S. cirsii* solid culture, recorded at 600 MHz

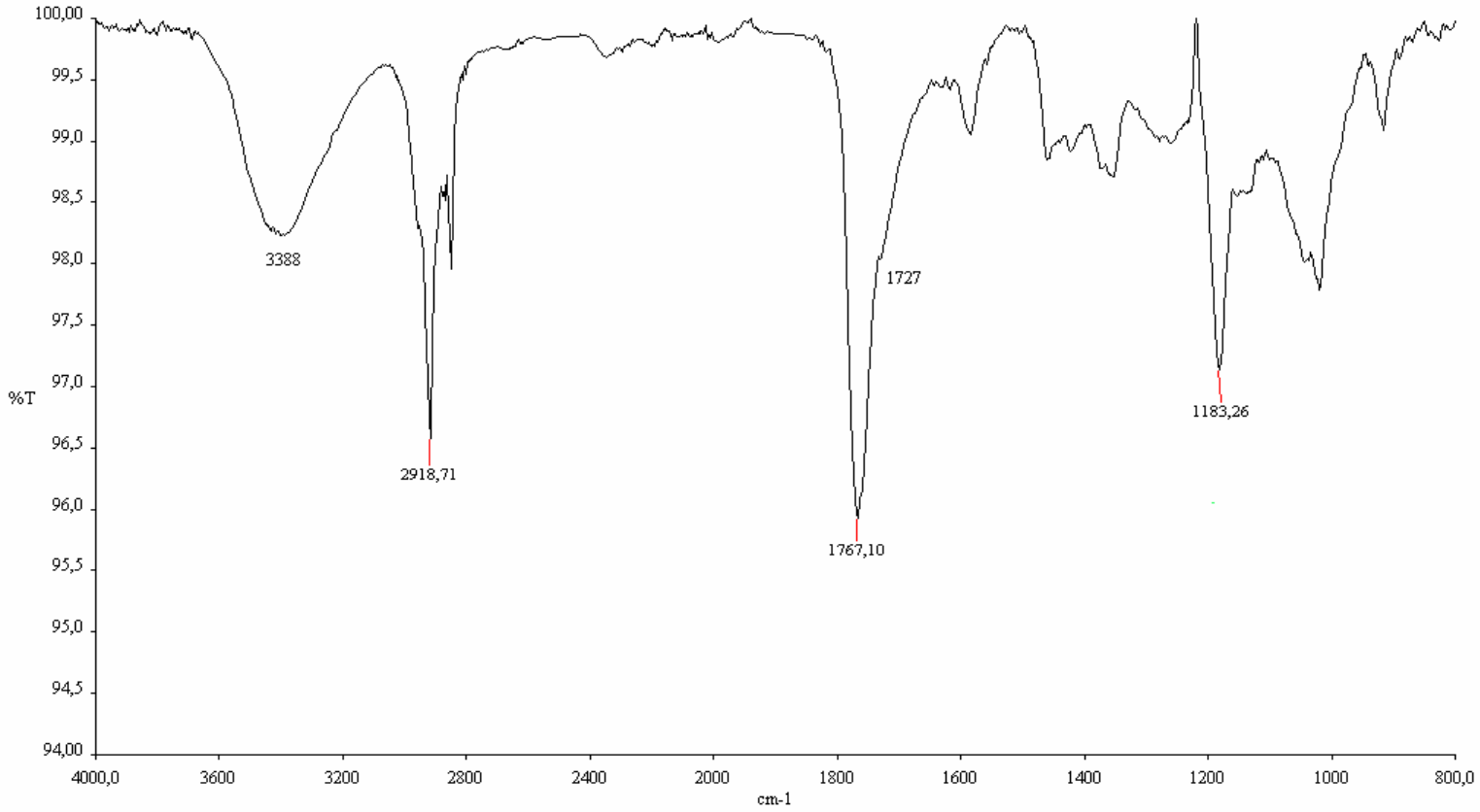

Figure 5.8.37. IR spectrum of stagonolide G, isolated from *S. cirsii* solid culture, recorded as neat

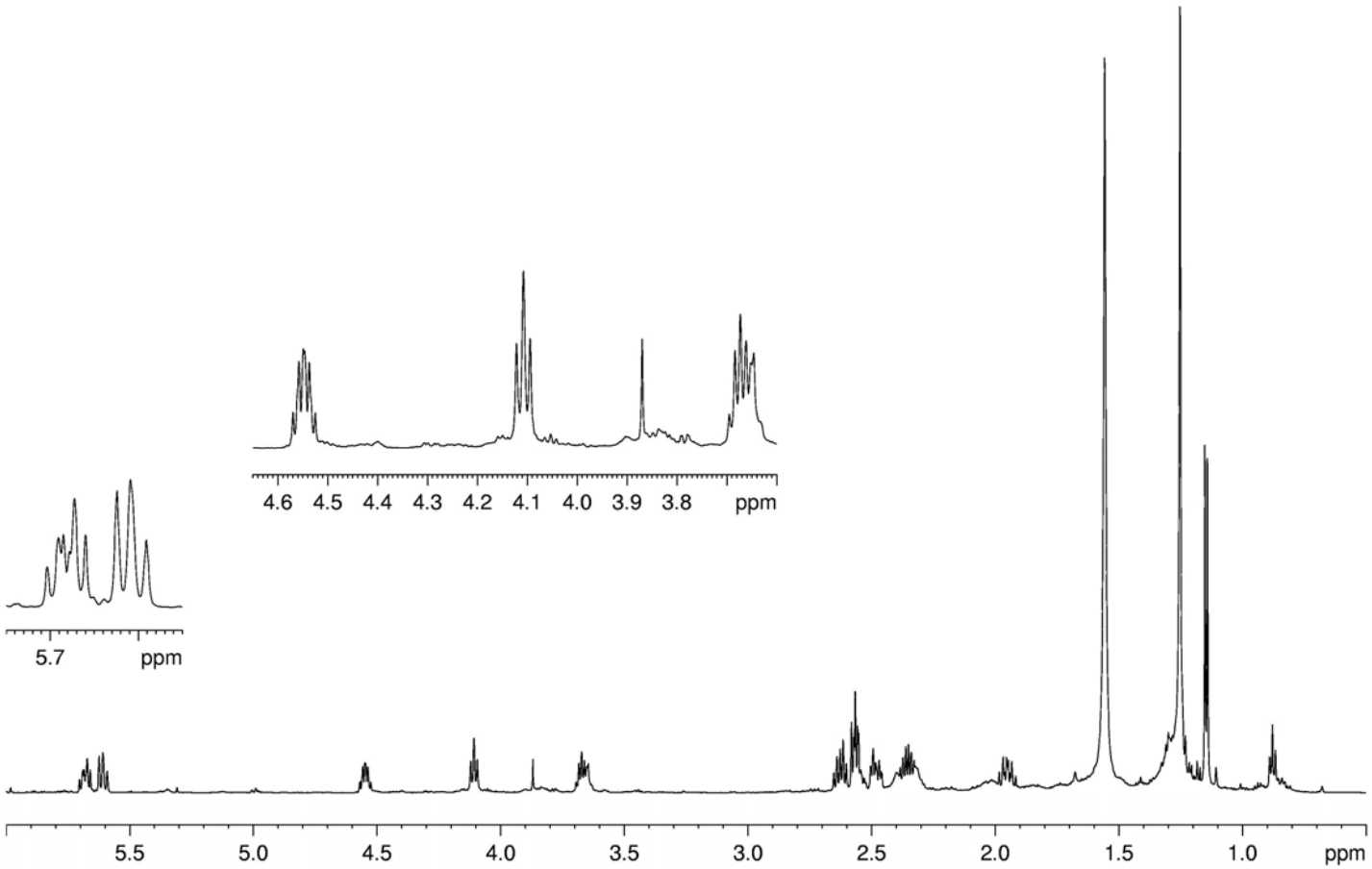

Figure 5.8.38. ^{1}H NMR spectrum of stagonolide G, isolated from *S. cirsii* solid culture, recorded at 600 MHz

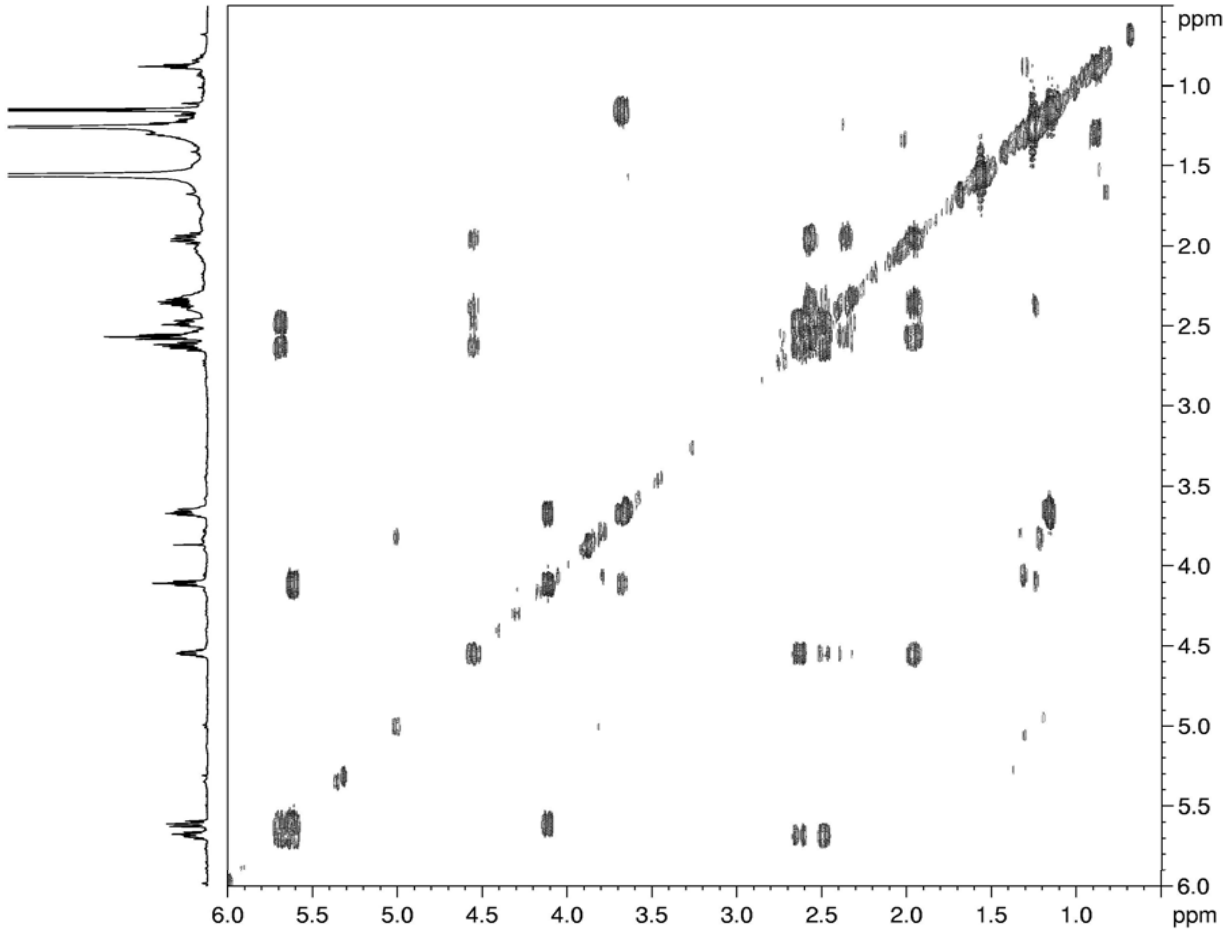

Figure 5.8.39. COSY spectrum of stagonolide G, isolated from *S. cirsii* solid culture, recorded at 600 MHz

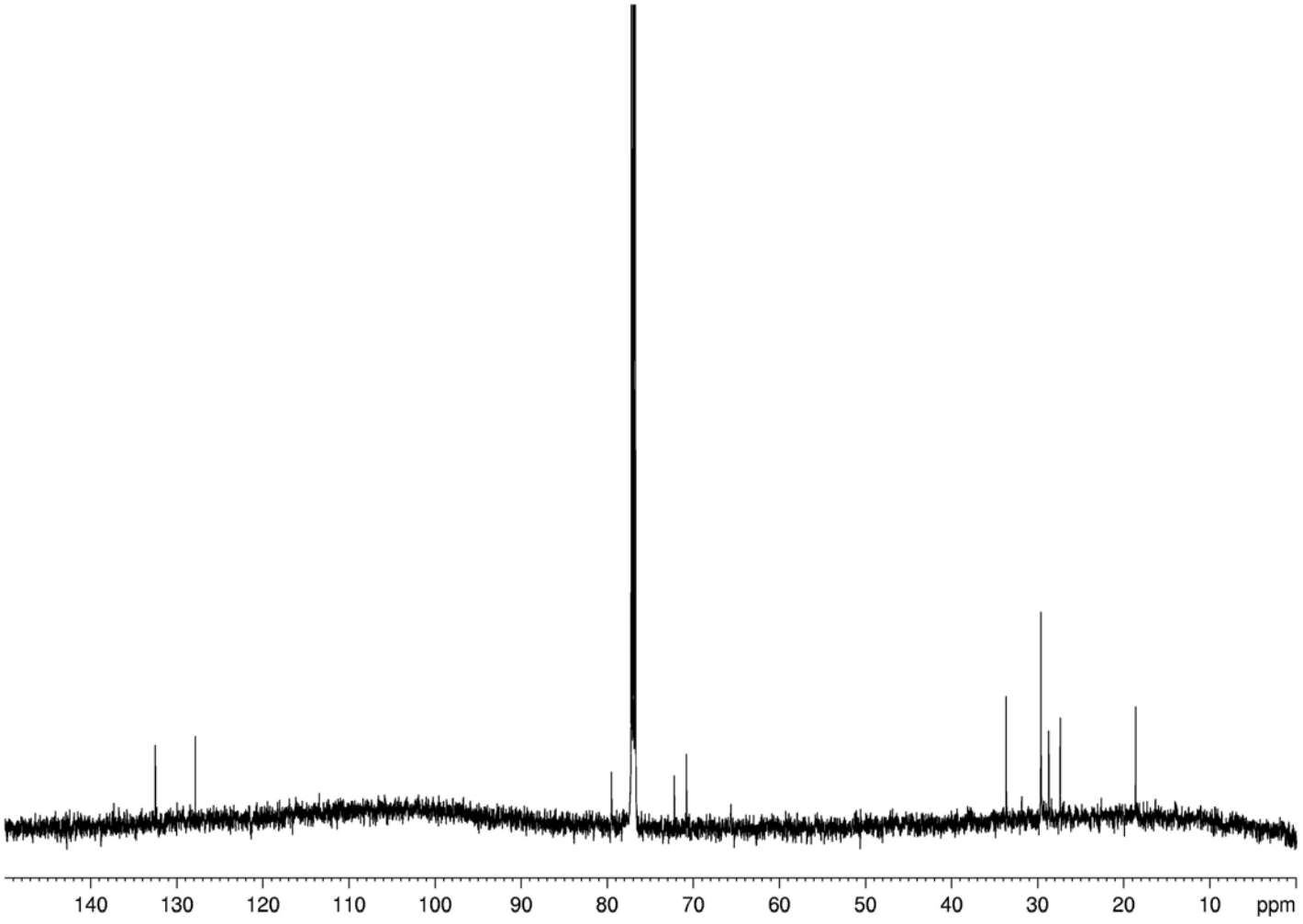

Figure 5.8.40. ^{13}C NMR spectrum of stagonolide G, isolated from *S. cirsii* solid culture, recorded at 600 MHz

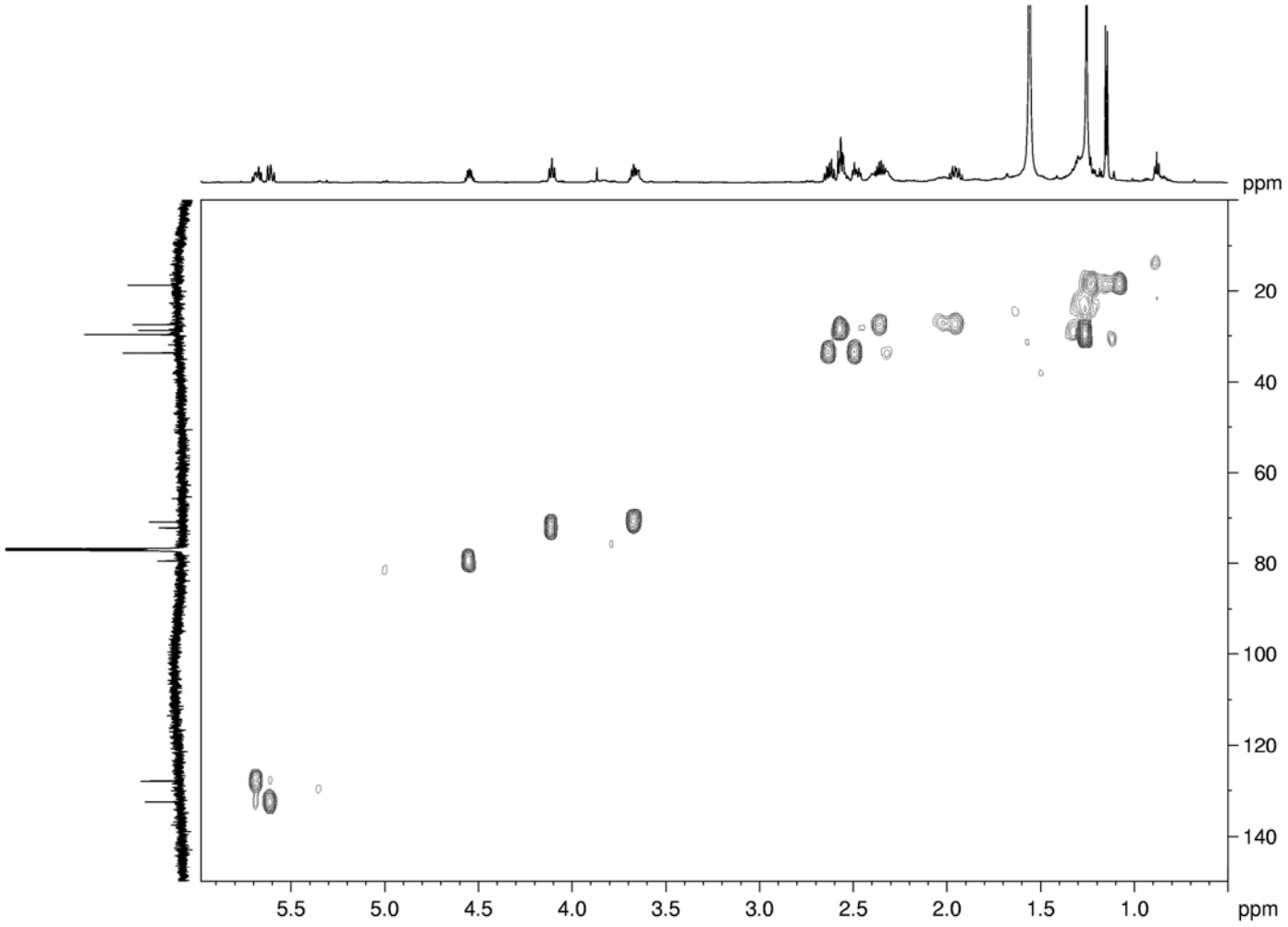

Figure 5.8.41. HSQC spectrum of stagonolide G, isolated from *S. cirsii* solid culture, recorded at 600 MHz

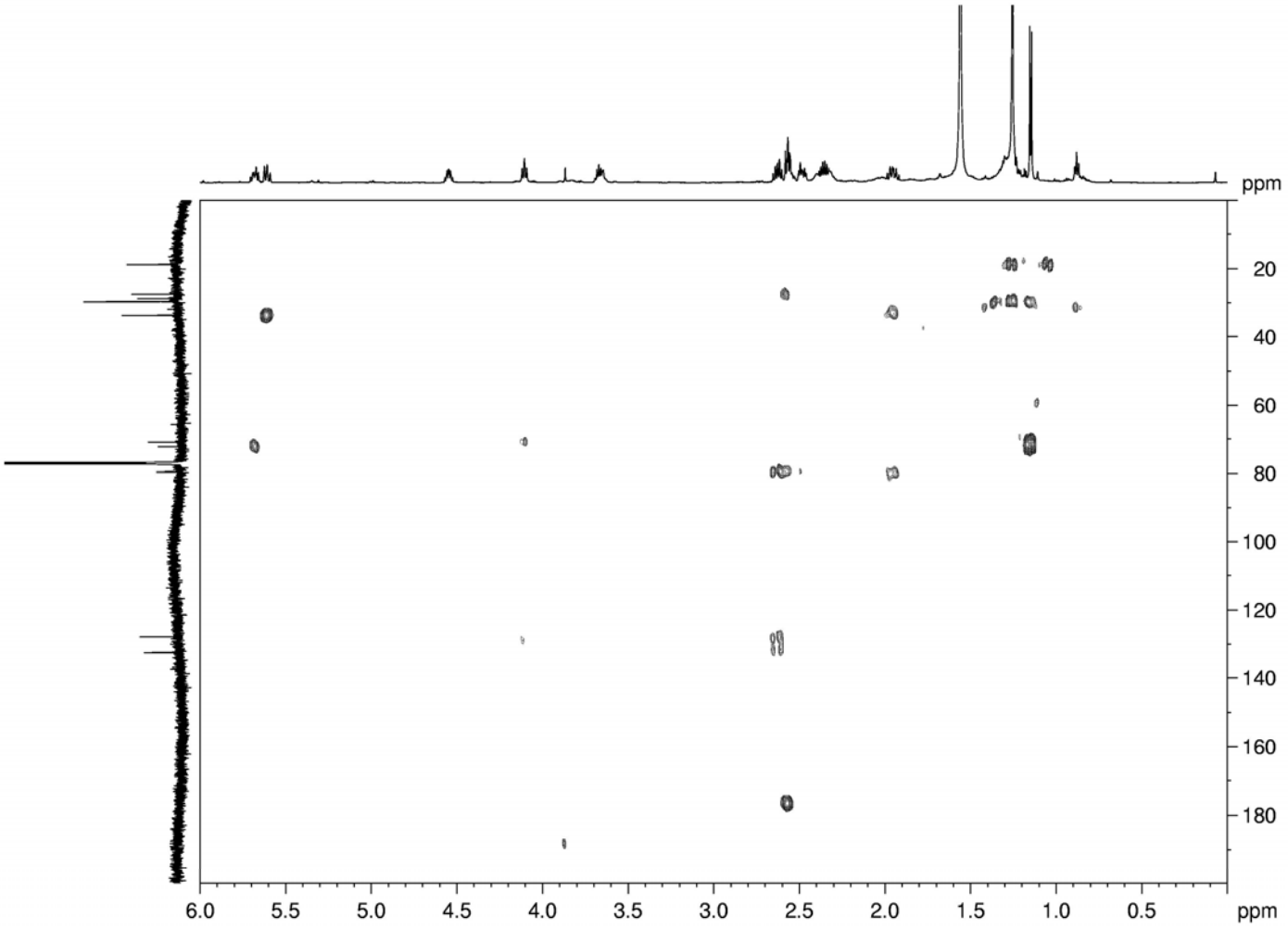

Figure 5.8.42. HMBC spectrum of stagonolide G, isolated from *S. cirsii* solid culture, recorded at 600 MHz

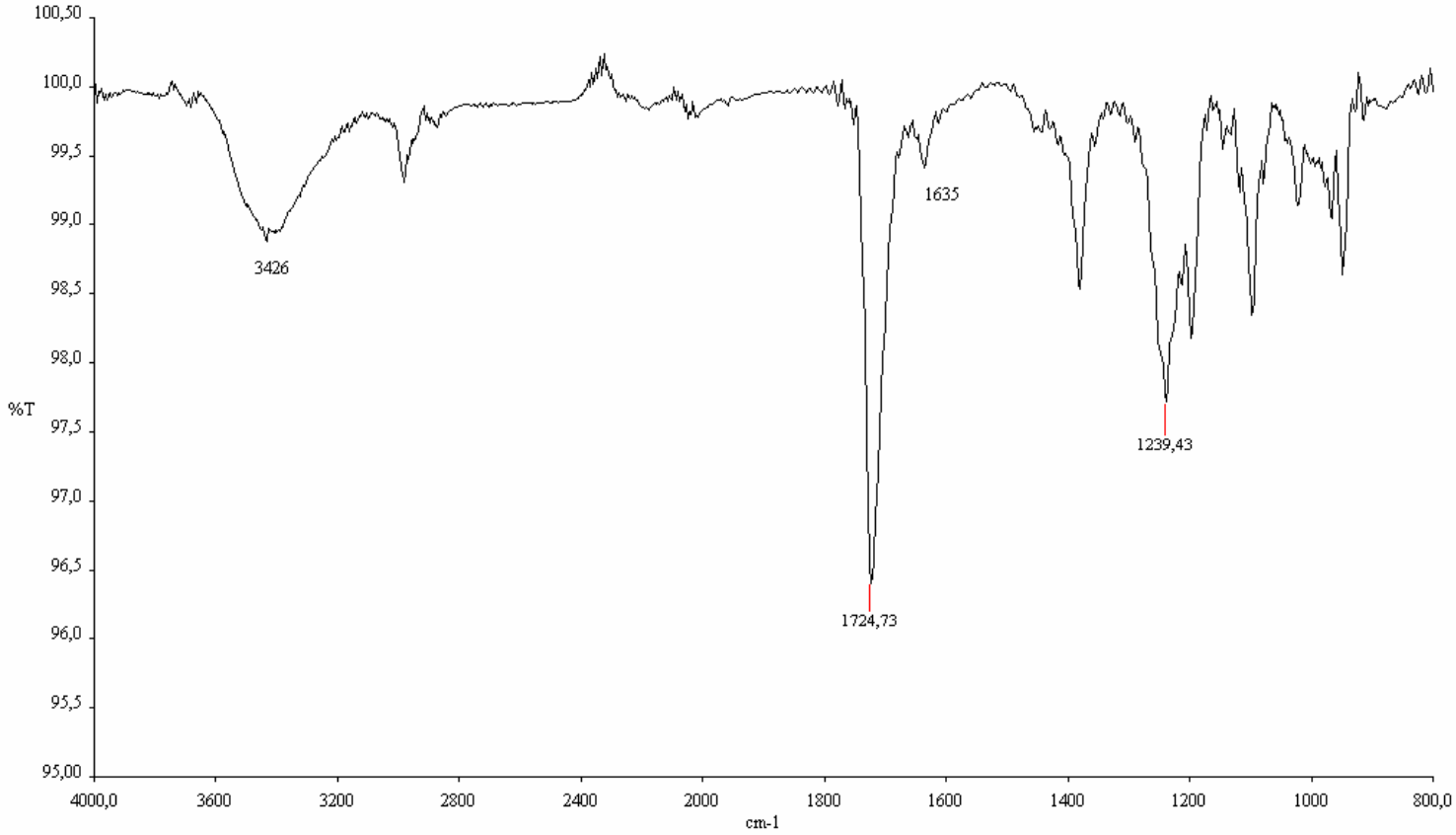

Figure 5.8.43. IR spectrum of stagonolide H, isolated from S. cirsii solid culture, recorded as neat

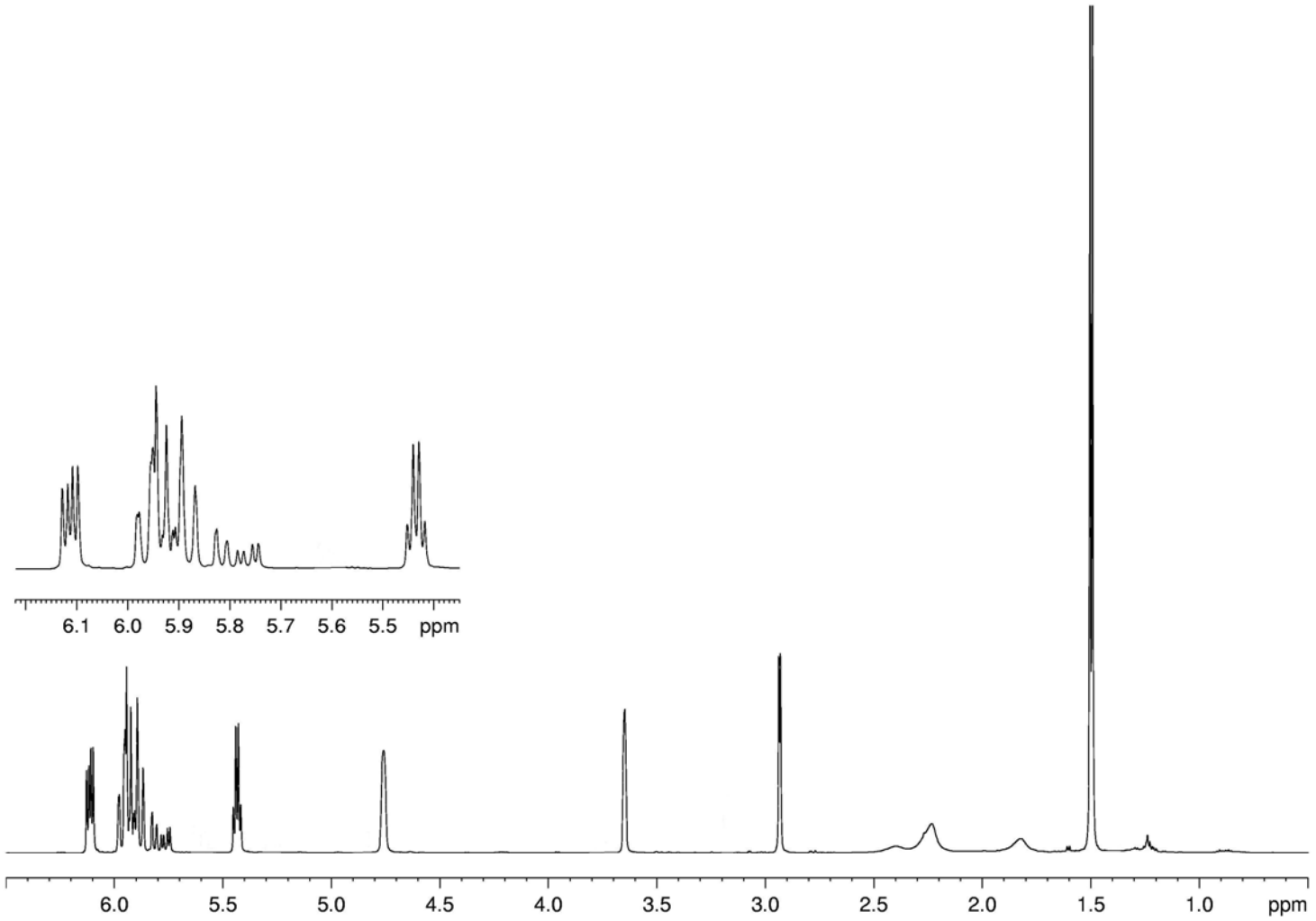

Figure 5.8.44. ^{1}H NMR spectrum of stagonolide H, isolated from *S. cirsii* solid culture, recorded at 600 MHz

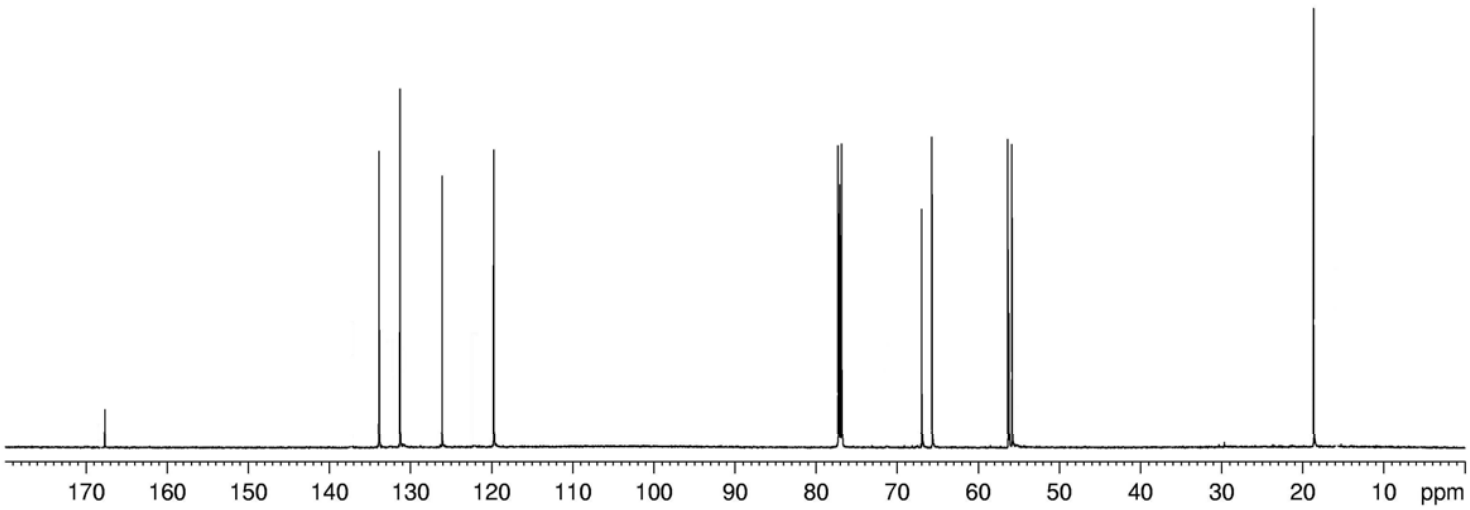

Figure 5.8.45. ^{13}C NMR spectrum of stagonolide H, isolated from *S. cirsii* solid culture, recorded at 600 MHz

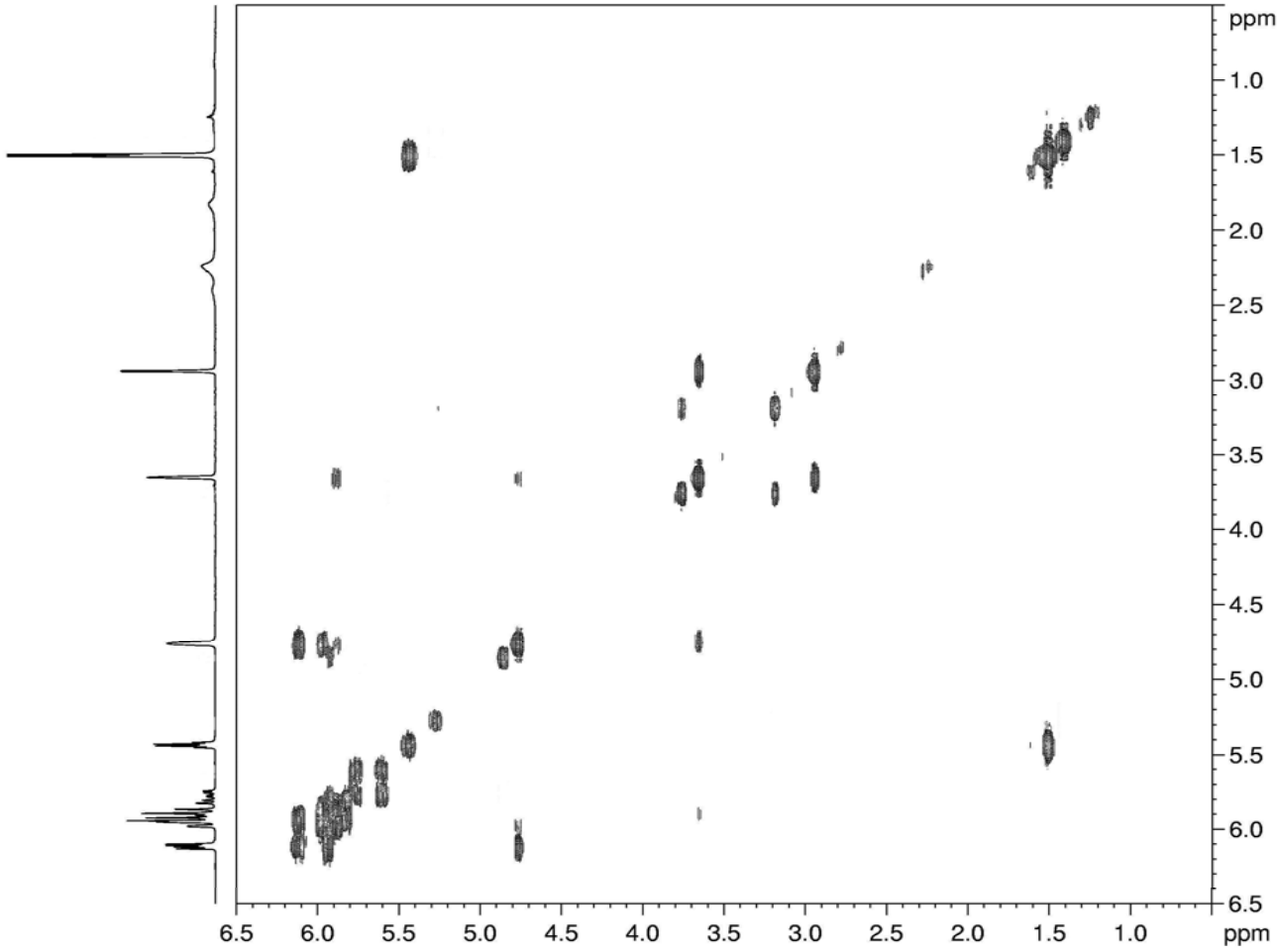

Figure 5.8.46. COSY spectrum of stagonolide H, isolated from *S. cirsii* solid culture, recorded at 600 MHz

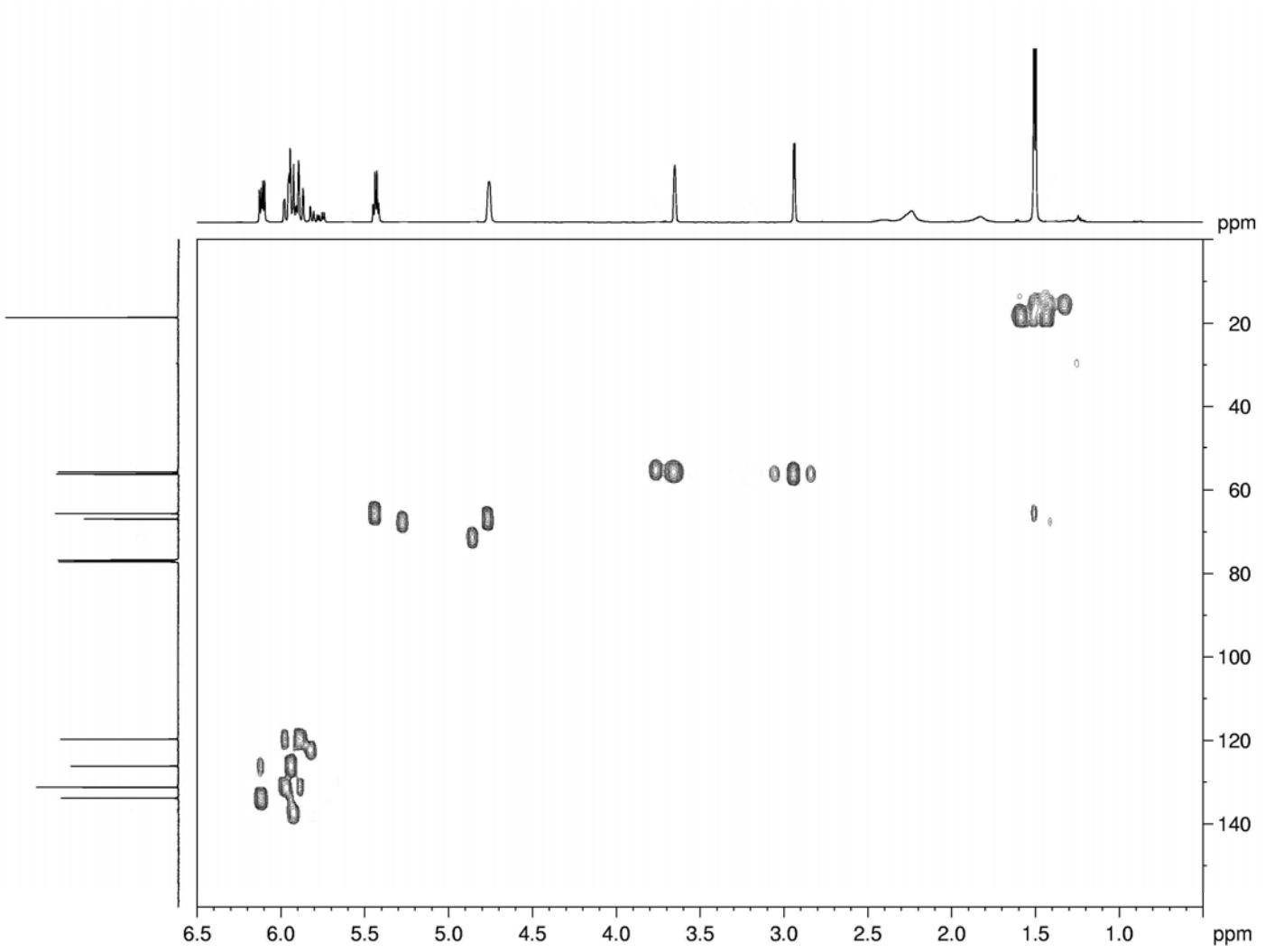

Figure 5.8.47. HSQC spectrum of stagonolide H, isolated from *S. cirsii* solid culture, recorded at 600 MHz

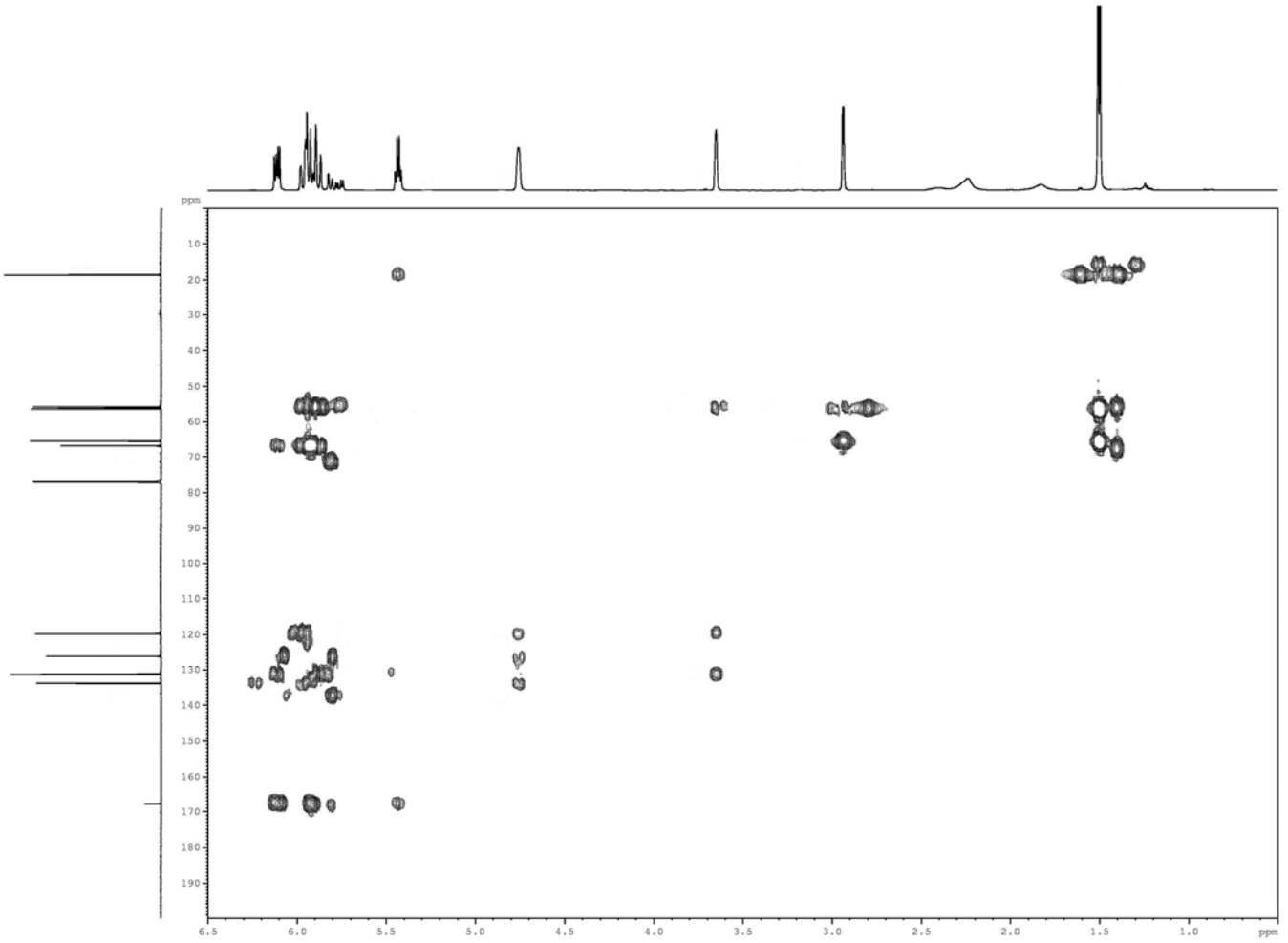

Figure 5.8.48. HMBC spectrum of stagonolide H, isolated from *S. cirsii* solid culture, recorded at 600 MHz

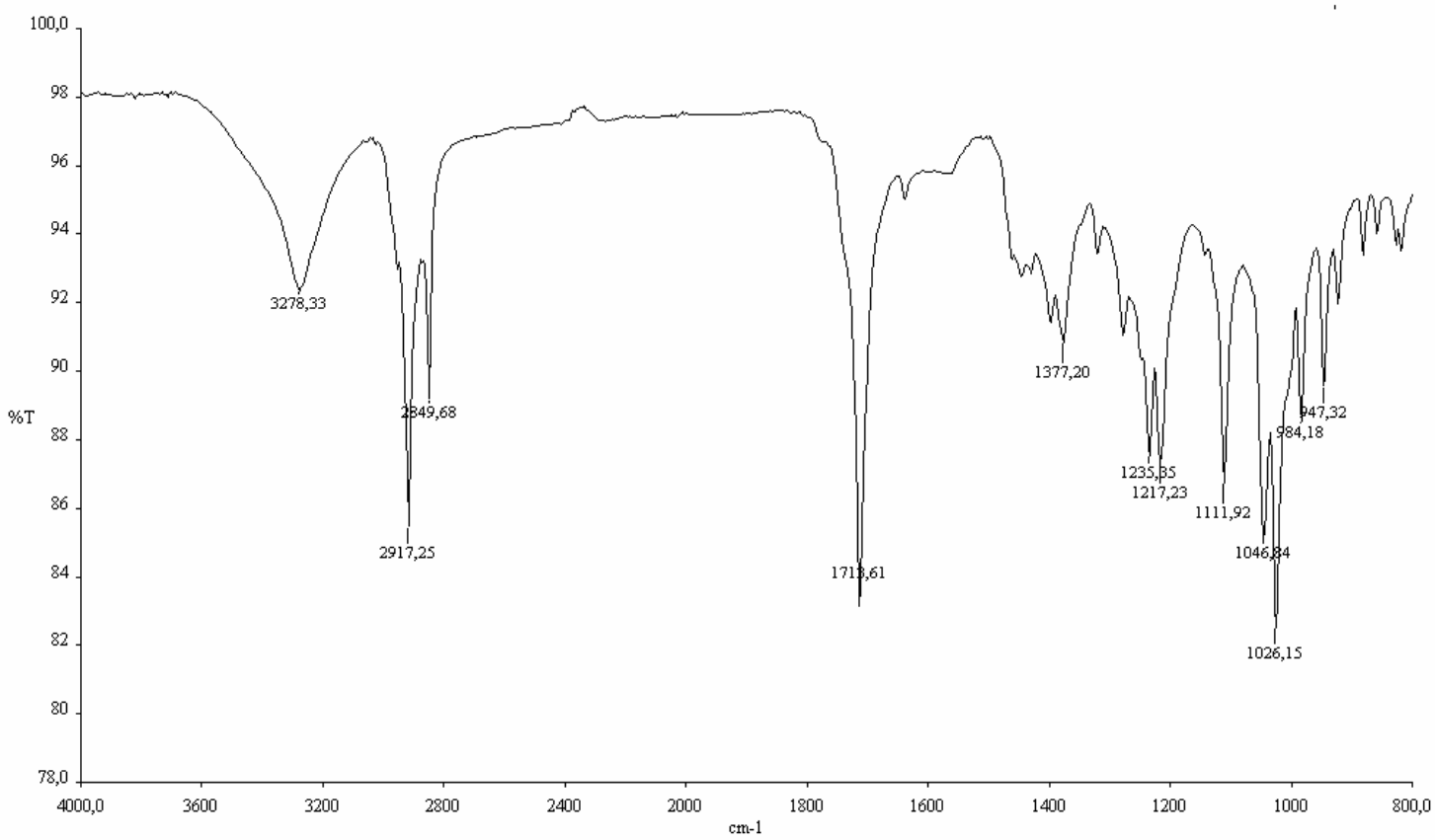

Figure 5.8.49. IR spectrum of stagonolide I, isolated from *S. cirsii* solid culture, recorded as neat

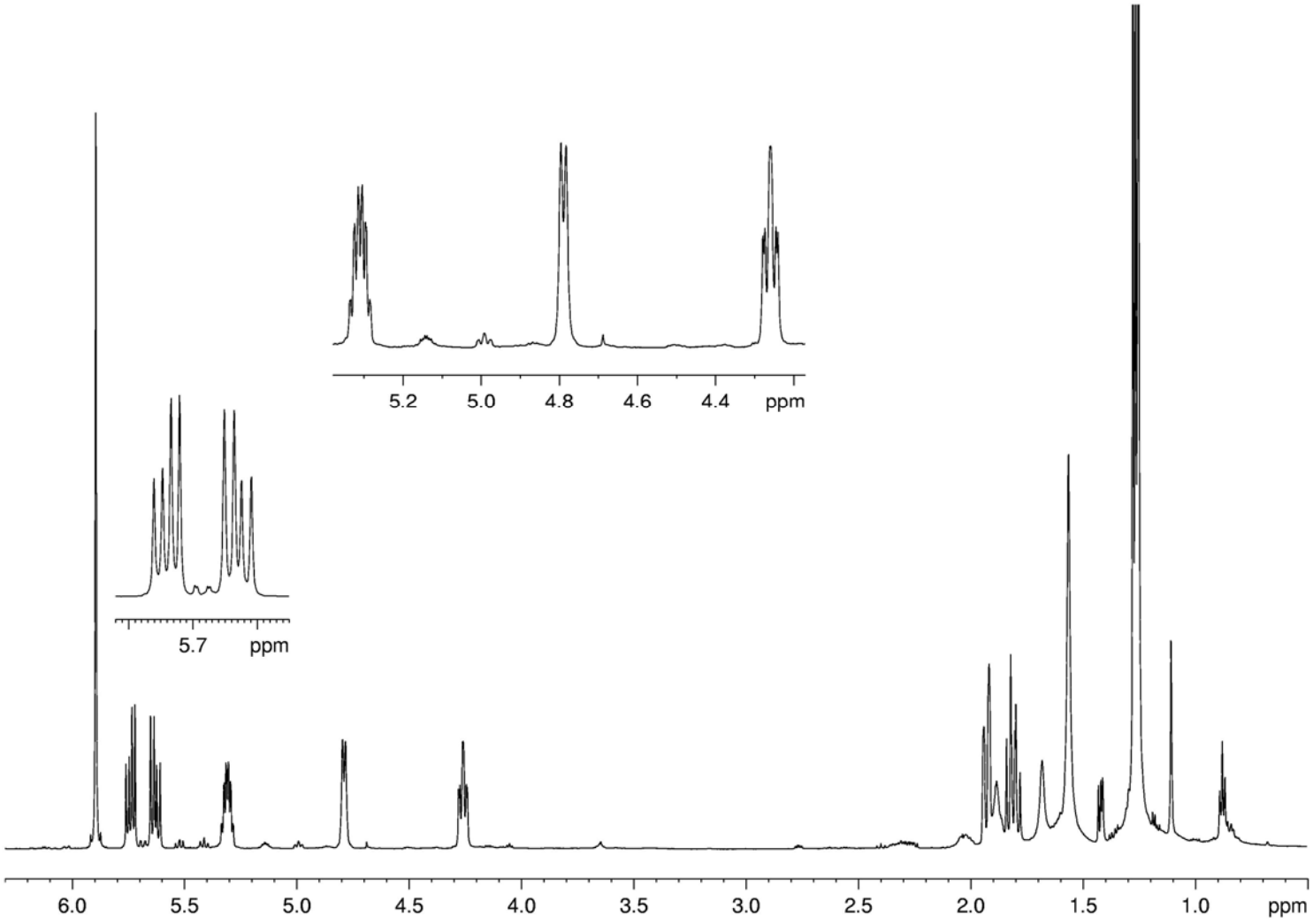

Figure 5.8.50. ^{1}H NMR spectrum of stagonolide I, isolated from *S. cirsii* solid culture, recorded at 600 MHz

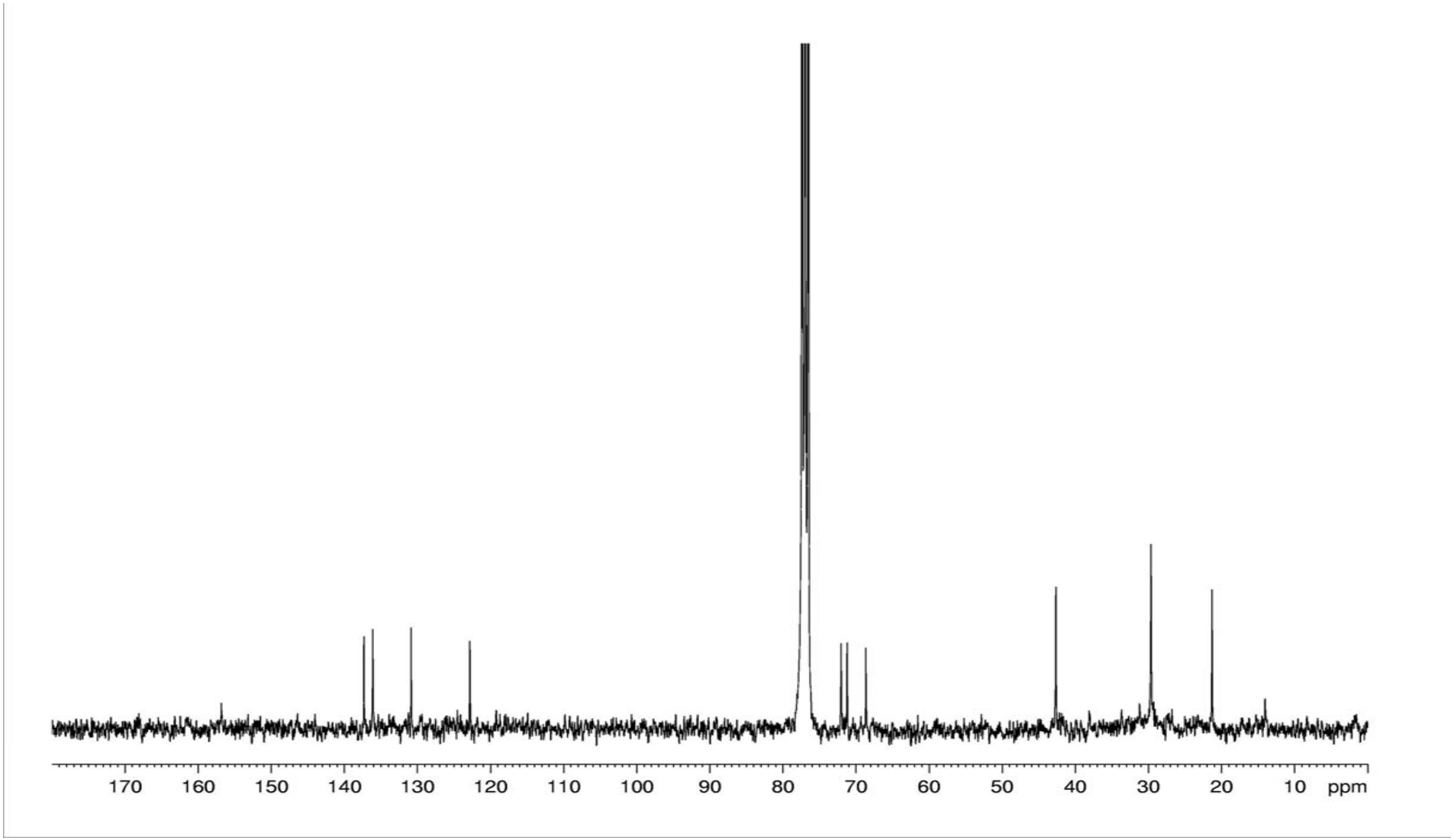

Figure 5.8.51. ^{13}C MR spectrum of stagonolide I, isolated from *S. cirsii* solid culture, recorded at 300 MHz

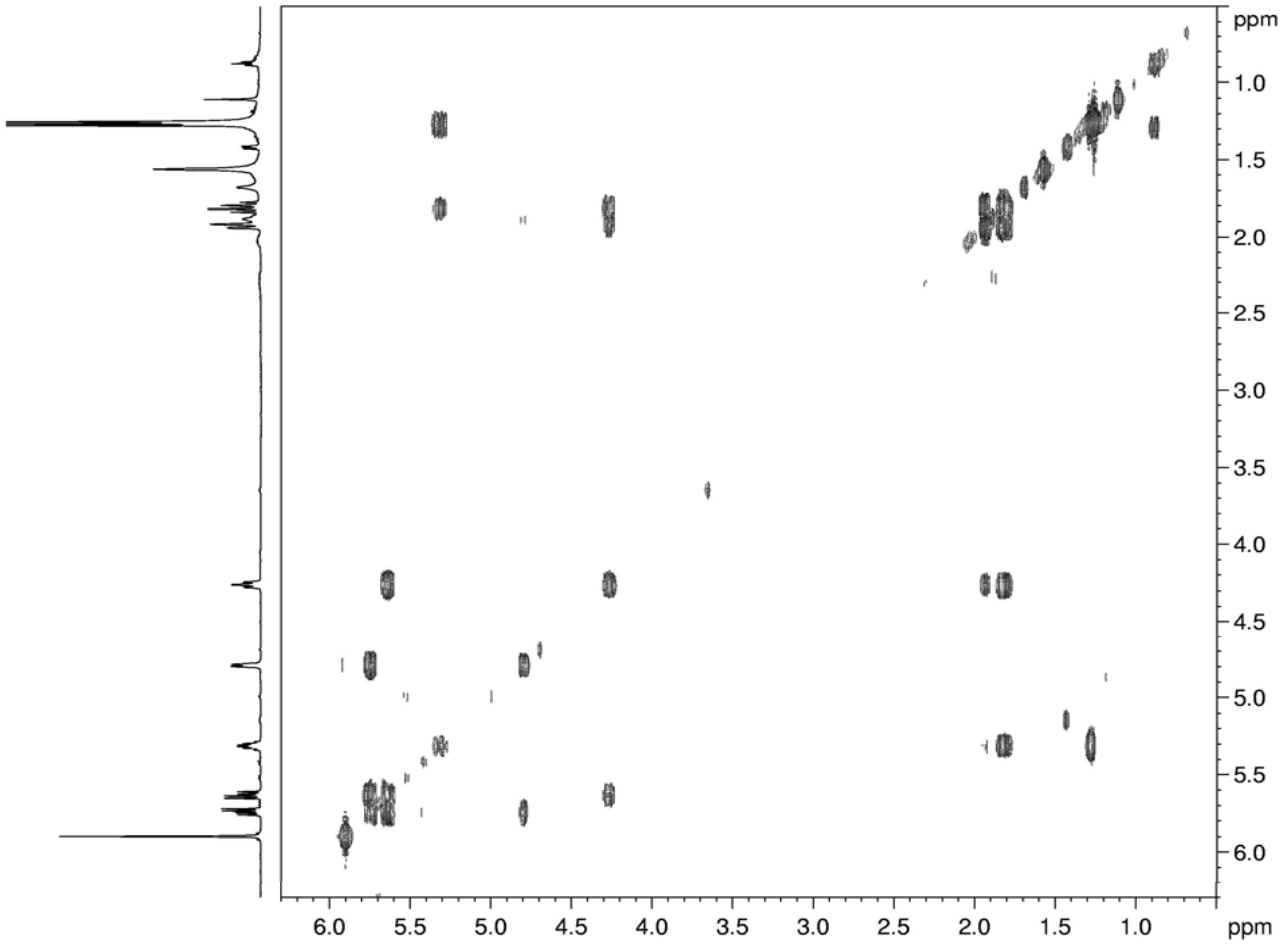

Figure 5.8.52. COSY spectrum of stagonolide I, isolated from *S. cirsii* solid culture, recorded at 600 MHz

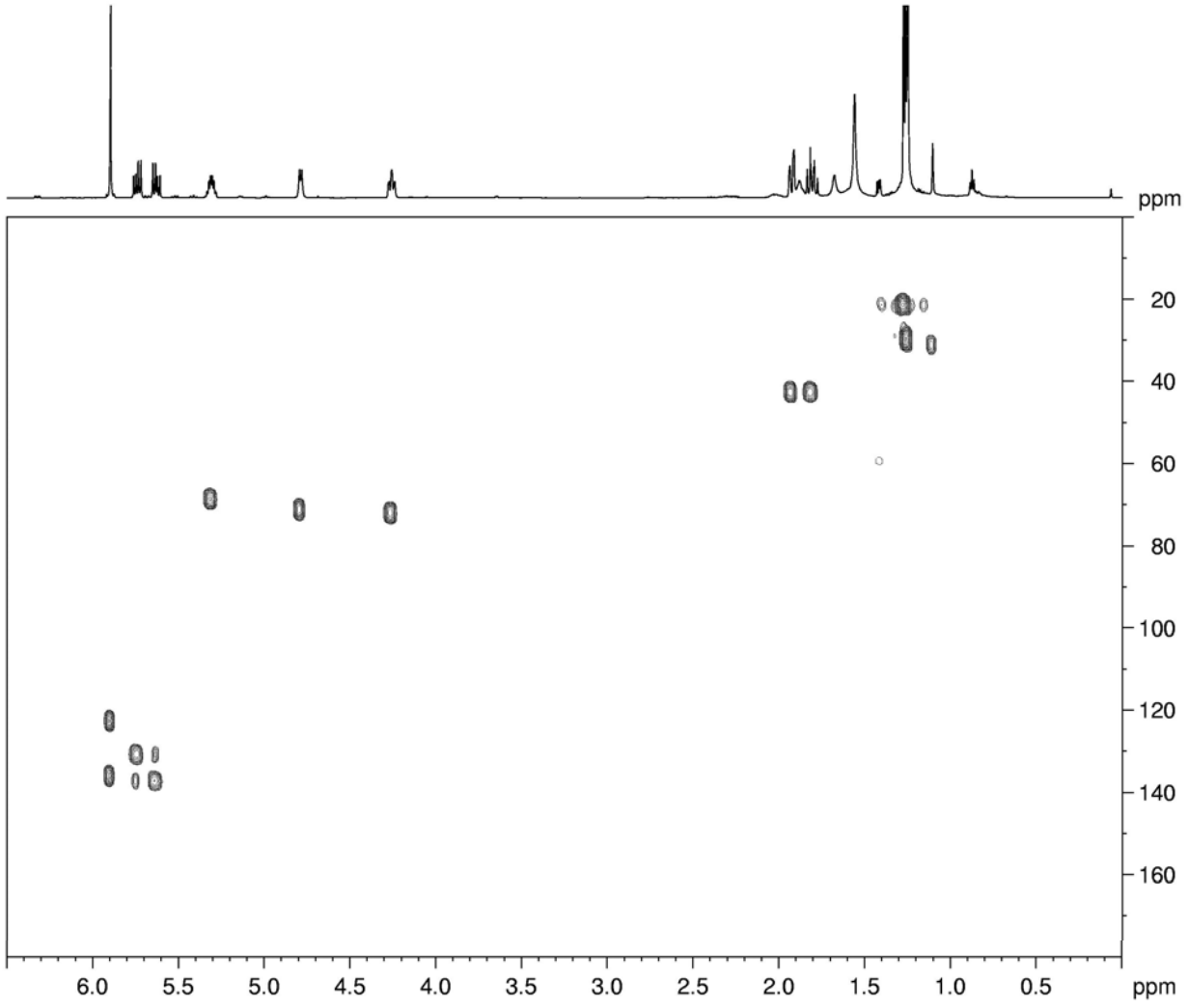

Figure 5.8.53. HSQC spectrum of stagonolide I, isolated from *S. cirsii* solid culture, recorded at 600 MHz

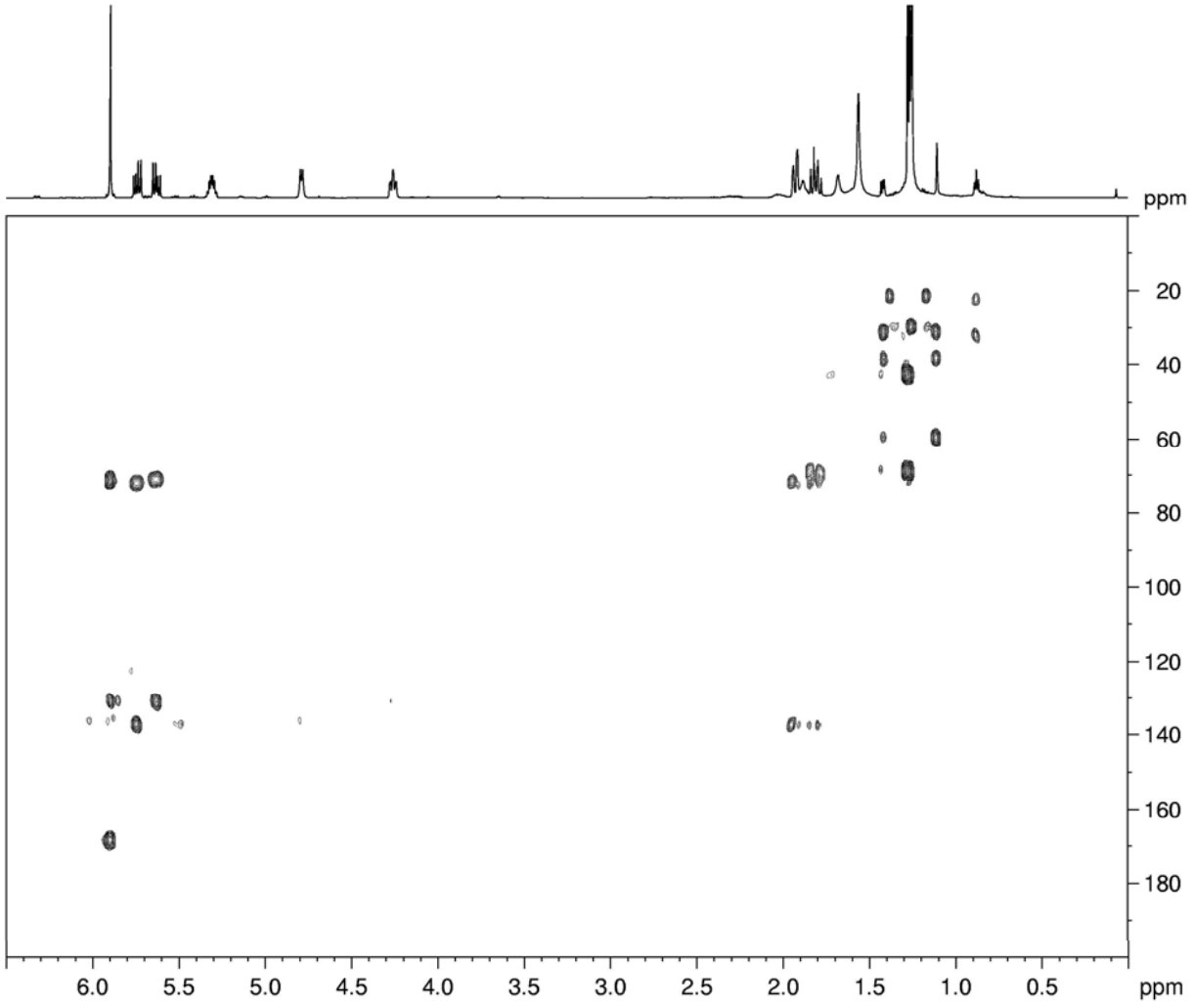

Figure 5.8.54. HMBC spectrum of stagonolide I, isolated from *S. cirsii* solid culture, recorded at 600 MHz

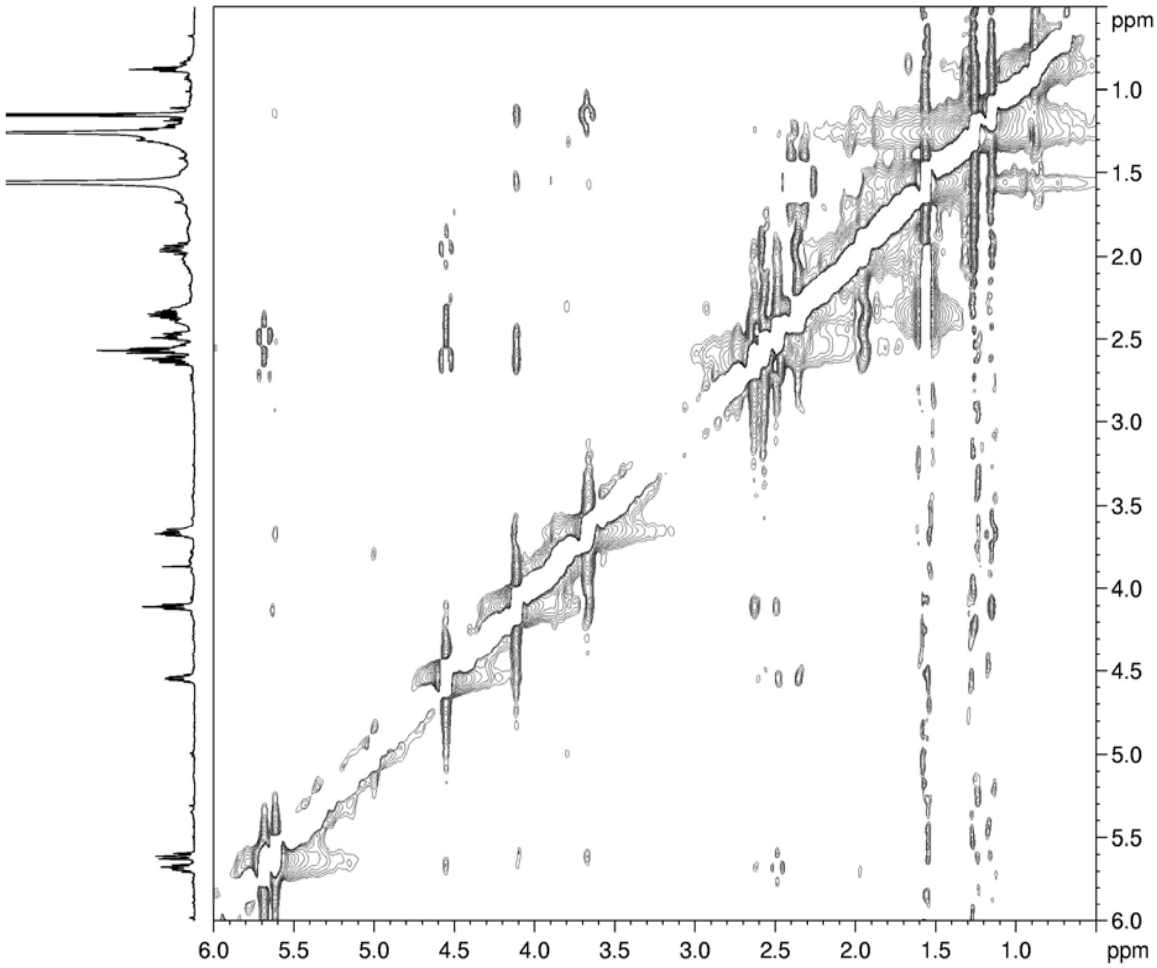

Figure 5.8.55. NOESY spectrum of stagonolide G, isolated from *S. cirsii* solid culture, recorded at 600 MHz

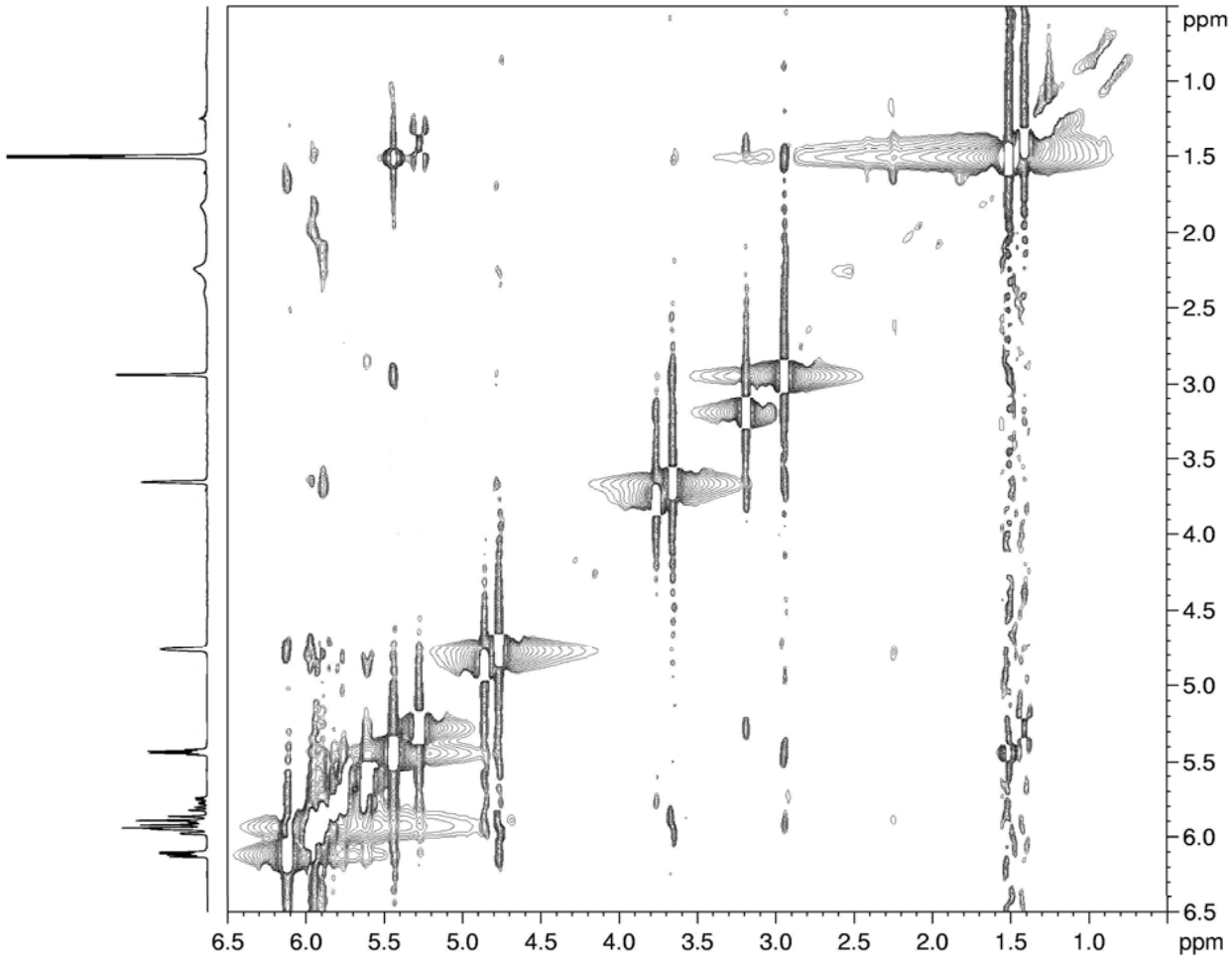

Figure 5.8.56. NOESY spectrum of stagonolide H, isolated from *S. cirsii* solid culture, recorded at 600 MHz

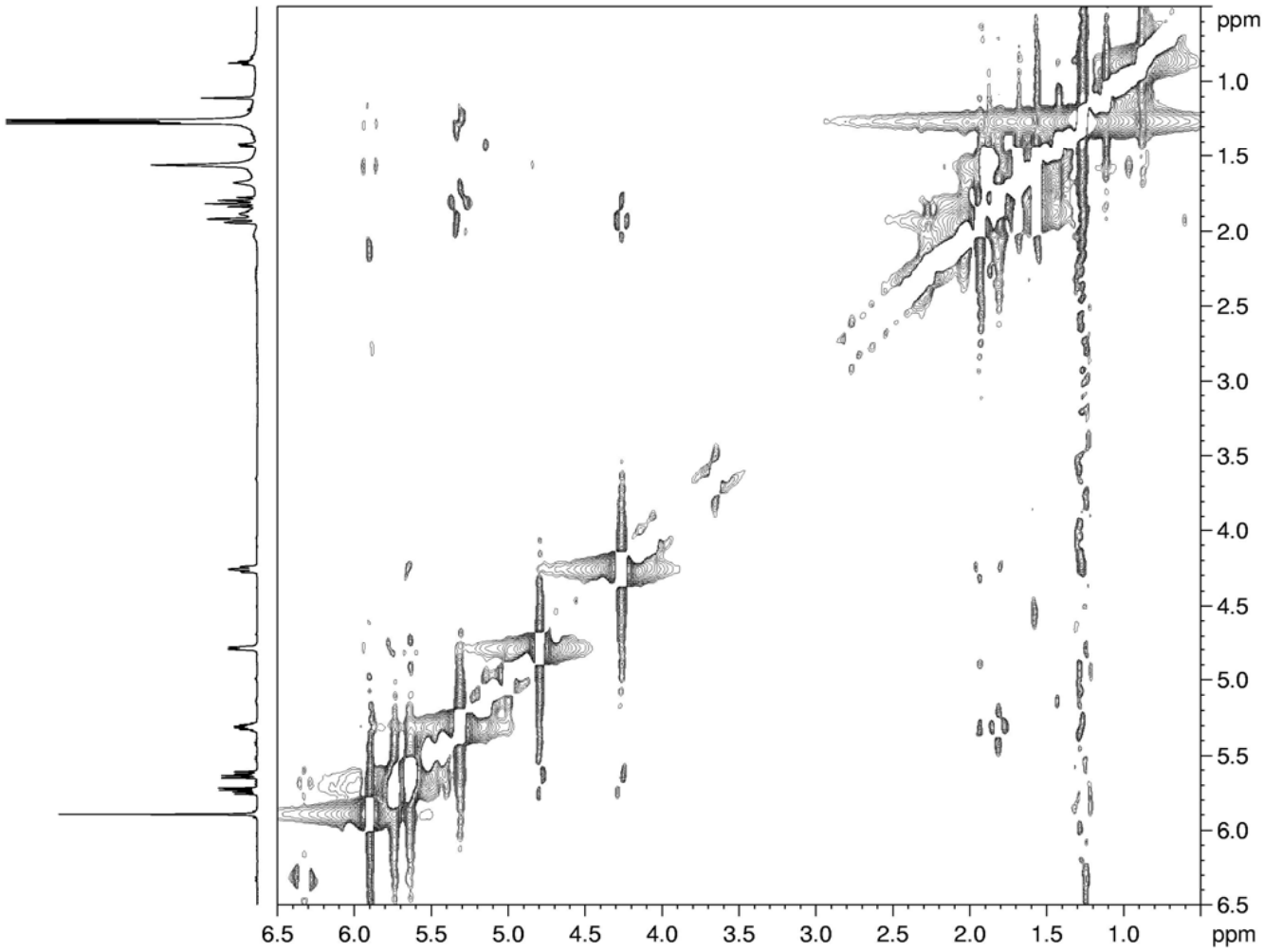

Figure 5.8.57. NOESY spectrum of stagonolide I, isolated from *S. cirsii* solid culture, recorded at 600 MH

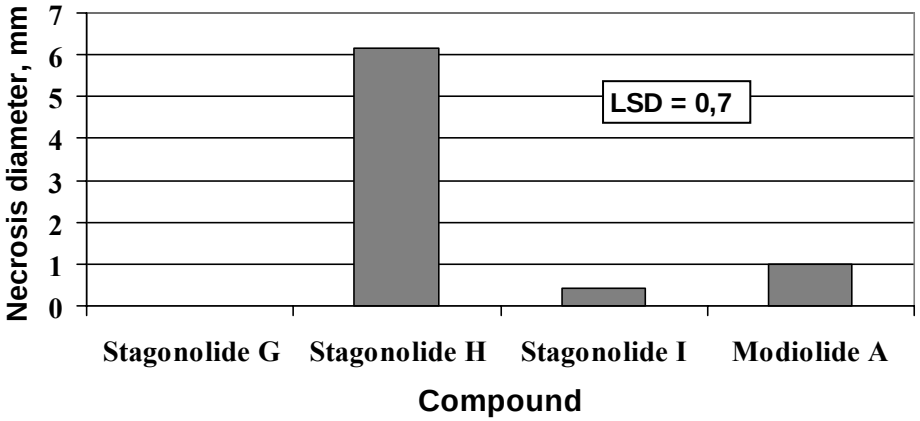

Figure 5.9.1. Phytotoxicity of nonenolides at 1 mg/ml in the *Cirsium arvense* leaf disk-puncture bioassay (48 hours post application)

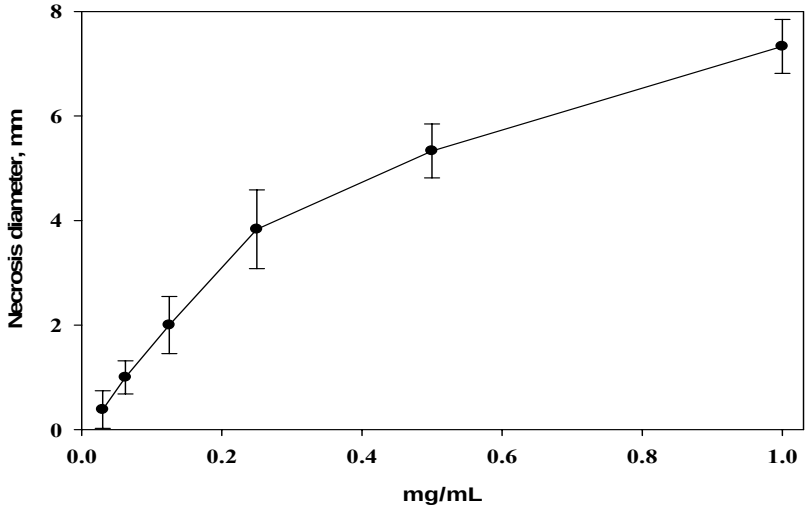

Figure 5.9.2. Dose-response relationship for stagonolide H by the *C. arvense* leaf disc-puncture bioassay (48 hours post application). Bars indicate standard deviation

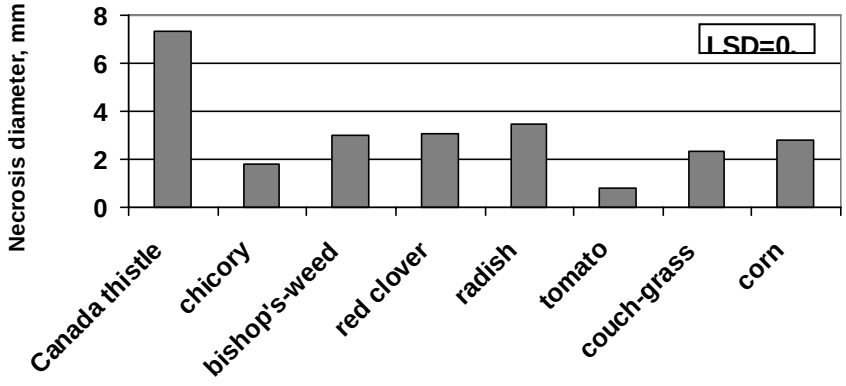

Figure 5.9.3. Effect of stagonolide H at 1 mg/ml on a range of various plant species using a leaf disc-puncture assay (72 hours post application)

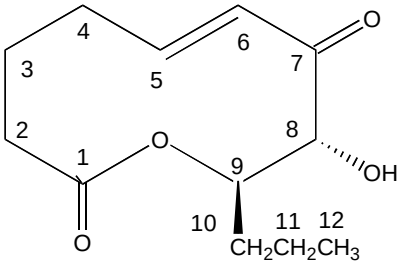

34

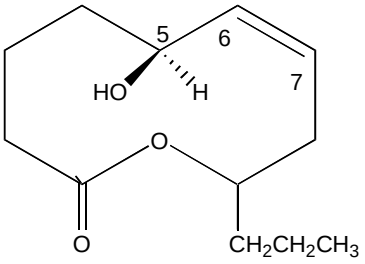

1

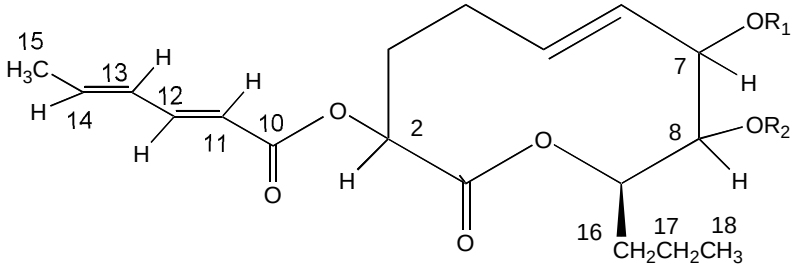

6 $R_1=R_2=H$

71 $R_1=Ac$ $R_2=Ac$

72 $R_1+R_2=-C(Me)_2-$

Figure 5.10.1. Structure of nonenolides and some their derivatives used in the structure-activity relationship study

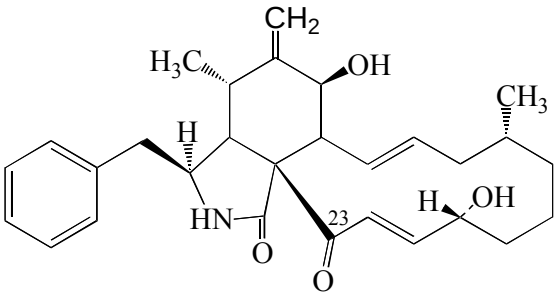

30

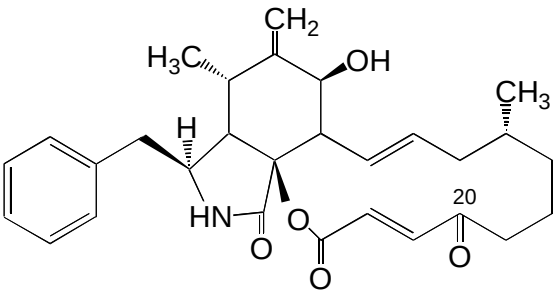

25

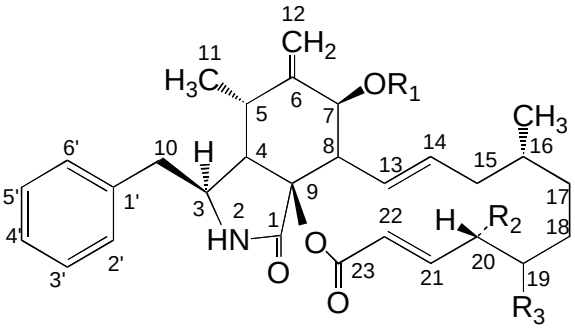

26 $R_1=R_3=H,\ R_2=OH$

27 $R_1=Ac,\ R_2=OH,\ R_3=H$

74 $R_1=Ac,\ R_2=OAc,\ R_3=H$

21 $R_1=R_2=H,\ R_3=OH$

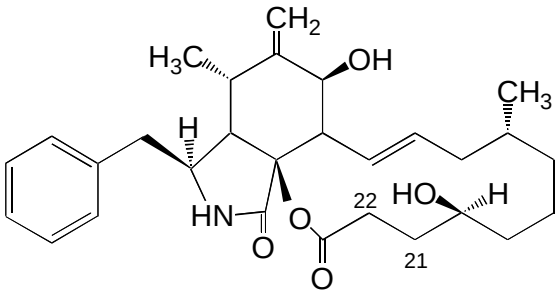

73

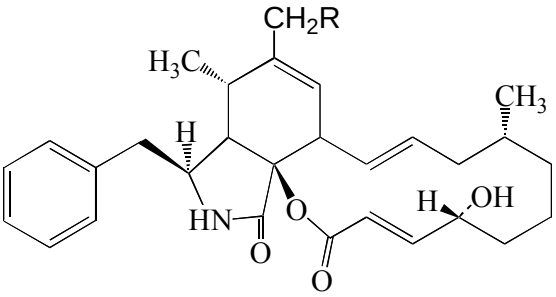

29 R=H

20 R=OH

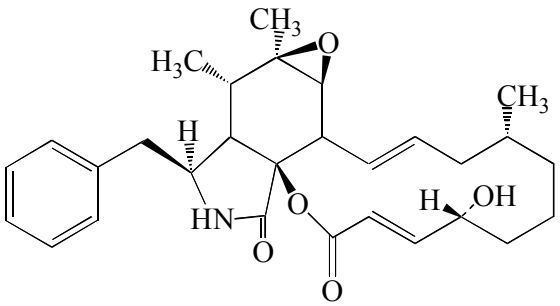

28

Figure 5.10.2. Structure of cytochalasins and some their derivatives used in the structure-activity relationship study

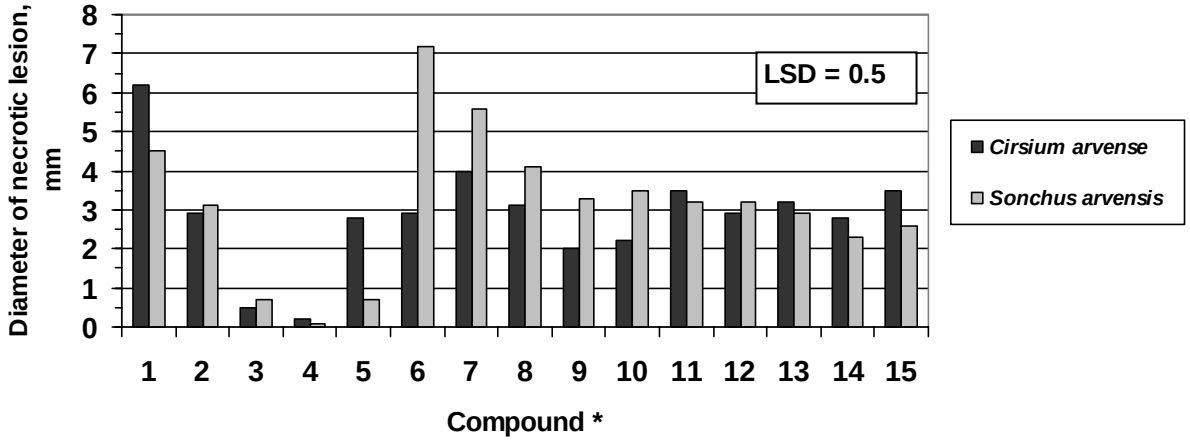

Figure 5.10.3. Effect of different toxins on *C. arvense* and *S. arvensis* using a leaf disc-puncture assay

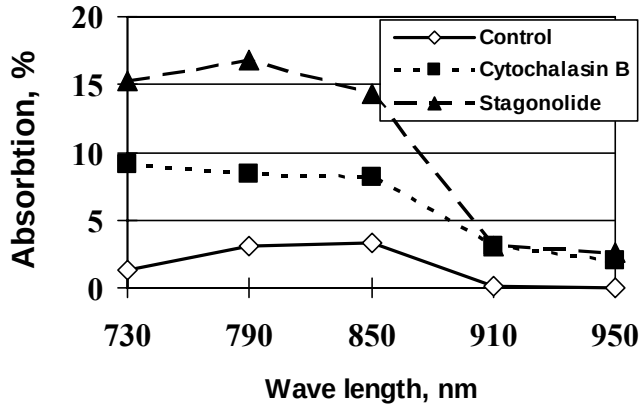

Figure 5.10. 4. Effect of toxins on light absorption by leaves of *C. arvense* in the range of 730-950 nm

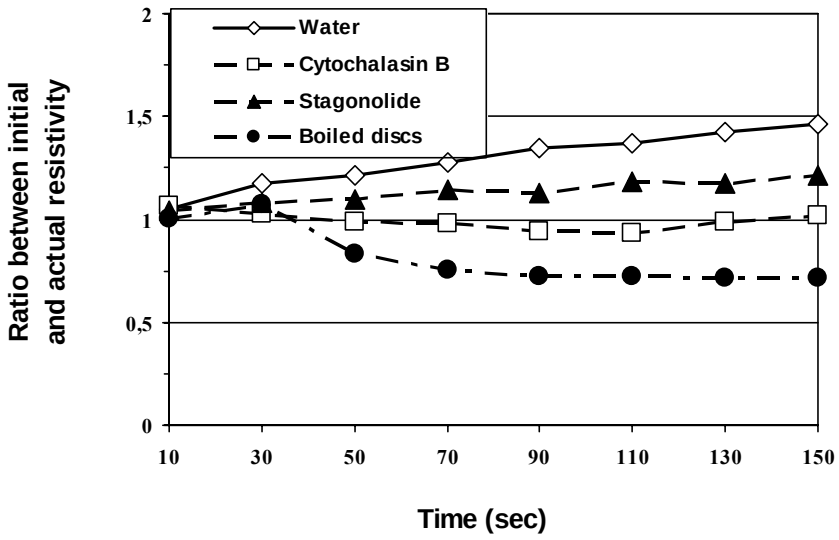

Figure 5.10.5. Effect of cytochalasin B and stagonolide on *in vivo* resistivity of *C. arvense* leaves

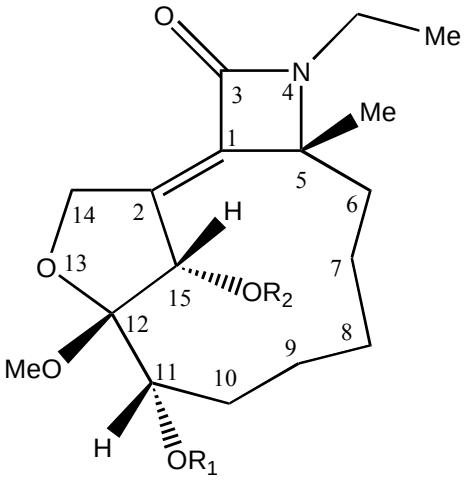

54 $R_1=R_2=H$
58 $R_1=H$, $R_2=Ac$
59 $R_1=R_2=Ac$
60 $R_1=H$, $R_2=S$-MTPA
61 $R_1=H$, $R_2=R$-MTPA

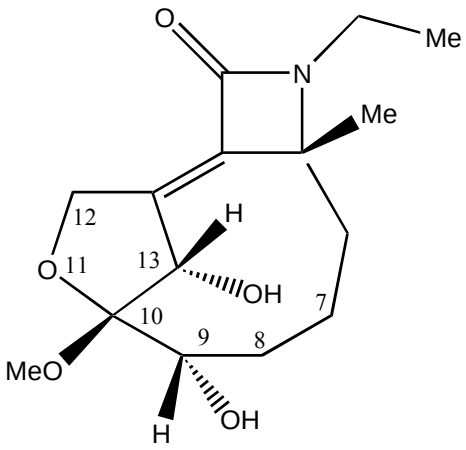

55

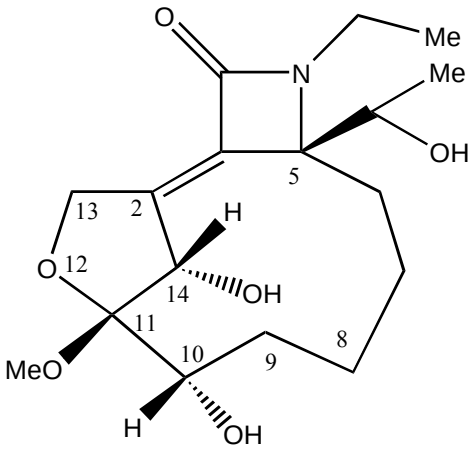

56

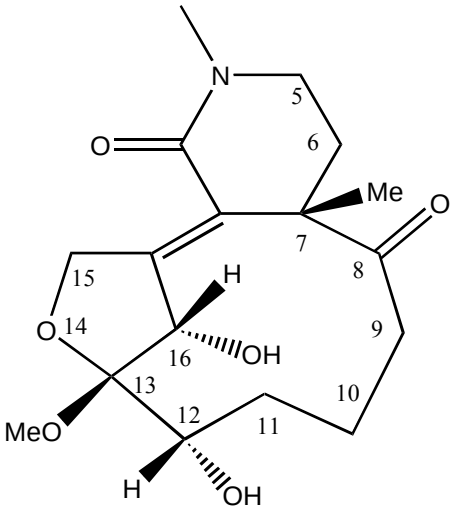

57

Figure 5.11.1. Structures of phyllostictines A-D isolated from *P.cirsii* culture filtrates

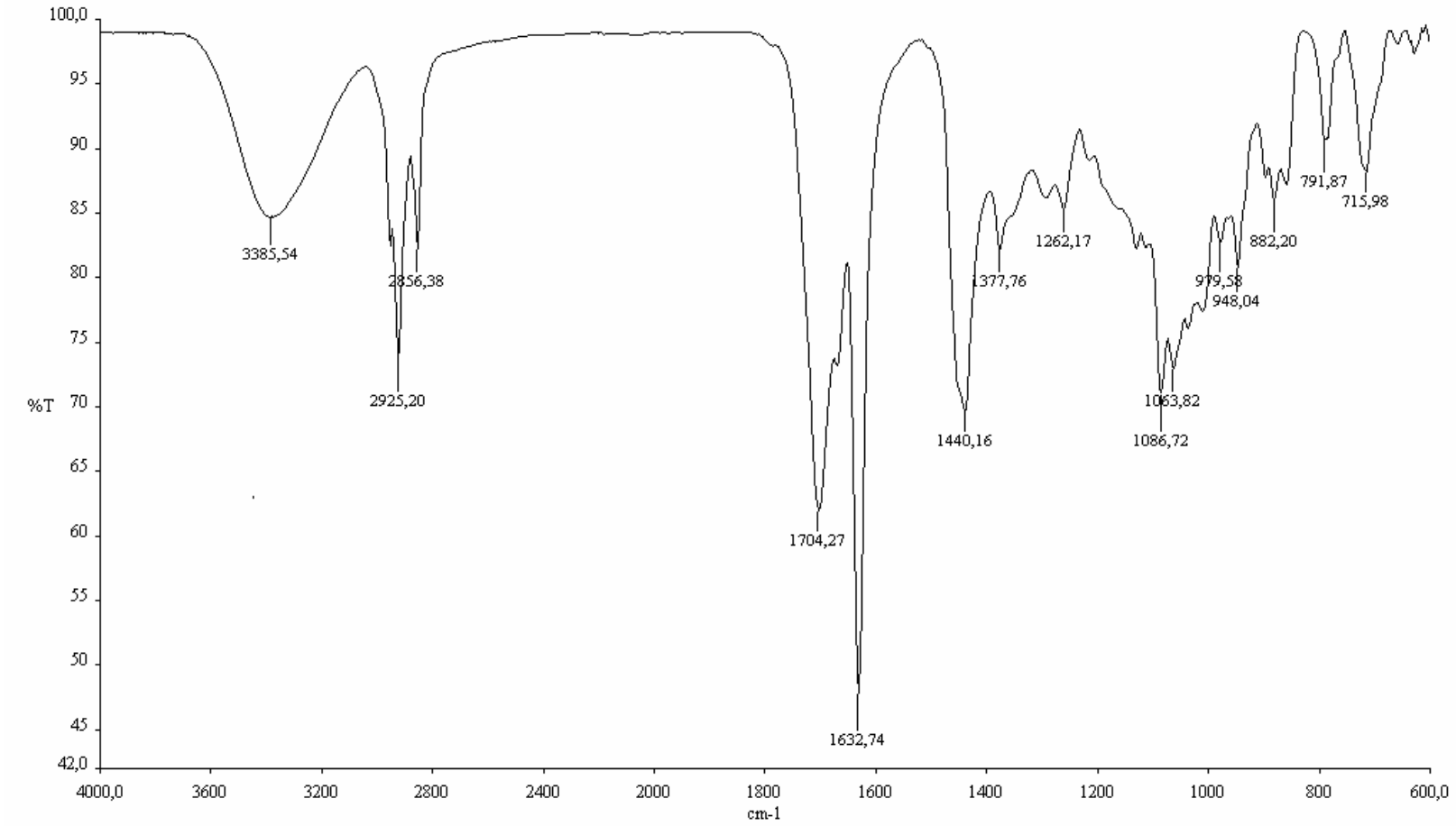

Figure 5.11.2. IR spectrum of phyllostictine A, isolated from *P. cirsii* culture filtrates, recorded as neat

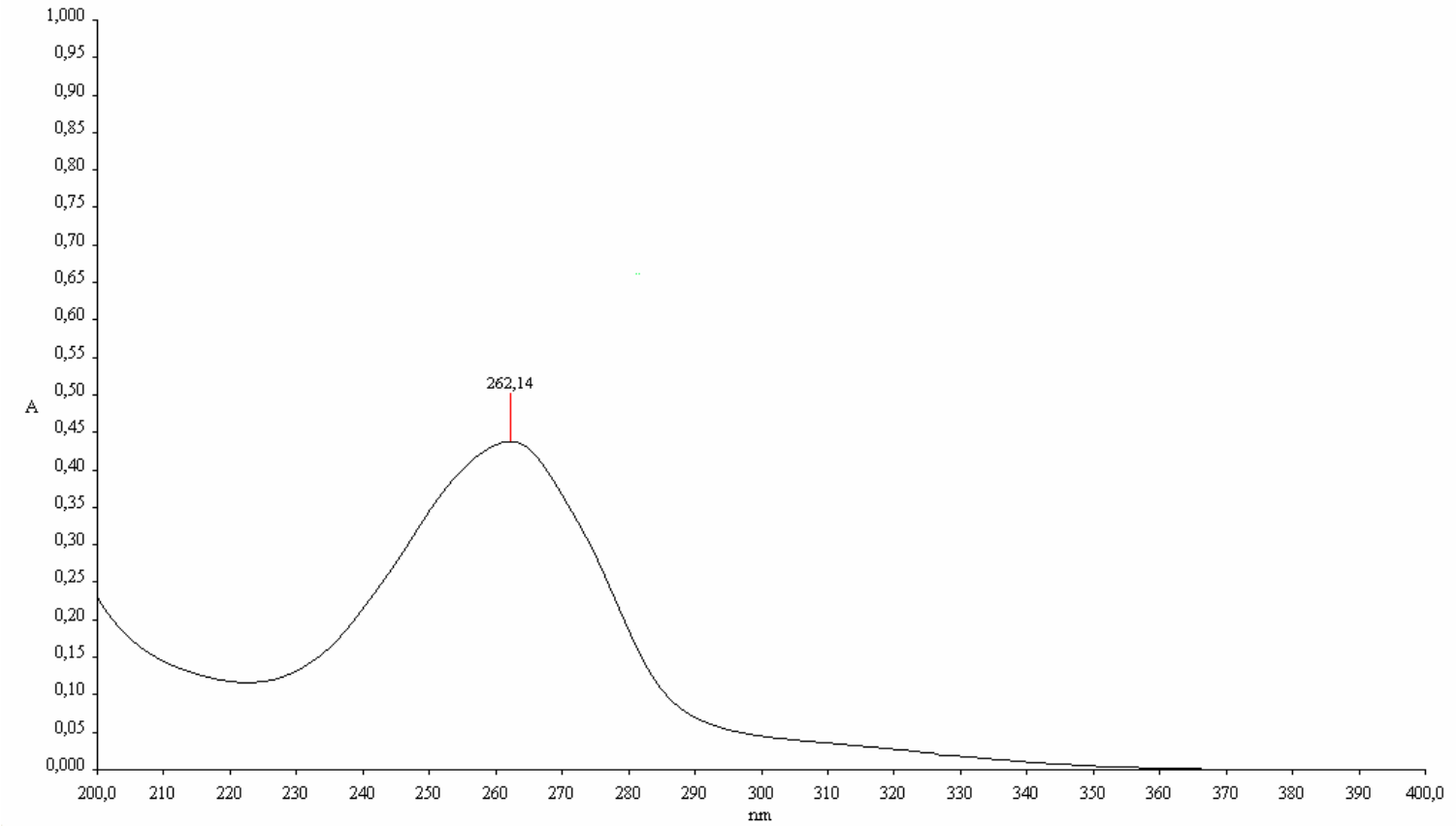

Figure 5.11.3. UV spectrum of phyllostictine A, isolated from *P. cirsii* culture filtrates, recorded in MeCN solution

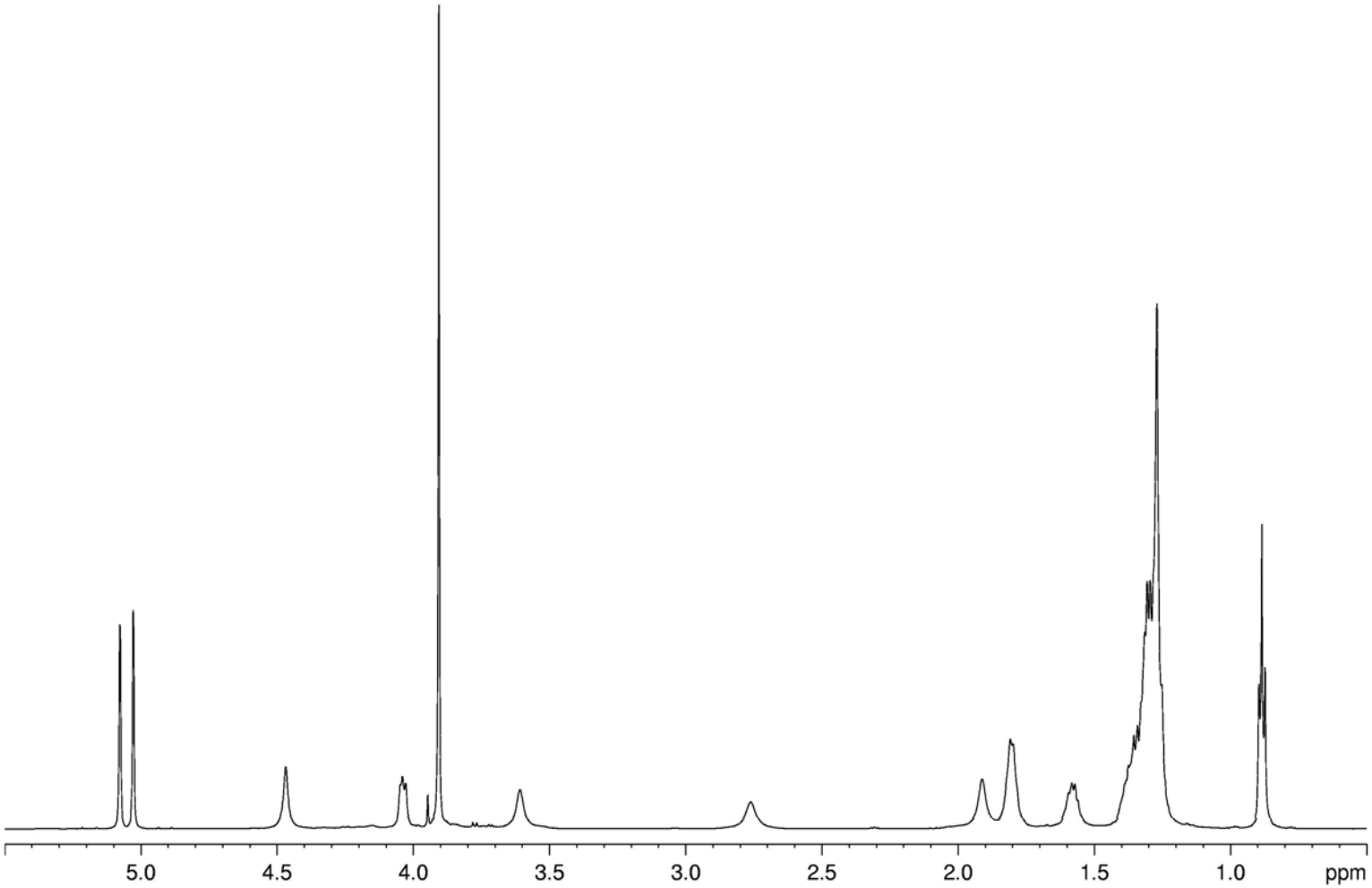

Figure 5.11.4. ^{1}H NMR spectrum of phyllostictine A, isolated from *P. cirsii* culture filtrates, recorded at 600 MHz

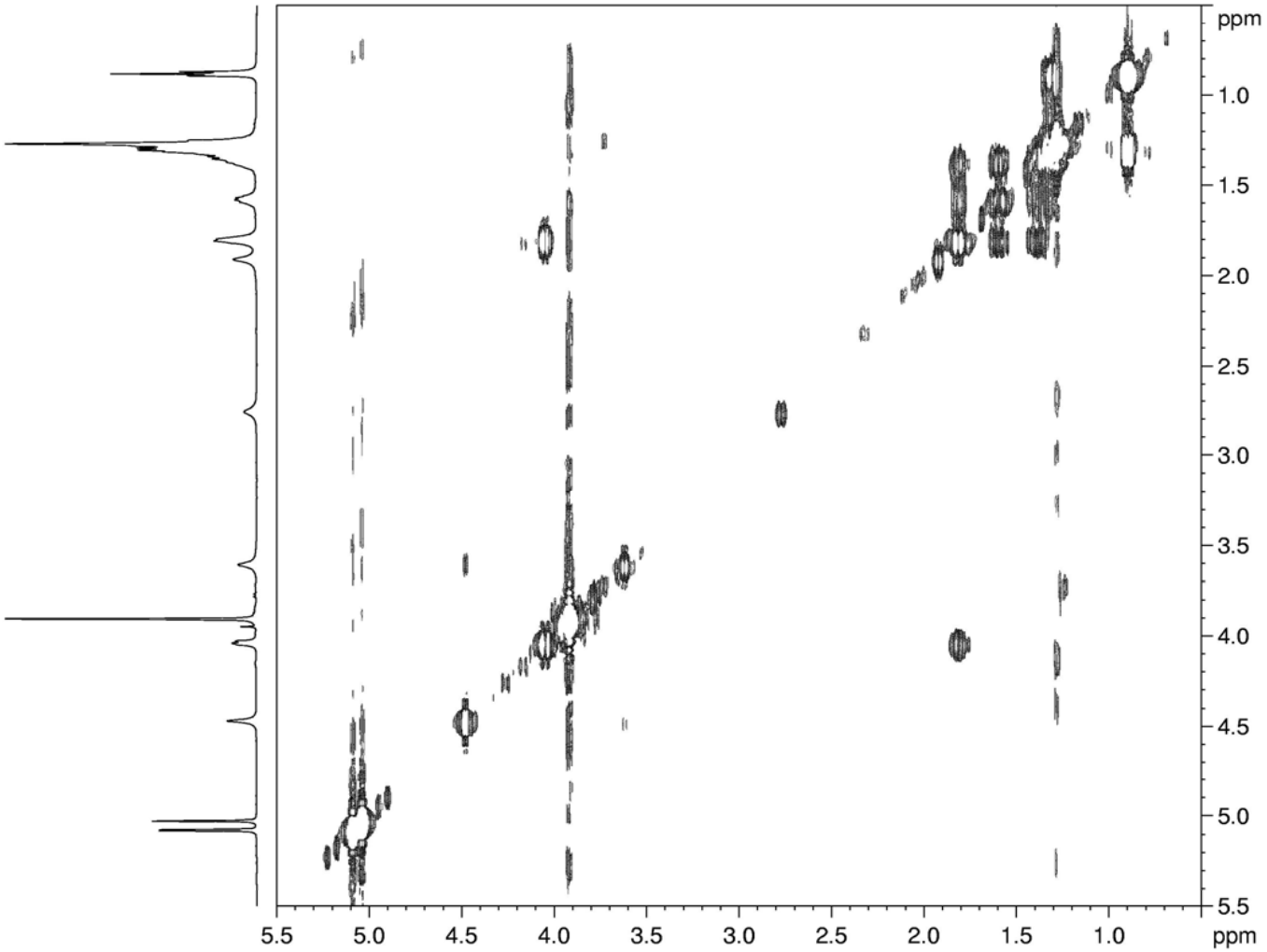

Figure 5.11.5. COSY spectrum of phyllostictine A, isolated from *P. cirsii* culture filtrates, recorded at 600 MHz

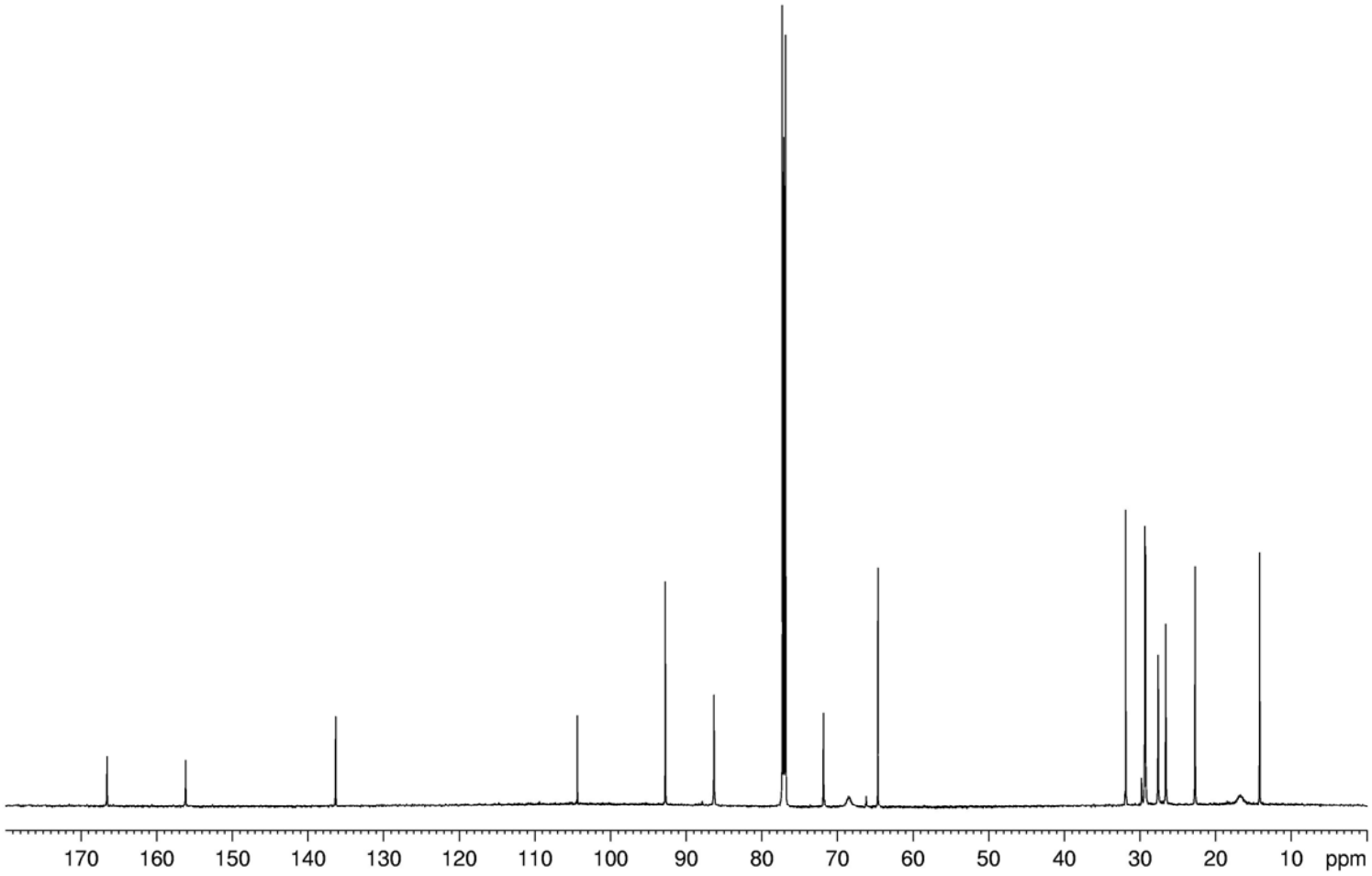

Figure 5.11.6. ^{13}C NMR spectrum of phyllostictine A, isolated from *P. cirsii* culture filtrates, recorded at 600 MHz

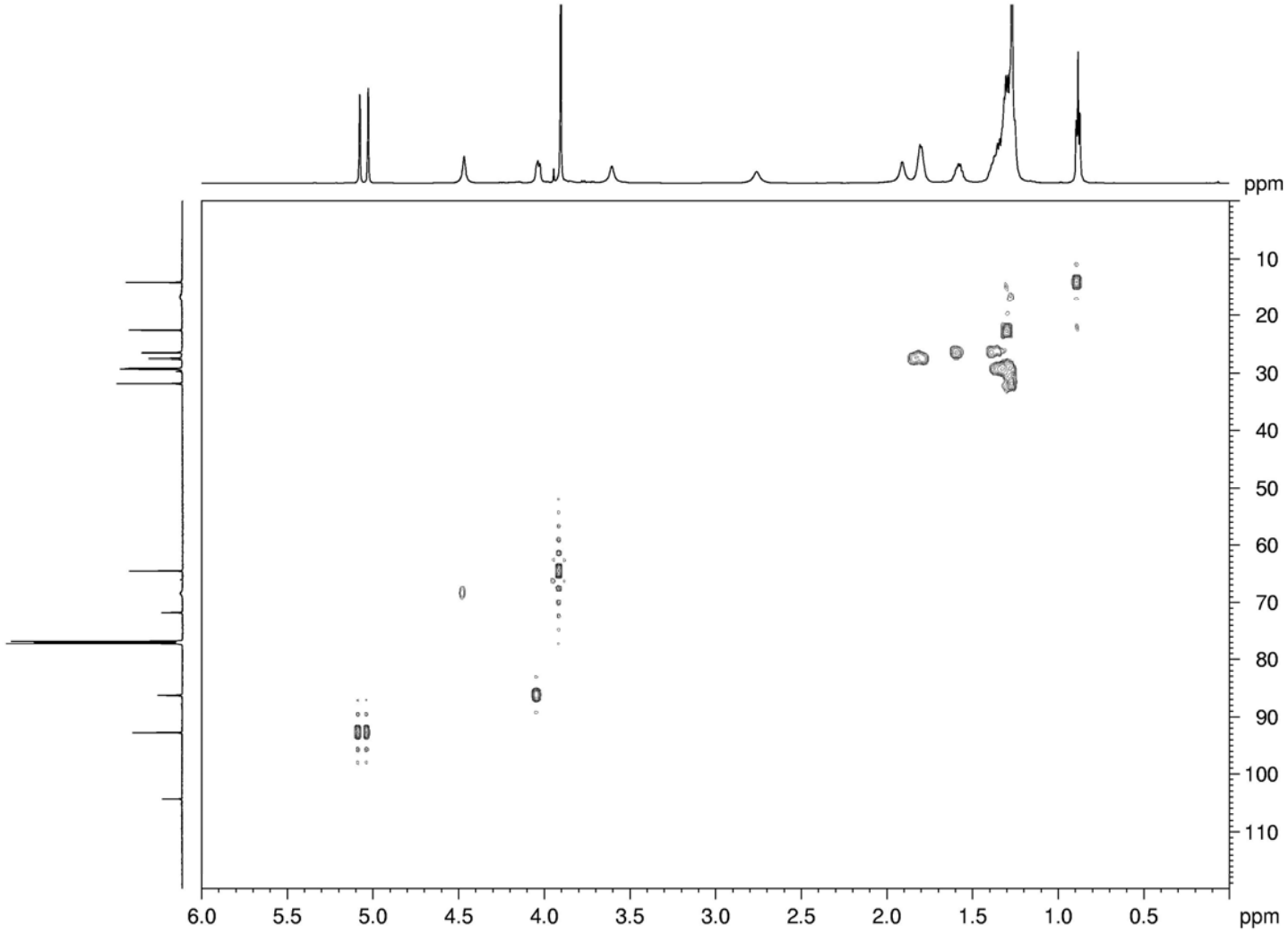

Figure 5.11.7. HSQC spectrum of phyllostictine A, isolated from *P. cirsii* culture filtrates, recorded at 600 MHz

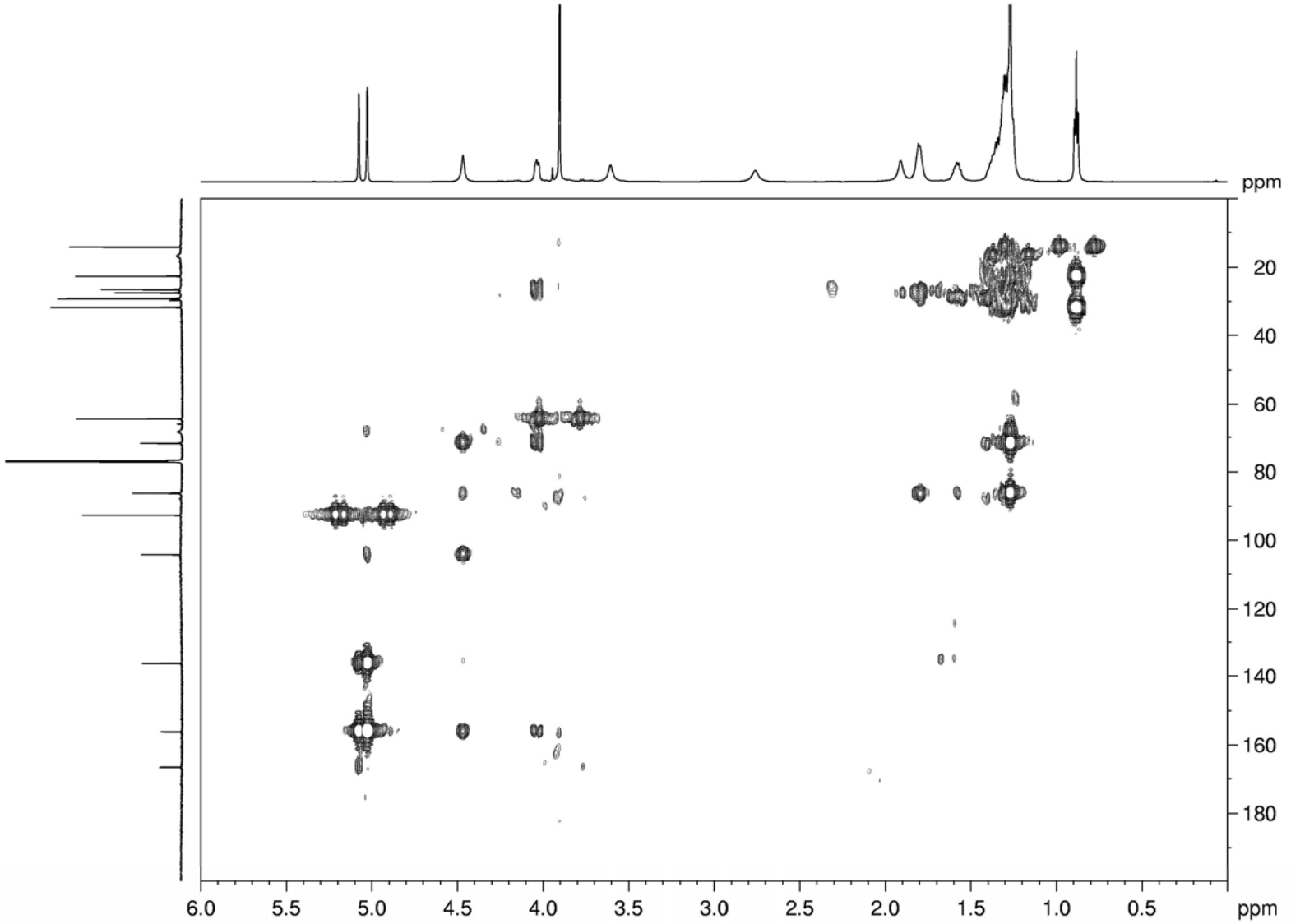

Figure 5.11.8. HMBC spectrum of phyllostictine A, isolated from *P. cirsii* culture filtrates, recorded at 600 MHz

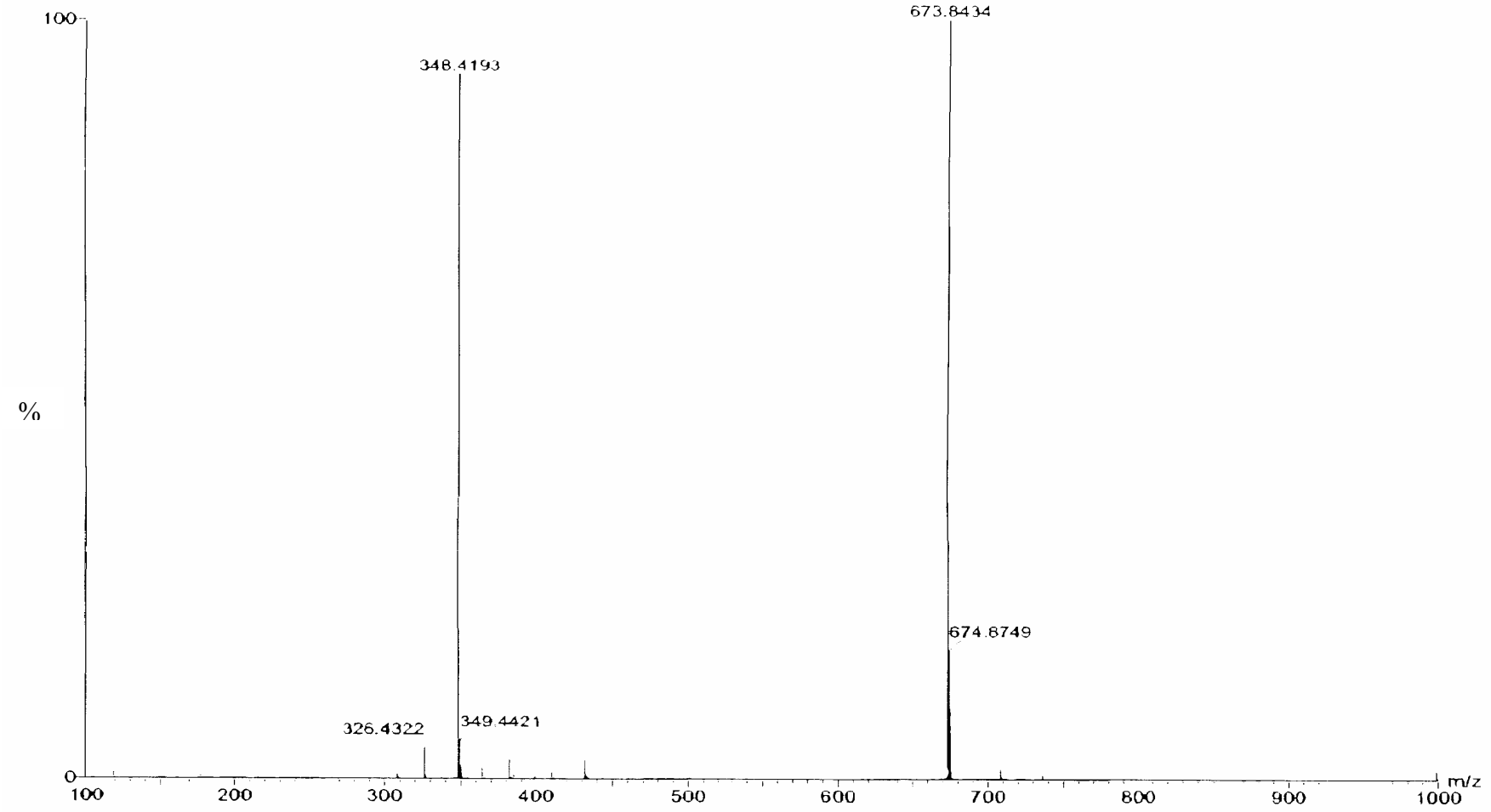

Figure 5.11.9. ESI MS spectrum of phyllostictine A, isolated from *P. cirsii* culture filtrates, recorded in positive modality

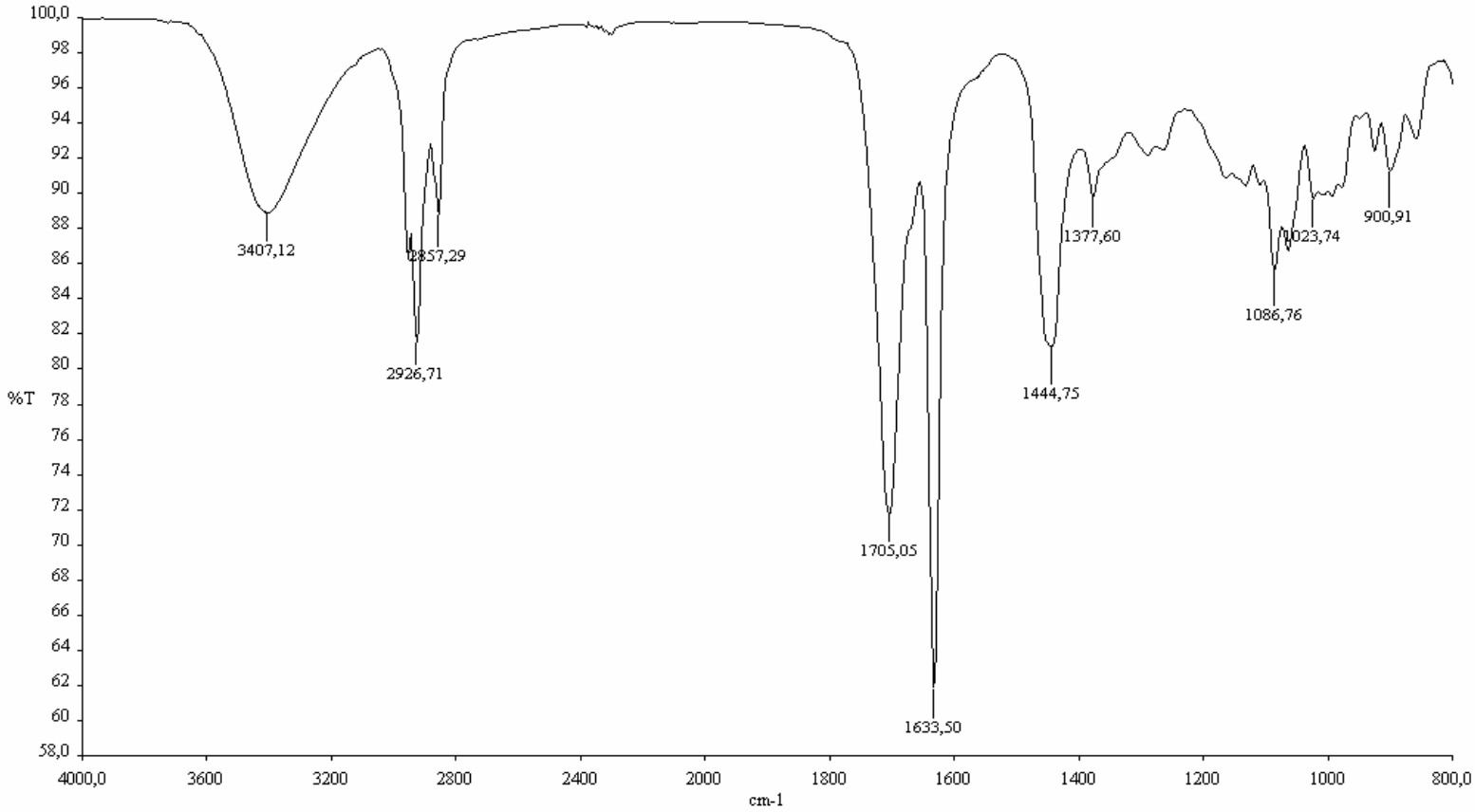

Figure 5.11.10. IR spectrum of phyllostictine B, isolated from *P. cirsii* culture filtrates, recorded as neat

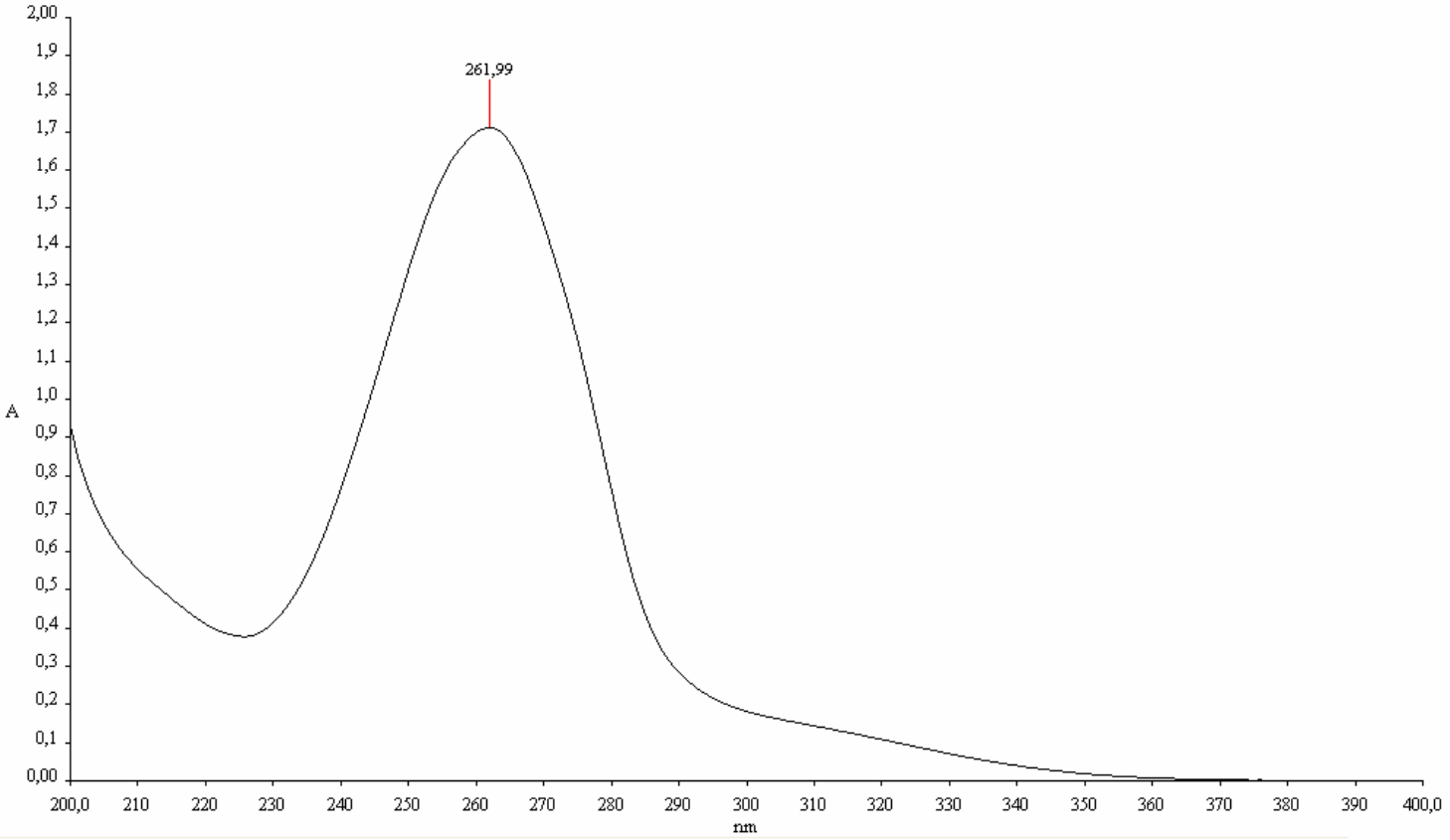

Figure 5.11.11. UV spectrum of phyllostictine B, isolated from *P. cirsii* culture filtrates, recorded in MeCN solution

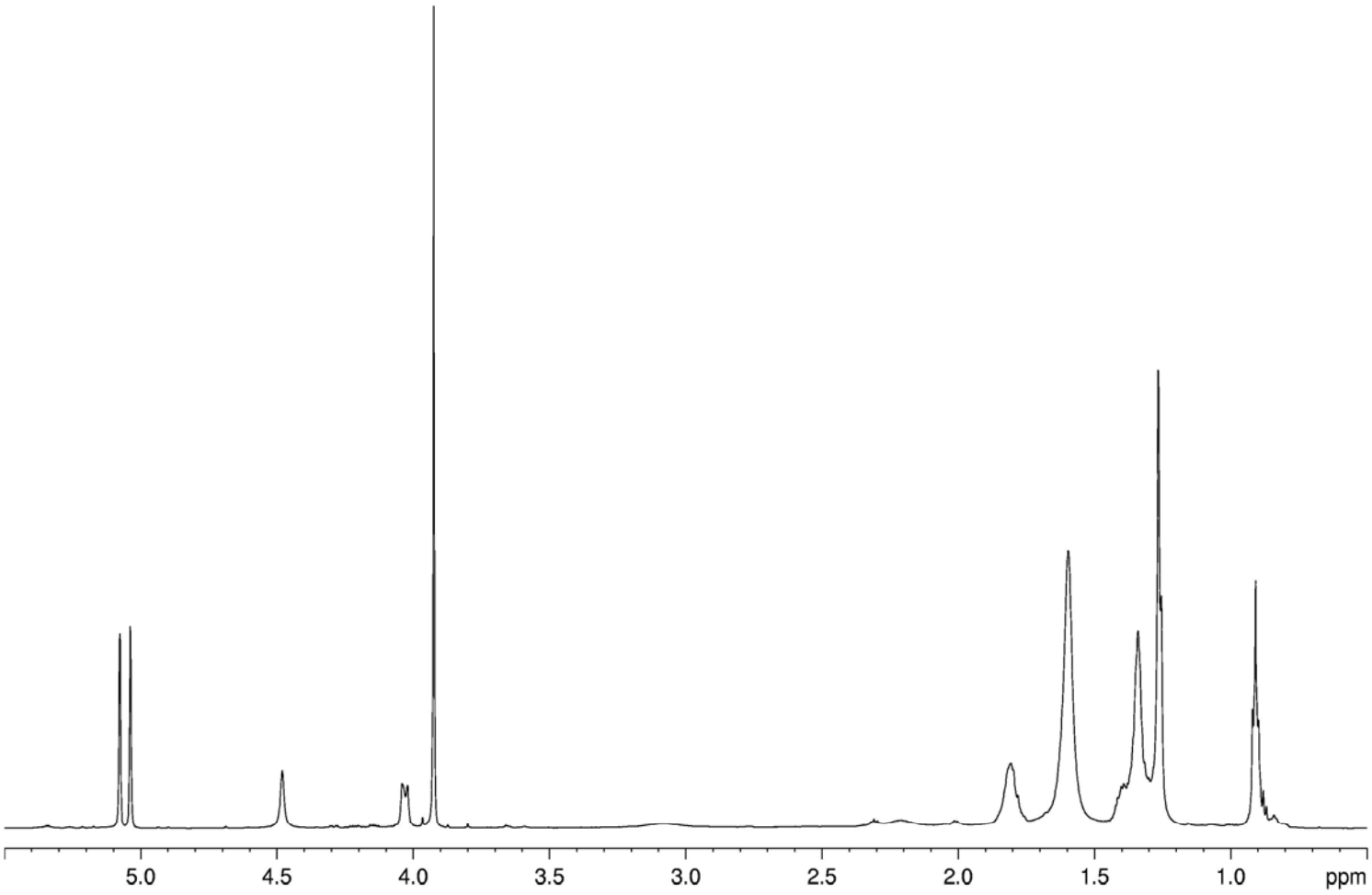

Figure 5.11.12. ^{1}H NMR spectrum of phyllostictine B, isolated from *P. cirsii* culture filtrates, recorded at 600 MHz

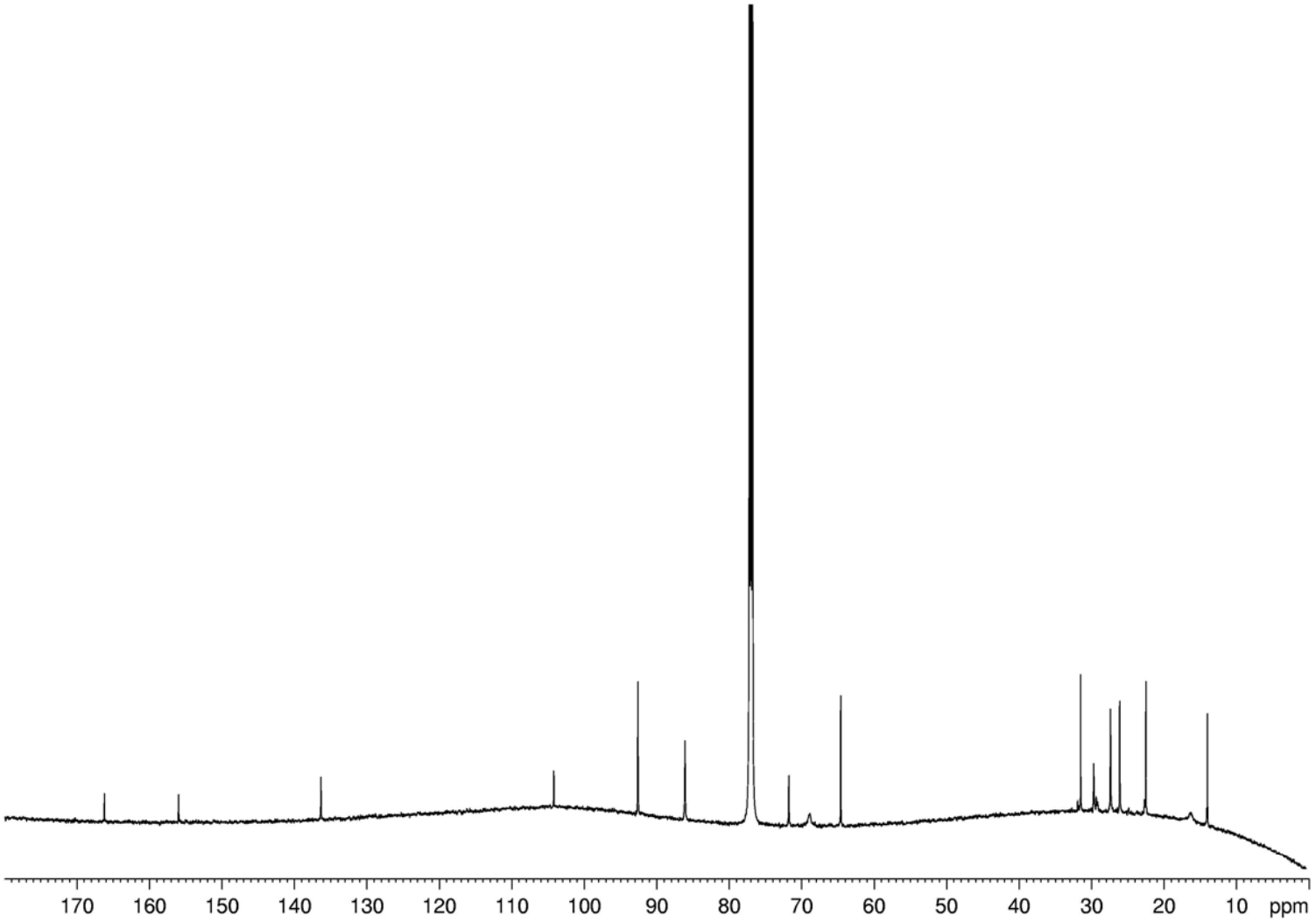

Figure 5.11.13. ^{13}C NMR spectrum of phyllostictine B, isolated from *P. cirsii* culture filtrates, recorded at 600 MHz

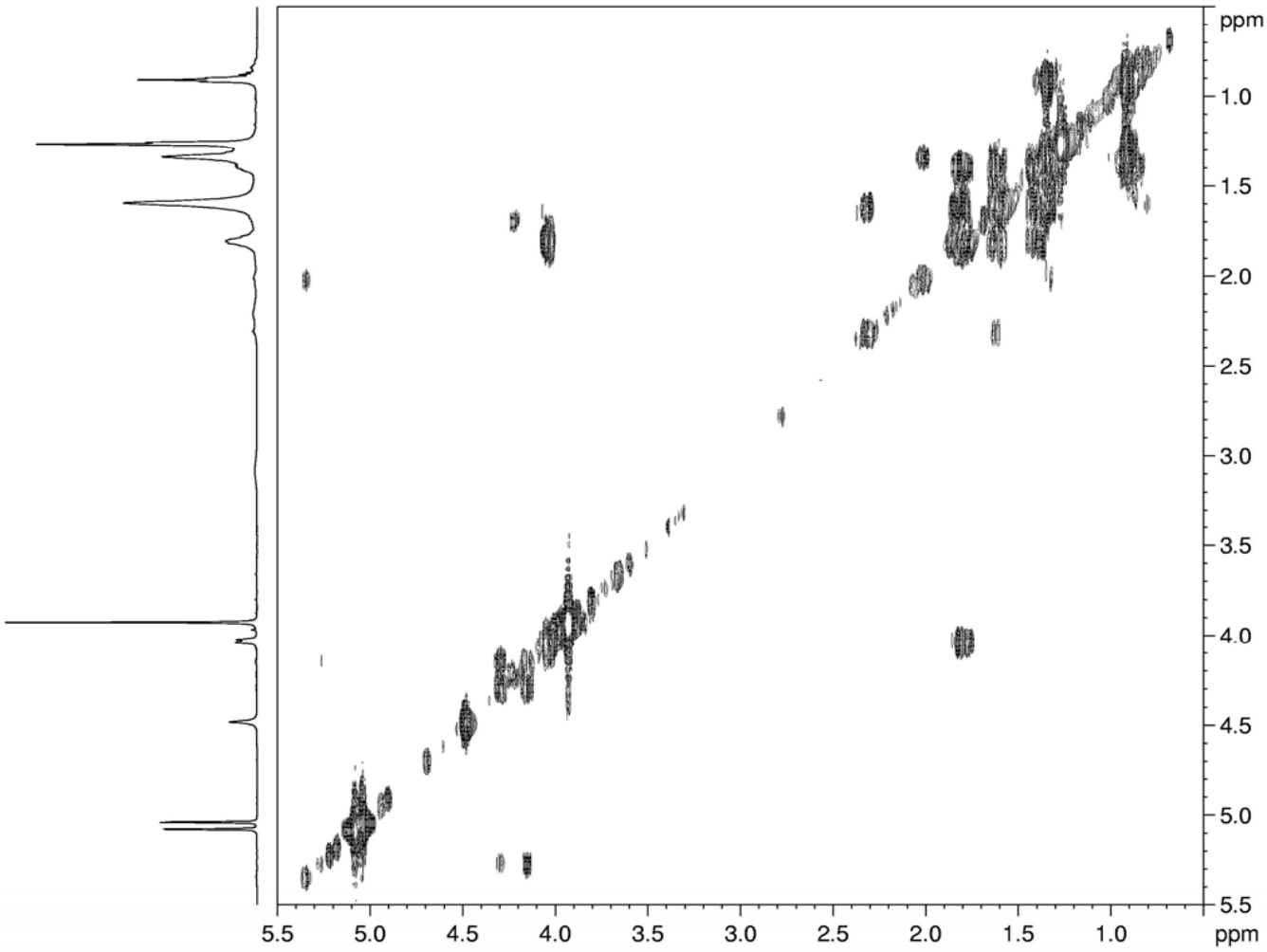

Figure 5.11.14. COSY spectrum of phyllostictine B, isolated from *P. cirsii* culture filtrates, recorded at 600 MHz

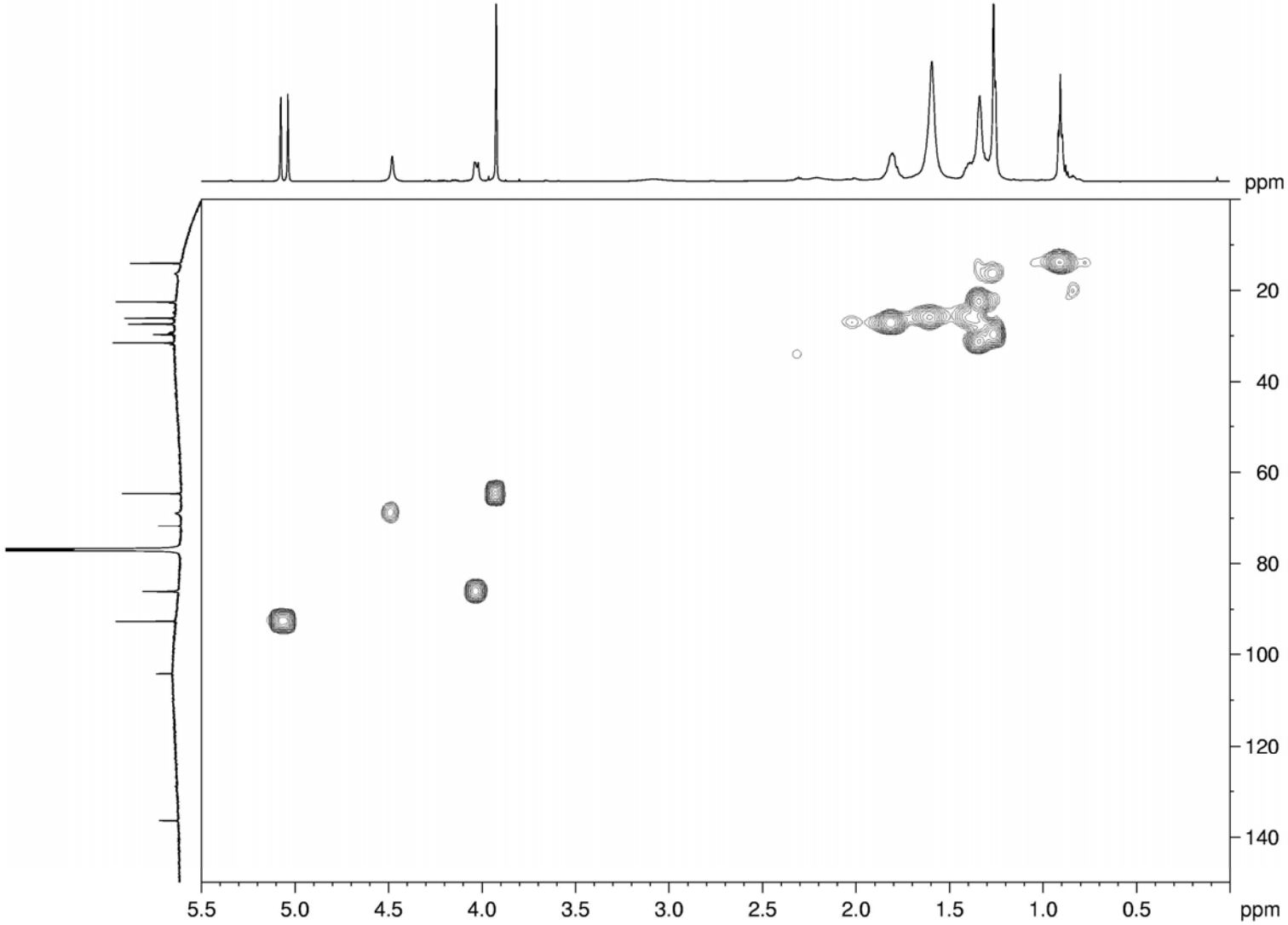

Figure 5.11.15. HSQC spectrum of phyllostictine B, isolated from *P. cirsii* culture filtrates, recorded at 600 MHz

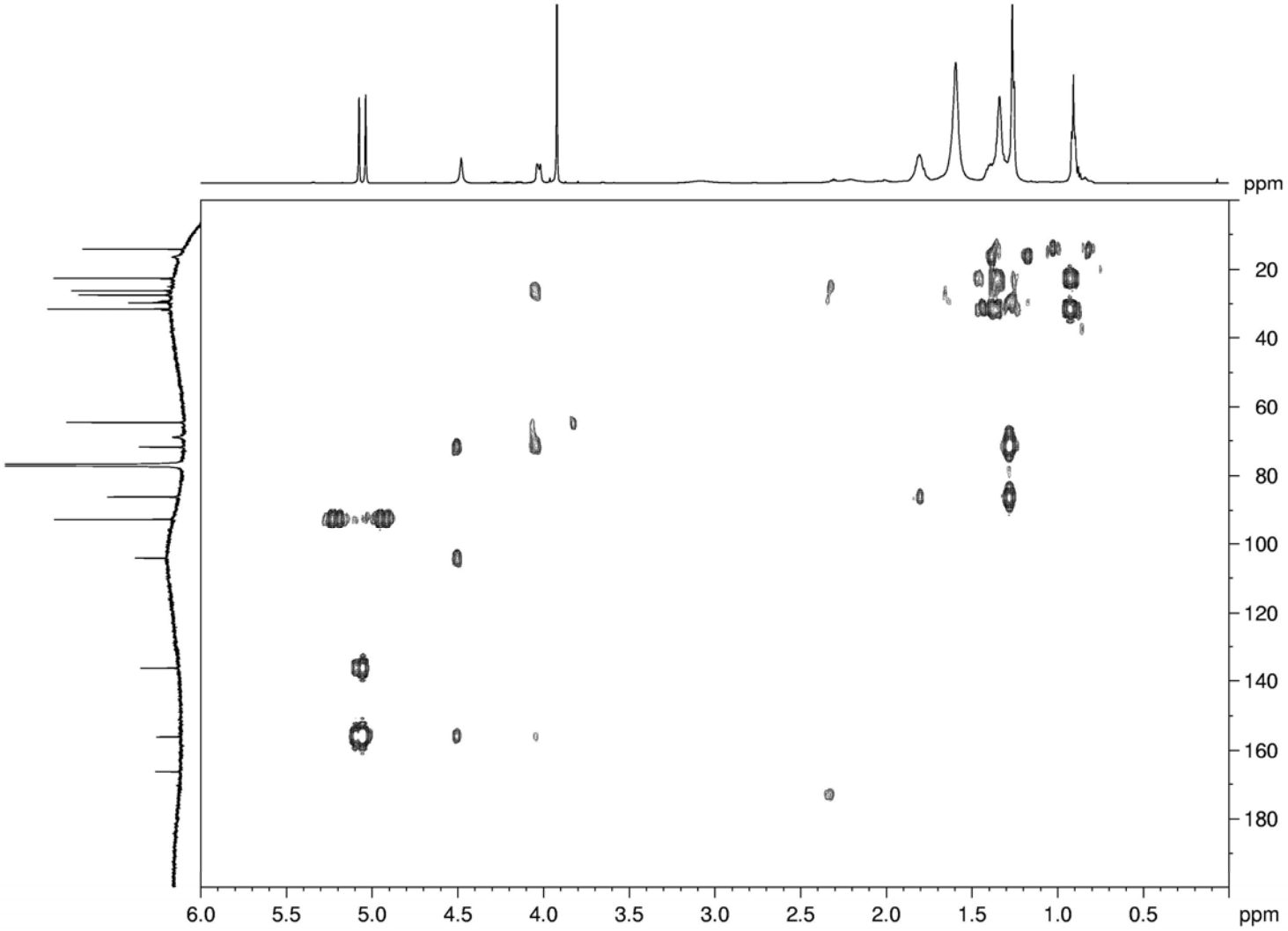

Figure 5.11.16. HMBC spectrum of phyllostictine B, isolated from *P. cirsii* culture filtrates, recorded at 600 MHz

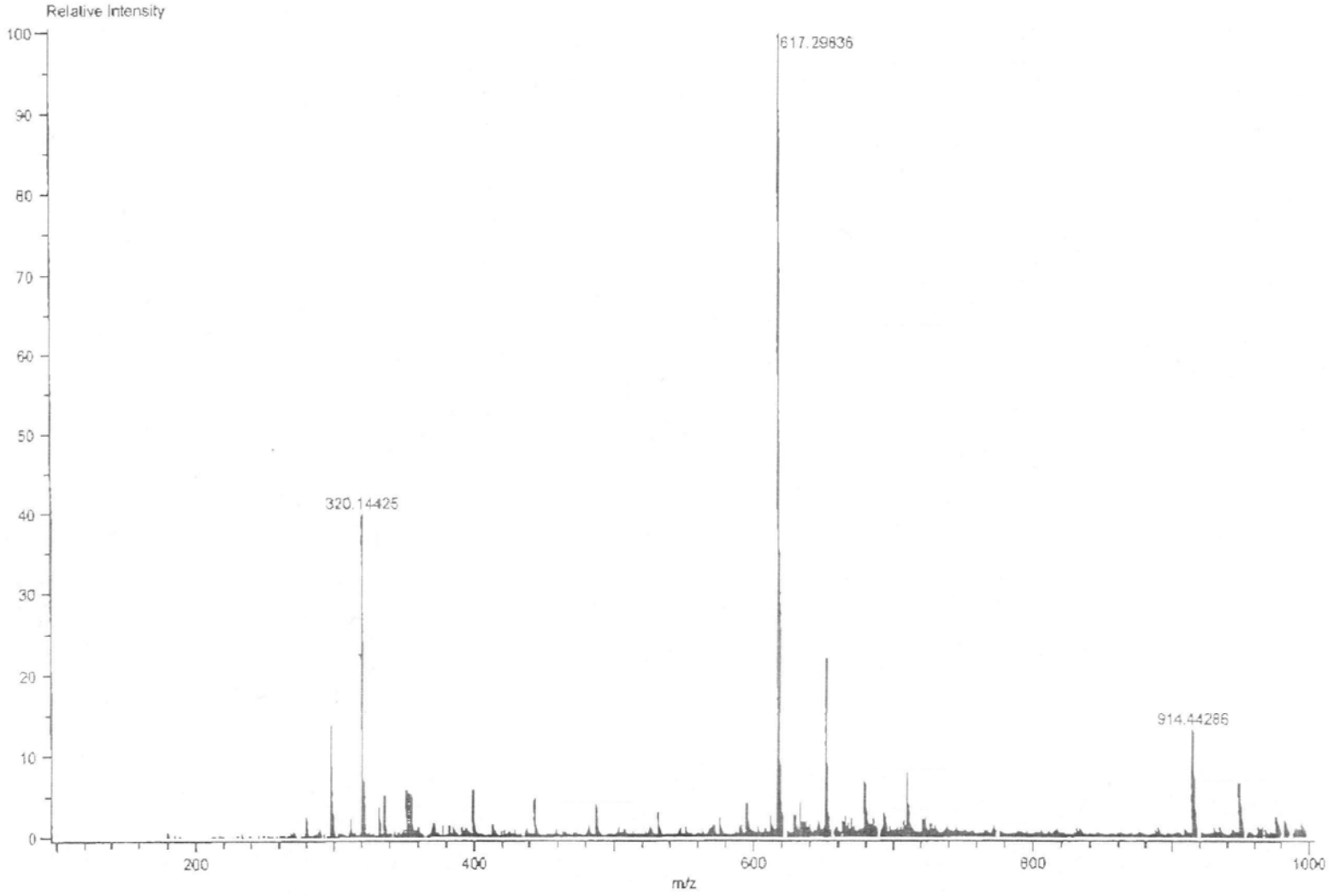

Figure 5.11.17. ESI MS spectrum of phyllostictine B, isolated from *P. cirsii* culture filtrates, recorded in positive modality

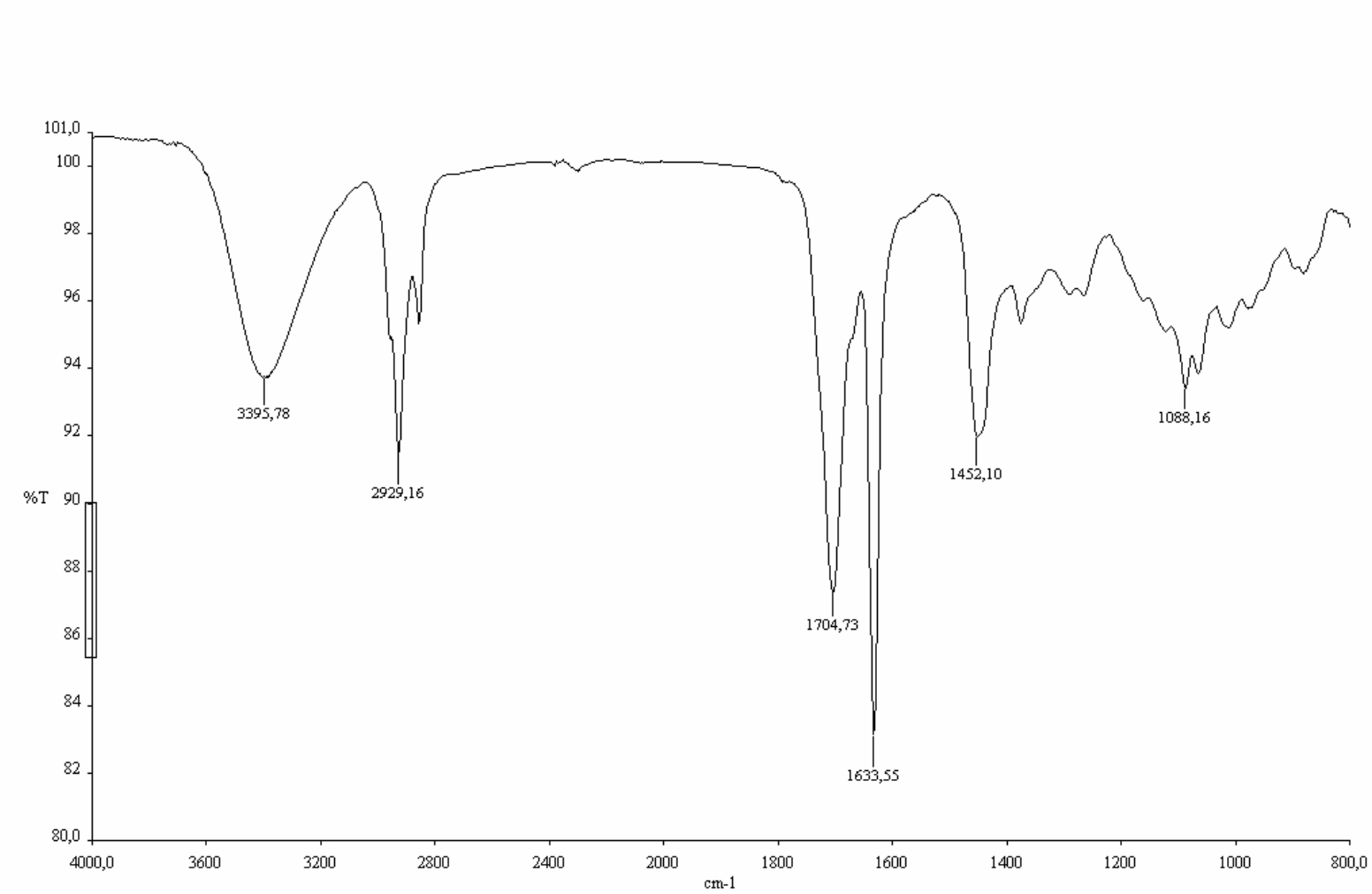

Figure 5.11.18. IR spectrum of phyllostictine C, isolated from *P. cirsii* culture filtrates, recorded as neat

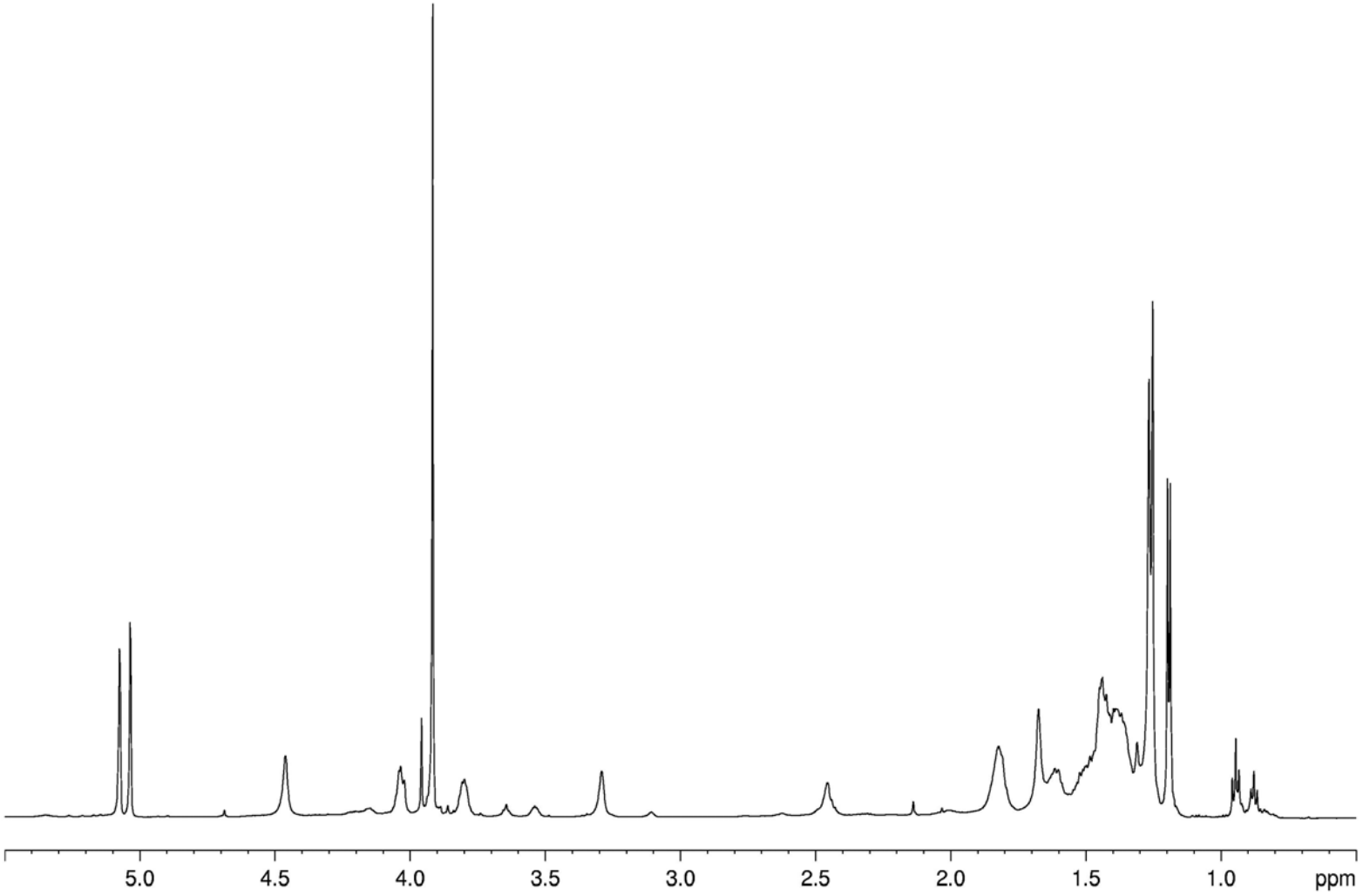

Figure 5.11.19. ^{1}H NMR spectrum of phyllostictine C, isolated from *P. cirsii* culture filtrates, recorded at 600 MHz

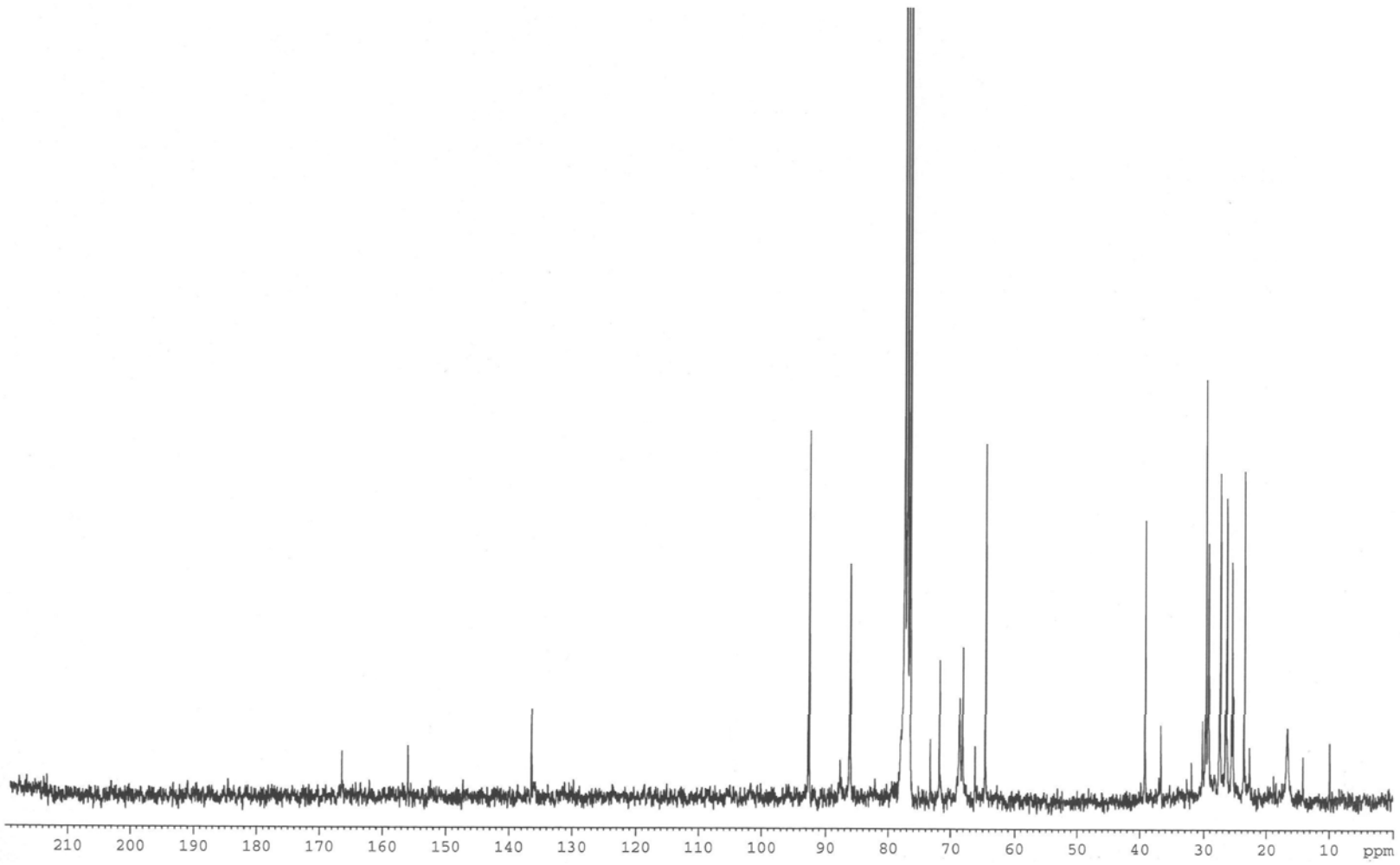

Figure 5.11.20. ^{13}C NMR spectrum of phyllostictine C, isolated from *P. cirsii* culture filtrates, recorded at 300 MHz

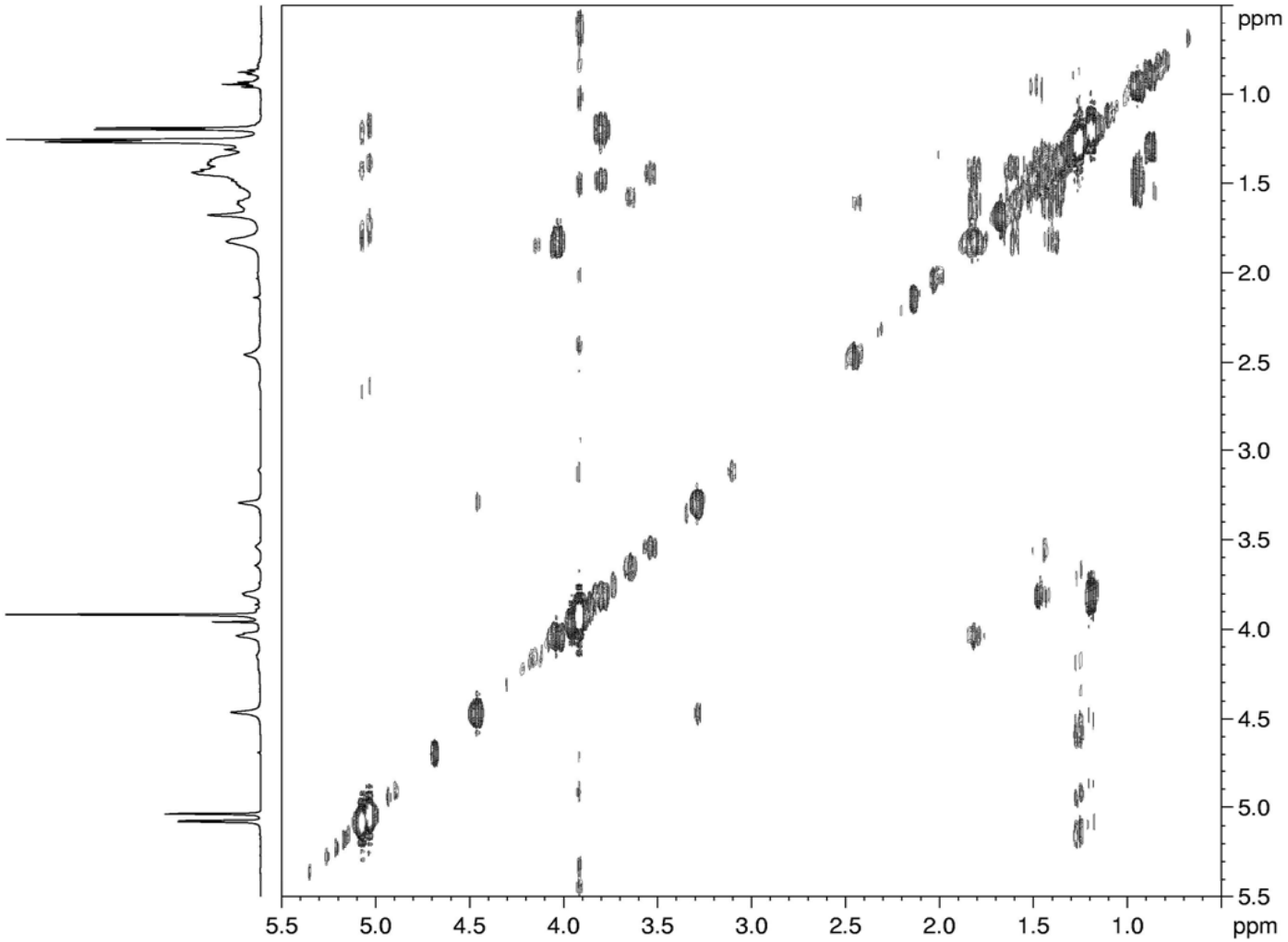

Figure 5.11.21. COSY spectrum of phyllostictine C, isolated from *P. cirsii* culture filtrates, recorded at 600 MHz

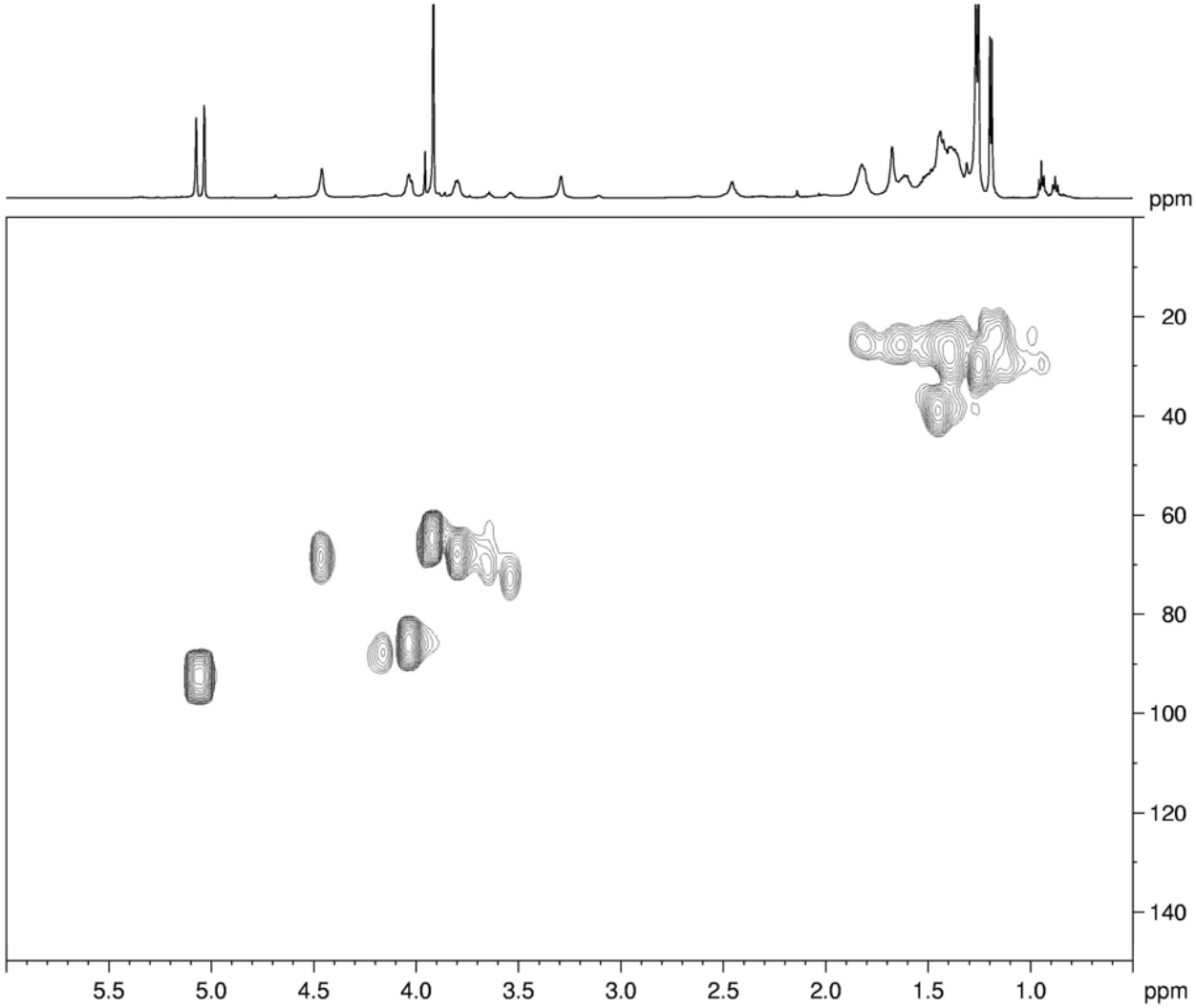

Figure 5.11.22. HSQC spectrum of phyllostictine C, isolated from *P. cirsii* culture filtrates, recorded at 600 MHz

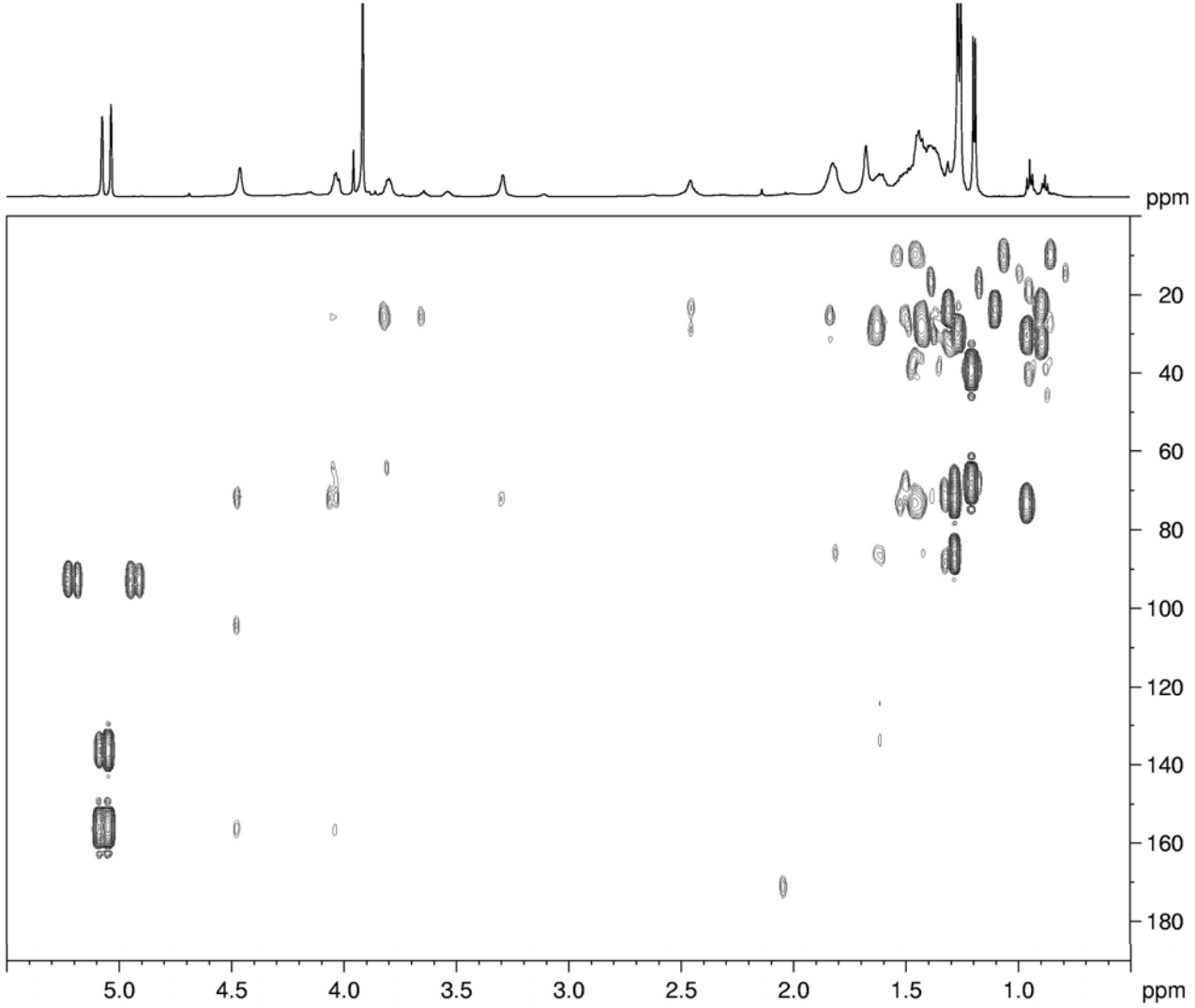

Figure 5.11.23. HMBC spectrum of phyllostictine C, isolated from *P. cirsii* culture filtrates, recorded at 600 MHz

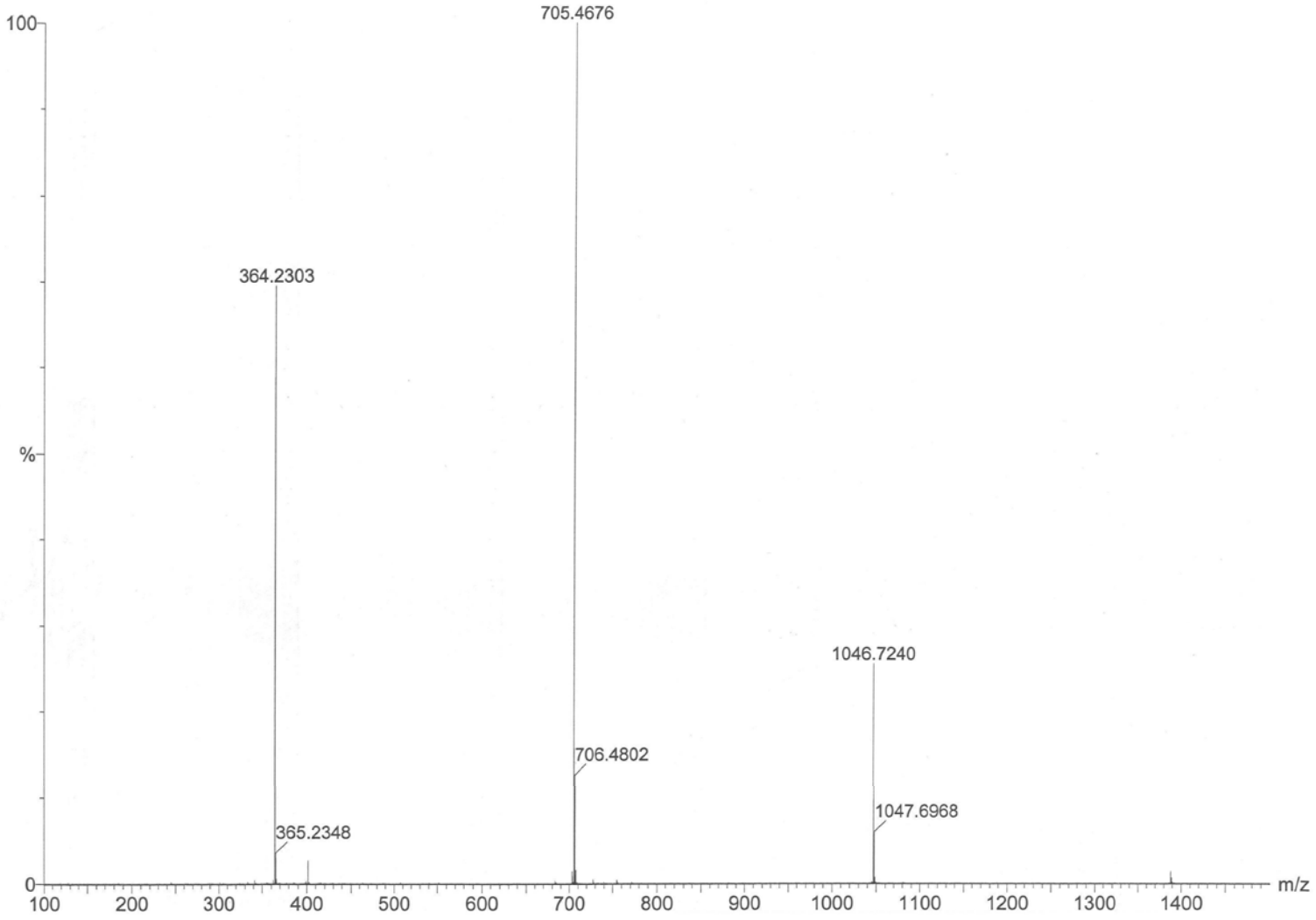

Figure 5.11.24. ESI MS spectrum of phyllostictine C, isolated from *P. cirsii* culture filtrates, recorded in positive modality

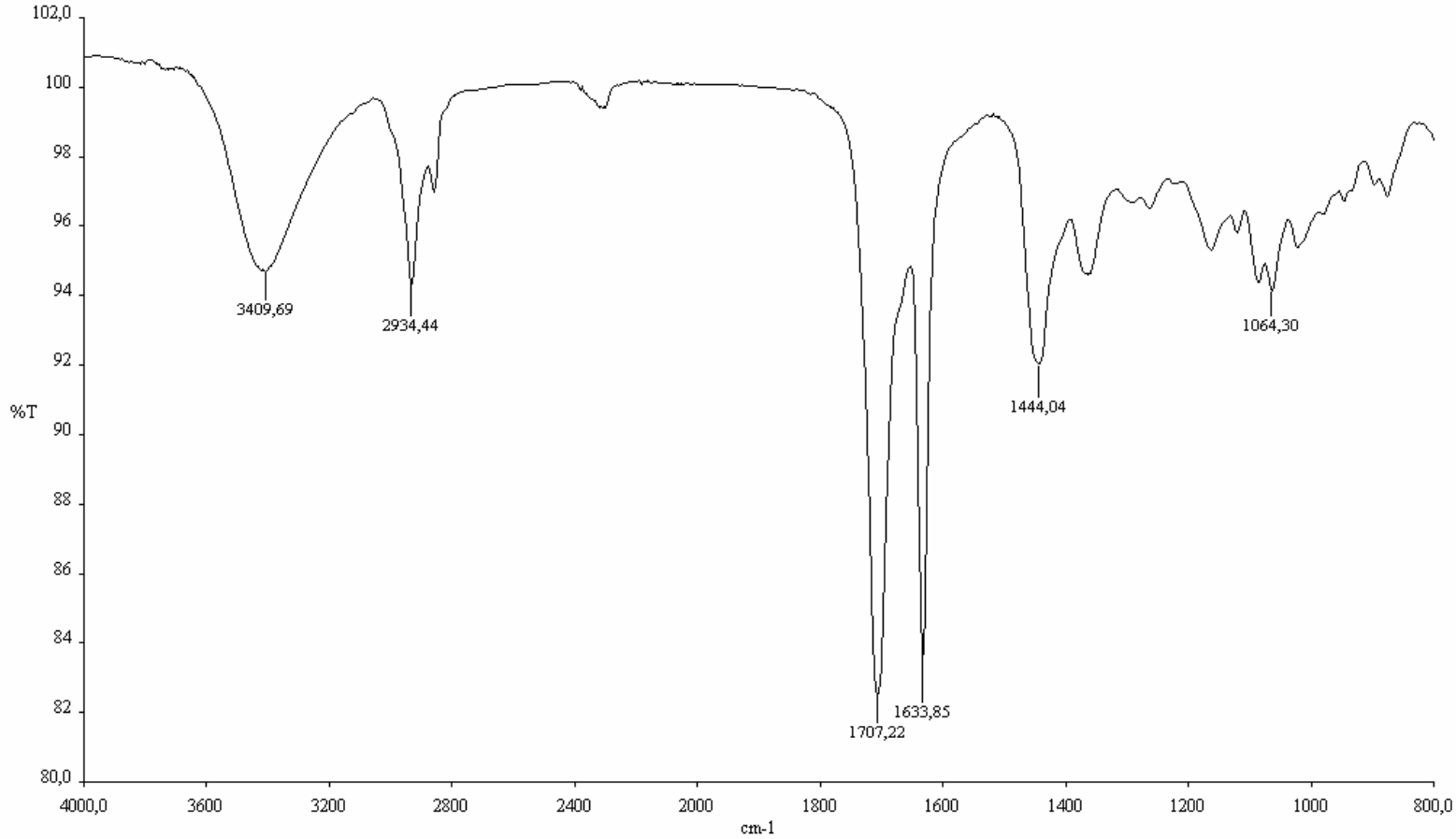

Figure 5.11.25. IR spectrum of phyllostictine D, isolated from *P. cirsii* culture filtrates, recorded as neat

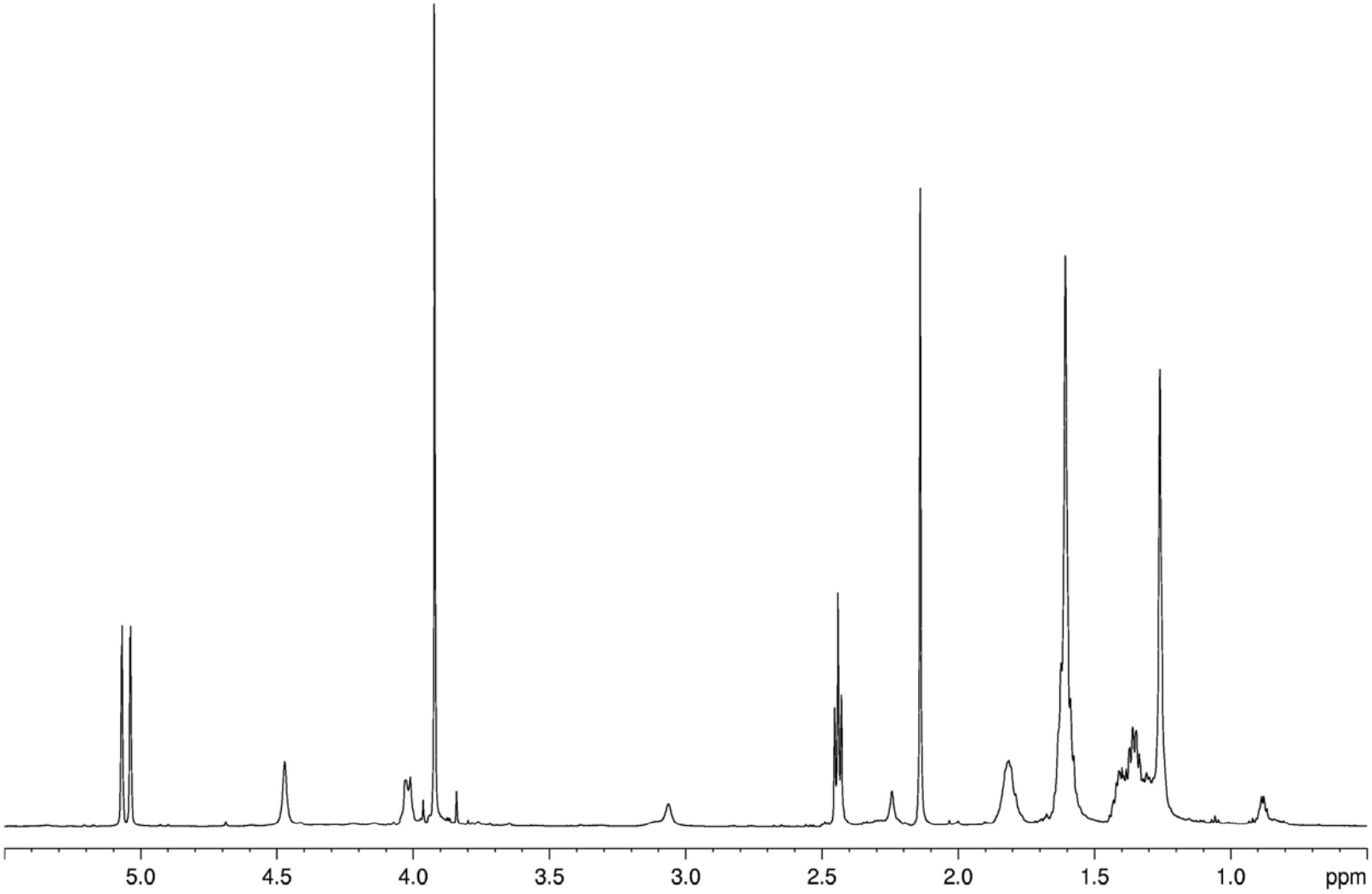

Figure 5.11.26. ^{1}H NMR spectrum of phyllostictine D, isolated from *P. cirsii* culture filtrates, recorded at 600 MHz

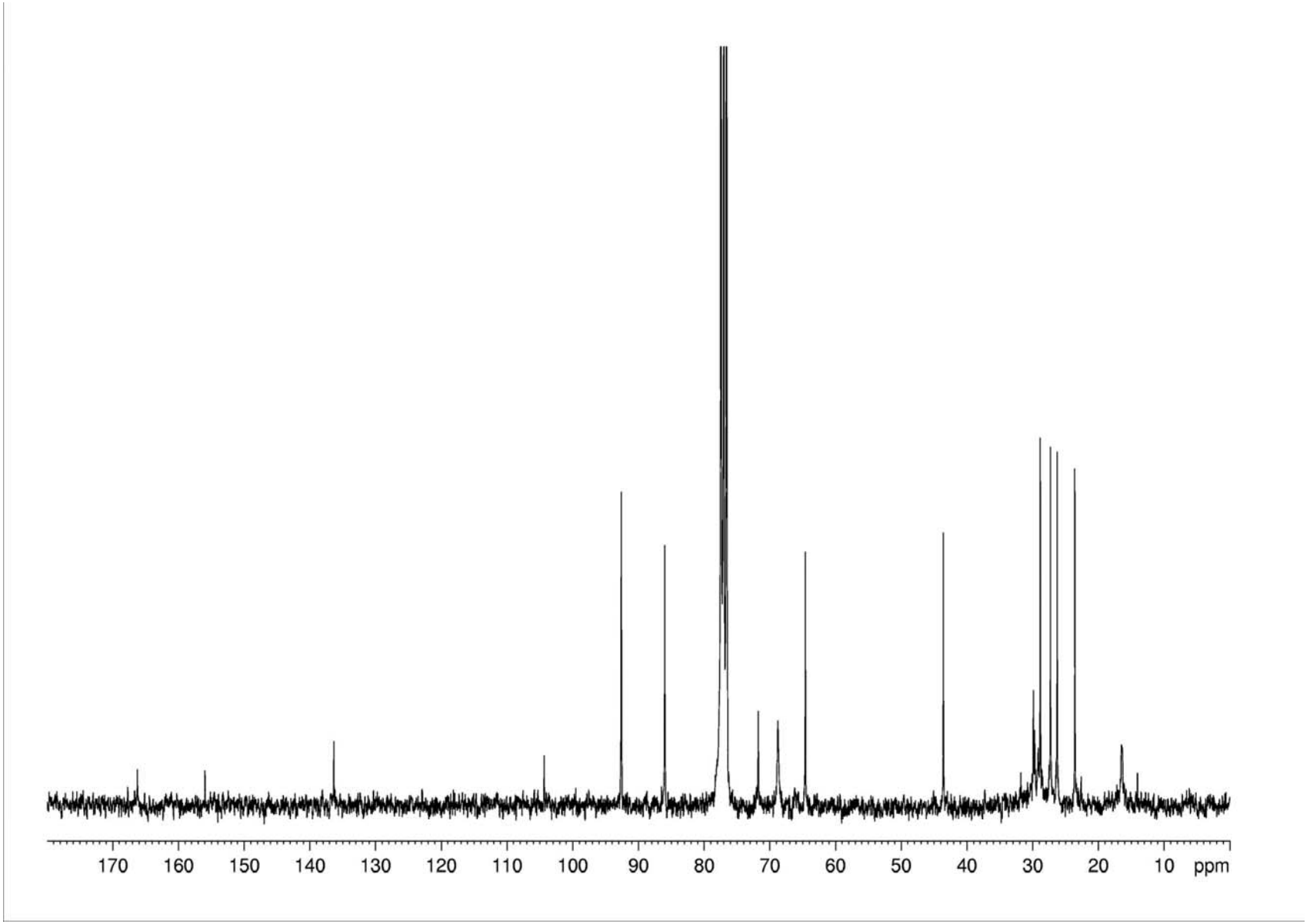

Figure 5.11.27. ^{13}C NMR spectrum of phyllostictine D, isolated from *P. cirsii* culture filtrates, recorded at 300 MHz

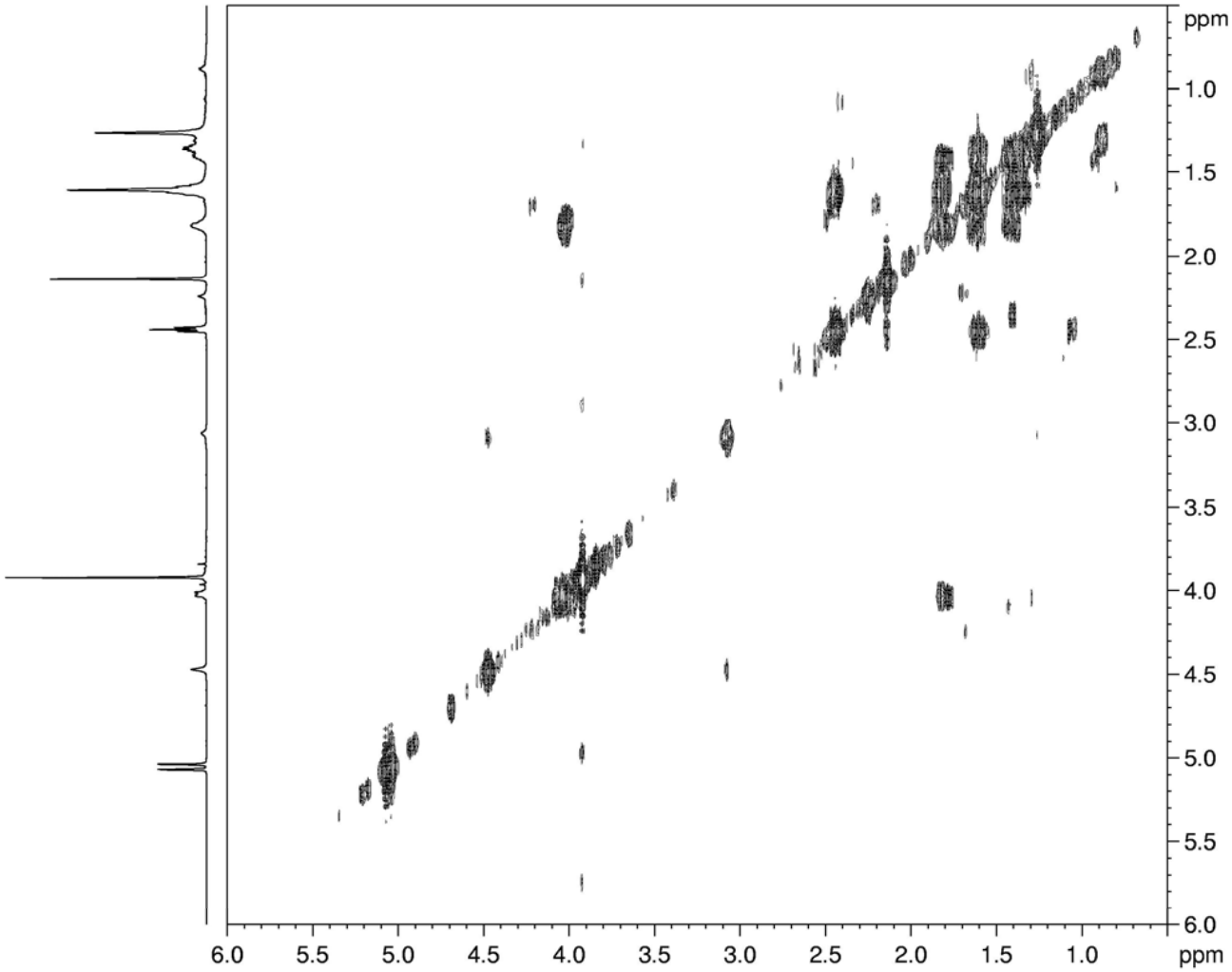

Figure 5.11.28. COSY spectrum of phyllostictine D, isolated from *P. cirsii* culture filtrates, recorded at 600 MHz

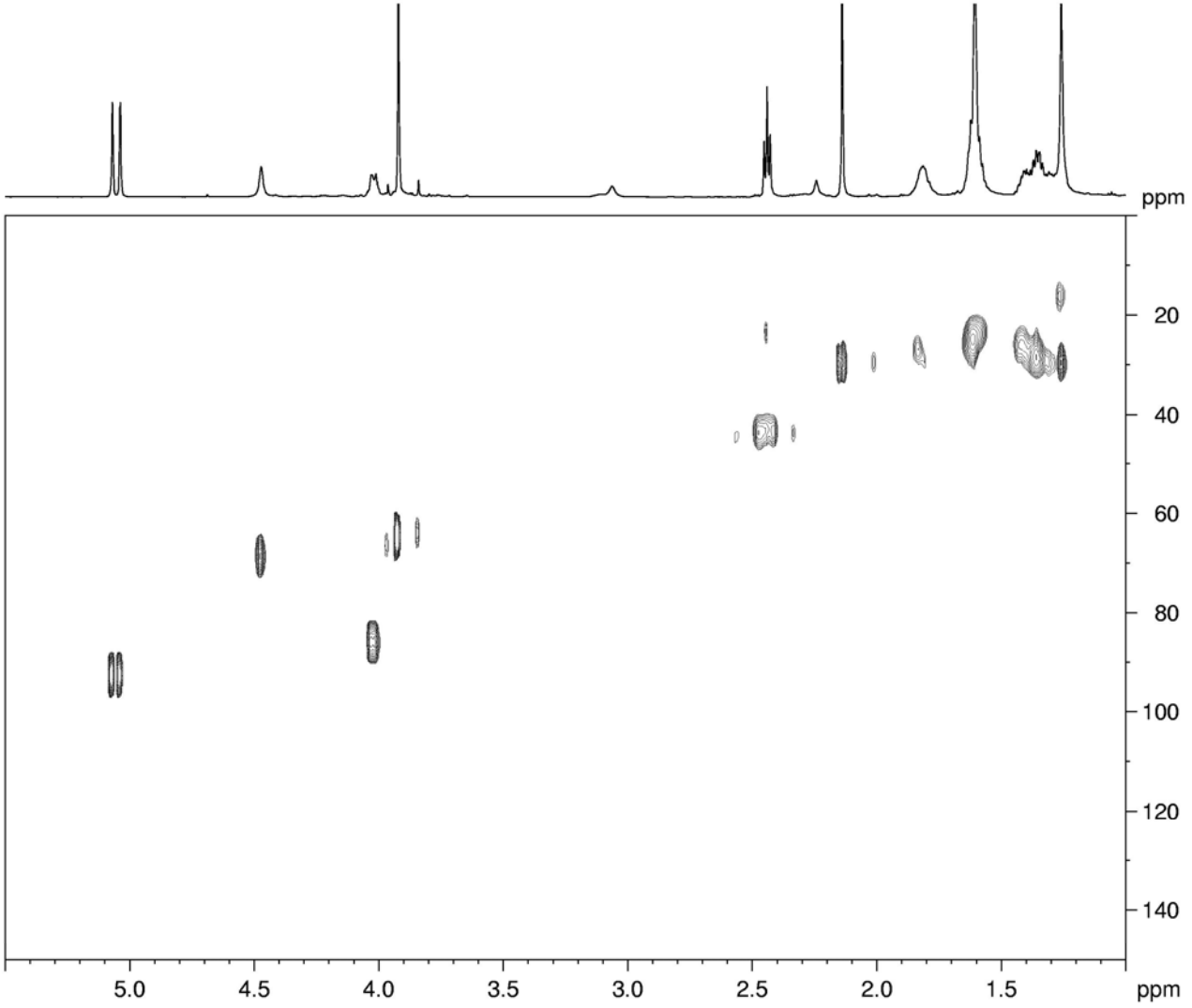

Figure 5.11.29. HSQC spectrum of phyllostictine D, isolated from *P. cirsii* culture filtrates, recorded at 600 MHz

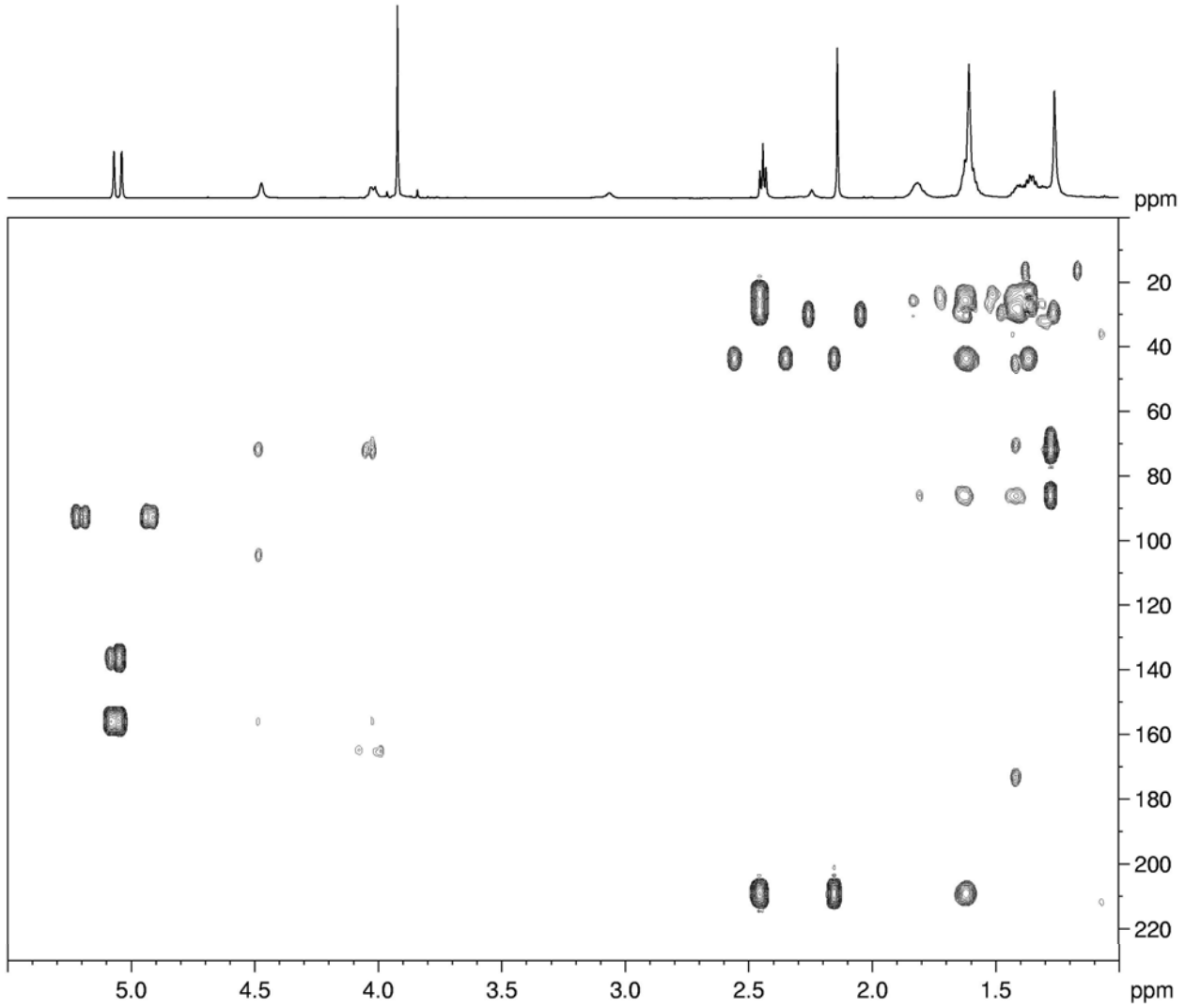

Figure 5.11.30. HMBC spectrum of phyllostictine D, isolated from *P. cirsii* culture filtrates, recorded at 600 MHz

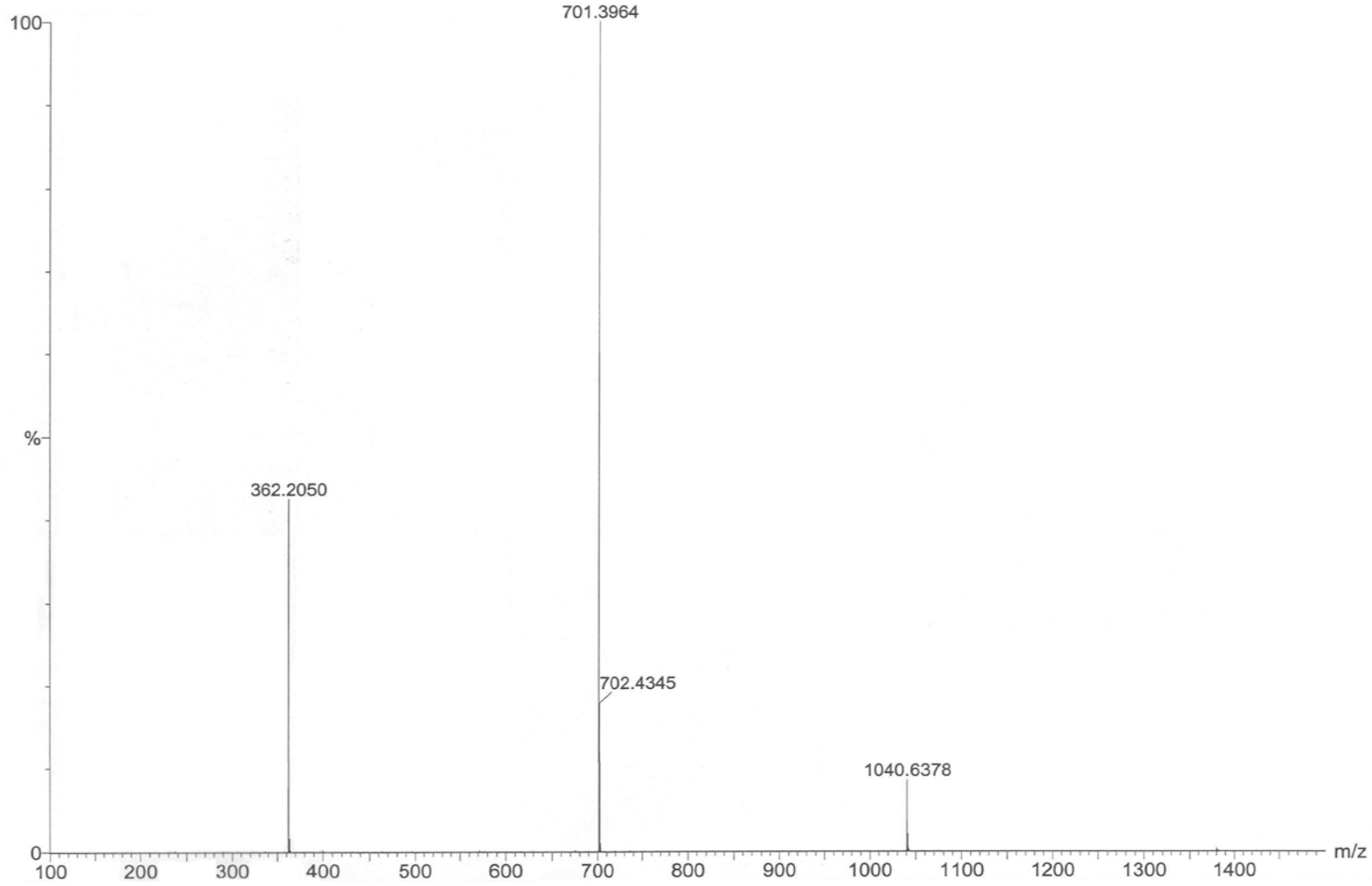

Figure 5.11.31. ESI MS spectrum of phyllostictine D, isolated from *P. cirsii* culture filtrates, recorded in positive modality

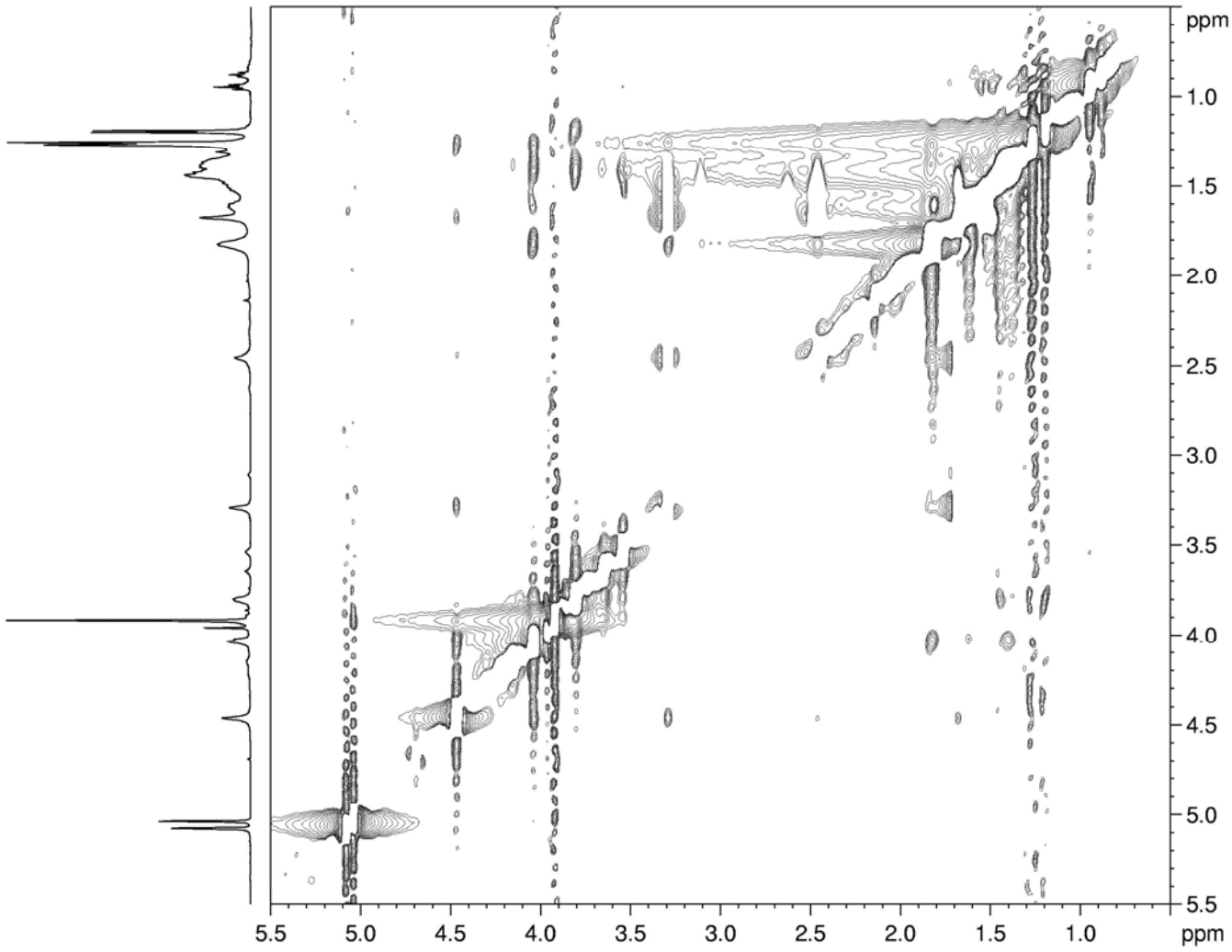

Figure 5.11.32. NOESY spectrum of phyllostictine C, isolated from *P. cirsii* culture filtrates, recorded at 600 MHz

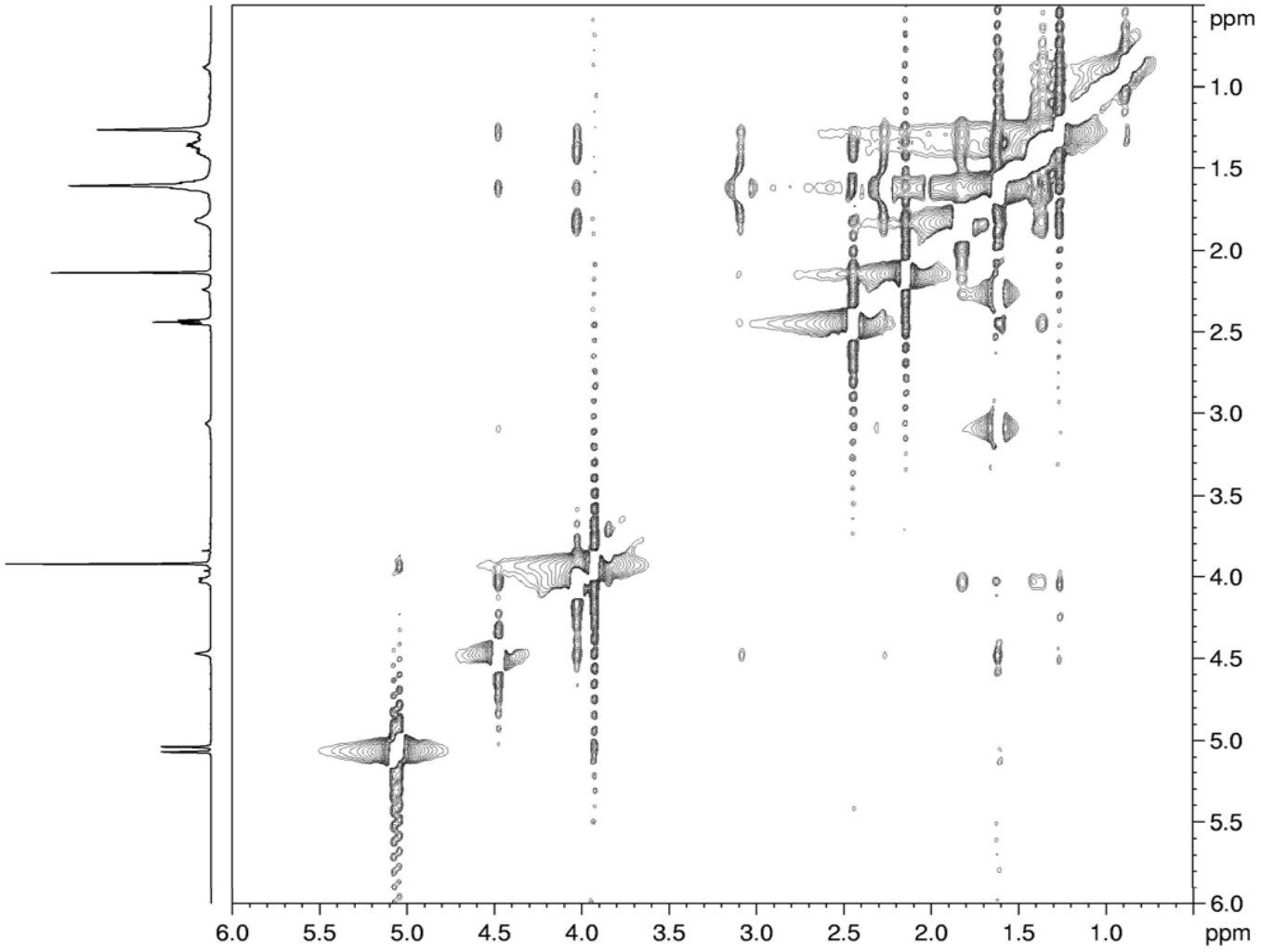

Figure 5.11.33. NOESY spectrum of phyllostictine D, isolated from *P. cirsii* culture filtrates, recorded at 600 MHz

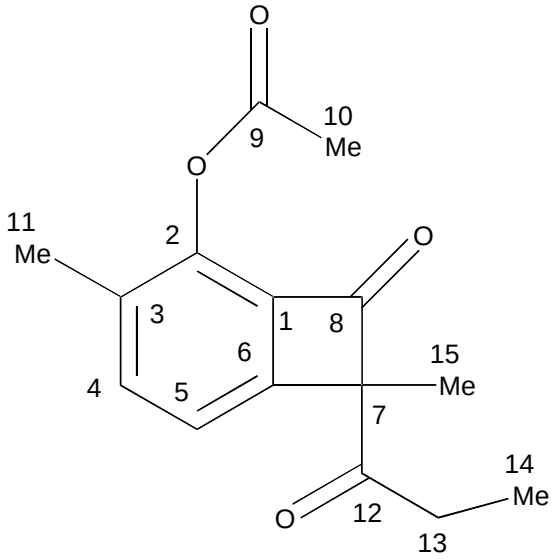

62

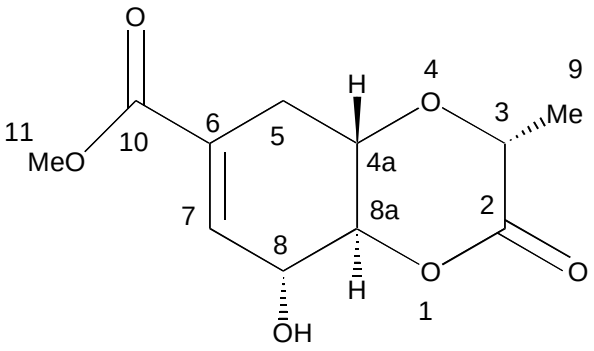

63

Figure 5.11.34. Structure of phyllostoxin and phyllostin isolated from *P. cirsii* culture filtrates

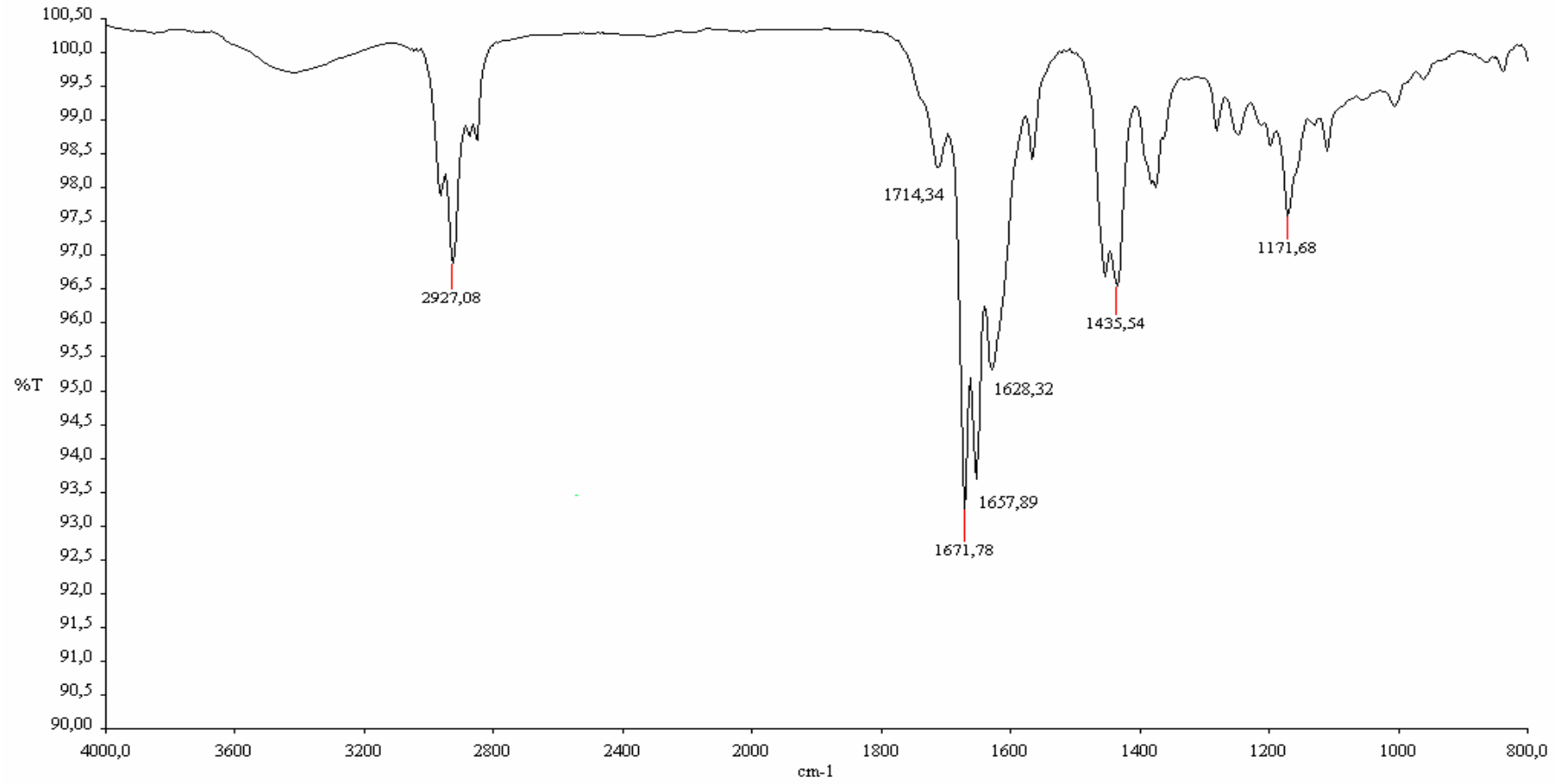

Figure 5.11.35. IR spectrum of phyllostoxin, isolated from *P. cirsii* culture filtrates, recorded as neat

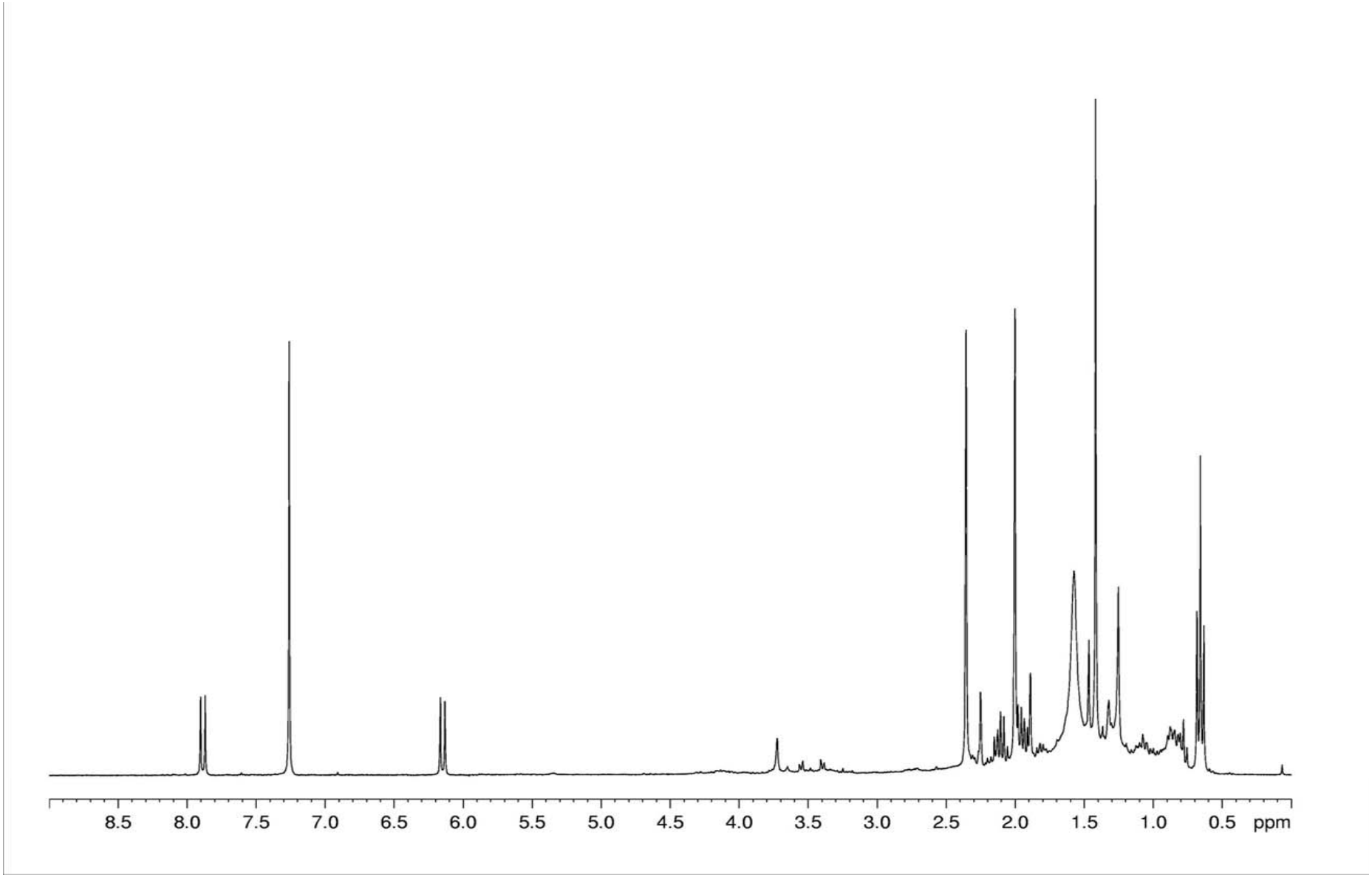

Figure 5.11.36. ^{1}H NMR spectrum of phyllostoxin, isolated from *P. cirsii* culture filtrates, recorded at 300 MHz

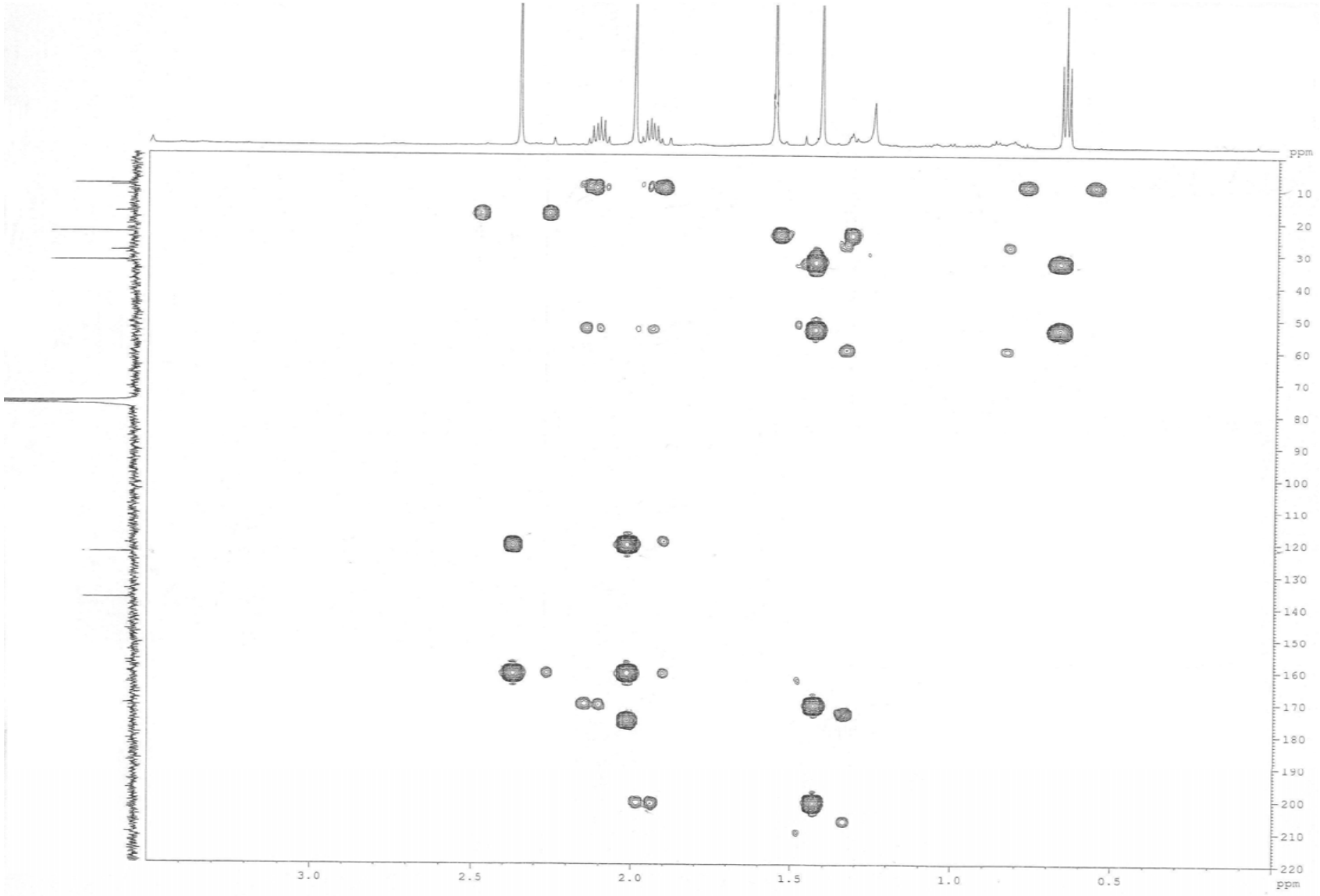

Figure 5.11.37. HMBC spectrum of phyllostoxin, isolated from *P. cirsii* culture filtrates, recorded at 600 MHz

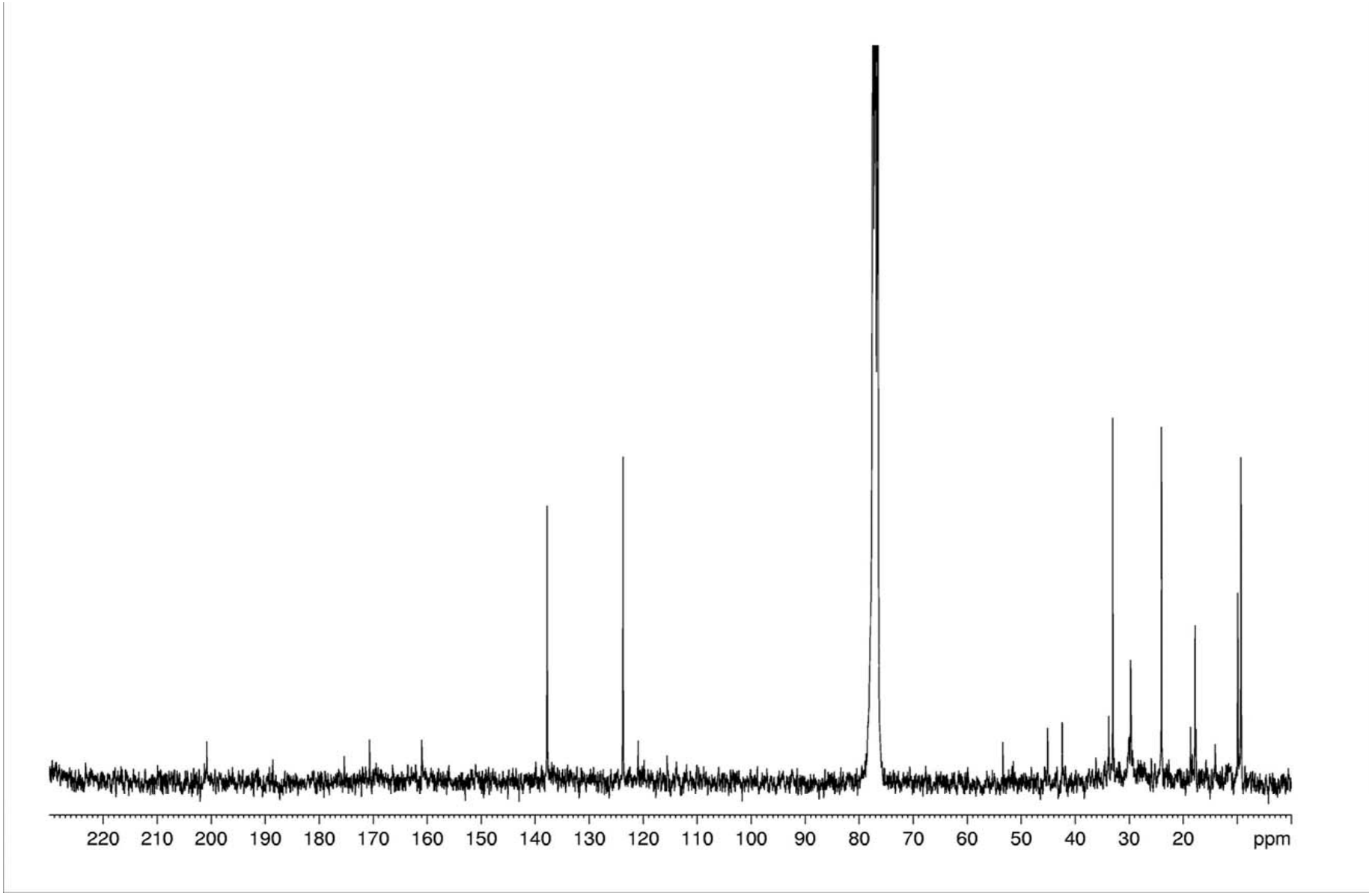

Figure 5.11.38. ^{13}C NMR spectrum of phyllostoxin, isolated from *P. cirsii* culture filtrates, recorded at 300 MHz

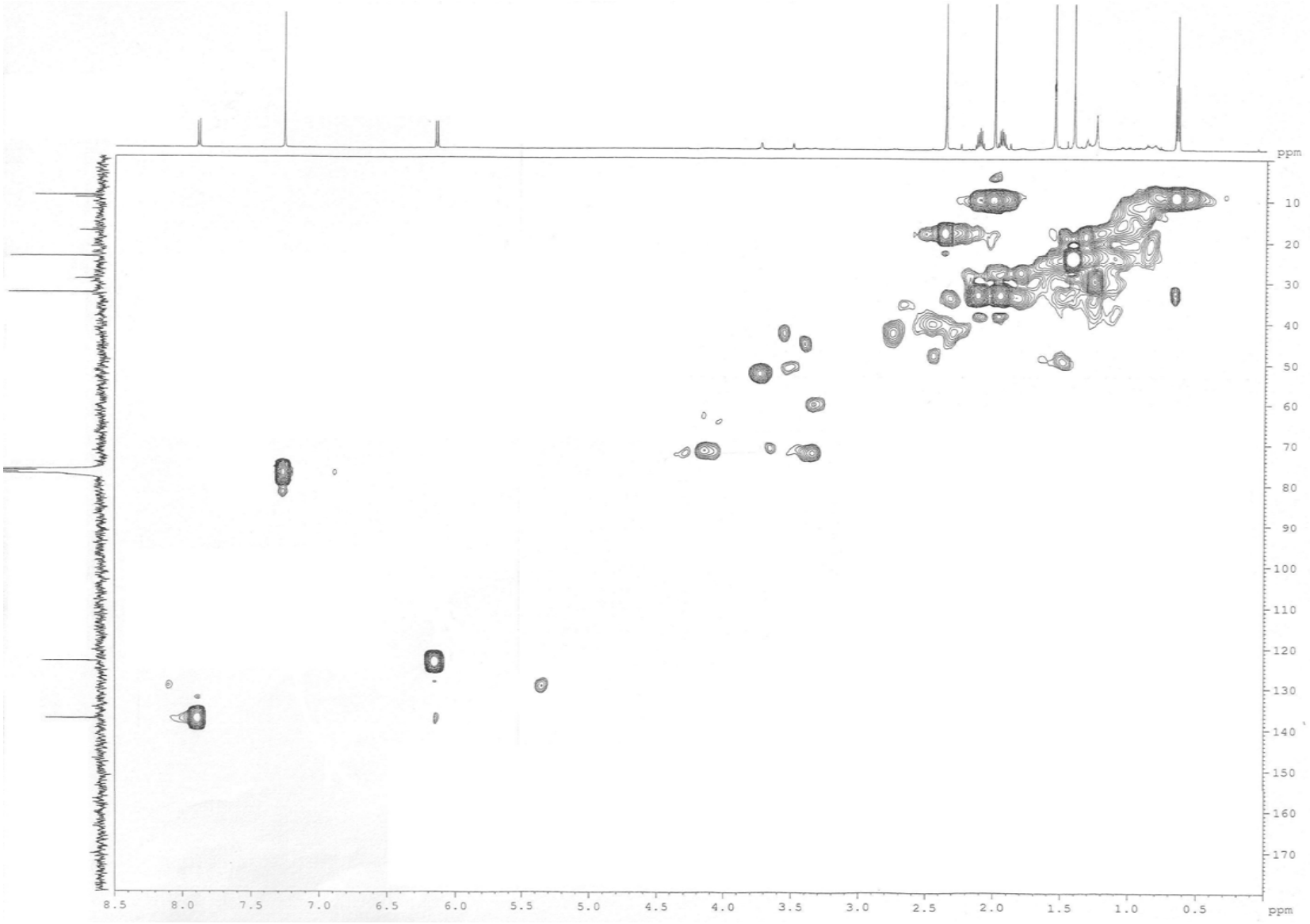

Figure 5.11.39. HSQC spectrum of phyllostoxin, isolated from *P. cirsii* culture filtrates, recorded at 600 MHz

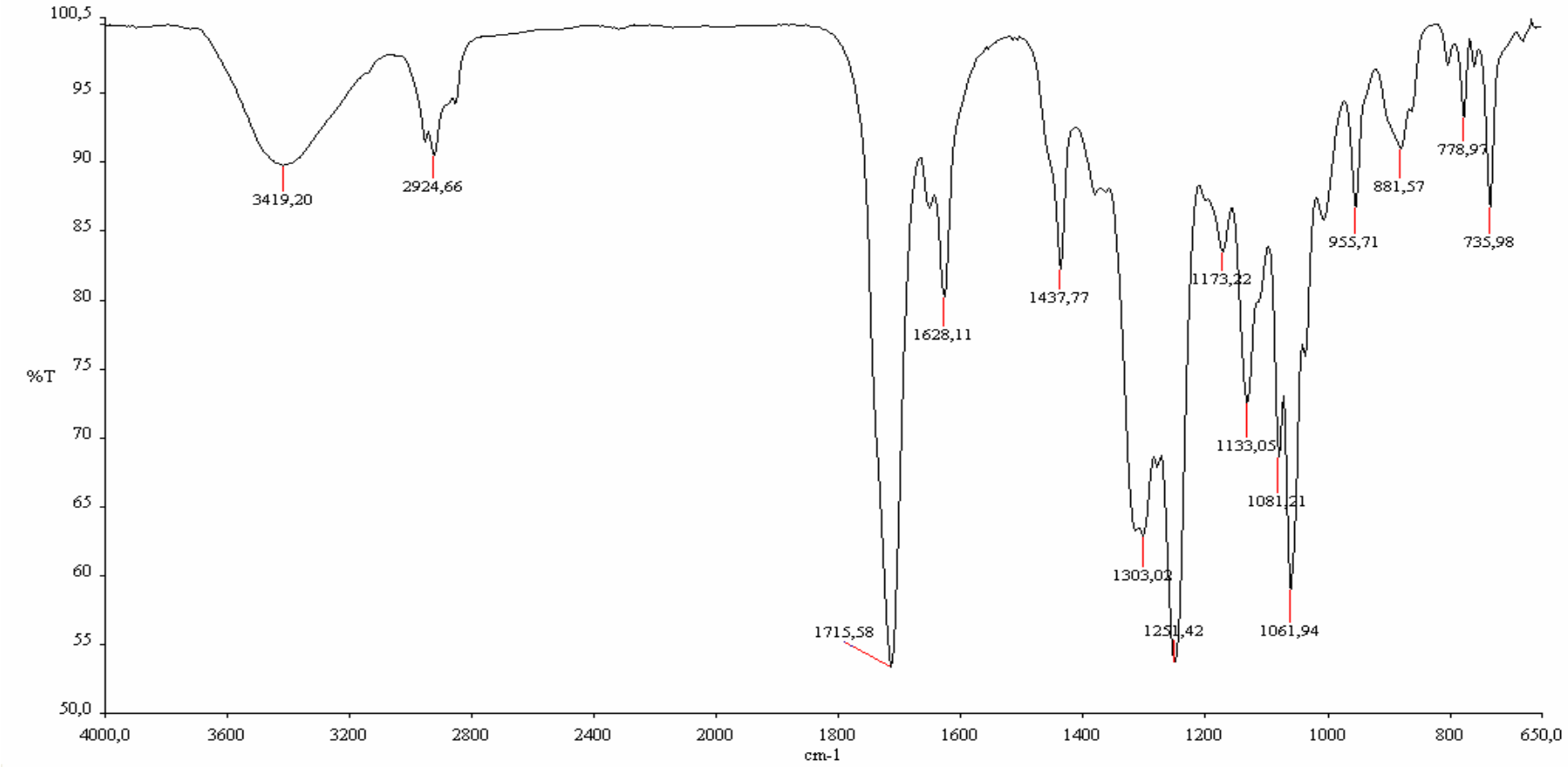

Figure 5.11.40. IR spectrum of phyllostin, isolated from *P. cirsii* culture filtrates, recorded as neat

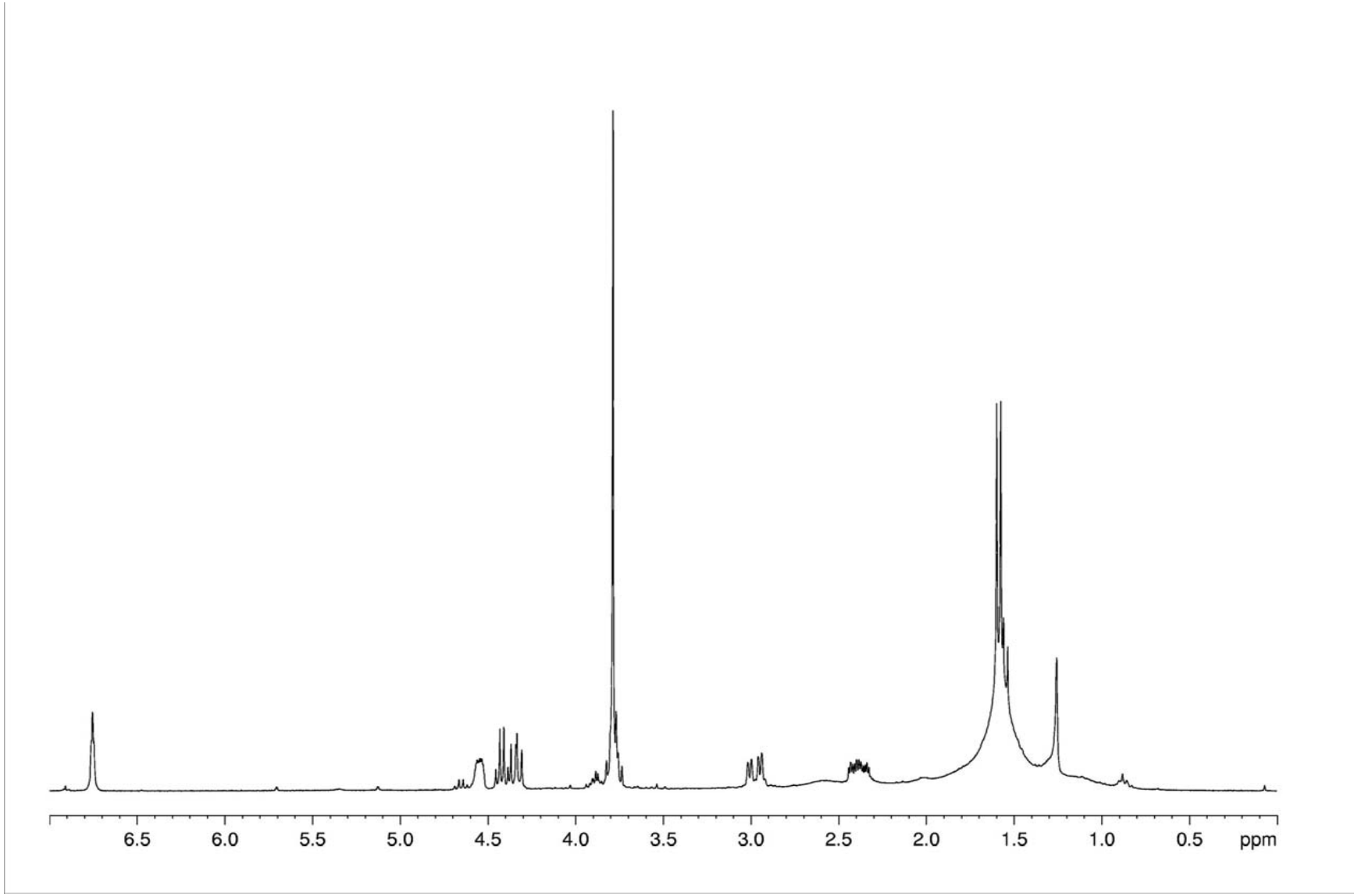

Figure 5.11.41. ^{1}H NMR spectrum of phyllostin, isolated from *P. cirsii* culture filtrates, recorded at 300 MHz

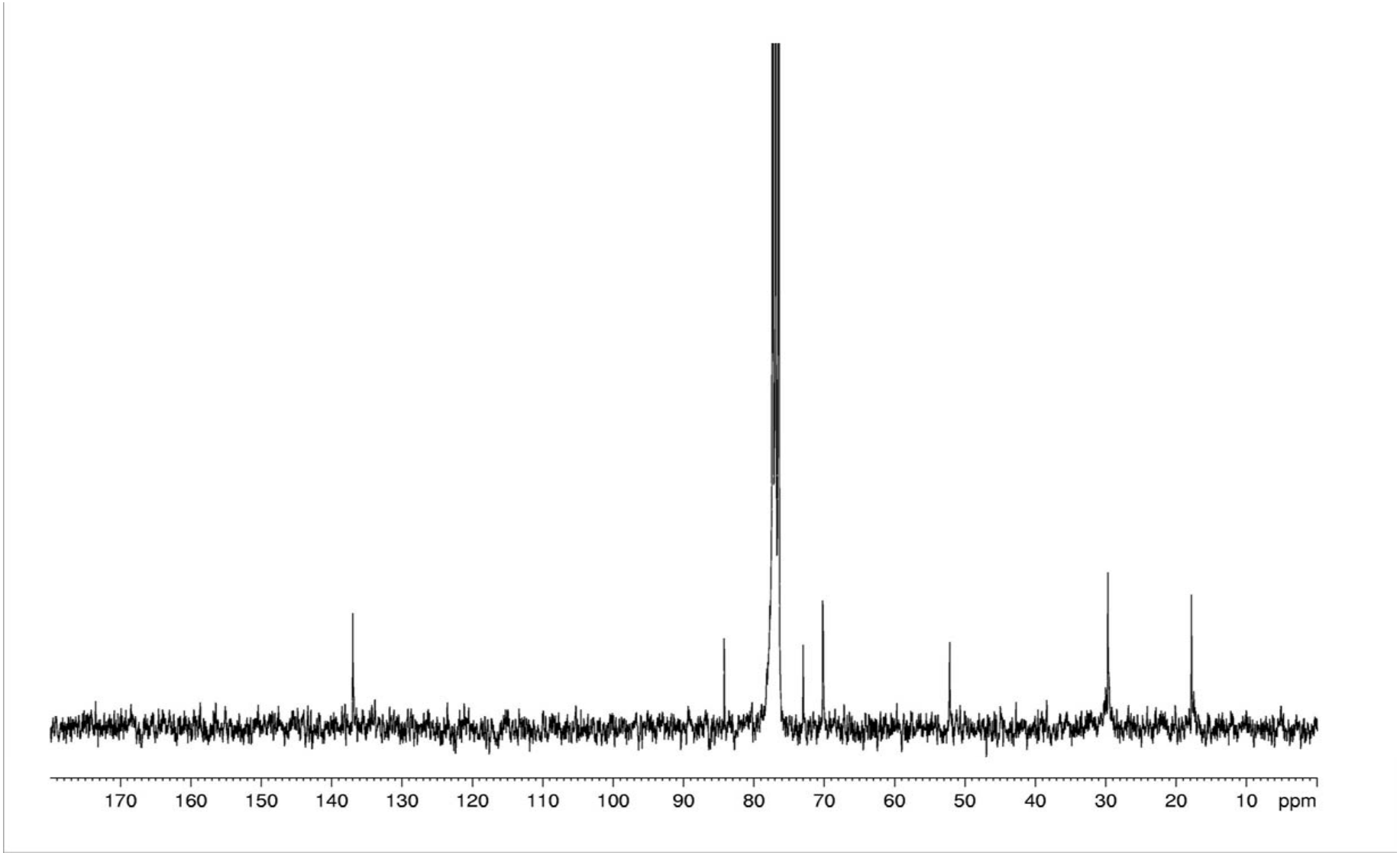

Figure 5.11.42. ^{13}C NMR spectrum of phyllostin, isolated from *P. cirsii* culture filtrates, recorded at 300 MHz

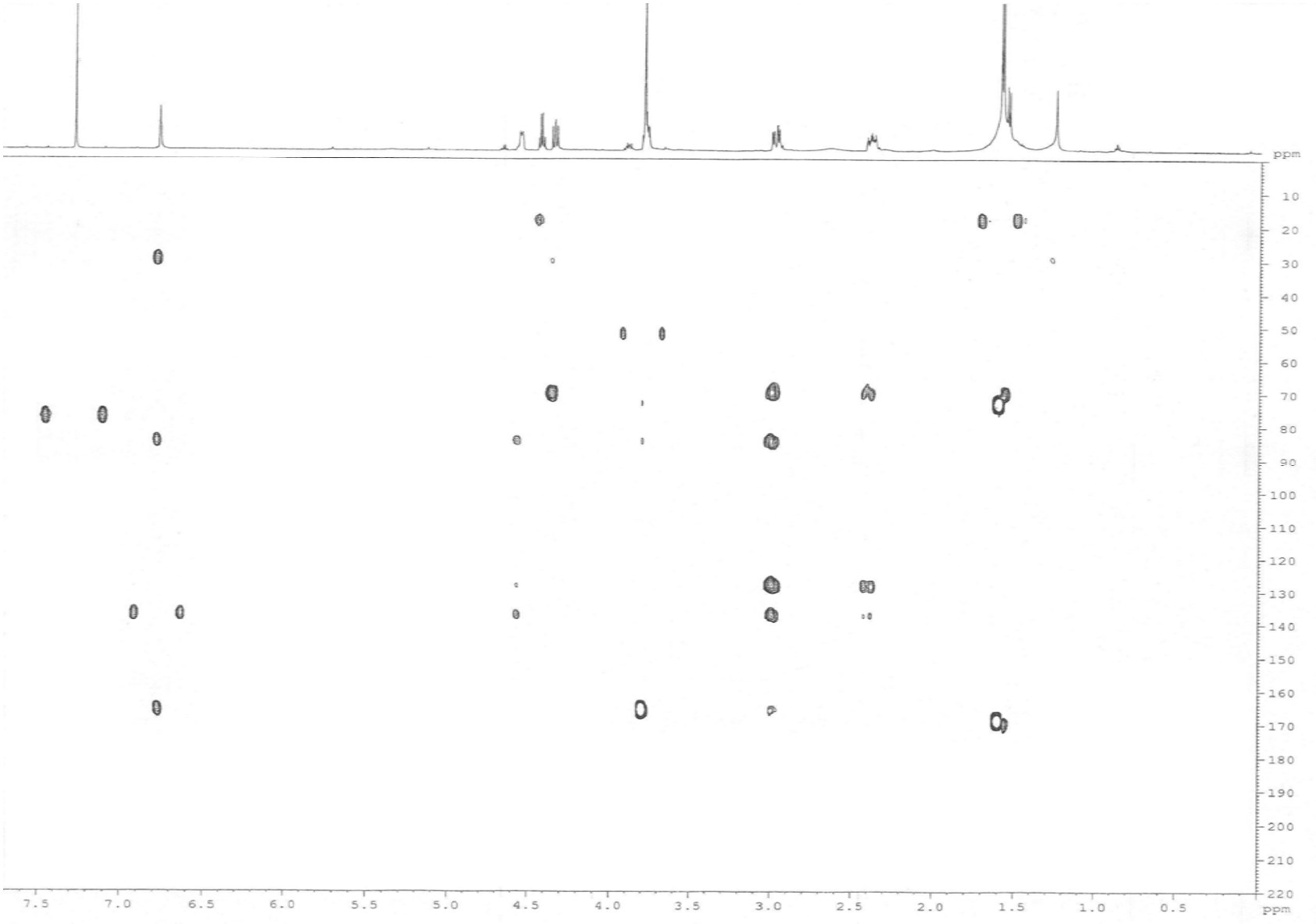

Figure 5.11.43. HMBC spectrum of phyllostin, isolated from *P. cirsii* culture filtrates, recorded at 600 MHz

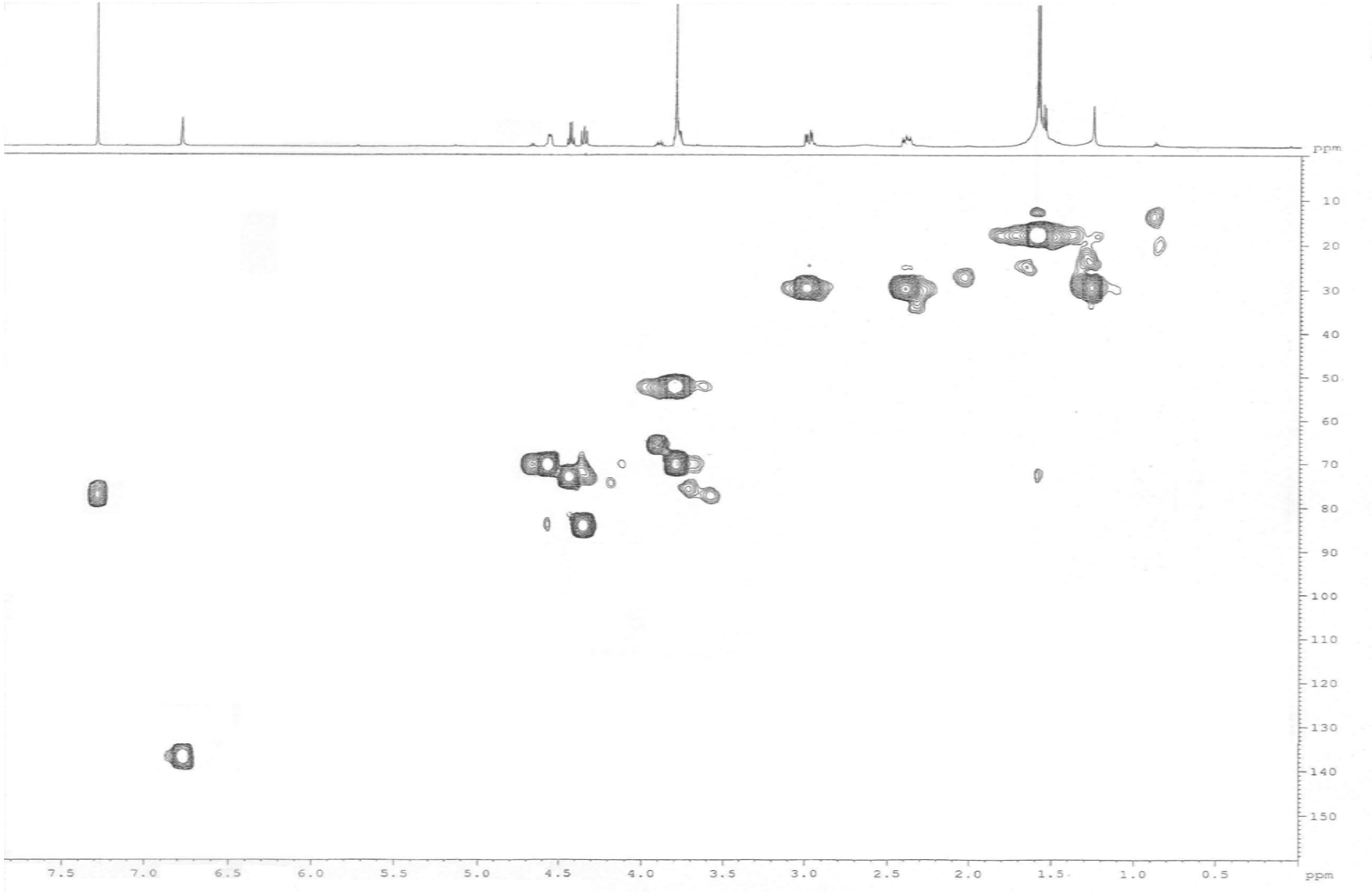

Figure 5.11.44. HSQC spectrum of phyllostin, isolated from *P. cirsii* culture filtrates, recorded at 600 MHz

Table 5.1.1. ^{1}H and ^{13}C NMR data of ophiobolin E and 8-*epi*-ophiobolin J (**40** and **43**). The chemical shifts are in δ values (ppm) from TMS [a]

	40				**43**			
C	δ[b]	δH	*J* (Hz)	HMBC	δ[b]	δH	*J* (Hz)	HMBC
1	30.4 t	1.50 m 1.17 m		2.85, 2.37, 0.89	49.7 t	1.96 dd 1.10 m	11.8, 1.4	3.16, 1.57, 1.34
2	45.7 d	2.37 bt	1.87	1.17, 0.89	45.8 d	3.16 d	11.8	2.08, 1.96, 1.10
3	78.9 s			2.85, 1.50, 1.34, 1.17	175.7 s			6.03, 3.16, 2.08, 1.96
4	53.2 t	2.45 d 1.50 m	13.1	1.69, 1.50, 1.34	131.9 d	6.03 s		3.16, 2.08
5	25.3 t	2.05 m 1.69 m	1.3		198.0 s			6.03, 3.16, 2.08
6	46.3 d	2.85 br d	6.99	9.49, 2.45, 1.50	138.6 s			6.03, 3.16, 2.08
7	141.5 s			9.49, 2.94, 2.85, 2.48, , 2.45	149.0 s			1.89
8	152.7 d	7.13 dd	5.3, 2.0	2.94, 2.85, 2.48, 1.50, 0.89	72.1 d	4.70 dd	10.0, 9.9	1.89
9	26.0 t	2.94 d 2.48 dd	19.7 19.7, 5.3	7.13	34.3 t	1.89 m (2H)		1.89
10	158.8 s			2.20	51.1 s	1.89 m		1.96, 1.89, 1.68, 1.51
11	58.0 s			7.13, 2.94, 2.85, 2.48	43.6 s			1.96, 1.89, 1.68, 1.57, 1.34, 1.51, 1.10
12	124.5 d	5.08 br t	5.4		30.3 t	1.68 m 1.51 m		2.20, 1.57, 1.34
13	159.6 s			5.84, 3.85, 0.93	42.4 t	1.57 m 1.34 m		
14	133.0 s				95.8 s			2.20, 1.89, 1.79, 1.68, 1.51, 1.34, 1.02
15	33.0 d	2.20 m		1.50	36.0 d	2.20 dq	13.7, 6.9	1.79, 1.68, 1.02
16	35.5 t	1.69 m 1.50 m		0.93	42.0 t	1.79 m 1.68 m		2.20, 1.02
17	85.7 d	3.85 br d	2.9	5.84	71.9 d	4.54 dd	15.7, 7.2	2.20, 1.79
18	125.8 d	5.84 br d	2.9	1.67, 1.59	127.0 d	5.16 br d	7.2	1.79, 1.69, 1.64
19	134.0 s			1.67, 1.59	134.5 s			4.54, 1.69, 1.64
20	29.2 q	1.34 s		1.50, 1.17	17.4 q	2.08 s		6.03
21	193.4 d	9.49 s		7.13, 2.94	56.7 t	4.74 br s		
22	14.1 q	0.89 s			22.7 q	1.10 s		1.96, 1.89, 1.57, 1.34, 1.10
23	22.7 q	0.93 d	7.0		16.3 q	1.02 d	6.9	2.20, , 1.79, 1.68
24 [c]	18.0 q	1.59 s			18.1 q	1.64 s		5.16, 1.79
25[c]	25.6 q	1.67 s			25.9 q	1.69 s		5.16, 1.79, 1.64

[a]2D ^{1}H, ^{1}H (COSY) and 2D ^{13}C, ^{1}H (HSQC) NMR experiments delineated the correlations of all protons and the corresponding carbons.
[b]Multiplicities determined by DEPT spectrum.
[c]These assignments can be exchanged (They were made by comparison with analogues Li *et al*., 1995).

Table 5.1.2. 2D ^{1}H-NOE (NOESY) data obtained for ophiobolin E and 8-*epi*-ophiobolin J (**40** and **43**)

40		**43**	
Considered	Effects	Considered	Effects
9.49 (H-21)	7.13 (H-8), 2.85 (H-6), 1.17 (H-1')	5.16 (H-18)	4.54 (H-17), 2.20 (H-15), 1.79 (H-16), 1.68 (H-16')
7.13 (H-8)	9.49 (H-21), 2.94 (H-9), 2.48 (H-9'), 0.93 (Me-23)	4.74 (H_2-21)	4.70 (H-8), 3.16 (H-2)
5.84 (H-18)	3.85 (H-17), 2.20 (H-15), 1.69 (H-16), 1.50 (H-16'), 0.93 (Me-23)	4.70 (H-8)	4.74 (H_2-21), 1.89 (H_2-9), 1.10 (Me-22)
5.08 (H-12)	2.20 (H-15), 1.69 (H-16), 1.50 (H-16')	4.54 (H-17)	5.16 (H-18), 1.79 (H-16), 1.68 (H-16'), 1.02 (Me-23)
3.85 (H-17)	5.84 (H-18), 1.50 (H-16'), 0.93 (Me-23)		
2.94 (H-9)	7.13 (H-8), 2.48 (H-9'), 2.20 (H-15), 0.93 (Me-23)	3.16 (H-2)	4.74 (H_2-21), 1.96 (H-1), 1.10 (Me-22)
2.85 (H-6)	9.49 (H-21), 2.37 (H-2), 1.50 (H-4'), 1.34 (Me-20)	2.20 (H-15)	5.16 (H-18)
2.48 (H-9')	9.49 (H-21), 2.94 (H-9), 0.89 (Me-22)	1.96 (H-1)	3.16 (H-2)
2.45 (H-4)	1.50 (H-4'), 1.34 (Me-20), 1.17 (H-1')	1.89 (H_2-9)	4.70 (H-8)
2.37 (H-2)	2.85 (H-6), 1.50 (H-1)	1.79 (H-16)	5.16 (H-18), 4.54 (H-17)
2.20 (H-15)	2.94 (H-9), 1.69 (H-16), 1.50 (H-16'), 0.93 (Me-23)	1.68 (H-16')	5.16 (H-18), 4.54 (H-17)
1.69 (H-16)	5.84 (H-18), 5.08 (H-12), 2.20 (H-15)	1.10 (Me-22)	4.70 (H-8), 3.16 (H-2)
1.50 (H-16')	5.84 (H-18), 5.08 (H-12), 3.85 (H-17), 2.20 (H-15)	1.02 (Me-23)	4.54 (H-17)
1.50 (H-4')	2.85 (H-6), 2.45 (H-4)		
1.50 (H-1)	2.37 (H-2)		
1.34 (Me-20)	2.85 (H-6), 2.45 (H-4)		
1.17 (H-1')	9.49 (H-21), 2.45 (H-4)		
0.93 (Me-23)	7.13 (H-8), 5.84 (H-18), 3.85 (H-17), 2.94 (H-9), 2.20 (H-15)		
0.89 (Me-22)	2.48 (H-9')		

Table 5.3.1. Effect of ophiobolins (**36-38**) in the leaf puncture assay on different weed species*

	36			**37**			**38**		
Species	$6.3x10^{-4}$	$2.5x10^{-4}$	$1.3x10^{-4}$	$6.3x10^{-4}$	$2.5x10^{-4}$	$1.3x10^{-4}$	$6.3x10^{-4}$	$2.5x10^{-4}$	$1.3x10^{-4}$
					monocotyledons				
Avena ludoviciana Dur.	3	3	3	2	2	2	0	0	0
Bromus sterilis L.	3	2	1	2	1	1	1	1	1
Cynodon dactylon (L.) Pers.	1	0	0	2	1	0	0	0	0
Digitaria sanguinalis (L.) Scop.	3	3	3	3	2	2	1	1	0
Echinochloa crus-galli (L.) Beauv.	3	3	3	2	2	1	1	1	1
Oryzopsis miliacea (L.) Aschers	3	2	1	2	1	1	1	1	1
Phalaris canariensis L.	3	3	3	3	2	1	1	1	1
Setaria viridis (L.) Beauv.	3	3	3	3	3	3	2	2	2
					dicotyledons				
Amaranthus retroflexus L.	3	2	2	1	1	1	0	0	0
Chenopodium album L.	3	2	2	3	2	2	1	1	0
Convolvulus arvensis L.	2	2	2	2	2	2	0	0	0
Diplotaxis erucoides (L.) DC.	2	2	2	2	2	2	3	3	2
Sonchus oleraceus L.	3	3	3	3	3	3	1	1	0

*Diameter of necrosis on leaves: 3 = necrosis > 3 mm; 2 = necrosis between 2 and 3 mm; 1 = necrosis between 1 and 2 mm; 0 = no necrosis

Table 5.3.2. Effect of ophiobolins B and J (**41** and **42)** on various weed species tested by leaf puncture assay

Species	Compound[a]	
	41	**42**
Avena sterilis	++[b]	+
Bromus sp.	++++	++
Hordeum murinum	++++	++
Oryzopsis miliacea	+	-

[a] 0.5 mg ml^{-1} - droplets 15 µl

[b]Diameter of necrosis on leaves: ++++ = necrosis diameter > 6 mm; ++ = necrosis between 4 and 2 mm; + = necrosis between 2 and 1 mm; - = no necrosis

Table 5.5.1. Origin, host and year of isolation of the *Ascochyta* strains used in the present work

Strain	Region	Host plant	Year of isolation
S-7	Saint-Petersburg, Russia	*Sonchus arvensis*	1998
S-9	Northern Osetia, Russia		2002
S-10			
C-177	Oslo, Norway	*Cirsium arvense*	
C-180	Northern Osetia, Russia		
C-182	Saint-Petersburg, Russia		
C-208			2003
C-216			
C-240	Northern Osetia, Russia		

Table 5.5.2. Analytical characteristics of calibration curve for ascosonchine

Rt (min)	Range (μg)	Slope[a]	Intercept[a]	SD,[a] y %	r^2	Number of data point	Detection limit (pg)
4.6	0.14-14	15599	917.7	0.73	0.9987	27	1.8

[a]Calculated in the form y=a+bx where y=chromatographic peak area and x=μg of toxin

Table 5.8.1. ^{1}H NMR data of stagonolides B-F (**45-49**)[a,b,c]

Position	**45** δH *J* (Hz)	**46** δH *J* (Hz)	**47** δH *J* (Hz)	**48** δH *J* (Hz)	**49** δH *J* (Hz)
2	2.47 br dd (14.6, 14.3)	2.03 (2H) m	2.28 ddd (13.0, 7.4, 1.8)	5.84 d (11.6)	2.35 t (7.5)
	2.08 ddd (14.3, 5.4, 2.8)		2.11 dd (13.0, 11.2)		2.00 m
3	2.10 br dd (15.0, 14.6)	2.29 m	2.05 dd (14.0, 1.8)	6.60 br d (11.6)	2.05 (2H)
	1.88 m	2.03 m	2.00 ddd (14.0, 11.2, 4.3)		
4	4.63 br s	4.10 m	4.13 ddd (8.4, 7.4, 4.3)	6.12 br d (15.4)	2.00 m
					1.60 m
5	5.65 dt (16.1, 2.6)	5.42 dd (15.6, 10.2)	5.52 dd (17.0, 8.4)	5.73 dd (15.4, 9.6)	4.06 ddd (10.2, 9.3, 3.3)
6	6.00 br d (16.1)	5.58 dd (15.6, 9.4)	5.64 dd (17.0, 4.8)	4.24 ddd (9.6, 9.0, 3.8)	5.27 br dd (15.1, 10.2)
7	4.51 br s	4.10 m	3.65 dd (4.8, 3.9)	2.08 ddd (14.2, 9.0, 3.8)	5.66 ddd (15.1, 10.7, 3.4)
				1.73 ddd (14.2, 9.5, 9.0)	
8	3.58 br dd (9.5, 2.4)	1.88 dd (13.8, 2.6)	3.05 dd (3.9, 2.6)	1.85 dd (15.8, 9.0)	2.30 m
		1.77 ddd (13.8, 11.2, 2.6)		1.60 m	2.05 m
9	4.94 td (9.5, 2.4)	5.14 dq (11.2, 6.2)	5.34 dq (6.7, 2.6)	4.98 dq (11.7, 6.5)	5.15 ddd (12.7, 6.4, 3.4)
10	1.88 m	1.22 d (6.2)	1.37 d (6.7)	1.21 d (6.5)	1.18 d (6.4)
	1.57 m				
11	1.37 m				
	1.25 m				
12	0.91 t (7.4)				

[a]The chemical shifts are in δ values (ppm) from TMS. [b]2D ^{1}H, ^{1}H (COSY) ^{13}C, ^{1}H (HSQC) NMR experiments delineated the correlations of all protons and the corresponding carbons.[c]The assignments are in agreements with the values reported for herbarumins (Rivero-Cruz *et al*., 2000), putaminoxin (Evidente *et al*., 1995) and aspinolides (Fucsher and Zeeck, 1997).

Table 5.8.2. ^{13}C-NMR data of stagonolides B-F (**45-49**)[a,b,c]

	45	**46**	**47**	**48**	**49**
Position	δC mult[d]	δC mult[d]	δC mult[d]	δC mult[d]	δC mult[d]
1	176.0 qC	174.5 qC	173.5 qC	168.2 qC	174.8 Qc
2	27.8 CH_2	34.4 CH_2	31.2 CH_2	125.6 CH	32.1 CH_2
3	31.7 CH_2	31.5 CH_2	35.0 CH_2	139.6 CH	31.5 CH_2
4	68.6 CH	74.4 CH	75.1 CH	126.6 CH	34.3 CH_2
5	127.5 CH	133.0 CH	134.2 CH	140.2 CH	71.8 CH
6	127.1 CH	135.8 CH	128.1 CH	73.7 CH	134.5 CH
7	73.7 CH	72.0 CH	55.4 CH	37.4 CH_2	131.3 CH
8	73.6 CH	43.4 CH_2	58.2 CH	30.4 CH_2	35.0 CH_2
9	70.2 CH	67.7 CH	65.7 CH	73.2 CH	75.4 CH
10	33.6 CH_2	21.3 CH_3	16.2 CH_3	21.4 CH_3	21.7 CH_3
11	18.0 CH_2				
12	12.1 CH_3				

[a]The chemical shifts are in δ values (ppm) from TMS. [b]2D ^{1}H, ^{1}H (COSY, TOCSY) ^{13}C, ^{1}H (HSQC) NMR experiments delineated the correlations of all protons and the corresponding carbons. [c]The assignments are in agreements with the values reported for herbarumins,[13] putaminoxin[20] and aspinolides.[23] [d]Multiplicities determined by DEPT spectrum.

Table 5.8.3. HMBC data of stagonolides B-E (**45-48**)

	45	**46**	**47**	**48**
C	HMBC	HMBC	HMBC	HMBC
1	H-9, H_2-2, H_2-3	H-9, H-4, H_2-2, H_2-3	H-9, H_2-2	H-9, H-3, H-2
2	H-4, H-3	H-5, H-4, H_2-3	H_2-3	H-4
3	H_2-2	H_2-2	H-5, H-4, H_2-2	H-2
4	H-6, H-5, H_2-2, H_2-3	H-6, H_2-3	H-6, H_2-3, H_2-2	H-6, H-5
5	H-6, H-4, H-3’	H-6, H-4, H_2-3	H-7, H-6, H-4, H_2-3	H_2-7, H-5
6	H-7, H-5,	H_2-8, H-7, H-5,	H-7, H-5, H-4	H_2-7, H-4
7	H-6, H-5,	H_2-8, H-5	H-8, H-5	H-9, H-5, H_2-8
8	H-9, H-7	H-7, H-6, Me-10	H-9, H-7,Me-10	H_2-7,Me-10
9	H-8, H-10’	H-8’, Me-10	Me-10	H_2-8, Me-10
10	H-9, H-8, Me-12	H_2-8	H-9	H-9, H-8
11	H-9, H_2-10, Me-12			
12	H-10’, H-11’			

Table 5.8.4. 2D ^{1}H-NOE (NOESY) data obtained for stagonolides B-E (**45-48**)

45		**46**		**47**		**48**	
Cosidered	Effects	Cosidered	Effects	Cosidered	Effects	Cosidered	Effects
H-9	H_2-10, H_2-11, Me-12	H-6	H-7, H-8’	H-6	H-7, H-8, H-4, H_2-3	H-3	H-4, H-2
H-8	H_2-11, H_2-10, H-7, H-6	H-5	H-4, H_2-2	H-5	H-7, H-8, H-4, H-2’	H-4	H-6
H-7	H-8, H-6,	H-7	H_2-8, H-6	H-9	H-8, Me-10	H-9	H-8, Me-10
H-6	H-8, H-7, H-2	H-9	Me-10, H_2-8, H-7	H-4	H_2-3	H-5	H-7’, H-6
H-5	H-4, H-2’	H-4	H-5, H-3’	H-7	H-8	H-6	H-8’, H-7, H-5, H-4
H-4	H_2-3			H-8	H-9, H-7, Me-10		
				Me-10	H-9, H-8		

Table 5.8.5. ^{1}H-NMR data for stagonolides G-I (**50-52**) and Modiolide A (**53**)[a,b,c]

	50	**51**	**52**	**53**
Position	δH (*J* in Hz)	δH (*J* in Hz)	δH (*J* in Hz)	δH (*J* in Hz
2	2.56 (2H) m	5.93 d (12.0)	5.68 dd (11.8, 2.1)	5.89 d (12.5)
3	2.35 m	6.11 dd (12.0,6.4)	6.31 dd (11.8, 4.0)	5.91 d (12.5)
	1.95 ddd (17.7, 10.9, 9.5)			
4	4.54 m	4.76 br dd (6.4, 2.2)	5.71 br ddd (9.6, 4.0, 2.1)	4.79 br d (8.7)
5	2.63 ddd (14.5, 7.7, 7.7)	5.96 dd (15.9, 2.2)	5.40 dd (10.3, 9.6)	5.74 dd (15.9, 8.7)
	2.48 ddd (14.5, 5.2, 5.2)			
6	5.67 ddd (11.1, 7.7, 5,2)	5.88 dd (15.9, 1.6)	5.50 dd (10.3, 8.2)	5.63 dd (15.9, 10.4)
7	5.60 dd (11.1, 8.2)	3.65 dd (4.3, 1.6)	4.97 br ddd (9.8, 8.2, 3.0)	4.26 br dd (10.4, 11.1, 3.2))
8	4.11 dd (8.2, 8.2)	2.94 br d (4.3, <1.0)	2.24 ddd (13.9, 9.8, 7.0)	1.92 ddd (12.9, 3.2, 1.2)
			1.87 ddd (13.9, 3.9, 3.0)	1.81 ddd (12.9,11.1, 10.8)
9	3.67 dq (8.2, 6.5)	5.43 br q (6.9, <1.0)	5.11 m	5.31 ddq (10.8, 6.3, 1.2)
10	1.15 d (6.5)	1.50 d (6.9)	1.41 d (6.5)	1.28 d (6.3)
OH	5.67 br s	4.85 br s	5.88 br s	1.67 br s
OH	3.64 s		5.72 br s	1.56 br s

[a]The chemical shifts are in δ values (ppm) from TMS. [b]2D ^{1}H, ^{1}H (COSY) ^{13}C, ^{1}H (HSQC) NMR experiments delineated the correlations of all protons and the corresponding carbons.[c]The assignments are in agreement with the values reported for stagonolides B-F, modiolides (Tsuda *et al*., 2003) and herbarumins (Rivero-Cruz *et al*., 2000)

Table 5.8.6. ^{13}C-NMR data for Stagonolides G-I (**50-52**) and Modiolide A (**53**)[a,b,c]

	50	**51**	**52**	**53**
Position	δC mult.[d]	δC mult.[d]	δC mult.[d]	δC mult.[d]
1	178.0 qC	167.7 qC	164.8 qC	167.0 qC
2	28.7 CH_2	126.1 CH	121.0 CH	122.8 CH
3	27.5 CH_2	133.9 CH	149.1 CH	136.1 CH
4	79.6 CH	66.9 CH	66.8 CH	71.3 CH
5	33.7 CH_2	131.3 CH	129.4 CH	131.0 CH
6	127.8 CH	119.7 CH	134.5 CH	137.3 CH
7	132.5 CH	55.8 CH	64.5 CH	72.1 CH
8	72.3 CH	56.3 CH	42.6 CH_2	42.7 CH_2
9	70.8 CH	65.6 CH	68.4 CH	68.7 CH
10	18.7 CH_3	18.6 CH_3	20.8 CH_3	21.3 CH_3

[a]The chemical shifts are in δ values (ppm) from TMS. [b]2D ^{1}H, ^{1}H (COSY, TOCSY) ^{13}C, ^{1}H (HSQC) NMR experiments delineated the correlations of all protons and the corresponding carbons. [c]The assignments are in agreement with the values reported for stagonolides B-F, modiolides (Tsuda *et a*l., 2003) and herbarumins (Rivero-Cruz *et al*., 2000) [d]Multiplicities determined by DEPT spectrum.

Table 5.8.7. HMBC data for Stagonolides G-I (**50-52**) and Modiolide A (**53**)

	50	**51**	**52**	**53**
C	HMBC	HMBC	HMBC	HMBC
1	H_2-2	H-3, H-2,	H-3, H-2	H-2
2		H-4, H-3	H-4	
3	H_2-2	H-4, H-2	H-5, H-2	
4	H_2-5, H-3’	H-6, H_2-3	H-6, H-5	H-6, H-3, H-2
5	H-7, H-3’	H-7, H-6, H-4, H-3	H-7, H-6, H-4	H-7, H-6, H-3
6	H-8, H_2-5,	H-7, H-5, H-4	H-7, H-5	H-5, H-4
7	H_2-5	H-8, H-6, H-5	H_2-8, H-5	H_2-8, H-5
8	H-7	H-7, H-6, Me-10	Me-10, H-7	Me-10, H-6
9	H-8, Me-10	H-8, Me-10	H_2-8	Me-10, H-8’
10		H-9, H-8	H-9, H-8	

Table 5.8.8. 2D ^{1}H-NOE (NOESY) data obtained for Stagonolides G-I (**50-52**) and Modiolide A (**53**).

50		**51**		**52**		**53**	
Considered	Effects	Considered	Effects	Considered	Effects	Considered	Effects
H-9	Me-10, H-8, H-7	H-9	Me-10, H-8	H-9	Me-10, H_2-8	H-9	H-8, Me-10
H-8	Me-10, H-9, H-7, H_2-5	H-8	H-9, H-7	H-7	H-8’	H-8	H-9, H-7, Me-10
H-7	H-9, H-8,	H-7	H-8, H-6	H-6	H-8’	H-7	H-8
H-6	H_2-5, H-4	H-4	H-5, H-3	H-3	H-2	H-6	H-7, H-8, H-4
H_2-5	H-8, H-6, H-4, H_2-3					H-5	H-7, H-8, H-4
H-4	H-6, H_2-5, H_2-3					H-4	H-3
						Me-10	H-9, H-8

Table 5.10.1. Effect of toxins on light absorption by leaves of *C. arvense* at 632.8 nm

Toxins	Absorption, %			Change after 4 hours (%)
	before treatment	after 2 hours post treatment	after 4 hours post treatment	
Stagonolide	68,1	63,4	53,5[a]	-21
Putaminoxin	62,0	53,4	47,8[a]	-24
Deoxaphomin	60,6	60,9	56,6	-7
Cytochalasin A	66,3	57,8[a]	58,8[a]	-11
Cytochalasin B	66,3	60,8	54,4[a]	-18
Control	63,8	61,6	61,8	-3

[a]Values marked with asterisk are significantly ($p<0.05$) differed from values before treatment

Table 5.10.2. Effect of toxins on light absorption by leaves of *C. arvense* in the range of 450–950 nm

Wavelength (nm)	Absorption, %			Comparison of means with Student's coefficient		
	Control	cytochalasin B	Stagonolide	Control vs. cytochalasin B	Control vs. stagonolide	cytochalasin B vs. stagonolide
450	62.6	58.6	58.5	4.40[a]	2.77[a]	0.07
470	77.1	76.8	76.8	0,31	0,10	0,02
490	74.1	74.9	71.1	0.36	1.98[a]	1.93
510	59.9	63.3	62.2	1.81	0.99	0.74
530	44.5	48.7	53.4	2,04[a]	3.70[a]	1.94
550	44.4	49.4	54.4	2.38[a]	4.85[a]	2,02[a]
590	65.2	66.4	63.9	0.84	0.87	1.61
610	68.4	69.8	66.1	0.70	1.37	1.71
630	70.9	72.4	66.7	0.84	2.14[a]	2.76[a]
650	78.5	78.2	70.5	0.15	2.15[a]	1.98[a]
670	85.6	85.7	76.1	0.12	3.65[a]	3.62[a]
690	62.6	64.8	55.0	0.98	3.46[a]	3.49[a]
710	19.1	21.9	26.0	0.97	3.02[a]	1.47
730	1.3	2.9	16.8	1.07	5.91[a]	4.79[a]
750	0.5	2.6	16.2	1.64	7.12[a]	5.44[a]
770	2.2	3.9	18.0	0.91	6.93[a]	5.39[a]
790	3.1	4.0	16.8	0.43	5.07[a]	4.31[a]
810	4.3	5.4	17.5	0.49	5.63[a]	2.60[a]
830	4.2	6.0	17.0	0.82	5.47[a]	4.27[a]
850	3.3	4.2	14.3	0.49	4.96[a]	3.95[a]
870	1.4	3.25	10.8	1.12	4.70[a]	3.25[a]
890	1,0	2.2	4.2	0.97	1.68	0.91
910	0.19	1.2	3.1	1.32	1.98	1.13
930	0.02	0.9	3.4	1.49	2.41[a]	1.61

[a]Values marked with asterisk significantly ($p<0.05$) differed from each other

Table 5.11.1. ^{1}H NMR data of phyllostictines A-D ()[a,b]

Position	δ_H			
	54	**55**	**56**	**57**
5				2.44 (2H) t (7.3 Hz)
6	1.30 (2H) m	1.33 (2H) m	1.34 (2H) m	1.61 m 1.36 m
7	1.30 (2H) m	1.58 m 1.38 m	1.40 (2H) m	
8	1.30 m 1.26 m	1.80 (2H) m	1.60 m 1.38 m	
9	1.58 m 1.37 m	4.02 m	1.80 (2H) m	1.36 (2H)m
10	1.80 (2H) m		4.03 m	1.61 m 1.40 m
11	4.04 m			1.81 (2H) m
12		5.08 d (*J*=1.0 Hz) 5.04 d (*J*=1.0 Hz)		4.02 m
13		4.48 br s	5.07 d (*J*=1.0 Hz) 5.05 d (*J*=1.0 Hz)	
14	5.08 d (*J*=0.9 Hz) 5.03 d (*J*=0.9 Hz)		4.46 br s	
15	4.45 br s			5.06 d (*J*=1.3 Hz) 5.04 d (*J*=1.3 Hz)
16				4.47 br s
MeN				2.14 s
$MeCH_2N$	1.30 (2H) m	1.33 (2H) m	1.48 (2H) m	
$MeCH_2N$	0.83 t (*J*=7.1 Hz)	0.91 t (*J*=6.6 Hz)	0.95 t (*J*=7.1 Hz)	
Me-C(5)	1.27 s	1.26 s		
MeCH(OH)-C(5)			3.80 m	
MeCH(OH)-C(5)			1.18 d (*J*=6.2 Hz)	
Me-C(7)				1.26 s
MeO	3.91 s	3.92 s	3.91 s	3.92 s
OH	3.61 (br s), 2.80 (br s)	3.10 (br s), 2.20 (br s)	3.29, 2.45, 1.61(all br s)	3.06 (br s), 2.24 (br s)

[a]The chemical shifts are in δ values (ppm) from TMS.
[b]2D ^{1}H, ^{1}H (COSY) ^{13}C, ^{1}H (HSQC) NMR experiments delineated the correlations of all the protons and the corresponding carbons.

Table 5.11.2. ^{13}C NMR data of phyllostictines A-D (**54-57**)[a,b]

Position	δC m[c]			
	54	**55**	**56**	**57**
1	136.3 s	136.3 s	136.4 s	136.4s
2	156.2 s	156.0 s	156.0 s	155.9 s
3	166.6 s	166.2 s	166.4 s	166.3 s
5	71.8 s	71.8 s	71.8 s	43.6
6	22.6 t	22.6	25.6 t	23.6 t
7	29.3 t	26.2 t	29.2 t	71.8 t
8	29.7 t	27.5 t	26.4 t	210.0 s
9	26.5 t	86.18 d	27.4 t	28.8 t
10	27.5 t	104.2 s	86.2 d	26.3 t
11	86.3 d			27.3 t
12	104.3 s	96.2 t		86.0 d
13		68.9 t	92.6 t	104.4 s
14	92.7 t		68.6 d	
15	68.4 d			92.6 t
16				68.1 d
Me$\underline{CH_2}$N	31.8 t	31.6 t	39.2 t	
$\underline{Me}CH_2N$	14.1 q	14.1 q	14.1 q	
MeN				29.9 q
Me-C(5)	17.1 q	17.1 q		16.5 q
Me$\underline{CH}$(OH)-C(5)			68.1 d	
$\underline{Me}$CH(OH)-C(5)			23.6 q	
Me-C(7)				
MeO	64.5 q	64.6 q	64.6 q	64.6 q

[a]The chemical shifts are in δ values (ppm) from TMS.

[b]2D ^1H, ^1H (COSY, TOCSY) ^{13}C, ^1H (HSQC) NMR experiments delineated the correlations of all the protons and the corresponding carbons.

[c]Multiplicities determined by DEPT spectrum

Table 5.11.3. HMBC data of phyllostictines A-D (**54-57**).

C	HMBC			
	54	**55**	**56**	**57**
1	H_2-14	H_2-12	H_2-13	H_2-15
2	H-15, H_2-14, H-11	H-13, H_2-12, H-9	H-14, H_2-13	H-16, H_2-15, MeO
5	H-15, H_2-6, Me-C(5)	H-13, Me-C(5)	H-14, H_2-6, $MeCH_2N$	H_2-6, MeN
6	Me-C(5)	$MeCH_2N$, H-9, H-7’		H_2-5, MeN
7		Me-C(5)		H_2-6, Me-C(7)
8		H-9		H_2-6, H_2-5
9	H_2-10	H_2-8	H-10	
10	H-11, H_2-9,	H-13	H_2-9, H_2-8	
11	H-15, H_2-10, H_2-9		H-14	
12	H-15			H_2-11, H_2-10
13				H-16
MeN				H_2-6, H_2-5
$MeCH_2N$	$MeCH_2N$	$MeCH_2N$	$MeCH_2N$	
MeCH(OH)-C(5)			MeCH(OH)-C(5)	

Table 5.11.4. 2D ^{1}H NOE (NOESY) data obtained for phyllostictines A-D (**54-57**)

54		**55**		**56**		**57**	
Considered	Effects	Considered	Effects	Considered	Effects	Considered	Effects
H-15	H_2-14, H-11, MeO, Me-C(5)	H-13	H_2-12, H-9, MeO, OH, OH, H-7, Me-C(5)	H-14	H_2-13, H-10, MeO, OH, OH, MeCH(OH)-C(5)	H-16	H_2-15, H-12, MeO, OH, OH, H_2-5, Me-C(7)
H-11	H-15, MeO, H_2-10, H-9’	H-9	H-13, MeO, OH, H_2-8, H_2-7	H-10	H-14, MeO, H_2-9, H_2-8	H-12	H-16, MeO, H_2-5, OH, H_2-11, H_2-10, Me-C(7)
MeO	H-15, H_2-14, H-11, OH, OH, Me-C(5)	MeO	H_2-12, H-13, H-9, OH, H_2-8, H-7	MeO	H-14, H_2-13, H-10, OH	MeO	H_2-15, H-16, H-12, H-10, Me-C(7)
				MeCH(OH)-C(5)	$MeCH_2N$	H_2-5	MeN

Table 5.11.5 ^{1}H and ^{13}C NMR data of Phyllostoxin (**62**)[a,b]

C	δ[c]	^{1}H	*J*, Hz	HMBC
1	115.8 (s)			6.15
2	161.0 (s)			2.00, 2.36
3	130.0 (s)			
4	124.0 (d)	6.15 (d)	9.9	2.36
5	138.0 (d)	7.88 (d)	9.9	
6	121.1 (s)			
7	53.6 (s)			6.15, 2.11, 1.95, 1.42, 0.66
8	170.0 (s)			7.88, 2.11, 1.42
9	175.0 (s)			2.00
10	10.6 (q)	2.00 (s)		
11	17.8 (q)	2.36 (s)		
12	201.0 (s)			7.88, 2.11, 1.95, 1.42
13	33.0 (t)	2.11 (dq)	14.8, 7.5	1.42, 0.66
		1.95 (dq)	14.8, 7.5	
14	9.6 (q)	0.66 (t)	7.5	2.11, 1.95
15	24.0 (q)	1.42 (s)		

[a]The chemical shifts are in δ values (ppm) from TMS. [b]2D ^{1}H, ^{1}H (COSY, TOCSY) ^{13}C, ^{1}H (HSQC) NMR experiments delineated the correlations of all protons and the corresponding carbons.
[c]Multiplicities determined by DEPT spectrum

Table 5.11.6. ^{1}H and ^{13}C NMR data of Phyllostin (**63**)[a,b]

C	δ[c]	^{1}H	*J*, Hz	HMBC
2	169.0 (s)			4.41, 1.58
3	73.1 (d)	4.41 (q)	7.0	3.76, 1.58
4a	70.3 (d)	3.76 (ddd)	9.9, 8,6, 6.1	4.41, 2.99, 2.40
5	29.8 (t)	2.99 (dd)	17.5, 6.1	6.75, 4.34, 3.76
		2.40 (ddd)	17.5, 9.9, 3.3	
6	132.0 (s)			3.76, 4.54, 2.99, 2.40
7	137.0 (d)	6.75 (br s)	7.4	4.54, 2.99, 2.40
8	70.2 (d)	4.54 (br d)	8.4	4.34
8a	84.3 (d)	4.34 (dd)	8.6, 8.4	6.75, 4.54, 3.76, 2.99
9	17.9 (q)	1.58 (d)	7.0	4.41
10	167.0 (s)			6.75, 3.76, 2.99,
11	52.4 (q)	3.78 (s)		
OH		2.63 (br s)		

[a]The chemical shifts are in δ values (ppm) from TMS. [b]2D ^{1}H, ^{1}H (COSY, TOCSY) ^{13}C, ^{1}H (HSQC) NMR experiments delineated the correlations of all protons and the corresponding carbons.[c]Multiplicities determined by DEPT spectrum.

Table 5.11.7. 2D ^{1}H NOE (NOESY) data Obtained for Phyllostoxin and Phyllostin (**62** and **63**)

	62		**63**
Considered	Effects	Considered	Effects
7.88 (H-5)	6.15 (H-4)	6.75 (H-7)	4.54 (H-8)
6.15 (H-4)	7.88 (H-5)	4.54 (H-8),	6.75 (H-7), 3.76 (H-4a)
2.36 (Me-11)	2.00 (Me-10)	4.41 (H-3)	3.76 (H-4a), 1.58 (Me-9)
2.11 (H-13)	1.95 (H-13'), 1.42 (Me-15), 0.66 (Me-14)	4.34 (H-8a)	2.40 (H-5')
1.95 (H-13')	2.11 (H-13), 1.42 (Me-15), 0.66 (Me-14)	3.78 (Me-11)	2.40 (H-5')
1.42 (Me-15)	2.11 (H-13), 1.95 (H-13')	3.76 (H-4a)	4.54 (H-8), 4.41 (H.-3), 2.99 (H-5)
0.66 (Me-14)	2.11 (H-13), 1.95 (H-13')	2.99 (H-5)	3.76 (H-4a), 2.40 (H-5')
		2.40 (H-5')	3.78 (Me-11), 4.34 (H-8a), 2.99 (H-5)

Table 5.11.7. Effect of phyllostictines A-D in the puncture assay on thistle leaves

Phyllostictine	**Toxicity (20 µl/droplet)**
A	++++ [a]
B	+++
C	-
D	+++

[a]Toxicity determined using the following scale: - = no toxic; +++ = necrosis 3-5 mm;
++++ = wider necrosis